LIFE COURSE INTERVENTIONS THAT MODULATE SHORT- AND LONG-TERM CARDIOVASCULAR FUNCTION

by

Ronan Malcolm Neuman Noble

A thesis submitted in partial fulfillment of the requirements for the degree of

Doctor of Philosophy

Medical Sciences - Pediatrics

University of Alberta

Abstract

The Developmental Origins of Health and Disease (DOHaD) theory posits that insults during critical developmental periods can cause permanent structural and functional changes in key organ systems and thereby predispose an individual to chronic disease later in life. During gestation, iron deficiency (ID) is one insult which can increase risks of non-communicable diseases in the offspring, including cardiovascular disease. However, others who develop even under ideal circumstances will still experience chronic disease, particularly as they age. Cardiovascular disease alone is the leading cause of death worldwide, and accounts for a third of all mortality in Canada. Cardiovascular disease is associated with an enormous economic burden, accounting for more than $18 billion per year in Canada. Preventing even a small fraction of cardiovascular disease cases, either by discovering new mechanisms by which it develops, or by developing novel treatments which decrease its incidence, could result in substantial healthcare savings. Here we investigated the how perinatal ID affects offspring cardiovascular health in the neonatal period, as well as how broccoli sprout (BrSp) supplementation improves cardiovascular health throughout adulthood.

To accomplish this female Sprague Dawley rats were fed either an iron restricted (3 or 10 mg/kg ferric citrate) or iron replete (37 mg/kg ferric citrate) purified diet prior to and throughout gestation; dams were fed an iron-replete diet at birth. Offspring were studied either during gestation or in the early neonatal period (postnatal days 0 through 28).

In the early postnatal period, perinatal ID resulted in anemia and asymmetric growth restriction, as well as changes in cardiac function which occurred in a sex-specific manner. Proteomic analysis revealed ID down regulated structural components and elevated proteins associated with cellular stress response, and histology revealed a reduction in cardiomyocyte endowment. While

the functional changes recovered, cellular differences persisted, implying ID may lead to long-term alterations in cardiac function.

When ID dams were supplemented with an exogenous ketone, the previously mentioned cardiac dysfunction was partially mitigated. ID increased expression of Il-1β whereas ketone supplementation further altered Il-1β, Sod2, and Cat expression, indicating oxidative stress and inflammation may be relevant pathways for future study.

We also assessed fetal and placental oxygen saturation (sO2) in ID and control offspring throughout gestation using photoacoustic imaging. We observed regional differences in sO2 within the placenta and between the placenta and fetus, however, ID had minimal effects on sO2 suggesting ID fetuses may require less oxygen during gestation when compared to controls.

To study the long-term effects of nutritional supplementation, male and female Long-Evans rats were fed a control diet with or without dried BrSp from four months of age until death. Here, various parameters of cardiometabolic syndrome were assessed periodically across their lifespan. BrSp feeding reduced female bodyweight and visceral adiposity while improving glucose tolerance and reducing blood pressure in males. Finally, broccoli sprouts improved lifespan in females and in the oldest 25% of males.

The studies herein show how perinatal ID affects fetal and neonatal circulatory physiology and provide two noteworthy therapies; ketones and BrSp, which may improve cardiovascular function in these models. Given the high incidence of perinatal ID as well as cardiovascular disease in adulthood, this work could have substantial implications for both the short- and long-term health of our population.

Preface

This thesis is an original work by Ronan Malcolm Neuman Noble. Ethics for the following research was received from the university of Alberta Animal Use and Care Committee, Under Animal Use Protocol #974 and #364

Dedicated to VP.

Acknowledgements

I would like to sincerely thank my supervisor Stephane for his mentorship and guidance in completing this research as well as furthering my career, I am incredibly grateful to train under you and hope this is just the beginning in terms of research projects we complete together.

I would also like to thank my committee members Ferrante Gragasin, Luke Eckersley, and Jerome Yager for not only their valuable time and insight, but also for providing a model of what exceptional clinician scientists look like.

A special thank you to all the current and former members of the Bourque lab who have been indispensable to complete these projects. First, I would not have made it to this stage without the help of Andrew Woodman, who has been both an outstanding mentor within the lab and friend outside of the lab. I would also like to thank Richard Mah again for the great times both inside and outside of the lab. Finally, I am thankful for the collaborations with my fellow trainee's Alyssa, Claudia, Jad, Si Ning, and Forough.

Thank you for all of the collaborations and feedback from our 'perinatal research group' from the Davidge, Hemmings, Riddell, Ospina, and Clugston labs. In particular, the collaborations with Dr. Davidge, as well as the opportunity to rotate through Dr. Hemmings lab as a MatCH student were incredibly rewarding experiences.

I am grateful for the financial support of the University of Alberta Women and Children's Health Research Institute, as well as the Canadian Institutes of Health Research.

Finally, words cannot express my gratitude to my family for their unfailing support, particularly Kent and Colin Noble, and Helen Neuman who's love and encouragement has had an enormous effect my well-being. I am eternally grateful to have you all in my corner.

Table of Contents

List of Tables

List of Figures

Chapter 1
Introduction

1.1 Overview

The Developmental Origins of Health and Disease (DOHaD) theory posits that insults during critical developmental periods can cause permanent structural and functional changes in key organ systems and thereby predispose an individual to chronic disease in later life (1). During gestation, iron deficiency (ID) is one insult which can increase risks of non-communicable diseases in the offspring, including cardiovascular disease.

Nonetheless, even individuals that developed under ideal circumstances will still experience disease later in life, particularly as they age. In fact, cardiovascular disease is the leading cause of death worldwide, and accounts for a third of all mortalities in Canada (2, 3). While the death rates are dramatic, what is perhaps even more important is the growing number of non-fatal cardiovascular events, which cause long term disability and co morbid conditions. Advancements in medicine have resulted in an improved survival of first cardiovascular events (4). While improved survival is unquestionably a positive, this also results in survivors who are discharged with long term morbidity and reduced physiological reserve (5). Improved survival rates for those with cardiovascular disease further add to an already growing aging population, which will require more care. In fact, as the world's population continues to grow older the global prevalence of cardiovascular disease is expected to further increase. The economic burden of cardiovascular disease is already enormous, accounting for more than 18 billion dollars per year in Canada (6).

Preventing even a small fraction of cardiovascular disease, either by identifying previously unknown causes which could be prevented, or by developing novel treatments which decrease the initial incident of cardiovascular disease, could result in substantial healthcare savings and improved quality of life for

those affected. The main research focus of this thesis is to evaluate the alterations in cardiovascular function due to nutritional restriction or supplementation.

1.2 The Developmental Origins of Health and Disease (DOHaD)

1.2.1 A Broad Introduction to DOHaD

Most mammals develop in the womb and are supported by a placenta which provides nutrients and oxygen from the mother to the developing fetus. This provides an optimal environment for fetal development, allowing the offspring to grow faster at this stage than at any other point in development. However, when abnormal maternal conditions lead to a compromised fetal environment (e.g., malnutrition, psychosocial stress) then the offspring's risk of developing long term diseases later in life increases; this can be described as the Developmental Origins of Health and Disease (DOHaD).

The concept that stressors in early life affects long-term health in humans has been appreciated in the literature for almost 100 years. The first epidemiological studies on the topic traced an increase in incident of diseases in adulthood with regions associated with either poor standard of living or morbidity/mortality in childhood (7-9). However, it was not until the 1980's that David Barker and colleagues published a series of landmark papers which brought major attention to this concept. Barker and colleagues identified an increase incident of ischemic heart disease mortality in lesser affluent regions of England and Wales; this was surprising as ischemic heart disease was considered at the time to be a disease of prosperity (10). Further investigation suggested mothers who were generally undernourished experienced an increased incident of low birthweight and neonatal death. Indeed, the specific regions with the highest incidents of infant mortality between 1920-25 had corresponding increased incidents of death from ischemic heart disease as well as bronchitis, stomach cancer, and rheumatic heart disease later in adult life (11). Further work linked indices of fetal growth to cardiovascular disease later in life. In this study by Barker *et al.*, 5654 men who were born during 1911-30 in Herefordshire England were weighed

at birth and the year following (12). In adulthood the men with the lowest weights experienced the highest mortality from ischemic heart disease, and the largest birthweight infants experienced the lowest mortality from heart disease. Barker argued two important findings from these results; first that poor nutrition in utero resulted in an increased susceptibility to ischemic heart disease, linking effects in the intrauterine environment to long-term outcomes, and secondly that the relationship was linear indicating even small reductions in nutrition may influence offspring health (i.e., there was no "cut-off"). Barker ultimately formed the "Fetal Programing Hypothesis" as a framework to describe this in utero programing of chronic disease (13).

The Fetal Programing hypothesis was supported by several studies throughout the 1990s. Because the quality of the intrauterine environment is challenging to quantify, parameters of fetal growth were, and still are, used as a surrogate of maternal nutritional status (14, 15). In 1993 another study by Barker *et al.* linked head circumference, thinness (ponderal index) or both with higher rates of cardiovascular death compared to heavier babies with larger heads (16). Other studies showed reduced fetal growth and increased placental size corresponded to elevated blood pressure, impaired glucose tolerance and diabetes, and elevated plasma fibrinogen and factor VII concentrations (17-20). These relationships remained even after controlling for confounders such as social class, cigarette smoking, alcohol consumption, and obesity.

Perhaps most famously, the association between poor fetal and infantile growth and increased glucose tolerance and metabolic syndrome in adult life was described by Barker as the 'Thrifty Phenotype Hypothesis' (21). This hypothesis proposed that poor fetal nutrition drives a developmental 'switch' in utero, leading to poor growth of certain organs (including pancreatic beta cells) with selective protection of brain growth. This would result in a smaller offspring with a tendency towards energy storage, which would improve survival in the nutrient scarce environment it may be born into. However, in cases where the childhood or adult environment instead offers adequate calories, a relative overnutrition occurs,

leading to glucose intolerance and obesity (18, 22). In the ten years following these landmark studies, 30 major papers were published showing similar findings in a variety of populations around the world (22). Further studies of the Herefordshire men again indicated a continuous relationship this time between infant growth and glucose tolerance (18), importantly solidifying the indication that offspring born small but above clinical cut-offs may still experience lasting cardiometabolic dysfunction later in life.

At a population level this can be practically shown by numerous famines but is perhaps best outlined best by the Dutch hunger winter. Near the end of 1944, embargos and dwindling supplies led to a period of starvation in the Netherlands over the course of five months; during this period, daily rations were reduced to between 400 and 800 calories per day (23). Though tragic, this event has provided valuable insights into mechanism by which early stressors can impact long-term health of the offspring due to the abruptness of this famine as well as the accuracy which the offspring were followed 50 years later. The sudden reduction of rations led to women who experienced famine exclusively in either late gestation, mid gestation, or early gestation; as well as control groups, which still experienced the poverty and general hardship of World War two but were not severely undernourished, in the year prior and year following.

This population showed a nuanced pathophysiology. Because different organ systems develop at different stages in pregnancy, the time of gestation during which mothers were exposed to famine lead to clear differences in chronic disease risk in the offspring. Offspring of women exposed to the famine in early gestation experienced reductions in clotting factor VII, increased LDL/HDL ratios and a corresponding increase in coronary artery disease and general poor health (24, 25). Offspring from mid gestation famine experienced increases in microalbuminuria and obstructive airway disease (26). Finally, offspring for the late gestation famine were born the smallest and experienced impaired glucose tolerance and insulin resistance in adulthood (27). These findings can be compared to the Siege of Leningrad, where the Russians experienced famine from 1941 to 1944. These offspring did not experience glucose intolerance,

dyslipidemia, or cardiovascular disease in later life (28, 29). There are important differences between these two famines where conclusions can be drawn. First the famine in Leningrad lasted for over 2 years, while the Dutch famine lasted 5-6 months. Furthermore, the years prior and following the Siege of Leningrad resulted in a poor standard of living and food scarcity for the Russians, this was not the case in the Netherlands (27). Ultimately Russian offspring developed in utero to survive a famine, these offspring were then either born into a famine, or a period which still consisted of poor nutrition and living conditions. The infants therefore benefited from adaptations in utero and ultimately lived relatively healthy lives. Because the Dutch famine ended either immediately after or during gestation the offspring which developed in utero to survive a famine instead experienced a relative over nutrition in the perinatal period. This led to rapid catch-up growth in the offspring either in late gestation or in the immediate postnatal period, depending on when the exposure occurred during gestation (27). What followed was a disease of the organ systems in adulthood which corresponded to the organs that were most susceptible to stressors during the period to which the fetus was exposed to malnutrition.

To understand the underlying mechanisms of this phenomena investigators then turned to preclinical research. One major finding was that while fetal life was critical for long term programing effects, the postnatal period and preconceptual period were also important. This led to the renaming from David Barkers "fetal programing" to the more encompassing "Developmental Origins of Health and Disease (DOHaD) Hypothesis" (1). Today, animal, clinical, and epidemiological studies have linked stressors such as macro and micronutrient deficiencies, hypoxia and ischemia, environmental exposures, and physiological stressors with numerous alterations in health such as cardiometabolic dysfunction, cognitive and behavioral defects, reproductive dysfunction, and cancer (1, 30-32). Later life health and disease susceptibility is firmly rooted in early life events.

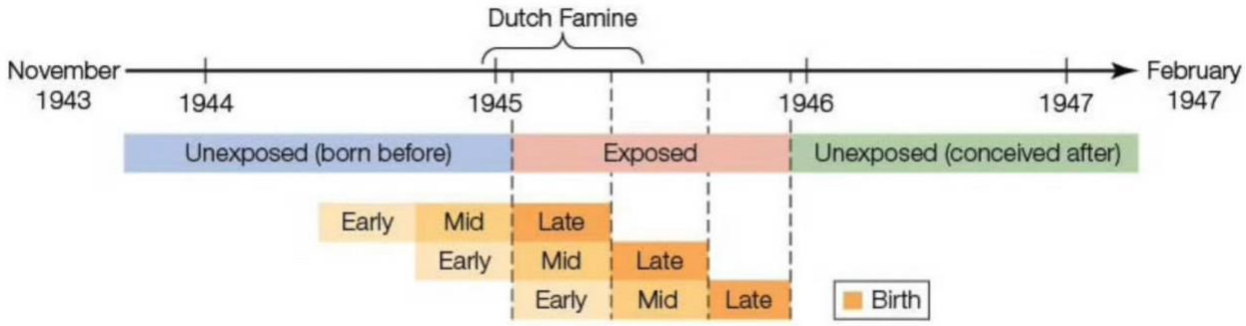

	Exposure to famine						
	Born before	Late gestation	Mid-gestation	Early gestation	Conceived after	All (S.D.)	*n*
Adult characteristics							
Number	264	140	137	87	284		912
Proportion of men	49%	47%	39%	41%	50%	47%	
Plasma glucose 120 min[a] (mmol/L)	5.7	6.3[b]	6.1	6.1	5.9	6.0 (1.4)	702
Plasma insulin 120 min[a] (pmol/L)	160	200[b]	190	207	181	181 (2.4)	694
LDL/HDL cholesterol[a]	2.91	2.82	2.69	3.26[b]	2.94	2.90 (1.53)	704
Fibrinogen (g/L)	3.02	3.05	3.05	3.21	3.10	3.07 (0.6)	725
Factor VII[a] (% of standard)	128	131	133	117[b]	133	129 (1.4)	725
Body mass index (kg/m^2)[a]	26.7	26.7	26.6	28.1	27.2	27.0 (1.2)	741
Coronary heart disease	3.8%	2.5%	0.9%	8.8%[b]	2.6%	3.3%	736
Microalbuminuria (ACR ≥ 2.5)	8%	7%	12%[b]	9%	4%	7%	724
Systolic blood pressure (mmHg)	126.0	127.4	124.8	123.4	125.1	125.5 (15.5)	739
Diastolic blood pressure (mmHg)	86.2	86.4	84.4	84.8	85.2	85.6 (9.9)	739
Obstructive airways disease	15.5%	15.0%	24.8%[b]	23.0%	17.3%	18.1%	733
General health poor	4.5%	6.4%	3.7%	10.3%[b]	5.3%	5.5%	912

Figure 1.1. Developmental Programing and the Dutch Famine from Stearns *Evolutionary Medicine*, 2017 (33)

1.2.2 Classic Features of Developmental Programing

There are several phenotypes which are common in the field of developmental programing. These include alterations in birthweight, catch-up growth, sex-differences, and varying responses based on the timing of insult.

1.2.2.1 Alterations in Birth Weight

Fetal growth represents a U-shaped curve where an exposure to developmental stressors can result in both increases and decreases in bodyweight, what follows is an increased risk of chronic disease.

Small for gestational age (SGA) is defined as <10th percentile at birth, while low birth weight (LWB) is defined as a birth weight of under 2500g (34, 35). Intrauterine growth restriction (IUGR) is currently defined as <10th percentile of predicted weight at any gestational age by ultrasound, which importantly is not due to genetics (36, 37). These changes in size are a commonly found in models of developmental programing, as well as epidemiological studies linking long term dysfunction to stressors in utero. However, an important caveat that must be recognized is that some offspring may be born small while remaining completely healthy (i.e., constitutional smallness, e.g., those born to large or small parents). Alternatively, because IUGR represents a pathological condition by which fetal growth deviates from its generically determined growth potential, IUGR is therefore likely present in babies which do not reach the cut-off's to be considered small. Recall that Barker found a continuous relationship between risk of cardiovascular disease and birth weight, at all birthweights. Therefore, the effects of IUGR can also result in long term programing effects in children which do not present as growth restricted (i.e., whose weights fall within the normal range) (38-40).

There are two main types of IUGR: asymmetric and symmetric. Asymmetric IUGR typically, occurs due to stressors in utero after 23 weeks of gestation. It is diagnosed by ultrasound and presents with a normal

for gestational age head circumference and a small abdominal circumference. The brain and heart are typically normal sized for gestational age, whereas the kidneys and liver are smaller. This is because stressors such as macro or micronutrient deficiencies, placental insufficiency, extremes in maternal BMI or weight gain, impose metabolic challenges on the developing fetus (41). The evolutionary adaptation is for the fetus is to ensure survival, and thus prioritize nutrient and oxygen delivery allowing essential organs (e.g., brain, heart) to remain "spared" at the expense of less critical organs (e.g., kidneys, liver). The resultant impairments in growth and development to these latter organs may predispose the offspring to long term health consequences (42, 43).

This is contrasted by symmetric IUGR which typically occurs in the first 23 weeks of pregnancy and is either due to chromosomal causes or the TORCH congenital infections (toxoplasmosis, rubella, cytomegalovirus, herpes, syphilis) (36). This manifests clinically as a growth restricted baby with a universal reduction in organ size, such that both the head and abdominal circumferences are small for gestational age. As the name implies there is a symmetric reduction in organ size, as opposed to typical "brain sparing" effects.

Regardless of the nature of the growth restriction, low birth weight and IUGR is considered by many to be the most common risk factors for neonatal morbidity and mortality (44). However, it is easy to speculate that this may in part be due to the ubiquity of prenatal ultrasounds allowing for fetal size, alongside birth weight, to be commonly documented. Other more sensitive predicators of fetal injury (e.g., amniocentesis) are not likely to be used at a large scale. Further, IUGR appears to be an important predictor of long-term programing effects in almost every organ system (36, 45-47).

Unfortunately, IUGR is incredibly common. A recent Lancet paper estimates 20.5 million infants are born growth restricted globally every year, making up about 15 percent of all births (41). There are several etiology's of IUGR, which can broadly be categorized as fetal (e.g., structural or genetic abnormalities),

placental (e.g., ischemic placental disease), and maternal factors (e.g., hypertension, cyanotic heart disease, medications). When a cause can be identified one-third of IUGR is found to be due to a genetic disease, whereas two-thirds is related to changes in fetal environment; however, in 40% of infants with an identified IUGR no underlying etiology is found.

Treating a newly born growth restricted infant comes with its own set of challenges. For example, infant weight is the main criterion for NICU/ hospital discharge. Normal growth trajectories may then be challenging to maintain as parents (as well as some healthcare providers) may be motivated to quickly increase neonatal bodyweight (48, 49). Rapid catch-up growth is dangerous for the newborn as it may further exacerbate harmful programing effects, which will be described in the following section.

Large for gestational age offspring also are important to identify, not only to ensure a safe delivery, but also because these offspring may experience altered developmental trajectories. Macrosomia is defined as a birth weight in a full-term infant of over 4000 grams or higher than 90th percentile bodyweight at any gestational age (50). Much like low birth weight it is important to note that some babies will reach this cut off due to genetic factors. However other factors such as gestational or pregestational diabetes, hypertriglyceridemia, obesity, excessive gestational weight gain, and even alcohol use can drive macrosomia (51-57). Furthermore, a study by Little *et al.* found that over 60% of babies born with macrosomia come from mothers with no identifiable risk factors (58). Much like IUGR and low birth weight, macrosomia is associated with several long-term consequences, these include a predisposition to obesity, diabetes, and cardiovascular disease (59, 60).

1.2.2.2 Catch Up Growth

In many cases the mechanism for long term programing in small for gestational age offspring stems from the previously mentioned idea that fetal survival in utero is prioritized at the expense of development. These adaptations result in decreased kidney growth (predisposing the offspring to cardiovascular

disease) as well as decreased liver and pancreatic growth, decreased insulin secretion and increased glucose uptake in peripheral tissues (61).

The thrifty phenotype hypothesis poises that if an offspring is then instead born into a more bountiful postnatal environment, further programing effects may occur (62, 63). At a minimum in the context of macronutrient deficiencies, catch up growth then reflects a relative overfeeding which these infants' metabolisms did not develop for. Catch up growth is loosely defined as either height velocity or weight gain above the statistical limits of normal (however the exact cut-offs are debated) (64) (65). There are likely several molecular mechanisms involved in mediating catch up growth and disease, some of which are still unclear. Regardless, the evidence that postnatal growth patterns are important for long term effects are apparent. Children with catch up growth show abnormalities at school age including precocious puberty, excess adiposity, insulin resistance, as well as low grade inflammation (66-69). Furthermore, children born small for gestational age and experienced subsequent catch-up growth are predisposed for cardiovascular disease, increased adiposity, and insulin resistance as adults (70, 71). IUGR offspring who are maintained on nutrient restricted diets however, had improvements in these long-term outcomes (72). There is evidence in animal models that catch up growth can be characterized by a proportionally larger increase in bodyfat than lean tissue gain, as well as a hyperinsulinemia signaled by adipose tissue (73-75). Ultimately these changes result in an increase in adipocytes in adulthood, which constitute maladaptive changes (75). Unfortunately, this is further complicated by potential contrasting beneficial effects of catchup growth regarding neurodevelopment. Some studies for example have suggested that in preterm infants, poor early growth may result in adverse neurodevelopmental outcomes. These studies typically recommend enhanced nutritional intake to promote rapid growth and brain development, all while recognizing the increased risk of long-term cardiometabolic syndromes (76, 77). Therefore, to manage long term consequences, an important strategy may involve balancing catch up growth for necessary skeletal and brain development, against excess growth which may lead to increased adiposity and eventual cardiometabolic syndromes (72).

1.2.2.3 Sex Differences

When referring to sex specific differences in this thesis we are referring to biological sex. Gender is a sociocultural construct that falls beyond the scope of this thesis as most research discussed utilizes animal models or newborns. A common theme in DOHAD is that biological sexes exhibit differences in developmental outcomes. In fact, it is far more common that male and female offspring respond differently than the same. In normal pregnancies female fetuses grow faster than males initially, but ultimately are born slightly lighter and smaller (78). However, while one would think females may then be more susceptible to subsequent catch-up growth, this does not appear to be the case in practice. Broadly speaking male offspring appear to develop more severe cardiometabolic dysfunction in the context of the DOHAD (79-81), though this is not always the case (82, 83).

At this point there is no singular clear mechanism to explain why developmental programing effects often present in a sex specific manner however, some hypothesize genetic, epigenetic, and hormonal causes, with the latter appearing to be the most important based on current literature. The presence of estrogen is higher in females than males in utero (84). In adults, testosterone is well known to exacerbate cardiovascular disease, while estrogen is generally considered to be cardioprotective; this is one of the reasons men experience cardiac events on average 10 years earlier than females (85).

When adult women reach menopause, many will look to hormone replacement therapy to control menopausal symptoms, as well as potentially prevent cardiovascular events. Unfortunately, hormone replacement therapy does not protect post-menopausal women from adverse cardiac events or reduce mortality (86), indicating there is more complex physiology at play. For example, in early development estrogen controls genes involved in antioxidant production, cellular survival, and mitochondrial function (87-89). This may be why even in adulthood females appear less susceptible to oxidative stress (90). However, despite this data the specific roles of testosterone and estrogen on the long-term programing

effects of developmental stressors are not clear. Understanding the mechanisms by which sex dependent programing effects occur could represent a critical step to better understand developmental programing, and eventually develop therapies. This emphasizes the necessity to study both sexes.

1.2.2.4 Timing of Insult

As previously mentioned, the same stress at a different period in development will lead to different programing effects. This is because different cell types (in early gestation) and different organ types (in late gestation) have periods where growth and development are incredibly plastic and sensitive, but also periods where development is not as critical. Therefore, stress in these critical periods could dramatically alter development, leaving lasting effects which could not be recovered from.

The previously mentioned "Dutch hunger winter" serves as a clear example, however this is of course not unique to famines. Toxic exposures (e.g., alcohol) during the embryonic period will produce severe and lasting effects across several different biology systems, even resulting in fetal loss. The same exposure later in development will typically result in a more moderate effect, typically constrained to less organ systems (91). Broadly speaking, the higher developmental plasticity earlier in life will correspond to a resulting increased susceptibility to insults. This highlights the importance of preventing diseases before they occur particularly during development when an individual may be more susceptible. For example, the Pathobiological Determinants of Atherosclerosis in Youth (PDAY) study suggests that lifestyle modifications such as healthy diet, physical activity, and an avoidance of smoking before the age of 15 could prevent 90% of myocardial infarctions in adulthood (92, 93). It is therefore important to focus on the health of the in the first and second decade of life, to ultimately prevent chronic disease in adulthood. Furthermore, the advancement of biomarkers and imaging modalities to detect pathophysiology earlier, may hopefully guide interventions prior to the progression of disease in the coming years.

1.2.3 Overview of Cardiovascular Development

The cardiovascular system is the first system to develop during organogenesis (94). In a healthy pregnancy, the following events occur as summarized from Leonard Lilly's textbook: Pathophysiology of Heart Disease (95). By gestational week 4, the heart has established four chambers and passive oxygen diffusion becomes insufficient to support the growth of the embryo alone (96, 97). Consequentially the fetal heart begins beating at gestational day 22 and at gestational day 28 fetal circulation is established (96, 97). After six weeks the cardiac outflow track splits from a single truncus arteriosus into the ascending aorta and pulmonary artery; this occurs through the spiraling of the aorticopulmonary septum. This spiraling causes the anatomical wrapping of the aorta and pulmonary artery as they leave the heart. At the same time, the heart and lungs descend into the thorax of the fetus. As a fun aside, this is what causes the left recurrent laryngeal nerve to be "pulled" down the neck, under the aortic arch, until it returns back to the larynx. By week 10 the fetus has grown too large for gas exchange to occur through diffusion, from this point forward the fetus relies completely on the placenta to connect to the mother's circulatory system (97). For the remainder of pregnancy, the heart continues to grow through cardiac hyperplasia, ultimately there are no other major changes in development and function until the heart is forced to transition from fetal to post-uterine life (98).

Despite low partial pressure of oxygen within the placenta, oxygen is adequately delivered to fetal tissues due a number of adaptations unique to in-utero life. First, fetal hemoglobin has a higher oxygen affinity than maternal and adult hemoglobin which allows for oxygen to easily transfer from maternal circulation to fetal circulation at the placental interface (97). Secondly, because the placenta allows for pulmonary circulation to be bypassed almost entirely, both the left and right ventricle may work to perfuse systemic circulation (99). Minimal pulmonary circulation (between 10 and 25 percent of that of a neonate) allows for the total workload of the fetal heart to be lower than that of the neonatal heart, all while fetal tissue perfusion is over double when compared to a neonate (100). This is further bolstered by the left ventricle carrying and delivering blood at a higher oxygen concentration than the right ventricle, which allows for a

higher oxygen concentration to be delivered to the heart muscles and brain compared to other organs (95). Finally, the fetal heart primarily uses carbohydrates as metabolic substrate and relies on glycolytic metabolism at a higher percentage, allowing the heart to work at a higher oxygen efficiently (101). Collectively these adaptations allow for rapid growth and development of the fetus, despite the lower oxygen environment of in utero life.

In the neonatal period the heart gradually progresses from a glycolytic state which relies on carbohydrates to almost entirely oxidative metabolism which (at least in healthy hearts) primarily relies on fatty acid oxidation. However it is worth noting that unlike the developing heart the mature heart can use a number of different energy sources. Mechanically as the neonatal heart develops it becomes more compliant and more efficient, both on a work per energy basis and a work per mass basis, this can be attributed to improvements in cardiomyocyte architecture as well as the previously mentioned changes in energy metabolism.

1.2.4 Developmental Programing of Cardiovascular Dysfunction

Although the underlying drivers of developmental programing were not examined in detail within this thesis, I would be remiss if I did not briefly speak about some of the mechanisms involved in the programing of cardiovascular disease. Here we first discus some classic "upstream" mechanisms (namely epigenetics, reactive oxygen species generation, and hypoxia) and how the downstream kidneys and heart are affected.

1.2.4.1 Epigenetic Modifications

It is likely that epigenetics is the first mechanism that comes to mind when discussing developmental programing; epigenetics has reached a point where they are almost used interchangeably with developmental programing outside of the field. Broadly, the concept can be drawn from the root of the word "epi" which is the Greek word for "over" or "above". Epigenetics therefore defines a process by

which gene expression can be modified "above the genome" without changing the underlying genome. There are several mechanisms by which this process occurs including post transcriptional modification by non-coding RNA, DNA methylation, as well as histone modification. The details of epigenetic modifications fall beyond the breadth of this thesis, however there are two broad takeaways which I believe to be important. First, epigenetic changes can occur rapidly. If these changes occur during critical periods of development, even if these periods are brief, they can cause lasting developmental consequences (102, 103). In the examples cited, it took under a week of perinatal hypoxia to drive DNA methylation, which led to long term changes in glucocorticoid receptor gene and protein expression potentially leading to lasting cardiovascular consequences (104). A second critical takeaway is that many other developmental stressors lead to epigenetic modifications including hypoxia (105, 106), reactive oxygen species generation (107), and undernutrition (108). Epigenetic modification could prove a common mechanism by which different stressors in pregnancy result in similar lasting cardiovascular outcomes, and therefore may become an important factor when guiding therapeutics.

The fetal heart may be particularly influenced by epigenetic modifications. Both DNA methylation and histone modification have been shown to regulate cardiomyocyte growth and development, in both the fetal and early neonatal environment (109, 110). Adult cardiomyocytes have a unique feature as non-dividing cells, which leaves them particularly vulnerable to perinatal environmental stressors. Epigenetic modifications of cardiomyocytes may represent a potential mechanism which leaves offspring at a higher risk of heart disease in the future.

1.2.4.2 Reactive Oxygen Species Generation

Reactive oxygen species (ROS) are products of oxidative respiration, which in appropriate amounts are important for cellular signaling but in excess can cause damage to biomolecules resulting in oxidative stress (111). In utero the amount of oxygen the fetus is exposed to is very low, so low that antioxidant systems do not develop until late gestation in preparation for the shift to the more oxygen available ex

utero life (112). Therefore, for the majority of pregnancy the fetus is vulnerable to oxidative stress because of the lack of antioxidant defense. Unfortunately, this lack of antioxidant defense has linked excess ROS to consequences during pregnancy such as IUGR, pregnancy loss, preeclampsia, and preterm rupture of membranes. Furthermore, in offspring ROS during pregnancy can program diseases such as bronchopulmonary dysplasia, respiratory distress, and necrotizing enterocolitis (113, 114).

Excess ROS generation can cause cellular damage as well as abnormal growth and development in utero, which can lead to a number of long-term cardiovascular consequences. Animal models of maternal nutritional imbalance, maternal illness, pregnancy complications, as well as exposure to medication or chemicals in utero have been shown to program cardiovascular disease; with many of these indicating the generation of excess ROS as a potential mechanism (115). This is further supported by the use of antioxidant therapies in pregnancy complications or models of pregnancy complications. In some cases, antioxidants appear to be protective, indicating a reduction of ROS in pathological pregnancies may be beneficial (116, 117). In other cases, antioxidants appear to be deleterious, suggesting some ROS generation is likely important for growth and development (118). Regardless it is clear that oxidative stress has some degree of involvement in cardiovascular programing.

1.2.4.3 Hypoxia

Lower than normal oxygen levels in pregnancy activate a variety of physiological responses, typically through the protein hypoxia inducible factor 1 and 2 which controls oxygen consumption and transport, growth and development, and the promotion of anaerobic metabolism (119). Therefore, hypoxia plays a major role in fetal development including placentation, angiogenesis as well as programing of numerous organ systems both directly and through epigenetic mechanisms (120, 121). Hypoxia causes an increase in apoptosis of cardiomyocytes, as well as an increase in collagen deposition in fetal and neonatal hearts (122). In the kidney offspring exposed to prenatal hypoxia in utero typically experience renal dysfunction and hypertension in adulthood (123, 124). Hypoxia is therefore clearly linked to long term cardiovascular

dysfunction; however, the exact mechanisms still remain to be determined (125). While models of prenatal hypoxia do not perfectly mimic real world senecios, intrauterine hypoxia is a common event. Emotional stress, nicotine, obesity, nutritional deficiencies, and even air pollution all cause intrauterine hypoxia to some degree (126, 127). Hypoxia is therefore a leading cause of fetal death and an important mechanism of cardiovascular programing (128, 129).

1.2.4.4 Kidney Programming

The nephron is the functional unit of the kidney, and much like cardiomyocytes of the heart, the total number of nephrons is determined before birth in humans (or shortly after birth in the case of rats). Many animal models of developmental programing have shown a reduction in nephron endowment in the offspring (130). Furthermore, a correlation has been made between total number of nephrons and birth weight, which continued across all sizes (131). The kidney initially maintains blood pressure and electrolyte balance, even if the total number of nephrons are reduced. However, this causes a hyperfiltration of the existing nephrons (132). Overtime this hyperfiltration can reduce the kidney's functional capacity, and either independently or when combined with a secondary stressor (e.g., high salt diet, obesity) the demand on the remaining nephrons can ultimately lead to kidney injury or hypertension (133-135). It is therefore not surprising that kidney size at birth, which correlates to total number of nephrons, has been identified as a risk factor for chronic kidney disease as well as hypertension in adulthood (133). This is particularly important in the context of fetal programing because, as previously mentioned, the kidney falls as a lower priority and therefore receives less blood flow in growth restricted fetuses to "spare" the brain and heart (136). This leaves the kidney particularly vulnerable in models of developmental adversity.

Maternal iron deficiency is no exception. Our group has previously shown a reduction in nephron endowment in our iron deficient offspring (137). As well as long term developmental effects including salt sensitivity, hypertension, altered renal function, and vascular dysfunction (138-140).

1.2.4.5 Heart Programing

Many stressors which cause developmental programing of the cardiovascular system, also acutely cause congenital heart defects (e.g., folate deficiency). While this helps identify potential insults many of these congenital defects may also lead to fetal demise (141). One may suspect that more subtle long term cardiac programing effects, without a resultant lethality are more common.

Maternal hypoxia exposure is likely the most common model to study the long-term consequences of developmental programing of the heart. The offspring of mothers exposed to maternal hypoxia have larger hearts and an increased collagen deposition in adulthood (142). Ultimately this leaves the offspring's hearts less resilient when exposed to ischemia reperfusion as well as exercise (143, 144). While the mechanism of this programing is still unclear, we do know hypoxia reduces cardiomyocyte proliferation (145), and increases apoptosis (146). This is critical because cardiomyocyte proliferation ends shortly after birth, forcing the heart to rely on hypertrophy for subsequent growth (147). While there is no definitive evidence that there are long-term consequences associated with reducing cardiomyocyte number, the potential for a greater absolute percentage of heart cells to die in any one ischemic insult could affect the heart's ability to recover from said injury. Furthermore, other histological changes to the heart, such as increased collagen deposition, could affect ventricular relaxation (148, 149). Finally, maternal hypoxia exposure has been linked to alterations in metabolism potentially increasing susceptibility to ischemic injury (143).

No human studies have shown lasting functional changes in hearts of offspring exposed to stressors in utero, however conclusions may be drawn from the hearts of pediatric IUGR offspring. These offspring reveal major cardiac changes in fetal life which persist into the postnatal period. This includes morphological changes such as: smaller and more spherical hearts, and a thicker ventricular septum (which could affect cardiac outflow in adulthood) (150). Functional changes include an inability to increase cardiac output and stroke volume as well as reduce heart rate in their first week following birth.

Furthermore, these children exhibit an increased myocardial performance index which indicates global ventricular dysfunction, diastolic dysfunction (i.e., impaired filling of the left ventricle); as well as vascular changes including increased mean arterial blood pressure, increased arterial wall thickness, vascular stiffness, and input impedance (150-152). Following autopsy, histology has shown IUGR fetuses with previous impaired cardiac function demonstrated significantly shorter sarcomere length which may help to explain some of the cardiac dysfunction described (153).

1.3 Aging and the Cardiovascular System

Aging is a complicated physiological process which is associated with several functional and cellular changes that result in the overall decline of organ systems. Aging has a dramatic effect on the body's cardiovascular system, with 86 percentage of the population over the age of 80 having some form of cardiovascular disease (154). In fact, age is the best predictor of an individual's cardiovascular health (155). Even in otherwise healthy individuals, aging causes morphological alterations including hypertrophy, stiffening of the heart and vessels, as well as a decrease in physiological reserve of the heart (156, 157). To make matters worse, the aging heart and vasculature antagonize each other to further progress physiological decline in each system.

Blood pressure generally increases with age, by the time an individual reaches 80 years old the incident of hypertension is almost 74%. This is important because uncontrolled hypertension can lead to complications in almost every organ system eventually resulting in death. Furthermore, in those with elevated blood pressure who are not yet hypertensive, the risk of a cardiovascular event is still substantial. The SPRINT trial showed that among patients at high risk for cardiovascular events, targeting a systolic pressure of less than 120 mmHg when compared to targeting pressures less than 140 mmHg resulted in lower rates of both fatal and non-fatal cardiovascular events (158).

Increases in blood pressure are in part due to arterial thickening, increased collagen deposition, as well as fibrosis. Ultimately, these changes raise the body's systemic vascular resistance and therefore blood pressure. These alterations increase the risk of atherosclerosis and atrial fibrillation (157). Furthermore, these vascular changes result in arteries losing their vascular compliance, and therefore being unable to buffer the high systolic blood pressure from the heart nor provide elastic recoil to continue to perfuse organs during ventricular diastole. This reduction in vascular compliance presents as a widened pulse pressure and an increased pulse wave velocity and can affect the heart in multiple ways.

First, a lack of vascular compliance needed to buffer high systolic pressures mean instead the heart will be required to resist backflow at end systole, this is a force which in ideal circumstances is primarily absorbed by the vessels. Secondly, this lack of compliance requires an increase in blood pressure to maintain perfusion of the organs during diastole. Collectively these changes increase internal pressure as well as the corresponding wall tension within the heart. To compensate the heart undergoes fibrosis as well as a concentric hypertrophy to offset this wall tension, as described by Laplace's law (159). Initially, these hypertrophic changes do successfully augment cardiac output in response to hypertension, however in the long term these changes are maladaptive and contribute to heart failure (95).

However, even in those adults who do not become hypertensive, cardiac function still declines with age due to a reduction in both heart rate and ventricular contractility (157). The heart attempts to compensate through increased atrial contraction to maintain ventricular filling and therefore sufficient output (160), as well as the same hypertrophic changes described previously. While these changes are effective in the short term, again they ultimately result in a further decrease in cardiac output (161). This is complicated by a resulting increase in ventricular mass as these hypertrophic changes increase myocardial oxygen demand. Furthermore, oxygen delivery to the myocardium is compromised by both a reduction in cardiac output, and a stiffening of the ventricles leading to elevated diastolic pressures which limits coronary artery perfusion. Collectively, increases in oxygen requirement and decreases in oxygen delivery and

perfusion put the heart at an increased risk of myocardial ischemia even in the absence of coronary artery disease (156, 157).

There are also cellular changes which drive aging of the heart. Despite an increase ventricular mass, an overall decrease in total cardiomyocytes due to either apoptosis or necrosis can be seen (162). Approximately one third of all cardiomyocytes are lost between the ages of 17 and 90, resulting in a reduced exercise capacity and decreased ability to respond to stressors (163). These losses are in part due to a reduction in cardiomyocyte resistance to the oxidative stress that occurs alongside aging (164). This is combined with an overall increase in oxidative stress due to the increased reactive oxygen species production associated with aging, which culminates in an increased incident of cardiomyocyte loss (165, 166). In addition, in those cardiomyocytes which necrose, the release of cellular components promotes a proinflammatory environment which affects neighboring cardiomyocytes (167, 168). This inflammatory response likely facilitates further injury, as well as promotes harmful remodeling leading to heart failure (169-171). Therefore, therapies which promote antioxidant and anti-inflammatory properties may provide a potential target to modulate the deleterious cardiovascular changes associated with aging. While the absolute number of cardiomyocytes decreases with age, the remaining cardiomyocytes hypertrophy (172). In addition, collagen content increases with age in the human heart, driven by several distinct pathways including ROS generation, chemokine recruitment of mononuclear cells and fibroblast progenitors, transforming growth factor-β activation, as well as angiotensin signaling (173). Autopsy studies show an almost 50% increase in collagen content between the third and seventh decade of life (172). Fibrotic tissue can then interfere with conduction which ultimately reduces heart rate and pacemaker function (174-178). Furthermore, the absolute number of pacemaker cells as well as control of the pacemaker, each decrease as an individual ages (179-181).

Vascular dysfunction due to aging can lead to several unique pathologies. Aging may cause excessive growth (i.e., neovascularization) which leads to injuries such as macular degeneration as well as

insufficient growth, which can cause hypertension or reduce tissue perfusion. The structural changes to vessels include an increased luminal diameter, wall thickening, as well as changes in endothelial function. As endothelial barriers become more porous with age, vascular smooth muscle can deposit matrix proteins in endothelial spaces resulting in a thickening of the intima. Furthermore, age causes the endothelium to lose its ability to proliferate following tissue injury, which combined with insufficient perfusion can impair wound healing (182).

Molecularly, as endothelial cells age, they exhibit a reduction in nitric oxide production (through endothelial nitric oxide synthase), a molecule which is essential for regulating vascular tone and therefore total peripheral resistance and blood pressure (183). Outside of vasodilation, nitric oxide is important for inhibiting cellular senescence, thrombotic events, irregular cellular proliferation, and vascular inflammation (184). Furthermore, as heart function declines and individuals become more sedentary, vasculature is therefore exposed to less hemodynamic stress. While this may sound beneficial, a certain amount of shear stress due to blood flow is important as it acts as a major contributor to endothelial nitric oxide synthase activity (183). Multiple factors therefore contribute to the decrease in nitric oxide levels, resulting in a decline in physiological function and exercise performance (185).

Fortunately, ultrasound allows for the elastic properties of arteries as well as cardiac function to be measured noninvasively. This allows for changes in cardiovascular function associated with aging to be measured serially in humans. Furthermore, animal models poise as a solution for mechanistic studies, as well as the ability to trial new supplements which may improve cardiovascular health.

1.4 Iron Status and Metabolism

1.4.1 Iron Metabolism, Transport, and Storage

Iron is a trace element essential to numerous biological processes including oxygen transport, redox reactions, DNA synthesis, and energy metabolism (186). Iron's high reduction-oxidation potential

represents a double-edged sword. This feature makes iron useful for cellular functions but makes unbound iron toxic for cells through the creation of excess reactive oxygen species (ROS). Iron homeostasis is therefore a highly regulated process.

One important factor of iron regulation is that the body's total iron stores are exclusively regulated by uptake from the gastrointestinal system, specifically the duodenum and proximal jejunum (187). In healthy individuals, 1-3 mg of iron is absorbed through the gastrointestinal system per day, compensating for losses due to sloughing of enterocytes and skin, as well as menstruation (188). Interestingly there are no excretory mechanisms to handle excess iron, which is why the main treatment for individuals with hemochromatosis (a disease associated with increased gastrointestinal iron absorption) is simply phlebotomy to physically remove excess iron, in the form of red blood cells, from the body.

Iron is absorbed with a lower efficiency than most other nutrients (189). Dietary iron is found in two forms, heme and non-heme iron. Heme iron (found in animal meat) is absorbed at a rate of about 25%, this is contrasted by non heme iron (found in plants and iron supplements) which is absorbed at a rate of about 10% (190). This is because iron can only be absorbed in its Fe2+ state, and non heme iron must then be converted from Fe3+ to Fe2+ by a ferric reductase enzyme, duodenal cytochrome B (Dcytb) on the brush border of enterocytes prior to passing through divalent metal transporter (DMT1) and entering the cell. Fe2+ is a divalent metal and is toxic due to its potential to react with components of the cell such as oxygen, to form ROS. As previously mentioned, ROS can cause damage to cellular membranes and organelles. Therefore, instead of flowing freely through the body or cells, iron must be bound to proteins, namely iron is stored in ferritin or transported in transferrin.

Once iron enters the enterocyte it is bound to ferritin. Some iron may then be stored within the enterocyte; however, most is transported through the basolateral membrane via ferroportin where it is then bound to transferrin to be transferred to target cells and taken up by transferrin receptors (186, 191). In fact,

ferroprotein is the only efflux route of cellular iron in the body. Ultimately the majority of iron is contained within hemoglobin as red blood cells (~2 g), with other storage sites including the liver (~ 1 g), macrophages (~600 mg), and myoglobin (~300 mg) (192).

Within the body, mobilization and storage of iron is mostly controlled by hepcidin, a peptide hormone (193, 194). As the name implies hepcidin is mostly synthesized in the liver by hepatocytes, however it can also be produced by the kidneys and heart (195). Hepcidin regulates iron uptake by binding to ferroportin resulting in lysosomal degradation, causing an overall decrease in iron absorbed by the GI system and decrease in iron taken up within the cells (195). A number of factors influence hepcidin expression, it is up-regulated (causing a decrease in iron stores) by inflammation, infection, and increased levels of circulating iron (196). Presumably hepcidin induction during infection and inflammation was evolved to help sequester iron from pathogenic microorganisms (which also rely on iron for the same cellular processes!) (197). Hepcidin levels decrease in situations where either an increase in RBC would be advantageous, such as hypoxia, anemia, and pregnancy; or when erythropoiesis is accelerated (e.g., in the setting of blood loss or exogenous erythropoietin) (191, 198).

1.4.2 Iron Deficiency and Anemia

Iron deficiency (ID) is the most common nutritional deficiency worldwide. The total burden of ID is challenging to estimate because it is not commonly screened for and definitions of ID vary, however over 2 billion people are anemic (199). ID is the chief cause of anemia, with up to 50% of all anemia cases being attributed to ID (193, 200). Because a greater subset of individuals are ID but have not yet reached anemia cut-offs, the incidence of ID is thought to be between 2 and 4 billion worldwide (199).

There are various mechanisms of ID which can be broadly categorized into issues with absorption (e.g., celiac disease, inflammatory bowel disease, medications such as proton pump inhibitors, parasites), reduced iron intake, blood loss (e.g., gastrointestinal bleed, menstruation), increased demands (e.g.,

growth, pregnancy), or an issue with organ systems (e.g., chronic kidney disease, heart failure) (201). Unfortunately, in the context of the Developmental Origins of Health and Disease, women of childbearing age as well as young children are some of the most susceptible populations to ID (202, 203). This is likely due to reduced liver size and increased losses due to menstruation, which ultimately cause diminished baseline iron stores (203). If a negative balance of iron persists and iron stores continue to deplete, then the following sequalae occurs. First, tissue iron stores are depleted in the liver and bone, which is reflected by a decrease in ferritin but perhaps not transferrin. This can be classified as iron deficient not anemic. After iron stores are eliminated, the body can no longer prioritize tissue oxygenation and a reduction in hemoglobin which is characterized by smaller than normal red blood cells will result (i.e., a macrocytic anemia) (193).

1.4.3 Diagnosis of Iron Deficiency and Iron Deficiency Anemia

Anemia is defined as a reduction in circulating hemoglobin or hematocrit levels below a set threshold which varies across different populations. Currently in men this is classified as a hemoglobin <13.6 g/dL or hematocrit <40 percent. In females the numbers are slightly lower at a hemoglobin <11.9 g/dL or hematocrit <35 percent. In pregnancy the diagnosis of anemia again falls lower with women not requiring an evaluation above 11 g/dL in the first trimester and 10.5 g/dL in the second and third trimester. Finally in children the lower limit of normal hemoglobin is between 11 and 11.2 g/dL or hematocrit between 31 and 35 percent. One important caveat is in scenarios with acute blood loss (such as a severe GI bleed), a patient may lose a significant amount of blood volume, however since the blood volume deficit is yet to be replaced, the hemoglobin or hematocrit will remain normal until fluid from either the extravascular space or fluid resuscitation enters the vasculature.

Clinically, patients with anemia present with signs and symptoms related to a reduction in oxygen carrying capacity. This may include fatigue, exercise intolerance, weakness, pallor, restless leg syndrome, dyspnea, headaches, as well as eating or craving things that are not food (also known as pica) in the case

of iron deficiency. However, because tissue level iron is responsible for several cellular processes, other symptoms typically associated with ID anemia (e.g., weakness, fatigue, difficulty concentrating, restless leg syndrome) can be present in ID but not anemic patients (204, 205). Furthermore, these symptoms persist after resolution of anemia, but before iron stores are adequately replenished (206). Upon physical examination of an ID anemic patient, one might observe pallor, brittle skin, fingernail changes such as koilonychia, and a loss of tongue papillae. The primary investigation for ID anemia is a complete blood count (CBC). The following abnormalities may be observed: low hemoglobin and hematocrit, low reticulocyte count, and low mean corpuscular volume (i.e., a small red blood cell) in severe anemias. In many cases, a CBC and history of potential blood loss or poor intake is enough to suspect ID anemia. Depending on resources a clinician could then either trial iron supplementation, search for the source of blood loss, or pursue further tests.

Further tests would first include a serum ferritin and then transferrin saturation (TSAT). If ferritin levels are low, no further investigation is needed and the patient can be diagnosed with iron deficiency, even with a normal CBC. However, a normal, or even high ferritin does not eliminate the possibility someone is iron deficient. This is because ferritin acts as an acute phase reactant and is released from cells during inflammation and infection (207). High ferritin concentrations could therefore either indicate either iron overload, or a shift of iron into reticuloendothelial cells in response to inflammation (208). Several factors linked to inflammation such as obesity, infection, and liver disease can raise an individual's ferritin, even if iron stores are low. While the cut-offs for ferritin are higher for individuals with these conditions (<41 ng/mL instead of <30 ng/mL), further tests are required. It is worth noting that a mathematical correction of ferritin concentration for the degree of inflammation has been proposed, however at this point it has not been implemented (208). If ferritin is high but ID is still suspected the transferrin saturation (TSAT) can be assessed, this is a ratio calculated using serum iron and total iron binding capacity (TSAT = serum iron/TIBC). While optimal thresholds have not been established most guidelines consider a TSAT <20 percent to confirm a diagnosis with a TSAT <10 percent to confirm a diagnosis with a high degree of

confidence. Finally, if TSAT is normal, other causes of anemia such as anemia of inflammation should be considered, or more specialized testing for iron deficiency such as a bone marrow biopsy stain for iron should be pursued if suspicion is high.

1.4.4 Iron Deficiency in Pregnancy

As previously mentioned, pregnant women and young children are both particularly susceptible to iron deficiency. In children this is due to their rapid growth, and in pregnant women this is due to blood volume expansion and the demands of the fetal-placental unit (209). The incidence of ID during pregnancy are not clearly reported, however approximately 38% of women worldwide become anemic during pregnancy, including 22% in developed countries (210). Furthermore, the proportion of anemia during pregnancy which was amenable to ID is even higher than non-pregnant populations, making up over 50% of all cases of anemia during pregnancy (211). Just like anemia in other populations, there is likely a larger group of pregnant women which are ID but not anemic.

There is also a physiological rationale that the developing fetus is more affected by ID. Because iron is required within the mitochondria and in cellular energy producing pathways, ID predominantly effects cells with the largest metabolic rates (212). The energy demands of a developing organism are much higher on a per weight bases, due to growth and cellular differentiation. A neonate requires three to four times the total body oxygen consumption of an adult; a fetus, even in the low oxygen environment of the womb still requires double the oxygen of an adult (212, 213). The increased in energy requirements associated with development may explain why the consequences of ID are more dramatic in the perinatal period. Because of the increased incidence of ID during pregnancy, as well as the large iron dependent energy demands of the fetus, ID represents an important field of study during pregnancy.

There are several impacts of ID on pregnancy outcomes. First, numerous studies have linked maternal ID with preterm birth, as well as being born small for gestational age or at a low birth weight (214-217). In

the worst cases, ID during pregnancy can lead to maternal and fetal demise (218, 219). Furthermore, there are clear correlations between growth & development and the severity of fetal iron deficiency; therefore, it is likely that iron directly affects fetal growth and development (220, 221). This could be due to several factors, including placental and fetal adaptations. The placenta's response to ID is reviewed wonderfully by Roberts *et al.* (222). In mild ID, studies show that the placenta can maintain the delivery of iron to the fetus. However, as ID becomes more severe the placental function begins to decline presenting with infarctions and necrosis. Therefore, much like other forms of intrauterine growth restriction (IUGR), alterations in the placenta can affect growth and development of the downstream fetus. Even in cases where placental function is maintained, hypoxia, which we have shown to be caused by maternal ID, may cause the classic "brain-sparing" effects previously described (223). This would result in a prioritization of blood flow to the brain and heart at the expense of organs which are less critical in the short term such as the liver, something our group has shown occurs in ID fetuses (224). Ultimately, ID induced hypoxia and growth restriction has been linked to numerous long-term cardiovascular, metabolic, neurobehavioral, and immunological effects in the offspring (225). Further, in offspring who are born healthy but with low iron stores, they must then develop without adequate iron stores in infancy and childhood. This is challenging as there is minimal iron in breast milk, and in many cases iron fortified foods may not be available (226, 227). In fact, postnatal iron status at up to 9 months of age are largely dependent on fetal iron loading (228).

1.4.5 Iron Intake

In men and postmenopausal women, the recommended daily iron intake by the U.S. Food and Drug Administration is 8 mg per day, in premenopausal women this number doubles at 18 mg per day (229). Unfortunately, most women report an intake of about 12 mg per day, meaning prior to pregnancy many women are already predisposed to ID (229). During pregnancy, a women’s daily iron requirement increases by about 1 mg per day in the first trimester, however by the third trimester this climbs as high as 8 mg per day (230). If intake guidelines are met, one gram of iron will be absorbed by the mother during

the course of pregnancy. Of this increased amount, ~360 mg is transferred to the fetoplacental unit, ~450 mg is used to make additional red blood cells for the mother, and ~230 mg is lost due to normal physiological processes (231, 232). An increase in iron intake must happen gradually, however. While there are some adaptations to improve iron absorption late in pregnancy, absorption of dietary iron is unlikely to ever be enough to compensate for ID if the mother begins their pregnancy with low iron stores (233). Ideally iron status would be assessed prior to pregnancy so that an individual who wished to be pregnant would have time to increase their iron stores. However, screening for ID is likely not feasible on a global scale, particularly while so many pregnancies go unplanned (218, 234, 235).

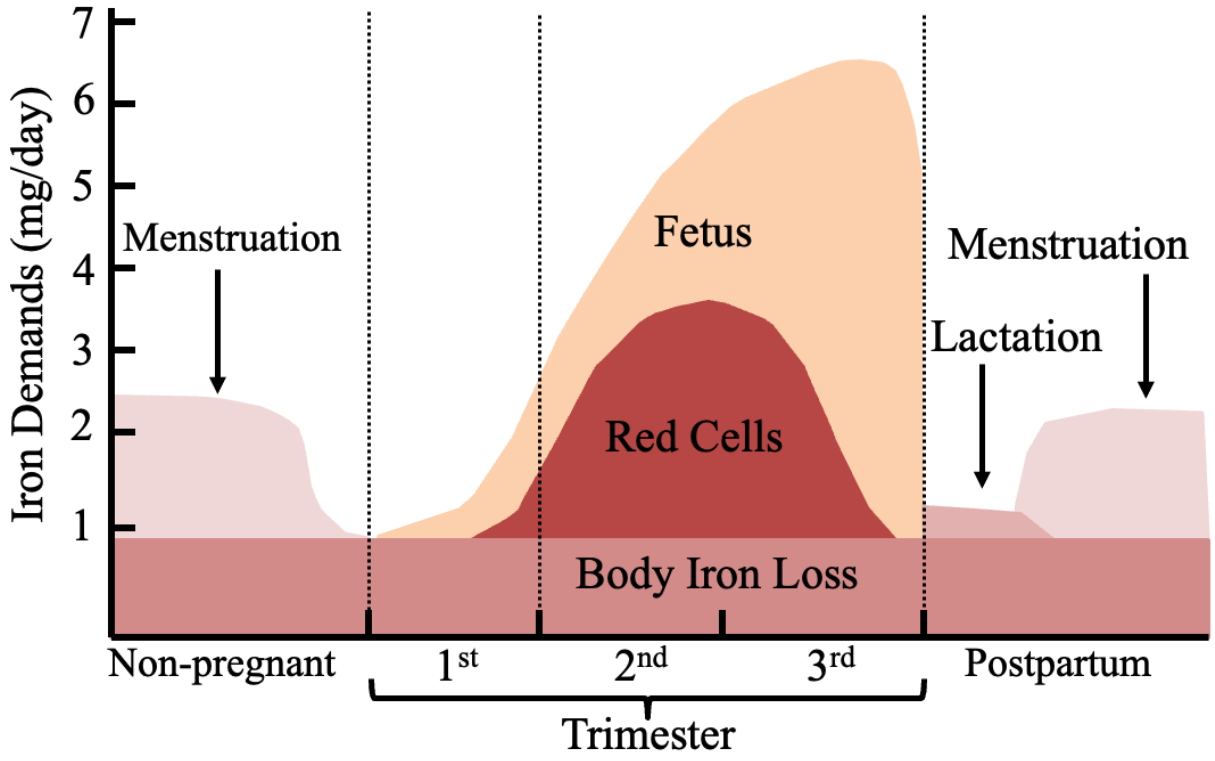

Figure 1.2. Iron demands during pregnancy, adapted from *WHO* (236)

1.4.6 Iron Supplementation

Many clinical studies support iron supplementation in pregnant women only when ID is diagnosed (defined by a reduction in hemoglobin, serum ferritin, or dietary intake) (237). However due to the large prevalence of ID, both health Canada and the World Health Organization recommend oral iron supplementation in all women during pregnancy (209, 238). On the other hand, the US Preventative Services Task Force as well as the European Food Safety Authority, each concluded that that iron supplementation should be reserves for those "at risk or with documented iron deficiency" (239).

Iron supplementation during pregnancy is therefore controversial, and while beneficial for those with ID, the practice comes with several challenges. Prenatal vitamins may not contain enough iron to meet demands, therefore higher dose supplementation may be required (240, 241). Larger doses of iron are associated with gastrointestinal discomfort, leading to issues with compliance (242). As a large portion of iron within the gut is not absorbed, iron poises as an essential micronutrient for pathogenic bacteria such as *Escherichia coli* and *Salmonella* (243). Probiotics, such as Bifidobacteria, which make up a large portion of the gut microbiome have low iron requirements (244). Aggressive oral iron supplementation therefore comes with some degree of risk.

A logical next step may be to consider intravenous iron supplementation, thereby bypassing issues with gastrointestinal absorption. Intravenous iron also allows large doses to be administered in a single infusion, up to 1 g per day, providing the entire gestational iron demand in one dose (214). This practice is consistent with United Kingdom's guidelines (245), and there is some evidence that IV iron is superior to oral iron supplementation in pregnancy. A meta-analysis based on data from randomized control trials showed a small increase in maternal hemoglobin, neonatal birth weight, and neonatal ferritin levels, however other maternal and neonatal outcomes (including neonatal hemoglobin) were not different (246). There are practical limitations regarding iron transfusion which include but are not limited to a high cost,

requirement to be done in a hospital under supervision, and occasionally resulting in infusion reactions in about 1% of individuals (247).

Much like other micronutrients, iron represents a U-shaped curve where prolonged supplementation can result in iron overload and damage from oxidative stress as previously described (248). Markers of oxidative stress in the fetoplacental unit have been associated with increased iron stores (249). Without supplementation, a hemoglobin above 14 g/dL has been associated with increased incidents of gestational hypertension, preeclampsia, as well as corresponding low birthweights and APGAR scores (248). Further clinical trials assessing iron supplementation in women with a hemoglobin above 13.2 g/dL found an increased incidence of preeclampsia and fetal growth restriction, likely due to maternal hypertension (250). Finally, a small number of pregnant women overdose on iron each year, which can result in organ failure, coma, and maternal and fetal demise (251). All together, a blanket iron supplementation in pregnant women must be met with some caution.

Finally, perhaps most interestingly, while iron supplementation improves maternal hematologic and iron indices, it is not entirely clear there is a benefit to the fetus (252). In fact, our group has recently shown that maternal indices of iron status have poor correlations with fetal and neonatal iron status (253). To further support this, two Cochrane systematic reviews evaluated the effectiveness of oral iron supplementation and found improvements in maternal anemia and iron deficiency, however other measures of neonatal outcome were not improved (242, 254). A study in pregnant rats also showed that iron supplementation corrected anemia in the mothers, however this was contrasted by an increase in oxidative stress and inflammation of the fetoplacental unit; hepatic damage was also found in the mothers (255).

There appears to be no additional benefit to iron supplementation in non-ID individuals, as this approach could lead to iron overload (237). The main solution to ID in pregnancy lies in prevention, while the

benefits of iron supplementation outweigh the risk in ID women, other therapies to treat the deleterious effects of maternal iron deficiency in pregnancy should be investigated.

1.5 Sulforaphane

The benefits of healthy nutrition on reducing the risks of both cardiovascular disease as well as all-cause mortality cannot be overstated. A meta-analysis by Kwok *et al.* highlighted how a number of dietary components are protective, with a particular emphasis on cruciferous vegetables (e.g., broccoli, cabbage) (256). This is best highlighted in a study of 134,796 Chinese adults who were divided by vegetable consumption. Here, the researchers found a dose response pattern highlighting an inverse association between fruit and vegetable intake, and total mortality. Importantly the association with mortality was even stronger when cruciferous vegetables were compared instead of all fruits and vegetables ($P<0.0001$ vs. $P=0.03$). Further, these associations were primarily related to cardiovascular disease but not cancer mortality (257).

There are several powerful associations between cruciferous vegetables and all cause mortality, cancer risk, survival following cancer, carcinogen excretion, and cardiovascular disease (258-263). These benefits likely come from a group of compounds called isothiocyanates. Isothiocyanates are formed from compounds known as glucosinolates through an enzyme called myrosinase. Myrosinase is activated when cruciferous vegetables are crushed, finely ground or chewed, they reach their optimal activity when they are slightly heated and are inactivated from sustained heat. Of the isothicyanates, perhaps the most studied and potent appears to be sulforaphane which forms from the glucosinolate precursor glucoraphanin. Among the best natural sources of sulforaphane are broccoli sprouts, which contain up to 50 times as much glucoraphanin per gram as mature broccoli (264).

1.5.1 Mechanisms of Sulforaphane

Sulforaphane acts as a phase II enzyme activator and upregulates intrinsic antioxidant mechanisms through nuclear factor erythroid 2-related factor 2 (NRF2) and the antioxidant response element (ARE)

pathway. In short, sulforaphane is small and lipophilic, allowing it to easily pass through the cell membrane. Sulforaphane can then bind to Kelch-like ECH associated protein 1 (Keap1), a protein responsible for suppressing NRF2 within the cytoplasm (265, 266). NRF2 then enters the nucleus and activate the ARE, which initiates a transcription of a series of protective genes or genes which code protective enzymes (267, 268). Sulforaphane appears to be on of the most potent naturally occurring inducers of the NRF2 pathway (269).

Oxidative stress activates the immune system and causes an inflammatory response which is hypothesized to further activate oxidative stress and together cause physiological decline (171). In fact, uncontrolled oxidative stress may be a primary cause of cardiovascular disease (270). One way antioxidants work is by directly decreasing oxidative stress (e.g., vitamin C), this is typically done through redox activity to scavenge reactive oxygen species, unfortunately this can be relatively short lived (271). Indirect antioxidants such as sulforaphane instead support endogenous antioxidant function, as described above. The binding of Keap1 to sulforaphane allows NRF2 to continue its transcriptional function for a longer period of time, as well as activate more frequently (272). How long antioxidant function is improved for is unclear, however sulforaphane has been shown to increase gene expression on the order of hours to days (273).

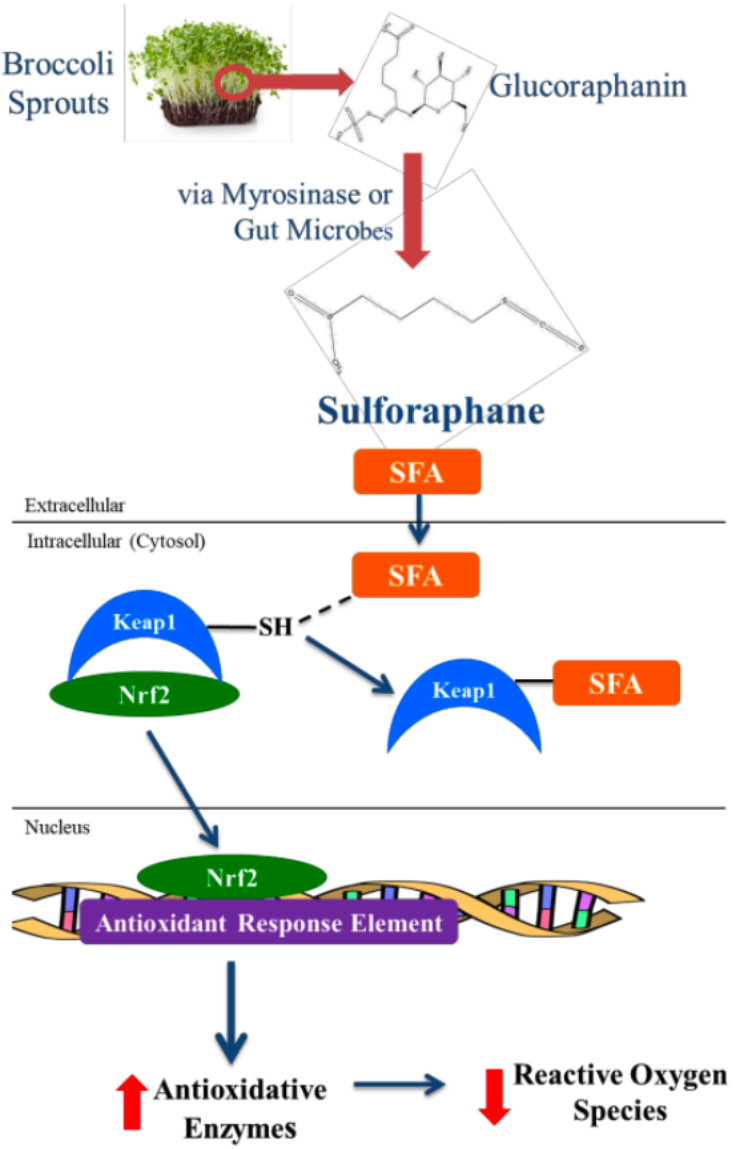

Figure 1.3. Antioxidant effects of broccoli sprouts from my friend *Zeenat Ladak,* 2021 (274)

One antioxidant particularly critical to the ARE is glutathione. Sulforaphane as a Phase II enzyme inducer will elevate glutathione levels (275). Glutathione is a direct antioxidant which is responsible for the protection against lipid and nucleotide peroxidation, and catecholamine quinones (276). Glutathione is also involved in the regeneration of vitamin C and E, and improves cellular proliferation, apoptosis, and mitochondrial function (275, 277). While the mechanisms have been highlighted in detail elsewhere, sulforaphanes ability to induce ARE and glutathione is critical in improving cellular function (278).

A decrease in inflammation is another factor associated with longer lifespan, improved physical function, and even improved cognition (279). Animal models have shown that an increase in systemic inflammation decreases survival, highlighting that inflammation may not just be a by-product of cardiovascular disease and aging but perhaps also a driver (280). Again, sulforaphane has been shown to inhibit inflammation through the NRF2 pathway in mice, as well as reduce systemic markers of inflammation in humans (281-283). These studies further highlight the protective effects of sulforaphane, in both unhealthy and healthy adults.

1.5.2 Sulforaphane and Longevity

If we recall the first study mentioned, improvement of all-cause mortality due to cruciferous vegetables was primarily related to a reduction in cardiovascular disease. In fact, numerous studies have linked cruciferous vegetable consumption with a reduction in cardiovascular disease, coronary artery disease, as well as stroke (258, 284). Furthermore, sulforaphane has been shown in rat studies to be protective against vascular remodeling through the inhibition of inflammation and oxidative stress (285-288). Finally in human's broccoli sprout supplementation improved serum triglyceride and oxidized LDL/LDL-cholesterol ratio, resulting in an improved atherogenic index, while also decreasing fasting blood glucose (289, 290). Therefore, there are a number of clear mechanisms by which sulforaphane exhibits protective effects on the cardiovascular system.

While these alterations, combined with the anti-cancer, and neuroprotective effects of sulforaphane could all improve longevity (275, 291, 292). This begs the question: does sulforaphane slow the aging process directly? Broccoli and sulforaphane supplementation have been shown to improve lifespan in beetles as well as larvae (293, 294). However, this data should be replicated in mammals which are physiologically closer to humans. This stands as the final chapter of my thesis.

1.6 Ketones

In times of low dietary sources of carbohydrates and depleted intercellular levels of glycogen the liver synthesizes ketones, also known as ketone bodies. This is hypothesized to be an evolutionary mechanism to preserve carbohydrates for the brain, which predominantly relies on glucose. Ketones then conserve glucose by providing another source of energy for the periphery, while also constituting neurological fuel if necessary. In addition, this decreases proteolysis required to support gluconeogenesis through amino acid catabolism. Therefore, ketones play a critical role as an alternative metabolic substrate in cases of glucose deprivation (295).

1.6.1 Ketone Metabolism

Ketone metabolism has been reviewed comprehensively by Selvaraj *et al.* as well as Lopaschuk *et al.* (296, 297); I will provide a summary bellow. Ketones are produced in the liver from fatty acids when liver glycogen levels become low. The process of generating ketones begins with β-oxidation within the mitochondrial matrix. Here fatty acids are catabolized into acetyl-CoA. At this point two acetyl-CoA are combined with β-ketothiolase to form acetoacetyl-CoA. Hydroxymethylglutaryl- CoA synthase (HMG-CoA synthase) and then combines the acetoacetyl-CoA with a final acetyl-CoA to generate β-hydroxy-β-methylglutaryl-CoA. HMG-CoA lyase can then convert the former to acetoacetate, a ketone body. Acetoacetate may then separate into its two products; acetone, and β-hydroxybutyrate which is the main ketone within human circulation. At this point ketogenesis is complete, these three molecules (acetoacetate, acetone, and β-hydroxybutyrate) can each be referred to as a ketone. However, as a signalling molecule β-hydroxybutyrate, plays a larger role than the other molecules.

β-hydroxybutyrate has two unique features to its sister molecule acetone, first β-hydroxybutyrate can convert back to acetoacetate, and secondly β-hydroxybutyrate may leave the liver to provide energy to other organs. β-hydroxybutyrate enters circulation via monocarboxylate transporters (MCT), a plasma membrane transporter which carries molecules having one carboxylate group (e.g., lactate, pyruvate, and ketones). Once in the circulation, ketones can travel to extrahepatic organs, particularly to fuel the heart, brain, and skeletal muscle.

These organs can then transport β-hydroxybutyrate into the cells through MCT. Within the cell β-hydroxybutyrate can enter the mitochondrial matrix through free diffusion or by the pyruvate carrier (298). In the myocardial mitochondria β-hydroxybutyrate is oxidized back into acetoacetate via β-hydroxybutyrate dehydrogenase 1 and then into acetoacetyl-CoA by succinyl-CoA-3-oxaloacid CoA transferase (SCOT). Acetyl-CoA acetyltransferase (ACAT) then converts acetoacetyl-CoA to acetyl-CoA, which can then enter into the tricarboxylic acid cycle. These enzymes are critical for ketolysis, as genetic defects of SCOT, ACAT, and MCT all result in recurrent ketoacidosis (299). Importantly, the process of metabolizing ketones for energy is more oxygen efficient than fatty acid metabolism. Since fatty acids are a major source of energy for the heart, in scenarios where oxygen supply is limited (such as heart failure, or in utero life) ketones may then be a preferred metabolic substrate.

1.6.2 Ketones as Signaling Molecules

β-hydroxybutyrate is by far the most studied ketone as, unlike acetoacetate and acetone, it has been shown to act as a signaling molecule (300). First, β-hydroxybutyrate has been shown to have antioxidant and anti-hypertrophic properties in the heart through inhibiting histone deacetylase and causing a subsequent increase in antioxidant stress molecules such as FOXO3A and MT2 (301). In addition to epigenetic modifications, β-hydroxybutyrate has been shown to modulate oxidative stress, inflammation, and immune cell function, at least in part through nucleotide binding domain like receptor protein 3

(NLRP3), causing a downstream reduction in inflammatory cytokines (301-304). In fact, because fasting, calorie restriction, and a ketogenic diet all can increase circulating levels of β-hydroxybutyrate (305), β-hydroxybutyrate may be a common molecule which links the health and longevity benefits between these three modalities. However, other studies have linked ketone derived acetyl-CoA with pathological remodeling and heart failure (297, 306). The effects of ketones therefore require much further study in animal models before its protective effects can be considered to alter cardiovascular disease.

1.6.3 Ketones in Pregnancy

The decision to study ketones in pregnancy is important, but also is associated with several drawbacks. Whenever a new treatment is studied during pregnancy its safety must be considered. Regarding exogenous ketone supplementation, there is minimal evidence on how animals, let alone humans, would respond during pregnancy. First, I would like to briefly overview physiology of ketone metabolism in pregnant women and why it is an important pathway to study.

During pregnancy, an individual undergoes numerous metabolic changes. Maternal insulin resistance increases starting in the second trimester due to the secretion of placental growth hormone, which functions as an insulin antagonist. Ultimately this leaves pregnant women in a state analogous to starvation, with a resultant increase in lipolysis and ketogenesis (307). In addition, maternal glucose utilization and fasting glucose levels fall in pregnancy, further signaling an increase in lipolysis and ketogenesis (308, 309). In fact, in a study of fasted women entering the hospital, serum ketone levels appeared three times higher in women in their third trimester of pregnancy compared to nonpregnant control subjects (310). Fortunately, the fetus is capable of using multiple energy substrates including ketones (311). A 1975 study on aborted fetuses showed that the fetal brain, kidney and liver all contain enzymes capable of catabolizing ketones, with the brain expressing these enzymes as early as 8 weeks into gestation (312).

As I have highlighted previously, an inappropriate gestational diet can cause permanent deleterious effects to both the mother and child (313). There is limited evidence whether the ketogenic diet (a diet which consists of eating minimal carbohydrates with a higher fat intake to increase circulating levels of ketones), has any meaningful effect on human pregnancies (314, 315). However, several rodent studies have associated the ketogenic diet with altered growth trajectories in offspring (316, 317). These findings, combined with an absence of folic acid in these diets, have caused most guidelines to recommend against a ketogenic diet during pregnancy (318).

Two studies in mothers have found an association between urine ketone levels and fetal outcomes. The first study looked at 360 nondiabetic mothers at greater than 40 weeks gestation (319). Here women experiencing vomiting, diarrhea, multiple pregnancy, history of renal disease, hypertension, and high-risk pregnancy were excluded. In 34 women (9.4%), ketonuria was identified and an association was found between the presence of urinary ketones and each of oligohydramnios, fetal heart rate decelerations, and non-reactive nonstress tests. A second study of 1,895 nondiabetic mothers greater than 41 weeks with the same exclusion criteria repeated these associations (320). Furthermore, in each of these studies there were no signs of dehydration, as assessed by urine specific gravity, which to the admission of the authors is a convenient but not sensitive measure of dehydration. At the very least these studies indicate that clinically detectable ketonuria is associated with abnormal fetal test results. However, post term pregnancies are already associated with a large degree of perinatal morbidity and mortality, and since ketonuria is a commonly used urinary marker of maternal starvation and dehydration, it is therefore unclear whether elevated serum ketone levels are directly harmful to the fetus. Further, a final study in 204 diabetic and 316 non diabetic first trimester women found zero association between maternal serum β-hydroxybutyrate levels and fetal malformations, however serum β-hydroxybutyrate was reversely correlated to crown rump length and birth weight (321).

While exogenous ketone supplementation, in particular β-hydroxybutyrate, has been studied in several other disease models, to the best of my knowledge it has only been studied in pregnancy once before. Hirata *et al.* injected 100 mg/kg of β-hydroxybutyrate 5 times across gestation, in a mouse model of chorioamnionitis (322). They found that β-hydroxybutyrate suppressed inflammation and reduced pregnancy losses induced by lipopolysaccharides, likely through inhibition of NLRP3 inflammation in the placenta.

Although the current literature is limited, it seems to indicate that exogenous ketone body supplementation during pregnancy may be safe for the fetus. Ketones do cross the placenta to be utilized by the fetus (311, 323), and have been shown to be protective in several other disease models. Therefore, testing if ketones are both safe, and potentially protective in models of pathological pregnancy proves an interesting field for potential study.

1.6.4 Ketones in the Failing Heart

Following completion of **Chapter 2**, I began to look for potential therapies to augment the reduction in cardiac contractility we found in our neonates. While the effects of exogenous ketone supplementation during the perinatal period have not been studied in detail, there is a growing body of evidence that ketones may have protective effects in heart failure. As this was the main rational to then test β-hydroxybutyrate salt in our model of perinatal iron deficiency I hope to summarize some of the more relevant finding's bellow.

First it is important to recognize that the heart is an incredibly active organ, weighing under a pound it is required to pump 7200 liters of blood per day against a systemic vascular resistance. Ultimately this effort requires 35 liters of oxygen per day, all while the heart turns over its ATP stores every 10 seconds (324). This is truly a remarkable organ. In part due to the heart's high metabolic demands, it demonstrates an

ability to adapt to the substrates it is provided, utilizing glucose, fatty acids, lactate, branch chain amino acids, as well as ketones for fuel; however fatty acid β-oxidation provides most of the ATP (325).

In heart failure there is a metabolic shift, such that the heart utilizes fewer fatty acids and instead relies on other substances such as glucose, lactate, and ketones (306, 326). In recent years altering cardiac metabolism has been investigated as a treatment for heart failure. For example, enhancing glucose oxidation at the expense of fatty acid oxidation in the heart has been shown by many studies to be protective (327-329). With the overall justification being that the change from fatty acid oxidation to the utilization of other substrates requires less oxygen to produce ATP (297). Furthermore, as oxidative stress is a driver of the development and progression of heart failure (330), one might assume that the swap to a more oxygen efficient form of fuel could reduce reactive oxygen species and therefore protect the heart.

It is also important to briefly address that heart failure is associated with an elevation of pro-inflammatory cytokines. Therefore, ketone supplementation, which in any form will increase β-hydroxybutyrate, may also be protective against heart failure through anti-inflammatory and immunomodulatory strategies (331).

However, this then begs the question: would an exogenous ketone supplementation reduce glucose utilization ultimately causing a maladaptive reduction in ATP supply? Fortunately, Ho *et al.* from the University of Alberta answered this question, in this study her group acutely added β-hydroxybutyrate to an isolated working mode mouse heart. Here the authors found no reduction in glycolysis, glucose oxidation, or palmate oxidation, and instead β-hydroxybutyrate simply supplied more energy (332). Therefore, given that ketone metabolism is more oxygen efficient than fatty acid metabolism, an exogenous ketone supplementation may benefit the heart by providing additional ATP with a smaller increase in oxygen consumption.

1.6.4 Ketone Salt as a Therapeutic

The idea of elevating ketones has been well established as a therapy and has been implemented since 1911 as a means for treating epilepsy (333). While a ketogenic diet is not recommended in pregnancy, exogenous ketone supplementation offers an interesting alternative to increase ketones directly. Exogenous ketones supplementation exists in three forms, medium-chain triglyceride oil, ketone esters, and sodium-β-hydroxybutyrate (aka ketone salts). Practically speaking, sodium-β-hydroxybutyrate was chosen for **Chapter 3** as a mechanism to deliver ketones because the alternative options required oral delivery. Initial pilot studies showed the unpalatability of ketone esters in particular made non injectable therapies challenging in pregnant rats. However, there are a number of benefits of ketone salts.

One advantage of sodium-β-hydroxybutyrate is the basic nature of its attached sodium. While β-hydroxybutyrate is acidic, sodium-β-hydroxybutyrate appears to act as a base and therefore may correct metabolic acidosis associated with heart failure. In fact, infusion of sodium-β-hydroxybutyrate in patients with reduced ejection fraction not only improved ventricular contractility and cardiac output, but also slightly increased blood pH (334). A second study, this time with oral intake, showed an increase in β-hydroxybutyrate in the blood, but no differences in any serum electrolytes or blood gas (335). While there are obvious issues with large sodium transfusion in patients with heart failure, lower concentrations may not affect blood pH as much as other alternatives. Ultimately while other β-hydroxybutyrate supplements exist, a number of studies have shown ketone salts are effective at elevating serum β-hydroxybutyrate levels, resulting in at least a temporal improvement of cardiac output and reduction in inflammation (336-338). Collectively it is tempting to speculate that β-hydroxybutyrate either as a metabolite, signaling molecule, or both, may prove a novel therapy in pregnancy.

1.7 Aims

Iron deficiency is the most common nutritional deficiency worldwide with pregnant women and infants being some of the most susceptible subgroups (199, 202, 203). Unfortunately, perinatal iron deficiency is

associated with several pregnancy complications including maternal and fetal demise, pre-term birth, and intrauterine growth restriction (214-219). Furthermore, perinatal iron deficiency can increase risks of non-communicable diseases, such as cardiovascular disease later in life (225). However, many who develop even under ideal circumstances will still experience cardiovascular disease as a product of ageing. In this thesis we aim to investigate the alterations in cardiovascular function due to nutritional restriction and nutritional supplementation. The specific aims of each study are as follows:

Chapter 2: To determine the structural and functional effects of maternal iron deficiency on the developing neonatal heart.

Chapter 3: To determine if exogenous ketone supplementation during gestation would reduce cardiac impairments observed in iron deficient neonates.

Chapter 4: To evaluate fetal and placental oxygen saturation in control and iron deficient dams using photoacoustic imaging.

Chapter 5: To determine the effects of long-term broccoli sprout feeding on cardiometabolic health and longevity in rats.

Chapter 2

Perinatal Iron Deficiency Causes Changes in Neonatal Cardiac Function and Structure in a Sex-Dependent Manner

Ronan M.N. Noble[1,2*], Claudia D. Holody[1,2*], Andrew G. Woodman[3], Chunpeng Nie[1,2], Si Ning Liu[1,2], Daniel Young[4], Alyssa Widemeyer[1,2], Shubham Soni[1,2], Jason R.B. Dyck[1,2], Daniel Graf[5], Luke G. Eckersley[1,2], Antoine Dufour[4], Stephane L. Bourque[1,2,3]

1. Department of Pediatrics, University of Alberta, Edmonton, Canada
2. Women and Children's Health Research Institute, University of Alberta, Edmonton, Canada
3. Department of Anesthesiology, University of Alberta, Edmonton, Canada
4. Department of Physiology and Pharmacology, University of Calgary, Calgary, Canada
5. School of Dentistry, University of Alberta, Edmonton, Canada

* denotes equal contribution

PUBLISHED:

Noble *at al.* Clinical Science 2023. Aug 14;137(15):1115-1130

2.1 Abstract

Iron deficiency (ID) is common during gestation and in early infancy and can alter developmental trajectories with lasting consequences on cardiovascular health. While the effects of ID and anemia on the mature heart are well documented, comparatively little is known about their effects and mechanisms on offspring cardiac development and function in the neonatal period. Female Sprague Dawley rats were fed an iron-restricted or iron-replete diet before and during pregnancy. Cardiac function was assessed in a cohort of offspring on postnatal days (PD) 4, 14, and 28 by echocardiography; a separate cohort was euthanized for tissue collection and hearts underwent quantitative shotgun proteomic analysis. ID reduced body weight and increased relative heart weights at all time points assessed, despite recovering from anemia by PD28. Echocardiographic studies revealed unique functional impairments in ID male and female offspring, characterized by greater systolic dysfunction in the former and greater diastolic dysfunction in the latter. Proteomic analysis revealed down-regulation of structural components by ID, as well as enriched cellular responses to stress; in general, these effects were more pronounced in males. ID causes functional changes in the neonatal heart, which may reflect an inadequate or maladaptive compensation to anemia. This identifies systolic and diastolic dysfunction as comorbidities to perinatal ID anemia which may have important implications for both the short and long-term cardiac health of newborn babies. Furthermore, therapies which improve cardiac output may mitigate the effects of ID on organ development.

2.2 Introduction

Iron deficiency (ID) is the most common nutritional deficiency worldwide, though prevalence varies depending on geographical location and population demographics (193). Among subgroups of the population, ID is notably prevalent among pregnant women and young children, due to increased iron demands during these periods of development. With increasing time and severity, ID can progress to anemia, a condition characterized by low levels of circulating hemoglobin (Hb). In high income countries, 1 in 5 women are expected to develop anemia during pregnancy (211), whereas in low and middle-income countries, rates can exceed 60% (211), with the majority of these cases attributed to ID (218). Its propensity to afflict pregnant women and children may reflect an evolutionary strategy to protect against disease-causing pathogens (339), but also increases the risk of perinatal health complications, including pre-term birth and intrauterine growth restriction (340). The consequences of impaired growth and development may extend beyond the neonatal period, and predispose the offspring to chronic disease later in life (1), as described by the developmental origins of health and disease (DOHaD) hypothesis. Indeed, we and others have reported that ID anemia causes lasting behavioral, metabolic, and cardiovascular abnormalities in adult offspring (138-140, 341-343). Yet despite extensive study, the mechanisms by which ID "programs" altered cardiovascular and metabolic risk profiles in offspring remains unclear.

Hb is primarily responsible for transporting oxygen from the lungs to the tissues. Most tissues receive an excess (~3-4 fold) of oxygen required for normal function (344); a notable exception is the heart, which, even at rest, extracts up to 80% of oxygen delivered (345). Despite a limited physiological reserve, the heart still exhibits a remarkable ability to adapt to "stressors" to improve maximal cardiac output in an effort to maintain systemic blood pressure and tissue perfusion. In human and animal studies, ID and anemia are associated with cardiac structural and functional changes that include increases in size, contractility, and heart rate (346-349). These changes appear largely reversible in the short-term (350), but over time the persistent stress can lead to inflammation and fibrosis, resulting in cardiac dysfunction, compromised hemodynamics and symptomatic heart failure (350). Intrinsic differences between mature

and developing heart (e.g. metabolic substrate utilization, mechanisms driving cardiac enlargement, neural and hormonal regulation) may affect its ability to adapt to stressors like anemia. Indeed, the neonatal myocardium is less compliant than the adult myocardium, and thus acute changes in cardiac output depend largely on increases or decreases in heartrate (100). However, as a chronic condition, anemia can induce cardiac morphological and structural changes in the fetus and neonate that increase physiological reserve. Indeed, in the early and middle stages of Hemoglobin Bart's disease (i.e. before the progression to heart failure), the severe anemia associated with alpha-thalassemia leads to dramatic enlargement of heart, which in turn enables the fetus to improve cardiac output without increasing contractility (351).

Perinatal ID is also associated with cardiomegaly (139, 223, 224), presumably as a means to improve cardiac output and tissue perfusion in the wake of hypoxemia caused by anemia. However, the accompanying structural and functional changes have not been explored in detail and may differ from conditions of anemia of other causes (e.g. thalassemia), in which the biochemical effects of ID are not present. We sought to determine the effect of maternal ID anemia and subsequent recovery in the offspring on cardiac structure and function in the immediate postnatal period. This period was chosen because the neonatal heart undergoes substantial growth and development during this time span, and therefore constitutes an important phase in the adaptation to extra-uterine life. In addition, since many short and long-term consequences of ID have been reported to be sexually dimorphic (138, 140), the present study examines outcomes in both male and female offspring.

2.3 Methods

2.3.1 Animals and Treatments

The protocols described herein were approved by the University of Alberta Animal Care and Use Committee in accordance with guidelines established by the Canadian Council for Animal Care, consistent with NIH guidelines for the Care and Use of Laboratory Animals. Sprague-Dawley rats aged six weeks were purchased from Charles River (Saint-Constant, QC, Canada) and housed at the University of Alberta Animal Care Facility, which maintains a 12-hour light/dark cycle and an ambient temperature of 23 °C. All animal experiments were completed at the University of Alberta. Rats had *ad libitum* access to food and water throughout the study. All purified diets used in this study were based on the AIN-93G formula and differed only by the amount of ferric citrate added (see below).

We used our well established model of maternal ID, which has been previously shown to reduce indices of iron status and cause ID anemia (223). Two weeks before mating, female rats were pseudorandomized by cage order to one of two groups: control rats (Ctl; n=22) were fed a purified control diet (containing 37 mg/kg elemental iron), and iron-deficient rats (ID; n=18) were fed an iron-restricted diet (containing 3 mg/kg elemental iron). After two weeks on their respective diets, rats were housed overnight with male rats (fed a standard rodent chow) until pregnancy was confirmed by presence of sperm in a vaginal smear (defined as gestational day [GD]0). Thereafter, dams were individually housed, and those in the iron-restricted group were fed a moderately iron-restricted diet containing 10 mg/kg elemental iron (thus ensuring a viable pregnancy), whereas Ctl dams remained on their prescribed control diet. From GD0, food consumption, body weight, and hemoglobin (Hb) levels were assessed weekly. Maternal Hb levels were assessed using a HemoCue Hb201+ hemoglobinometer from approximately 10 μL of blood collected via saphenous venipuncture.

On the day of birth (defined as postnatal day [PD]0), all dams were fed the standard rodent chow and litters were reduced to ten offspring (five males and five females) to standardize postnatal conditions. At PD0, PD4, PD14, and PD28, male and female pups were weighed, and euthanized by decapitation (at PD0 and PD4) or by cardiac excision (at PD14 and PD28; pups were anesthetized with 5% isoflurane in pure oxygen prior to euthanasia). Free flowing blood was collected for hemoglobin assessments (Hemocue Hb201+) and arterial blood was collected via a carotid catheter or the descending aorta for blood gas analysis (AB Flex 80, Radiometer Canada, Mississauga, Canada). Offspring hearts were excised, weighed, and either flash-frozen in liquid nitrogen. All tissues were stored at -80 °C prior to analyses. At PD21, pups were separated from their mothers, housed with their same-sex littermates, and fed standard rodent chow until PD28.

2.3.2 Echocardiography

Cardiac structure and function were assessed by thoracic echocardiography (Vevo 2100, Visualsonics, Toronto, ON, Canada) in offspring in a supine position using two linear array transducers ranging from 18 to 55 MHz. Animals were anesthetized (isoflurane in oxygen; 2.5% for induction and 1.5-1.8% for maintenance). PD4 was chosen as the first timepoint for echocardiography as it proved challenging to maintain a consistent heart rate (a necessity to ensure consistency between neonates) under anesthesia at earlier timepoints. For rats at PD14 and PD28, the chest and upper abdomen were shaved, and depilatory cream was used. Limbs were fixed to electrodes with tape and conductive electrode gel (SignaGel, WA, USA); electrocardiogram and respiratory rate were continuously recorded. Body temperature was maintained with heated ultrasound transmission gel, a heated table surface, and a heat lamp.

A single operator who was blinded to experimental groups performed all assessments, if anatomy limited an optimized measurement the particular image would be discarded. Parasternal long axis M mode tracings of the left atrium were taken at the level of the aortic valve. Parasternal short axis M mode tracings of the left ventricle (LV) were recorded at the widest point of the heart, with the M mode cursor

placed perpendicular to the anterior and posterior wall of the left ventricle. LV end-diastolic and end-systolic diameters (LVID), and septal (IVS) and posterior wall (LVPW) thicknesses were measured; at this point heart rate was also recorded over the same cardiac cycles. Ejection fraction (EF), fractional shortening (FS), stroke volume (SV), cardiac output (CO), and oxygen delivery (DO_2) was calculated as:

$EF = (LVEDV - LVESV)/LVEDV$

$FS = (LVID_d - LVID_s)/LVID_d$

$SV = LVEDV - LVESV$

$CO = SV \times \text{heart rate}$

$DO_2 = CO \times Hb \times (1.34 \times 0.97)$

where LVEDV is the left ventricular end-diastolic volume, LVESV is the left ventricular end-systolic volume, Hb is the hemoglobin of the pup measured shortly after echocardiography, 1.39 is the oxygen binding capacity of Hb in mL/g, and 0.97 is an estimated hemoglobin oxygen saturation.

The trans mitral flow velocity was obtained from the apical four chambers view. The ratio of peak early filling (E) and atrial velocity (A) was measured with pulse wave Doppler imaging; the corresponding mitral annulus velocities were evaluated using tissue Doppler imaging. The E and A wave images were also used to quantify isovolumetric relaxation time (IVRT), isovolumetric contraction time (IVCT), and aortic ejection time (AET) which were then combined to calculate a TEI index. Pulmonary artery Doppler imaging was used to measure pulmonary acceleration time (PAT), pulmonary ejection time (PET), and pulmonary valve peak velocity (PV peak velocity). Pulmonary vein doppler imaging was used to measure S (systolic) wave, D (diastolic) wave, A (atrial systolic reversal) wave, as well as the atrial systolic reversal duration. Aorta doppler imaging was used to measure descending aorta velocity. All values were measured under steady state conditions and averaged from at least three cardiac cycles taking care to exclude cycles that took place during inhalation. Organ weights were collected from offspring which

underwent echocardiography (and therefore isoflurane exposure) however subsequent biochemical analysis was not performed on these tissues.

2.3.3 Quantitative Real-Time PCR

Total RNA was isolated from frozen hearts using TRIzol reagent (Invitrogen®) according to the manufacturer's instructions. First strand cDNA synthesis was performed using 5× All-In-One RT MasterMix (Applied Biological Materials, G592), according to the manufacturer's instructions. Quantitative real-time PCR was performed in white 384-well reaction plates with PowerUp SYBR Green Master Mix (Applied Biosystems, A25742) in the LightCycler 480 (Roche Life Science), as previously described (323). Quantitative PCR data was analyzed using the relative gene expression (ΔΔCt) method with *Actb* as the housekeeping gene. The following gene specific primers (Integrated DNA Technologies, Coralville, IA) were used:

ACAGAGTGCTTCGTGCCTGAT (5' *Myh6*)

CGAATTTCGGAGGGTTCTGC (3' *Myh6*)

CGCTCAGTCATGGCGGAT (5' *Myh7*)

GCCCCAAATGCAGCCAT (*3'Myh7*)

AACCCTAAGGCCAACCGTG (5' *Actb*)

TACGTACATGGCTGGGGTGT (3' *Actb*)

2.3.4 Quantitative Shotgun Proteomics

Isolated cardiac ventricles from neonatal rats were subjected to a quantitative shotgun proteomics analysis as previously described (352); the proteomics workflow is depicted in **Figure 2.1**. Briefly, hearts were lysed in 200 mM HEPES buffer (pH 8.0) containing 1% SDS, 100 mM ammonium bicarbonate, 10 mM EDTA and protease inhibitor cOmplete tablets (Roche, 4693159001), and then treated with 10 mM dithiothreitol (DTT) to denature proteins, followed by incubation for 25 min in 15 mM iodoacetamide (VWR) in the dark at room temp to alkylate proteins. Samples were then digested with Trypsin (Promega,

Madison, WI, United States). Next, to label peptide α- and ε-amines, samples were incubated for 18 h at 37° C with isotopically heavy (40 mM $_{13}CD_2O$ + 20mM $NaBH_3CN$ (sodium cyanoborohydride)) or light formaldehyde (40 mM CH_2O + 20 mM $NaBH_3CN$). Samples were subjected to C18 chromatography using Pierce™ C18 columns (Thermo chromatography™, ON, Canada) before being subjected to liquid chromatography and tandem mass spectrometry (LC-MS/MS).

Proteomics analyses were performed by the Southern Alberta Mass Spectrometry (SAMS) core facility at the University of Calgary, Canada using a Thermo Scientific Easy-nLC (nanoflow Liquid Chromatography) 1200 system coupled to a Orbitrap Fusion Lumos Tribrid mass spectrometer (Thermo Fisher Scientific) operated with Xcalibur (version 4.0.21.10). Tryptic peptides (2 μg) were loaded onto a C18 trap (75 μm × 2 cm; Acclaim PepMap 100, P/N 164946; Thermo Fisher Scientific) at a flow rate of 2 μL/min of solvent A (0.1% formic acid and 3% acetonitrile in LC mass spectrometry grade water). Peptides were eluted using a 120 min gradient from 5 to 40% (5% to 28% in 105 min followed by an increase to 40% B in 15 min) of solvent B (0.1% formic acid in 80% LC- mass spectrometry grade acetonitrile) at a flow rate of 0.3 μL/min and separated on a C18 analytical column (75 um × 50 cm; PepMap RSLC C18; P/N ES803; Thermo Fisher Scientific). Peptides were then electrosprayed using 2.3 kV voltage into the ion transfer tube (300 °C) of the Orbitrap Lumos operating in positive mode. The Orbitrap first performed a full mass spectrometry scan at a resolution of 120,000 FWHM to detect the precursor ion having a mass-to-charge ratio (m/z) between 375 and 1,575 and a + 2 to + 4 charge. The Orbitrap AGC (Auto Gain Control) and the maximum injection time were set at 4 x 10^5 and 50 ms, respectively. The Orbitrap was operated using the top speed mode with a 3 s cycle time for precursor selection. The most intense precursor ions presenting a peptidic isotopic profile and having an intensity threshold of at least 2 × 10^4 were isolated using the quadrupole (isolation window of m/z 0.7) and fragmented with HCD (38% collision energy) in the ion routing Multipole. The fragment ions (MS2) were analyzed in the Orbitrap at a resolution of 15,000. The AGC, the maximum injection time and the

first mass were set at 1×10^5, 105 ms and 100, respectively. Dynamic exclusion was enabled for 45 s to avoid of the acquisition of same precursor ions having a similar m/z (plus or minus 10 ppm).

Spectral data were matched to peptide sequences in the rat UniProt protein database using the Andromeda algorithm as implemented in the MaxQuant software package v.1.6.10.23, at a peptide-spectrum match FDR<0.01 (353, 354). Search parameters included a mass tolerance of 20 p.p.m. for the parent ion, 0.5 Da for the fragment ion, carbamidomethylation of cysteine residues (+57.021464 Da), variable N-terminal modification by acetylation (+42.010565 Da), and variable methionine oxidation (+15.994915 Da). N-terminal and lysine heavy (+34.063116 Da) and light (+28.031300 Da) dimethylation were defined as labels for relative quantification. The cleavage site specificity was set to Trypsin/p for the proteomics data, with up to two missed cleavages allowed. Significant outlier cutoff values were determined after log (2) transformation by boxplot- and-whiskers analysis using the BoxPlotR tool (355). The data were deposited into ProteomeXchange via the PRIDE database and are freely available (PXD028922).

To identify protein–protein interactions, the STRING (Search Tool for the Retrieval of Interacting Genes) database was used to illustrate interconnectivity among proteins (354). Protein-protein interactions relationship were encoded into networks in the STRING v11 database (https://string-db. org). Data were analyzed using the *homo sapiens* as the organism (FDR=0.05). Metascape analysis was also used to identify enriched pathways (354). Protein-protein interactions relationship were encoded into networks using the Metascape website (https://metascape.org/), and the enriched pathways were plotted as heatmaps.

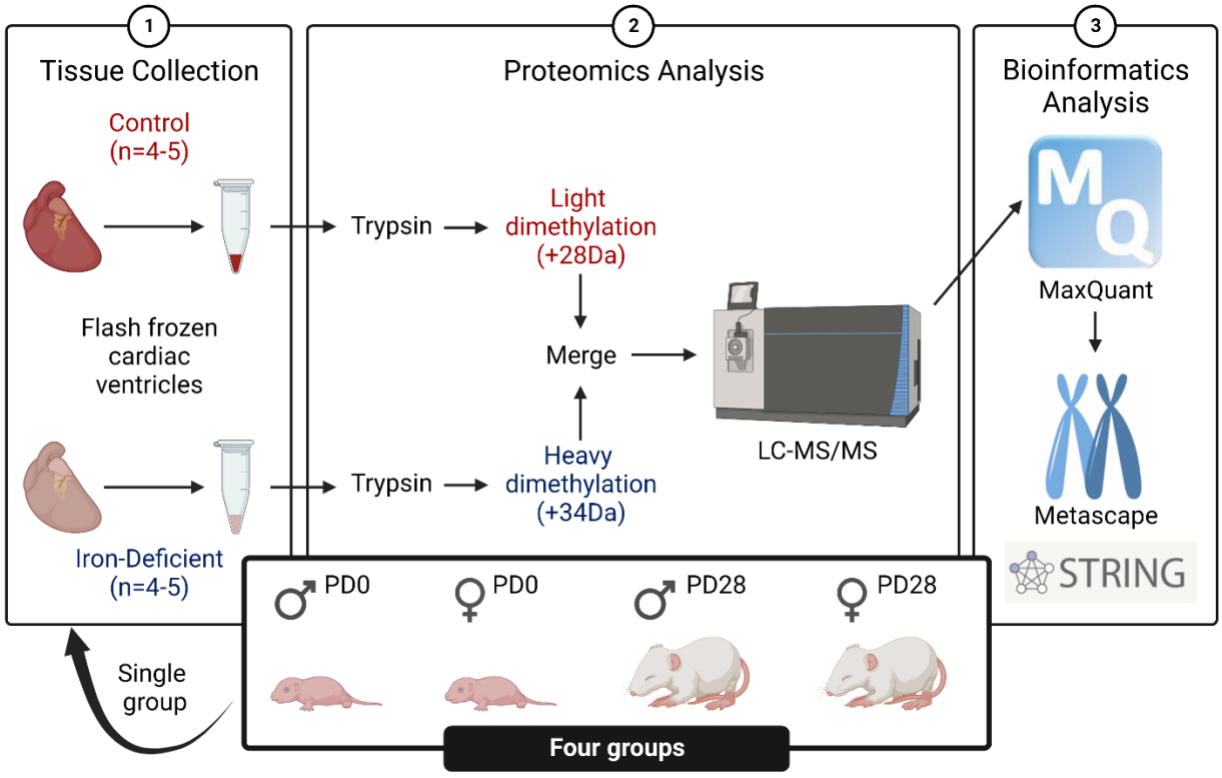

Figure 2.1. Proteomics workflow.

2.3.5 Western Blotting

Hearts from 1 male and 1 female pup from each litter at each timepoint were homogenized in lysis buffer at 0.1 mg tissue per milliliter that contained sodium orthovanadate (2 mM), phosphatase inhibitor (20 µg/ml; Calbiochem, San Diego, CA, USA), and protease inhibitor (10 µl/ml; Sigma-Aldrich). Total protein concentration of the lysate was determined by bicinchoninic acid assay (Pierce, Rockford, IL, USA). Total protein (100 µg/well) was separated on 12% SDS polyacrylamide gels—with a 3.5% stacking gel—and transferred onto a nitrocellulose membrane. Membranes were incubated with 100% blocking reagent (Odyssey PBS Blocking Buffer; Li-Cor Biosciences, Lincoln, NE, USA) for 1 h at room temperature. After washing with PBS solution, membranes were incubated overnight at 4°C in 5% blocking buffer and 0.05% Tween-PBS with primary antibodies. Secondary antibodies were incubated with 25% blocking buffer in 0.05% Tween-PBS for 1 h at room temperature, and blots were visualized by using an Odyssey near-infrared fluorescence imager and quantified by densitometry by using Odyssey v.3.0 software (Li-Cor Biosciences). Antibodies were purchased from ProteinTech Group, ProSci Incorporated, and Novus Biologicals.

2.3.6 Statistical Analyses

n values throughout represent the number of treated dams or litters; any replicates obtained from littermates of the same sex were pooled and treated as n=1. Data were analyzed by two-way ANOVA or by fitting a mixed-effects model for the effects of ID and time as implemented in GraphPad Prism 8.3.0. Sidak's post-hoc test was used for multiple comparisons of Ctl and ID groups within age groups.

2.4 Results

2.4.1 Pregnancy and Neonatal Outcomes

Prolonged dietary iron restriction caused a progressive decline in maternal Hb levels throughout gestation (**Figure 2.2 a**), though there was no evidence of reduced body weight gain (**Figure 2.2 b**) or changes in maternal food intake (data not shown). Hb levels were reduced in ID male and female pups from PD0 to PD14 but were no longer different by PD28 (P=0.85 for males; P=0.58 for females) (**Figure 2.2 c, d**).

Both male and female ID offspring were growth restricted compared to their respective controls ($P<0.001$ for both sexes; **Figure 2.2 e, f**), ranging from -20% (at PD0) to -32% (at PD4) in males, and -19% (at PD0) to 34% (at PD4) in females.

Neonatal arterial blood gas analysis (**Table 2.1**) confirmed the reduced Hb concentrations in ID offspring. Male and female ID offspring exhibited signs of reduced pCO_2 and increased pH levels compared to their respective controls at PD4, as well as reduced actual $cHCO_3^-$ levels, but no differences in standard $cHCO_3^-$. No differences in electrolytes were observed between Ctl and ID offspring of either sex at any time points assessed.

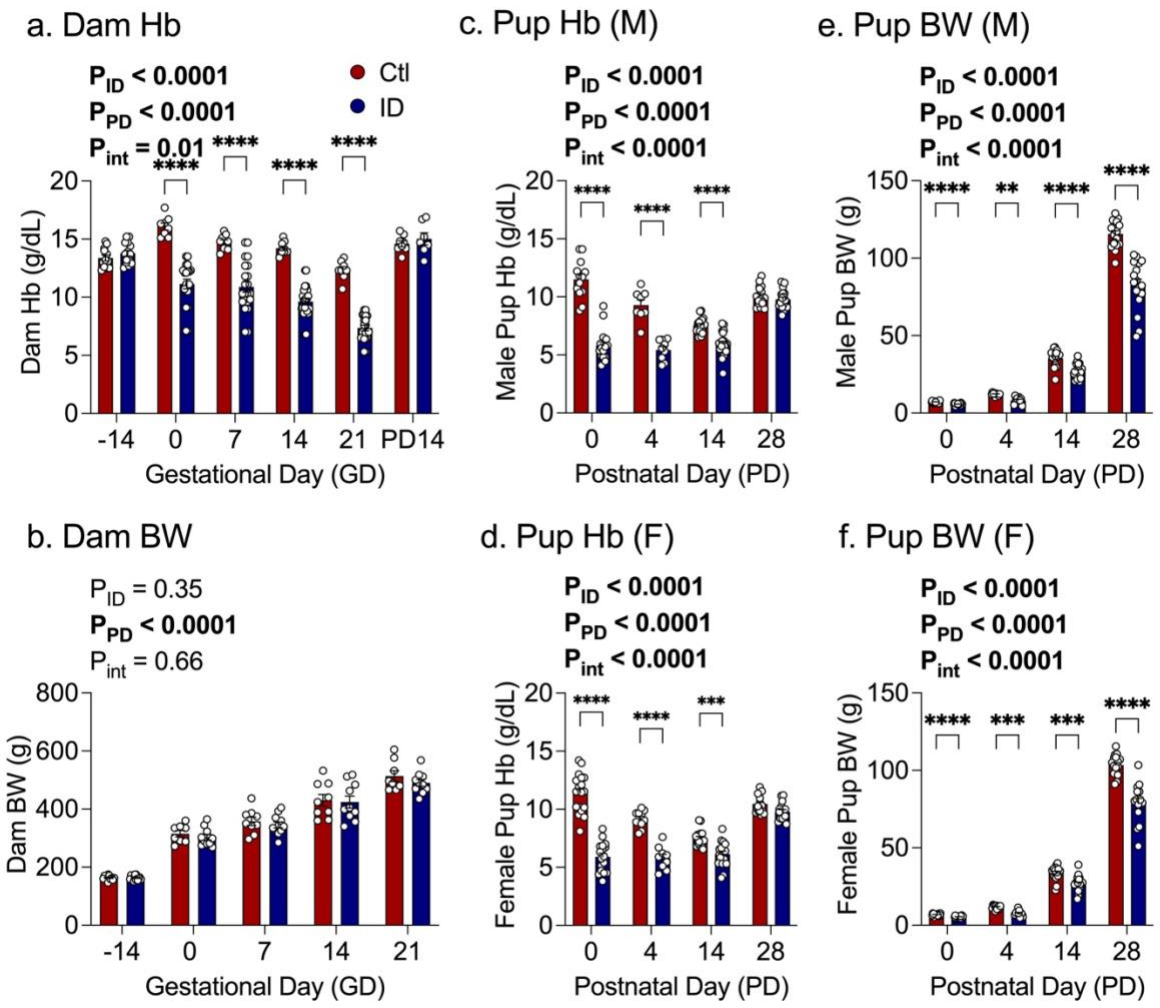

Figure 2.2. Maternal and fetal outcomes. Effects of maternal iron restriction on maternal (a) hemoglobin (Hb) and (b) body weight (BW) prior to and throughout gestation, and on offspring (c,d) Hb and (e,f) BW from postnatal day (PD)0 to 28. Male (M; left panels) and female (F; right panels) offspring data are shown separately. Each bar represents data from n=9-22 litters. **P<0.01, ***P<0.001, ****P<0.0001 for multiple comparisons.

Table 2.1. Neonatal blood gas analysis in control (Ctl) and perinatal iron deficient (ID) offspring

Male Offspring	**PD4**		**PD14**		**PD28**		**P Values**		
	Ctl (n=9-10)	**ID** (n=9-11)	**Ctl** (n=8)	**ID** (n=6)	**Ctl** (n=9-10)	**ID** (n=6)	**PD**	**ID**	**Int.**
Hct (%)	30.8±2.2	22.6±1.7****	26.0±1.5	20.7±1.7**	33.7±1.7	32.3±1.3	**<0.0001**	**<0.0001**	**0.01**
Hb (g/dL)	10.0±1.3	7.3±1.0****	8.4±0.8	6.6±1.0*	10.9±1.0	10.5±0.8	**<0.0001**	**<0.0001**	**0.01**
ctO_2 (mL/dL)	13.2±1.7	10.4±1.2**	12.8±0.9	10.2±1.2*	16.3±1.2	15.6±0.9	**<0.0001**	**0.0002**	0.18
pO_2 (mmHg)	244.9±14.4	283.8±14.2	409.1±9.3	323.5±11.1	414.2±9.2	369.2±7.6	**0.001**	0.74	0.26
sO_2 (%)	92.3±2.8	95.2±2.6	100.0±0.2	99.9±0.4	100±0.3	100.0±1.2	**0.0001**	0.39	0.78
pCO_2 (mmHg)	100.0±3.6	83.3±4.6*	42.9±2.0	42.6±2.7	46.8±3.7	40.4±1.7	**<0.0001**	**0.05**	0.21
pH	7.08±0.27	7.16±0.32*	7.40±0.21	7.39±0.25	7.39±0.29	7.44±0.15	**<0.0001**	0.09	0.20
HCO_3^- (mmol/L)	29.7±1.3	28.0±1.5*	26.1±1.0	24.9±1.1	27.0±1.2	26.6±1.0	**<0.0001**	**0.02**	0.43
$stHCO_3^-$ (mmol/L))	23.0±1.2	23.7±1.5	26.0±1.1	24.9±1.0	26.3±1.2	26.9±0.8	**<0.0001**	0.89	0.20
Na^+ (mmol/L)	137.5±1.8	145.1±3.5	131.4±1.3	129.5±1.3	137.6±1.3	138.2±1.6	**<0.0001**	0.11	0.11
K^+ (mmol/L)	3.96±0.77	3.85±0.78	4.34±0.64	4.68±0.86	4.1±0.8	4.5±0.5	**0.02**	0.21	0.32
Ca^{2+} (mmol/L)	1.41±0.41	1.46±0.36	1.31±0.40	1.24±0.41	1.16±0.39	1.20±0.36	**<0.0001**	0.91	0.45
Cl^- (mmol/L)	89±1	97±4	90±1	90.2±1.3	93.8±1.3	96.7±1.6	**<0.0001**	0.12	**0.04**
Female Offspring	**PD4**		**PD14**		**PD28**		**P Values**		
	Ctl (n=5-9)	**ID** (n=11-12)	**Ctl** (n=7-8)	**ID** (n=7-8)	**Ctl** (n=9-10)	**ID** (n=6)	**PD**	**ID**	**Int.**
Hct (%)	33.0±1.6	23.1±1.8****	24±2	21.7±1.7	33.7±1.5	34.7±1.4	**<0.0001**	**0.0007**	**<0.0001**
Hb (g/dL)	10.6±0.9	7.4±1.0****	7.8±1.0	7.0±1.0	10.9±0.9	11.2±0.8	**<0.0001**	**0.0003**	**<0.0001**
ctO_2 (mL/dL)	13.3±1.6	10.7±1.4**	12.0±1.3	10.7±1.1	16.4±1.1	16.6±1.0	**<0.0001**	0.13	**0.02**
pO_2 (mmHg)	177.2±13.3	319.9±14.3	365±11	350±11	423±10	349±7	**0.0179**	0.6693	0.0838
sO_2 (%)	86.5±3.4	95.5±2.7**	99.9±0.4	99.8±0.5	100.0±0.2	99.9±0.2	**<0.0001**	0.09	**0.04**
pCO_2 (mmHg)	123.3±4.3	86.6±3.9****	40.5±2.1	40.8±1.6	40.6±2.4	38.5±2.0	**<0.0001**	**0.0005**	**0.0002**
pH	7.03±0.25	7.13±0.27***	7.42±1.21	7.40±1.7	7.43±0.21	7.44±0.15	**<0.0001**	**0.045**	**0.003**
HCO_3^- (mmol/L)	30.8±1.3	27.6±1.3****	25.8±1.3	24.8±1.0	26.5±1.1	25.8±1.2	**<0.0001**	**0.001**	**0.04**
$stHCO_3^-$ (mmol/L)	21.9±1.4	22.9±1.4	26.0±1.3	25.0±1.0	26.7±0.9	26.3±1.0	**<0.0001**	0.83	0.11
Na^+ (mmol/L)	138.2±1.8	145.8±3.7	130±1	129±1	139.1±1.2	135.8±1.1	**<0.0001**	0.11	0.19
K^+ (mmol/L)	3.52±0.72	3.74±0.74	4.47±0.94	4.38±0.69	4.02±0.70	4.46±0.75	**0.002**	0.88	0.15
Ca^{2+} (mmol/L)	1.53±0.41	1.50±0.48	1.15±0.46	1.20±0.36	1.27±0.29	1.20±0.38	**<0.0001**	0.85	0.71
Cl^- (mmol/L)	87±1	98±4	89±1	90±1	95±1	96±1	**0.0009**	0.05	0.07

Data are mean±SEM. P values denote 2-way ANOVA outcomes for postnatal day (PD), ID, and interaction (Int.). *P<0.05, **P<0.01, ***P<0.001, ****P<0.0001 for Sidak posthoc tests within the same PD. ctO_2, oxygen content; HCO_3^-, actual bicarbonate; stHCO3-, standard bicarbonate.

2.4.2 Cardiac Morphology and Function

Male and female perinatal ID pups had enlarged hearts (when normalized to body weight) throughout the entire postnatal period (**Figure 2.3 a, b**). This increase in relative heart size was more pronounced than all other organs studied (**Table 2.2**). Cardiac measurements assessed by echocardiography (**Table 2.3**) revealed increased left ventricular wall thicknesses and interventricular septal widths, as well as increased ventricular diameters and volumes when normalized to body weight. Interestingly, cardiomyocyte size was not appreciably altered by perinatal ID in either sex (**Figure 2.3 c, d**). Thus, when absolute heart weight was normalized to cardiomyocyte size as an estimate for cardiomyocyte numbers, these values were decreased in PD28 ID male and female offspring (**Figure 2.3 e, f**) – a time-point when cardiomyocytes no longer retain their proliferative ability (356). Furthermore, cardiac β-myosin heavy chain (β-MHC) to α-MHC protein expression (**Figure 2.3 g, h**) as well as gene expression ratio for Myh7 to Myh6 (data not shown), which encode β-MHC to α-MHC proteins, respectively, were elevated at PD14 in perinatal ID male offspring. Myh7 to Myh6 ratios were also increased in Perinatal ID females at PD14 and PD28 (data not shown), albeit these were not accompanied by corresponding increases in protein levels (**Figure 2.3 i**).

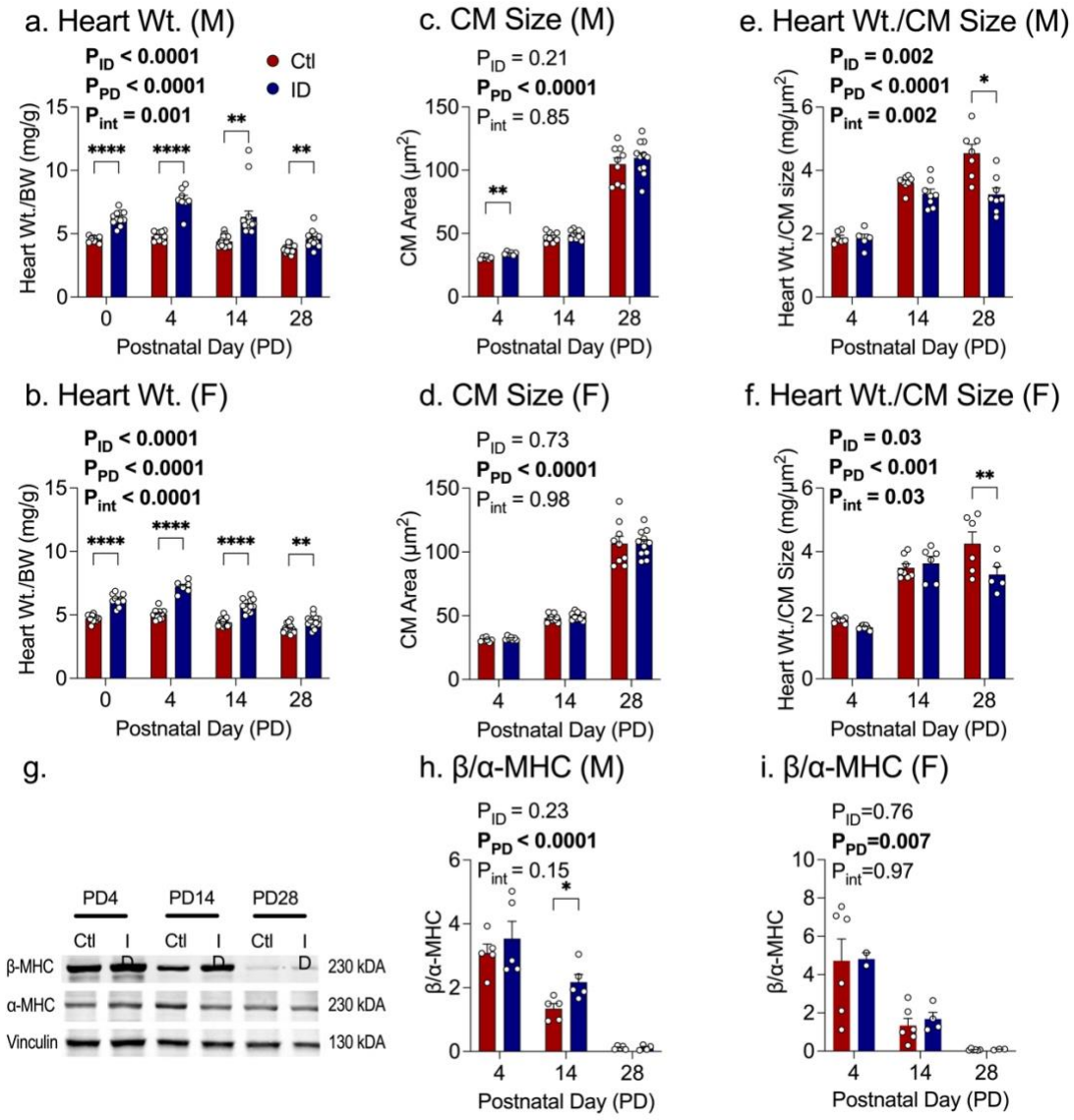

Figure 2.3. Cardiac weigh, histology, and protein expression. Effects of perinatal iron deficiency (ID) throughout the neonatal period on (a, b) heart weights (Wt.) normalized to body weights (BW); (c, d) cardiomyocyte (CM) size; (e, f) CM size normalized to absolute heart Wt. (g) representative western blot depicting male offspring cardiac β-myosin heavy chain (β-MHC) and α-MHC protein expression, and (h, i) β-MHC to α-MHC ratios (depicted in solid bars) and gene expression ratio for Myh7 to Myh6 (shown in open bars), which encode β-MHC to α-MHC proteins, respectively, from PD4-PD28. Male (M) and female (F) offspring data are shown separately. Each bar represents data from n=7-20 litters. Data are analyzed by two-way ANOVA with Sidak's *post hoc* test where *P<0.05, **P<0.01, ****P<0.0001 for multiple comparisons.

Table 2.2. Organ weights. Control (Ctl) and perinatal iron deficient (ID) offspring

Male Offspring	**PD4**		**PD14**		**PD28**		**P Values**		
	Ctl (n=9-10)	**ID** (n=4-7)	**Ctl** (n=6-7)	**ID** (n=6-10)	**Ctl** (n=8-9)	**ID** (n=7-11)	**PD**	**ID**	**Int.**
Hb (g/dL)	9.4±0.4	5.3±0.3****	7.5±0.2	5.5±0.3****	9.9±0.2	9.6±0.3	**<0.0001**	**<0.0001**	**<0.0001**
Bodyweight (g)	12.13±0.28	7.98±0.81**	39.2±0.7	27.0±1.7****	117.1±2.6	81.1±5.2****	**<0.0001**	**<0.0001**	**<0.0001**
Kidneys (g)	0.152±0.007	0.105±0.010**	0.454±0.014	0.345±0.029*	1.34±0.07	1.08±0.08	**<0.0001**	**0.008**	**0.05**
Brain (g)	0.355±0.010	0.260±0.029	0.991±0.021	0.775±0.038**	1.19±0.02	1.05±0.03*	**<0.0001**	**<0.0001**	**0.03**
Liver (g)	0.338±0.001	0.298±0.027*	1.16±0.041	0.819±0.090*	5.15±0.25	3.98±0.30*	**<0.0001**	**0.002**	**0.009**
Heart (g)	0.048±0.0001	0.058±0.005	0.171±0.006	0.154±0.009	0.452±0.022	0.368±0.026	**<0.0001**	**0.01**	**0.01**
Kidneys (mg/g)	12.6±0.3	13.9±0.5*	11.5±0.3	13.1±0.5**	11.5±0.4	12.9±0.3	**0.004**	**0.0009**	0.87
Brain (mg/g)	29.5±0.7	36.4±2.2***	25.2±0.7	29.9±1.5**	10.3±0.2	13.0±1.0	**<0.0001**	**0.0002**	0.08
Liver (mg/g)	33.8±1.4	39.0±2.1*	29.1±0.7	30.7±0.8	43.7±1.8	46.6±1.2	**<0.0001**	**0.02**	0.39
Heart (mg/g)	4.8±0.1	7.7±0.4****	4.3 ± 0.1	6.3±0.4****	3.9±0.1	4.9±0.4*	**<0.0001**	**<0.0001**	**0.004**
Female Offspring	**PD4**		**PD14**		**PD28**		**P Values**		
	Ctl (n=5-10)	**ID** (n=6-8)	**Ctl** (n=6-7)	**ID** (n=6-9)	**Ctl** (n=6-9)	**ID** (n=9-11)	**PD**	**ID**	**Int.**
Hb (g/dL)	9.3±0.2	5.7±0.3****	7.2±0.1	5.7±0.3**	10.6±0.2	9.7±0.2*	**<0.0001**	**<0.0001**	**<0.0001**
Bodyweight (g)	11.58±0.42	7.74±0.75**	36.6±0.6	27.1±2.1**	102.9±1.8	77.7±4.4***	**<0.0001**	**<0.0001**	**0.0002**
Kidneys (g)	0.144±0.007	0.104±0.009*	0.447±0.013	0.386±0.024	1.20±0.02	1.12±0.09	**<0.0001**	**0.02**	0.77
Brain (g)	0.352±0.012	0.254±0.026*	0.941±0.020	0.805±0.038	1.16±0.02	1.08±0.02*	**<0.0001**	**<0.0001**	0.48
Liver (g)	0.394±0.016	0.280±0.027*	1.11±0.028	0.918±0.085	4.59±0.19	3.88±0.33	**<0.0001**	**0.006**	0.08
Heart (g)	0.057±0.002	0.052±0.005	0.166±0.006	0.183±0.013	0.418±0.017	0.373±0.027	**<0.0001**	0.31	0.09
Kidneys (mg/g)	12.4±0.2	14.9±0.9	12.1±0.2	13.4±0.1	11.4±0.3	13.2±0.6	**0.04**	**<0.0001**	0.45
Brain (mg/g)	30.6±0.6	35.3±1.9	25.5±0.6	25.5±0.6	11.2±0.2	12.1±0.8	**<0.0001**	**0.009**	0.28
Liver (mg/g)	34.9±1.0	39.2±1.4	33.0±1.3	30.0±0.3	43.5±1.0	46.6±1.7	**<0.0001**	**0.005**	0.48
Heart (mg/g)	5.0±0.1	7.4±0.3***	4.5±0.1	6.8±0.6*	4.0±0.2	4.5±0.3	**<0.0001**	**<0.0001**	**0.004**

Data are mean±SEM. P values denote 2-way ANOVA outcomes for postnatal day (PD), ID, and interaction (Int.). *P<0.05, **P<0.01, ***P<0.001, ****P<0.0001 for Sidak posthoc tests within the same PD.

Table 2.3 Neonatal cardiac measurements. In diastole in control (Ctl) and perinatal iron deficient (ID) offspring

Male Offspring	**PD4**		**PD14**		**PD28**		**P Values**		
	Ctl (n=9-10)	**ID** (n=7-8)	**Ctl** (n=6-10)	**ID** (n=8-10)	**Ctl** (n=9)	**ID** (n=9-11)	**PD**	**ID**	**Int.**
LVPW / BW (mm/g)	0.071±0.003	0.117±0.015****	0.028±0.002	0.043±0.004	0.013±0.0002	0.018±0.002	**<0.0001**	**<0.0001**	**0.002**
IVS / BW (mm/g)	0.069±0.003	0.115±0.010****	0.024±0.002	0.035±0.003	0.011±0.001	0.015±0.001	**<0.0001**	**<0.0001**	**0.0002**
Diameter / BW (mm/g)	0.25±0.007	0.38±0.034****	0.12±0.003	0.16±0.009	0.051±0.001	0.063±0.004	**<0.0001**	**<0.0001**	**0.0004**
LVPW / Diameter	0.24±0.01	0.33±0.03**	0.24±0.02	0.28±0.02	0.24±0.01	0.24±0.01	0.08	**0.002**	0.07
IVS / Diameter	0.27±0.009	0.31±0.03	0.21±0.01	0.23±0.01	0.22±0.009	0.24±0.02	**<0.0001**	**0.02**	0.72
Volume / BW (µL/g)	3.1±0.14	4.0±0.38*	2.5±0.17	3.0±0.21	1.5±0.03	1.5±0.12	**<0.0001**	**0.003**	0.09
Female Offspring	**PD4**		**PD14**		**PD28**		**P Values**		
	Ctl (n=9)	**ID** (n=8)	**Ctl** (n=7)	**ID** (n=8)	**Ctl** (n=9-10)	**ID** (n=11)	**PD**	**ID**	**Int.**
LVPW / BW (mm/g)	0.065±0.003	0.11±0.01****	0.029±0.003	0.047±0.005*	0.014±0.001	0.017±0.001	**<0.0001**	**<0.0001**	**<0.0001**
IVS / BW (mm/g)	0.064±0.005	0.11±0.01****	0.026±0.001	0.042±0.005*	0.012±0.001	0.016±0.001	**<0.0001**	**<0.0001**	**<0.0001**
Diameter / BW (mm/g)	0.27±0.01	0.37±0.03****	0.12±0.002	0.17±0.02*	0.05±0.002	0.07±0.005	**<0.0001**	**<0.0001**	**0.02**
LVPW / Diameter	0.24±0.01	0.32±0.02**	0.24±0.02	0.28±0.03	0.26±0.02	0.24±0.01	0.24	**0.02**	**0.01**
IVS / Diameter	0.23±0.01	0.29±0.02*	0.22±0.01	0.25±0.02	0.23±0.02	0.22±0.02	**0.04**	0.06	0.05
Volume / BW (µL/g)	3.4±0.17	3.8±0.25	2.4±0.08	3.3±0.43**	1.5±0.09	1.9±0.12*	**<0.0001**	**0.002**	0.36

Data are mean±SEM. P values denote 2-way ANOVA outcomes for postnatal day (PD), ID, and interaction (Int.). *P<0.05, **P<0.01, ***P<0.001, ****P<0.0001 for Sidak posthoc tests within the same PD. Bodyweight, BW; interventricular septum, IVS; left ventricle posterior wall, LVP.

Cardiac function was assessed in neonates by echocardiography. Indices of systolic function are shown in **Table 2.4**; all parameters assessed changed with PD. Despite increased heart size in perinatal ID offspring, neither males nor females exhibited increased CO (normalized to body weight). With no changes in HR due to ID (under anesthesia), the lack of CO increase could be attributed to systolic dysfunction, resulting from reduced ejection fraction and fractional shortening. Correspondingly, offspring oxygen delivery (DO_2) was markedly reduced in ID offspring, even when normalized to body weight. S' peak velocity, as well as aortic peak velocity in males were also reduced with ID.

Indices of diastolic function are shown in **Table 2.5**. IVCT, E-to-e' ratio, and TEI index were reduced in ID females, but not in males, throughout the entire postnatal period. Mitral valve velocities, which are additional markers of diastolic dysfunction, were assessed by tissue Doppler imaging, and revealed reduced e' wave peak velocity in ID female offspring from PD4 to 28, whereas no differences were evident in male offspring. Altogether, these data suggest a profound diastolic dysfunction in female offspring. However, a' wave peak velocities were reduced in both male and female offspring. Moreover, left atrial enlargement, a hallmark of chronic pressure and volume overload (357), was evident in both male and female ID offspring (after normalizing to bodyweight) from PD4 through PD28, suggesting males are not completely spared.

Table 2.4. Neonatal systolic function. In control (Ctl) and perinatal iron deficient (ID) offspring

	PD4		PD14		PD28		P Values		
Male Offspring	**Ctl** (n=8-10)	**ID** (n=6-8)	**Ctl** (n=6-7)	**ID** (n=10)	**Ctl** (n=5-10)	**ID** (n=10-11)	**PD**	**ID**	**Int.**
HR (bpm)	298±9	273±23	344±9	329±13	368±8	370±10	**<0.0001**	0.22	0.57
EF (%)	72±2	62±5	63±2	50±2***	70.±2	74±2	**<0.0001**	**0.001**	**0.03**
FS (%)	41±2	33±3*	34±2	26±1*	43±2	43±2	**<0.0001**	**0.002**	**0.04**
SV / BW (mL/g)	2.2±0.09	2.5±0.33	1.6±0.06	1.5±0.10	1.1±0.04	1.1±0.10	**<0.0001**	0.37	0.72
CO / BW (mL/min*g)	0.67±0.03	0.69±0.09	0.53±0.02	0.49±0.04	0.40±0.01	0.41±0.03	**<0.0001**	0.78	0.97
DO2 / BW (mL/min*g)	0.084±0.005	0.050±0.008****	0.051±0.003	0.035±0.003**	0.056±0.002	0.054±0.004	**<0.0001**	**<0.0001**	**0.007**
MV S' (mm/s)	13±1	12±1	20±2	17±1	31±2	28±1	**<0.0001**	**0.03**	0.86
Desc Aorta Vel (mm/s)	585±31	517±35	720±33	601±35	1073±45	913±29**	**<0.0001**	**0.0003**	0.42
Female Offspring	**Ctl** (n=9-10)	**ID** (n=8-11)	**Ctl** (n=9-10)	**ID** (n=8-11)	**Ctl** (n=9-10)	**ID** (n=8-11)	**PD**	**ID**	**Int.**
HR (bpm)	310±12	295±16	318±13	335±8	404±14	353±8	**<0.0001**	0.08	**0.02**
EF (%)	71±3	68±4	61±2	54±2**	77±2	70±3	**<0.0001**	**0.009**	0.61
FS (%)	39±2	37±4	32±1	28±1	47±2	41±3	**<0.0001**	**0.01**	0.65
SV / BW (mL/g)	2.4±0.15	2.5±0.12	1.5±0.05	1.8±0.18	1.1±0.06	1.3±0.08	**<0.0001**	**0.03**	0.79
CO / BW (mL/min*g)	0.72±0.04	0.73±0.04	0.47±0.02	0.59±0.06	0.46±0.03	0.47±0.02	**<0.0001**	0.14	0.23
DO2 / BW (mL/min*g)	0.090±0.005	0.058±0.004****	0.047±0.003	0.044±0.004	0.068±0.004	0.062±0.003	**<0.0001**	**0.0001**	**0.0009**
MV S' (mm/s)	16±2	14±1	20±1	17±1	31±2	27±1	**<0.0001**	**0.02**	0.81
Desc Aorta Vel (mm/s)	502±28	527±32	677±46	656±47	926±35	930±46	**<0.0001**	0.85	0.89

Data are mean±SEM. P values denote 2-way ANOVA outcomes for postnatal day (PD), ID, and interaction (Int.). *P<0.05, **P<0.01, ***P<0.001, ****P<0.0001 for Sidak posthoc tests within the same PD. Bodyweight, BW; cardiac output, CO; descending aorta velocity, Desc Aorta Vel; ejection fraction, EF; fractional shortening, FS; heart rate, HR; mitral valve systolic wave, MV S'; oxygen elivery, DO2; stroke volume, SV.

Table 2.5. Neonatal diastolic function. In control (Ctl) and perinatal iron deficient (ID) offspring.

Male Offspring	**PD4**		**PD14**		**PD28**		**P Values**		
	Ctl (n=9-10)	**ID** (n=4-7)	**Ctl** (n=6-7)	**ID** (n=6-10)	**Ctl** (n=8-9)	**ID** (n=7-11)	**PD**	**ID**	**Int.**
L Atrium / BW (mm/g)	0.16±0.01	0.27±0.05****	0.07±0.01	0.09±0.01	0.03±0.00	0.04±0.00	**<0.0001**	**<0.0001**	**0.0008**
E/A	1.0±0.02	0.9±0.03	1.3±0.09	1.1±0.04	1.2±0.05	1.4±0.07	**<0.0001**	0.30	**0.02**
AET (ms)	86±3	89±5	71±4	77±4	60±3	61±2	**<0.0001**	0.33	0.77
IVCT (ms)	17±1	16±1	21±1	21±2	20±2	16±1	**0.03**	0.30	0.27
IVRT (ms)	27±2	27±1	25±1	27±1	23±1	23 ±0.6	**0.004**	0.47	0.47
MV A (mm/s)	480±14	493±34	553±38	523±54	705±38	661±45	**<0.0001**	0.68	0.77
MV E (mm/s)	473±15	445±33	695±28	643±41	851±30	864±29	**<0.0001**	0.67	0.78
MV a' (mm/s)	14±1	12±1	24±3	19±2	36±2	30±2	**<0.0001**	**0.01**	0.70
MV e' (mm/s)	13±1	11±1	25±3	22±2	33±2	30±2	**<0.0001**	0.09	0.99
TEI index	0.48±0.03	0.49±0.04	0.66±0.03	0.65±0.05	0.74±0.08	0.66±0.04	**0.0002**	0.62	0.52
e'/a'	0.92±0.07	0.88±0.10	1.1±0.11	1.1±0.09	0.93±0.05	1.0±0.09	0.21	0.77	0.73
a'/e'	1.1±0.10	1.2±0.13	0.98±0.08	0.73±0.17	1.1±0.06	1.1±0.09	**0.02**	0.32	0.35
E/e'	39±3	43±5	30±3	31±3	27±2	29±2	**<0.0001**	0.19	0.99
Female Offspring	**PD4**		**PD14**		**PD28**		**P Values**		
	Ctl (n=5-10)	**ID** (n=6-8)	**Ctl** (n=6-7)	**ID** (n=6-9)	**Ctl** (n=6-9)	**ID** (n=9-11)	**PD**	**ID**	**Int.**
L Atrium / BW (mm/g)	0.18±0.01	0.23±0.02**	0.07±0.005	0.10±0.008*	0.03±0.002	0.04±0.004	**<0.0001**	**0.0002**	0.19
E/A	1.10±0.03	1.00±0.04	1.76±0.18	1.2±0.13	1.3±0.06	1.3±0.07	**0.007**	0.16	0.17
AET (ms)	80±3	85±6	72±2	76±2	56±3	62±3	**<0.0001**	0.09	0.84
IVCT (ms)	20±1	16±1	22±2	19±2	22±2	18±1	0.18	**0.01**	0.78
IVRT (ms)	26±2	24±2	27±1	26±1	23±1	22±1	**0.03**	0.49	0.78
MV A (mm/s)	414±16	462±22	382±27	544±64	715±35	644±26	**<0.0001**	0.29	**0.03**
MV E (mm/s)	502±38	460±21	647±17	638±37	887±35	831±34	**<0.0001**	0.27	0.54
MV a' (mm/s)	14±1	13±1	20±3	18±3	43±4	25±2****	**<0.0001**	**0.0007**	**0.007**
MV e' (mm/s)	15±1	10±2	26±1	18±2	40±4	27±2***	**<0.0001**	**0.0002**	0.13
TEI index	0.58±0.05	0.49±0.05	0.68±0.04	0.61±0.04	0.84±0.08	0.66±0.05	**0.0004**	**0.01**	0.42
e'/a'	1.1±0.12	0.82±0.10	1.5±0.29	1.1±0.18	0.97±0.11	1.1±0.05	0.29	0.47	0.40
a'/e'	0.99±0.11	1.4±0.20	0.79±0.11	0.98±0.13	1.1±0.13	0.95±0.04	0.39	0.65	0.09
E/e'	35±1	44±8	25±1	37±3	24±2	33±3	**0.008**	**0.002**	0.99

Data are mean±SEM. P values denote 2-way ANOVA outcomes for postnatal day (PD), ID, and interaction (Int.). *P<0.05, **P<0.01, ***P<0.001, ****P<0.0001 for Sidak posthoc tests within the same PD. Aortic ejection time, AET; early left ventricular filling velocity, E or MV E; late left ventricular filling velocity, A or MV A; early mitral valve filling velocity, e' or MV e'; isovolumetric contraction time, IVCT; isovolumetric relaxation time, IVRT; late left ventricular filling velocity, A or MV A; late mitral valve filling velocity, a' or MV a'; left atrium diameter, LA diameter; myocardial performance index, TEI index.

Indices of pulmonary artery and venous flow are shown in **Table 2.6**. The PAT and PAT-to-PET ratio were similar between groups, albeit the PET increased overall in both male and female ID offspring (after normalizing to bodyweight) from PD4 through PD28, suggesting males are not completely spared.

Indices of pulmonary artery and venous flow are shown in **Table 2.6**. The PAT and PAT-to-PET ratio were similar between groups, albeit the PET increased overall in both male and female ID offspring. Pulmonary artery peak velocity was increased in female ID offspring from PD4 through 28. In ID females the s-to-d wave ratio was increased, and the d wave velocity was decreased, whereas in males, a wave velocity was increased. While an increase in pulmonary artery peak velocity may indicate increased pulmonary artery pressures in the females, there were no changes in PAT and PAT-to-PET ratio, which are more specific measures of elevated pulmonary arterial pressures.

Table 2.6. Neonatal pulmonary function. In control (Ctl) and perinatal iron deficient (ID) offspring.

Male Offspring	**PD4**		**PD14**		**PD28**		**P Values**		
	Ctl (n=5-10)	**ID** (n=6-8)	**Ctl** (n=3-7)	**ID** (n=8-10)	**Ctl** (n=7-9)	**ID** (n=8-11)	**PD**	**ID**	**Int.**
S wave (mm/s)	216±15	260±26	224±34	255±21	259±18	274±18	0.25	0.06	0.76
D wave (mm/s)	219±16	271±11	289±17	282±21	397±10	347±23	**<0.0001**	0.76	**0.02**
A wave (mm/s)	68±10	149±34	114±8	155±23	165±32	187±32	**0.049**	**0.02**	0.55
A duration (ms)	13±2	22±3	18±4	23±3	17±1	20±3	0.69	**0.005**	0.45
S/D	1.06±0.13	0.98±0.07	0.65±0.04	0.89±0.04	0.66±0.05	0.80±0.03	**0.0008**	0.12	0.15
PAT (ms)	23±1	25±2	27±2	28±2	31±2	29±1	**0.0006**	0.67	0.21
PET (ms)	91±2	96±6	82±2	90.03±2	76±3	77±1	**<0.0001**	**0.03**	0.38
PV (mm/s)	601±30	543±22	595.28±28	649.97±37	780±41	858±40	**<0.0001**	0.23	0.11
PAT/PET	0.25±0.01	0.26±0.01	0.33±0.01	0.31±0.01	0.41±0.02	0.37±0.01	**<0.0001**	0.32	0.31
Female Offspring	**PD4**		**PD14**		**PD28**		**P Values**		
	Ctl (n=5-10)	**ID** (n=6-8)	**Ctl** (n=6-7)	**ID** (n=8-9)	**Ctl** (n=7-9)	**ID** (n=8-11)	**PD**	**ID**	**Int.**
S wave (mm/s)	200±14	235±23	197±20	257±17*	270±22	243±12	**0.048**	0.06	**0.01**
D wave (mm/s)	258±17	241±13	325±17	295±29	422±28	343±20*	**<0.0001**	**0.047**	0.21
A wave (mm/s)	92±11	106±17	107±12	123±15	203±34	156±26	**0.002**	0.76	0.29
A duration (ms)	15±2	21±4	21±3	20±2	17±2	19±2	0.78	0.19	0.68
S/D	0.78±0.04	1.02±0.17	0.62±0.07	0.94±0.09*	0.64±0.04	0.73±0.05	**0.03**	**0.001**	0.27
PAT (ms)	22±1	25±2	28±1	29±2	31±2	29±1	**0.0002**	0.46	0.29
PET (ms)	85±0.86	92±3	86±3	88±2	78±3	81±1	**<0.0001**	**0.02**	0.45
PV (mm/s)	536±14	674±48**	624±28	717±30	749±15	952±38****	**<0.0001**	**<0.0001**	0.22
PAT/PET	0.25±0.01	0.27±0.01	0.33±0.02	0.33±0.02	0.39±0.02	0.36±0.02	**<0.0001**	0.80	0.34

Data are mean±SEM. P values denote 2-way ANOVA outcomes for postnatal day (PD), ID, and interaction (Int.). *P<0.05, **P<0.01, ***P<0.001, ****P<0.0001 for Sidak posthoc tests within the same PD. Control, Ctl; pulmonary artery acceleration time, PAT; pulmonary artery ejection time, PET; pulmonary artery peak velocity, PV; pulmonary vein atrial reversal, A wave; pulmonary vein atrial reversal duration, A duration; pulmonary vein diastolic wave, D wave; pulmonary vein systolic wave, S wave.

2.4.3 Proteomic Analysis

Quantitative shotgun proteomics analyses of offspring heart tissues at PD0 and PD28 were performed and analyzed using MaxQuant at 1% false discovery rate (FDR) and as determined by interquartile boxplot analysis (**Figure 2.4** and **2.5**). In PD0 male offspring hearts, 54 and 45 proteins were downregulated and upregulated, respectively, with ID. By PD28, despite recovering from anemia, 59 and 67 proteins were downregulated and upregulated, respectively in ID offspring (**Figure 2.4**). STRING-db analysis revealed reduced expression at PD0 in ID male offspring related to supramolecular fiber organization and actin cytoskeleton (FDR=0.007, FDR=0.01; respectively) (**Figure 2.6 a**), which was more statistically significant by PD28 (FDR=8e-7, FDR=4e-5; respectively) (**Figure 2.6 b**). Notable downregulated proteins at PD0 included ELN, COL1A2, FBLN5, MYH8 MYH11, whereas at PD28, MYH1, MYH2, MYH11, MYH13, MYH15, COL1A1, COL1A2, and FBLN5 were downregulated in ID offspring. Other enriched pathways appeared in male ID offspring by PD28 including cellular responses to stress (FDR=0.02), RNA metabolism (FDR=0.049), and organelle structure (FDR=0.03). Though not explored to any appreciable extent here, it is noteworthy that male ID hearts were enriched in proteins related to mitochondrial oxidative phosphorylation at both time points studied (FDR=0.04 at PD0; FDR=0.0001 at PD28).

In PD0 female offspring hearts, 63 and 18 proteins were downregulated and upregulated, respectively, with ID (**Figure 2.6 c**). STRING-db analysis revealed reduced pathway expression in ID females at PD0 related to supramolecular fiber organization (FDR=0.008) as well as actin cytoskeleton (FDR=0.03); specific proteins included MYH3 and MYH8 isoforms, CALM1 and ATP2A1, but tended to be diverse in their gene ontology. As with males, by PD28 proteome changes were more marked, with 82 and 56 proteins downregulated and upregulated in ID offspring (**Figure 2.6 d)**. As with males, by PD28 proteome changes were more marked, with 82 and 56 proteins downregulated and upregulated in ID offspring (**Figure 2.6 d)**. STRING-db analysis revealed more pronounced reductions in pathway

expression related to supramolecular fiber organization (FDR=5e-6) as well as actin cytoskeleton (FDR=0.003). At this time, downregulation of MYH multiple isoforms, as well as ACTN1, COL4A1, and FBN1 were most apparent. Notably, there was also protein enrichment in ID females at PD28, which included TTN, MYL isoforms, among others.

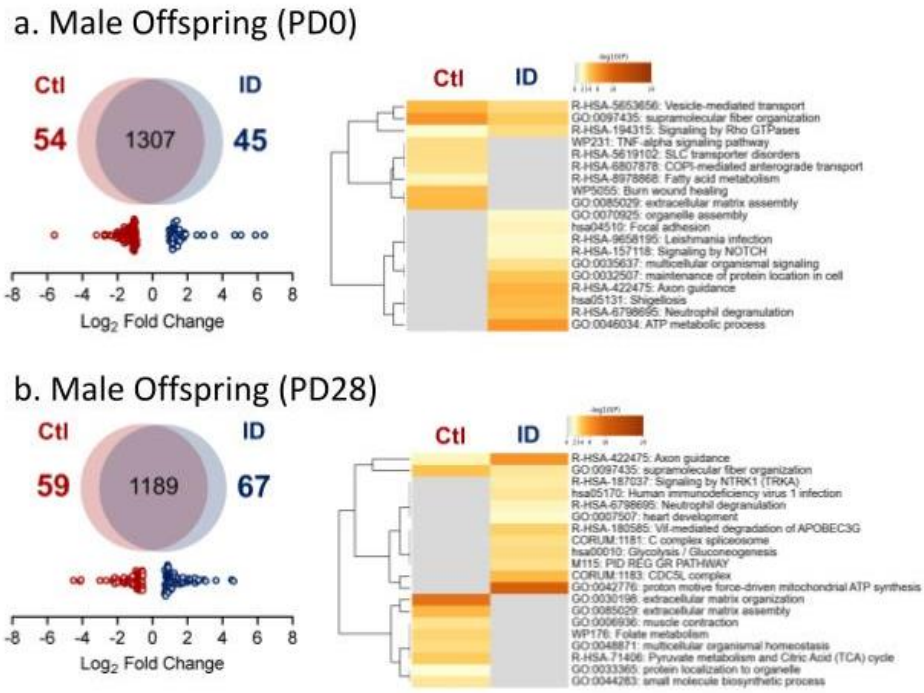

Figure 2.4. Total proteins upregulated in males. In (a) postnatal day (PD)0 and (b) PD28. Heatmaps generated using Metascape show pathway enrichment. Each group used 4-5 biological replicates.

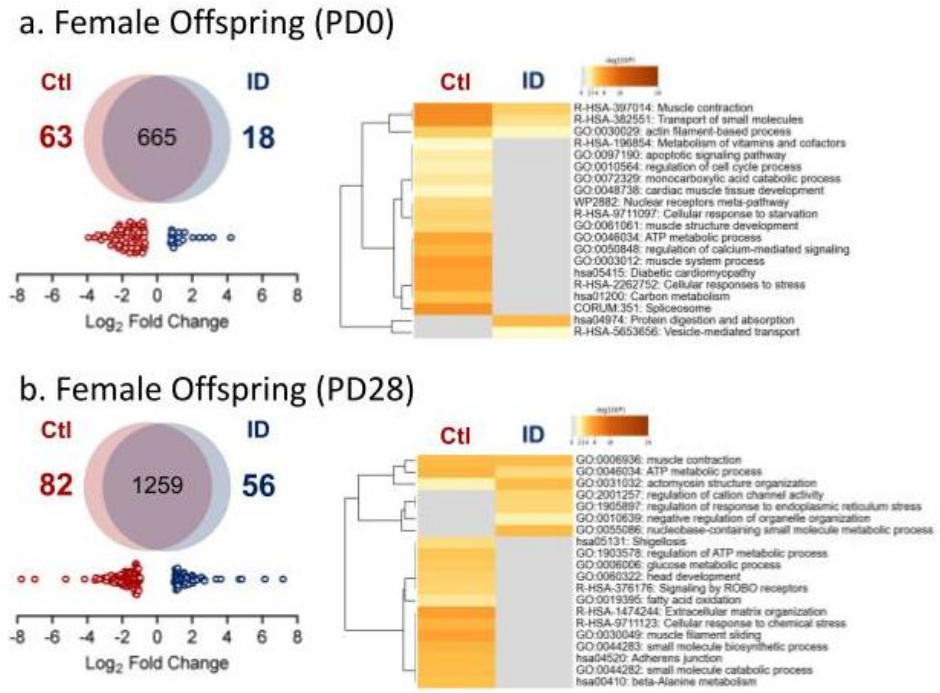

Figure 2.5. Total proteins upregulated in females. In (a) postnatal day (PD)0 and (b) PD28. Heatmaps generated using Metascape show pathway enrichment. Each group used 4-5 biological replicates.

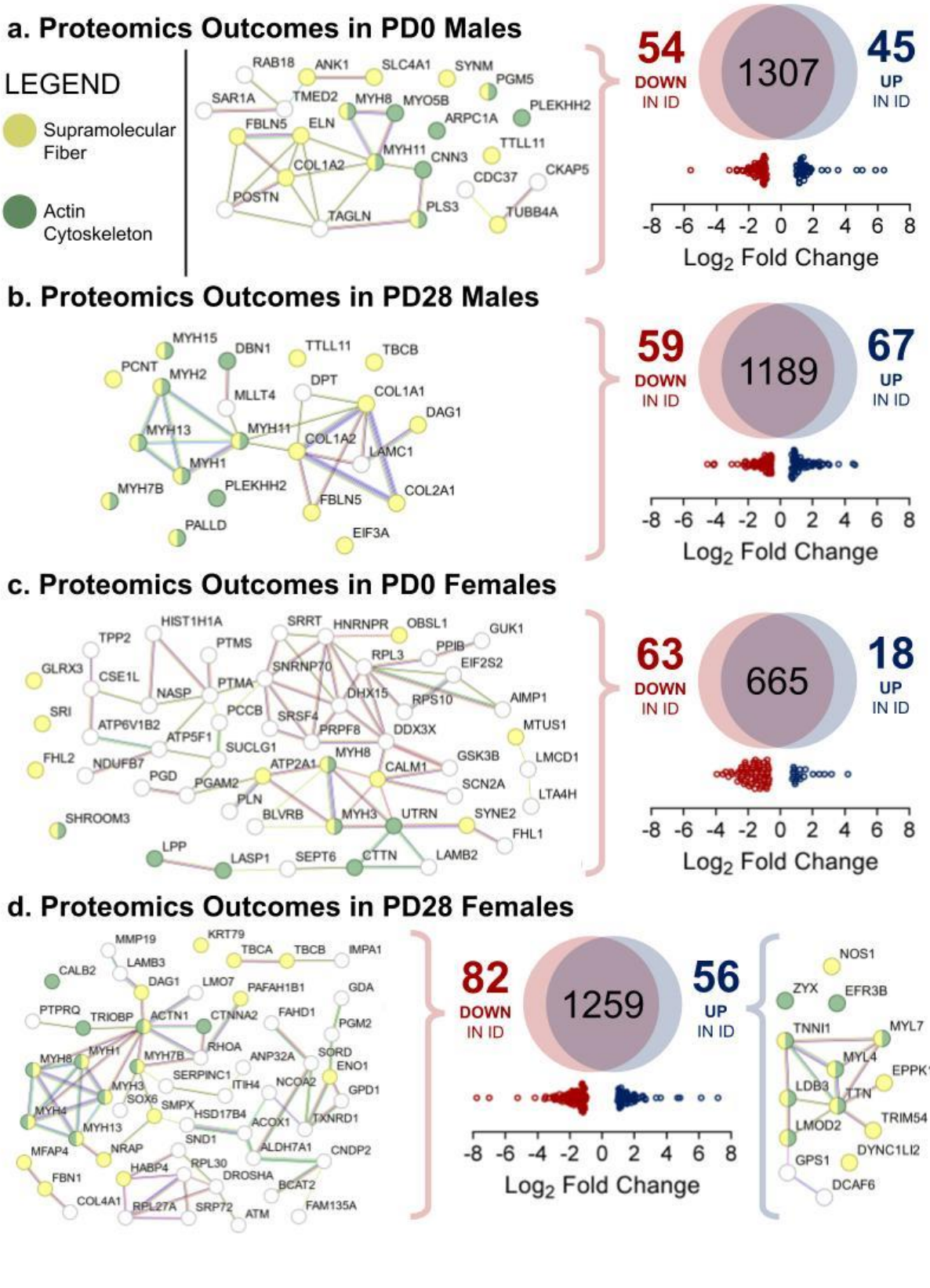
a. Proteomics Outcomes in PD0 Males
LEGEND
Supramolecular Fiber
Actin Cytoskeleton
RAB18
ANK1
SLC4A1
SYNM
PGM5
SAR1A
TMED2
MYH8
MYO5B
PLEKHH2
ARPC1A
FBLN5
ELN
TTLL11
MYH11
CNN3
COL1A2
CDC37
CKAP5
POSTN
TAGLN
PLS3
TUBB4A
54
DOWN IN ID
1307
45
UP IN ID
-8 -6 -4 -2 0 2 4 6 8
Log2 Fold Change
b. Proteomics Outcomes in PD28 Males
MYH15
DBN1
TTLL11
TBCB
PCNT
MYH2
DPT
MLLT4
COL1A1
DAG1
MYH13
MYH11
COL1A2
LAMC1
MYH1
MYH7B
PLEKHH2
FBLN5
COL2A1
PALLD
EIF3A
59
DOWN IN ID
1189
67
UP IN ID
-8 -6 -4 -2 0 2 4 6 8
Log2 Fold Change
c. Proteomics Outcomes in PD0 Females
HIST1H1A
SRRT
HNRNPR
OBSL1
GUK1
TPP2
PTMS
PPIB
RPL3
GLRX3
CSE1L
SNRNP70
EIF2S2
PTMA
NASP
DHX15
RPS10
AIMP1
SRI
PCCB
SRSF4
ATP6V1B2
PRPF8
DDX3X
MTUS1
ATP5F1
SUCLG1
FHL2
NDUFB7
ATP2A1
MYH8
GSK3B
LMCD1
PGD
PGAM2
CALM1
SCN2A
LTA4H
PLN
SHROOM3
BLVRB
MYH3
UTRN
SYNE2
FHL1
LPP
LASP1
SEPT6
CTTN
LAMB2
63
DOWN IN ID
665
18
UP IN ID
-8 -6 -4 -2 0 2 4 6 8
Log2 Fold Change
d. Proteomics Outcomes in PD28 Females
MMP19
KRT79
TBCA
TBCB
IMPA1
CALB2
LAMB3
DAG1
LMO7
PAFAH1B1
GDA
PTPRQ
TRIOBP
ACTN1
CTNNA2
FAHD1
PGM2
MYH1
MYH8
MYH7B
RHOA
ANP32A
SORD
SERPINC1
ENO1
ITIH4
NCOA2
MYH3
GPD1
SOX6
SMPX
MYH4
HSD17B4
ACOX1
TXNRD1
MYH13
SND1
MFAP4
NRAP
ALDH7A1
CNDP2
HABP4
RPL30
FBN1
DROSHA
BCAT2
COL4A1
RPL27A
SRP72
ATM
FAM135A
82
DOWN IN ID
1259
56
UP IN ID
-8 -6 -4 -2 0 2 4 6 8
Log2 Fold Change
NOS1
ZYX
EFR3B
TNNI1
MYL7
MYL4
EPPK1
LDB3
TTN
TRIM54
LMOD2
DYNC1LI2
GPS1
DCAF6

Figure 2.6. STRING visualization of select pathway enrichment in hearts, as well as Venn diagrams depicting global protein changes. For STRING visualizations: Nodes represent a single down- or upregulated protein. Colored nodes indicate proteins responsible for supramolecular fiber (green, GO:0099512) and/or actin cytoskeleton (yellow, GO:0015629) pathway enrichment. White nodes represent proteins interacting with those belonging to enriched pathways (as indicated by linear connections). Linear connections indicate protein associations based on the following evidence: known interactions from curated databases (turquoise), known interactions experimentally determined (fuschia), predicted interactions by gene neighbourhood (green), predicted interactions by gene fusions (red), predicted interactions by gene co-occurrence blue), textmining (yellow), co-expression (black), and protein homology (purple). Each group used 4-5 biological replicates.

2.5 Discussion

Severe anemia has been shown to cause cardiovascular developmental aberrations, resulting in cardiac congenital malformation in mice (358), establishing a clear link between adequate iron supply and proper heart development. However, even with less severe iron-restriction during gestation, ID and anemia have been reported to result in cardiac adaptations (i.e. cardiomegaly). It may be theorized that the increase in heart size is an adaptive response to increase cardiac output to overcome the hypoxemia caused by reduced circulating Hb levels. However, the exact mechanisms remain unclear, and therefore we investigated the effects of maternal iron restriction on neonatal cardiac function, followed by an unbiased proteomics profiling to assess global changes in cardiac protein expression and signaling networks. To summarize our findings, we report that perinatal maternal iron restrictions caused: (1) anemia and growth restriction with concomitant cardiomegaly in both male and female neonatal offspring; (2) systolic dysfunction that was more pronounced in males, and diastolic dysfunction that was more pronounced in female offspring; (3) impaired oxygen delivery to tissues in all offspring; (4) broad but distinct proteomic changes in males and females that persisted beyond postnatal recovery from anemia. This study to identify ID as a cause of cardiac dysfunction in neonates in the absence of congenital defects, as well as identify proteome changes which may drive this dysfunction. Together, these data suggest perinatal ID is associated with cardiac morphological and functional changes which are incapable of compensating for the reduced oxygen carrying capacity caused by anemia. These alterations may in turn result in persistent structural changes that predispose the offspring to long-term cardiovascular consequences over time.

Hb concentration is the primary determinant of circulating oxygen content, and thus anemia had profound effects on blood O_2 content (CtO_2), irrespective of PO_2 and SaO_2 levels, which resulted in reduced oxygen delivery (DO_2) to organs and tissues. Neonates had signs of primary respiratory alkalosis, characterized by lower pCO_2 levels and increased pH levels compared to Ctl at PD4, which was likely secondary to anemia-induced hyperventilation. This notion is consistent with reduced actual HCO_3^- levels, which reflects a metabolic acid-base compensation, but no change in standard HCO_3^-. However, despite no

change in anion gap due to ID, we cannot exclude the possibility of a secondary metabolic acid/base disturbance. Indeed, we have previously shown that this model of ID anemia is associated with impaired oxygen delivery to fetal organs (notably the kidneys and liver), albeit not all were affected (i.e. brain and placenta were spared) (223). Together, these data suggest ID anemia results in impaired systemic oxygen delivery that cannot be overcome with respiratory or metabolic compensation.

Echocardiographic data and heart weights revealed proportionally larger hearts (relative to body weight) in both male and female ID offspring, although CO was unchanged. A larger and more dilated heart with no corresponding increase in CO indicates systolic dysfunction and reflects maladaptive or inadequate compensation to overcome the hypoxemia caused by anemia, resulting in growth restriction in the offspring. The greater and prolonged decrease in DO_2 in male offspring, combined with intrinsically higher growth rates in early life, are likely responsible for the more severe growth restriction compared to female offspring, and may contribute, at least in part, to the sex-differences in long-term health outcomes observed in this model (137, 140, 224). In cases of fetal anemia without concomitant ID, such as in Hb Bart's syndrome, cardiomegaly is associated with increased CO (at least in the high-output phase) and improved tissue oxygen delivery (351), suggesting the fetal heart has intrinsic functional reserve and can adapt to systemic effects of anemia *per se*. Although the present study focused on neonatal heart function, which may exhibit different adaptive capacities than the fetal heart, our previous work demonstrating fetal ID is associated with tissue-specific patterns of hypoxia in late gestation (223) suggests the hearts of ID fetuses are similarly dysfunctional. It is therefore tempting to speculate that the inadequate compensation observed herein may be due to the biochemical effects of ID. This notion is supported by a wealth of clinical data showing ID worsens heart failure with reduced ejection fraction (359), even without concomitant anemia (360).

Though evidence of systolic dysfunction was evident in all offspring, the reduction in aortic peak velocity as well as a greater decrease in ventricular contractility indicates a more severe systolic dysfunction in

male offspring. Conversely, while perinatal ID was associated with signs of diastolic dysfunction (left atrium diameter and a' wave peak velocities) in both male and female offspring, the decreased IVCT and TEI index, and increased E-to-e' ratio (each of which indicate increased ventricular filling pressures) altogether suggests a more profound diastolic dysfunction in females. Compared to men, adult women are more than twice as likely to develop heart failure with preserved ejection fraction (361) – a condition generally (albeit not exclusively) attributed to diastolic dysfunction; to our knowledge, the present study is among the first to show a propensity for diastolic dysfunction in female newborn rats. Thus, while this study contributes to the growing body of evidence which highlights sex-specific mechanisms behind cardiovascular programming and challenges the often-held assumptions that females are 'protected' from developmental stressors compared to their male counterparts.

We identified several cardiac structural alterations associated with ID that may underlie the observed functional deficits and could predispose offspring to long-term cardiovascular complications. The ratio of absolute heart weight to cardiac cell size, which was taken as a surrogate for cardiomyocyte number, was found to be lower in perinatal ID offspring by PD28. and thus, have long-term consequences for cardiac health. Newborn hypoxemia has been shown to inhibit cardiomyocyte proliferation in the developing heart (145). It follows that hypoxia may have contributed to reduced cardiomyocyte proliferation, since oxygen delivery was decreased with ID, and these offspring had proportionately thicker ventricular walls, which would impose greater oxygen demands. Beyond the early postnatal phase, cardiomyocytes no longer proliferate and instead respond to physiological and pathological stimuli by undergoing hypertrophy (362). A reduced cardiomyocyte endowment could therefore reduce adaptive capacity of the heart, and in turn impair recovery from injury, or predispose the offspring to accelerated age-related cardiovascular decline, as we and others have reported (138-140, 341, 342).

Other structural changes observed in the hearts of perinatal ID offspring included delayed maturation of the heart, as indicated by greater beta to alpha-MHC. In rodents, β- and α-MHC are characterized by

temporal expression patterns, with the former expressed predominantly in fetal life, and the latter in adulthood (as shown with the gradual decline in beta-MHC expression with postnatal day [Fig. 2G]). α-MHC has higher ATPase activity than the β-chain, and thus have higher contractile velocity, and hence greater efficiency in force generation (363). Despite ultimately recovering, the slower transition to the α-MHC may deprive the perinatal ID offspring of much needed cardiac efficiency in the context of ID anemia. Moreover, the extent of cardiac structural changes extends beyond altered β- and α-MHC expression. Indeed, the effects of ID on the neonatal heart were perhaps most evident in proteomics analysis. In perinatal ID offspring, diminished expression in pathways related to supramolecular fibre assembly (which relates to the assembly, arrangement, or disassembly of polymers that form a fibre shaped structure), and integrity of the actin cytoskeleton may, at least in part, contribute to the cardiac dysfunction observed in the perinatal period. Though evident at PD0, many pathway alterations were more pronounced at PD28, despite recovery from anemia, which occurs shortly after the third week in this model (unpublished observations). This delayed recovery could reflect a residual deficit in functional iron despite recovery from anemia, since replenishment of tissue iron levels only occur after restoration of Hb levels (364). Indeed, in a mouse model of ID without anemia, hearts and skeletal muscle were associated with left ventricular dysfunction (365, 366). Alternatively, if they persist indefinitely, these structural changes could also contribute to long-term alterations in cardiac function in the offspring.

In summary, our findings suggest that perinatal ID causes cardiac adaptations that do not result in increased cardiac output, despite the increase in heart size. This contrasts with models of anemia without concurrent ID (e.g., thalassemia), suggesting the biochemical effects of ID impose constraints on the heart's ability to adapt. Although the specific mechanisms underlying these maladaptive changes remain to be clarified, contractile and structural pathways were attenuated in response to ID in our untargeted proteomics analysis. Given their role in dictating muscle contractility, these could be important contributors to the cardiac dysfunction observed in ID offspring. Altogether, the findings have implications for the health of iron deficient babies and suggest that interventions to improve cardiac

output during the perinatal period may constitute an effective strategy to mitigate the effects of ID anemia on various organ systems. However, the marked differences in postnatal responses to ID between male and female offspring suggest intervention strategies should be tailored to meet the unique needs of each sex.

Clinical Perspectives:

- Iron deficiency (ID) is the most common nutritional deficiency worldwide and is highly prevalent among pregnant women and young children, however, how ID affects cardiovascular adaptations in early life remains unclear.
- Here we show that while ID causes increased heart size in the neonate, it is also associated with systolic and diastolic cardiac dysfunction, resulting in inadequate compensation to overcome the reduced oxygen carrying capacity caused by anemia.
- These findings have important implications for both the short and long-term cardiac health of newborn babies. Furthermore, therapies which improve cardiac output may mitigate the effects of ID on organ development.

Data Availability:

All supporting data are included within the main article and the supplementary file, the proteomics dataset has been deposited to the ProteomeXchange Consortium via the PRIDE partner repository with the dataset identifier PXD043588 (367-369). The datasets generated and/or analyzed for accomplishing the current study are available on request.

Funding:

This research was funded by the Canadian Institutes of Health Research (MOP142396 and PS183846 SLB), the Heart and Stroke Foundation of Canada (G-20-0029380 to SLB), the Stollery Children's Hospital Foundation and the Alberta Women's Health Foundation through the Women and Children's Health Research Institute. SLB is a Canada Research Chair (Tier 2) in developmental and integrative pharmacology.

Author contributions:

Conception and/or design: RMNN, CDH, AGW, JRBD, DG, LGE, AD, SLB

Data acquisition and analysis: RMNN, CDH, CN, SL, DY, AW, AD, SLB

Data interpretation: RMNN, CDH, AGW, CN, SL, DY, LGE, AD, SLB

Writing manuscript: RMNN, CDH, SLB

Revising manuscript: RMNN, CDH, AGW, CN, SL, DY, AW, SS, JRBD, DG, LGE, AD, SLB

Conflict of Interest: none declared.

Chapter 3

Gestational Ketone Supplementation Protects against Cardiac Dysfunction in Neonates Subjected to Maternal Iron Deficiency

Ronan M.N. Noble[1,2,3*], Si Ning Liu[1,2,3*], Shubham Soni[1,2,3], Alyssa Wiedemeyer[1,2,3], Jad-Julian Rachid[1,2,3], Claudia D. Holody[1,2,3], Richard Mah[2,3], Andrew G. Woodman[2,3,4], Mourad Ferdaoussi[1,2,3], Jason Dyck[1,2,3], Stephane L. Bourque[1,2,3,4]

1. Department of Pediatrics, University of Alberta, Edmonton, Canada
2. Women and Children's Health Research Institute, University of Alberta, Edmonton, Canada
3. Cardiovascular Research Institute, University of Alberta, Edmonton, Alberta, Canada
4. Department of Anesthesiology, University of Alberta, Edmonton, Canada

* denotes equal contributions

PUBLISHED:

Not yet published

3.1 Abstract

Iron deficiency (ID) is common during gestation and in early infancy and can alter developmental trajectories leading to lasting cardiovascular consequences. Ketone supplementation has been shown to exhibit cardioprotective effects in numerous disease models. We hypothesized that maternal ketone supplementation during gestation would reduce the cardiac impairments previously observed in ID neonates. Female Sprague Dawley rats were fed an iron-restricted or iron-replete diet before and throughout pregnancy, during gestation pregnant rats on the iron-restricted diet were given either a daily subcutaneous injection of β-Hydroxybutyrate (a type of ketone body) or saline. Neonatal cardiac function was assessed via echocardiography; offspring were then euthanized for tissue collection where hearts and livers were assessed for transcript markers of metabolism, oxidative stress, inflammation, and organ damage. ID reduced body weight and increased relative heart and brain weight at all time points assessed, in both the ketone and saline ID groups. Echocardiography revealed clear cardiac dysfunction in ID offspring, which was reversed by ketone supplementation causing an improved ejection fraction and a corresponding increase in cardiac output and total oxygen delivery. Furthermore, ID increased expression of *Il-1β* whereas ketone supplementation further altered *Il-1β, Sod2,* and *Cat* expression, indicating oxidative stress and inflammation may be relevant pathways for future study. Ketone supplementation could be protective against cardiac dysfunction in neonates secondary to ID. These findings could have important implications for the treatment ID during pregnancy, as well as the health of anemic babies.

3.2 Introduction

Iron is an essential element that plays an important role in many biochemical functions, including redox reactions, DNA synthesis, and energy metabolism (370). Most of the iron in the body is found in hemoglobin within red blood cells, whose primary function is to transport oxygen throughout the body. Iron deficiency (ID) is the most common nutritional deficiency worldwide affecting over 20% of the global population. Common causes of ID include issues with absorption (e.g. celiac disease), low iron intake, blood loss (e.g. gastrointestinal bleed, heavy menstruation), or increased iron demands (201). Iron demand increases substantially during pregnancy (230), due to requirements for fetal growth and development. As ID progresses it will eventually result in anemia which is characterized by a fall of circulating hemoglobin below a clinical threshold (371). 38% of pregnant women become anemic, with most cases being attributed to ID (210, 211).

Maternal ID is associated with adverse pregnancy outcomes, including preterm birth, maternal and fetal demise, and low birth weight (217-219). The consequences in the offspring extend beyond perinatal health outcomes; indeed, consistent with the DOHaD concept, offspring exposed to ID in gestation exhibit increased susceptibility to chronic diseases, such as cardiovascular disease (225). Given the prevalence of ID and its tendency to affect pregnant women, ID could be an important contributor to the overall burden of disease at both ends of lifespan.

Iron supplementation is currently recommended for all pregnant women (209, 238), however this is often not effective. Standard prenatal vitamins often do not have enough iron to treat anemia (240, 241), and larger doses are associated with gastrointestinal side effects, as well as

occasional toxicity to the mother and fetus (237). To make matters worse, some cases of iron deficiency during pregnancy are caused by poor intestinal absorption of iron, making iron supplementation ineffective in these circumstances (242). Finally, while iron supplementation does improve indices of anemia in mothers, their effectiveness in improving iron status and hematological indices in the fetus or newborn are not established (242). On the basis of these challenges, there is a clear necessity to develop other therapies to treat the deleterious effects of maternal iron deficiency, both to improve perinatal health of the neonate and in turn improve long-term health trajectories.

Ketones are molecules produced by the liver from fatty acids that can be used as a source of energy. Compared to fatty acids (a major source of energy for the heart), ketones produce more energy per unit of oxygen rendering them, potentially, a more efficient source of energy in the context of anemia (372). Ketones, specifically β-hydroxybutyrate (βOHB), also have signaling effects that provide resistance against oxidative stress and directly inhibit inflammation (301, 302, 373). Others have shown increasing βOHB in the blood can directly improve renal function through the reduction of oxidative stress and inflammation (374), we have shown that βOHB can also prevent the worsening of cardiac dysfunction (and therefore preserve cardiac output) through anti-inflammatory mechanisms (375).

We have previously shown that perinatal ID causes cardiomegaly of the ID neonate, as well as systolic dysfunction resulting in a reduction in total oxygen delivery (Noble et al. submitted). Because perinatal ID is also associated with organ-specific patterns of hypoxia late in gestation (223), a therapy which augments ID's maladaptive changes within the heart may effectively

mitigate the effects of ID on various organ systems. We and others have identified a number of pathological mechanisms associated with perinatal ID where βOHB may cause protective effects, including mitochondrial dysfunction, increased ROS generation, and the generation of inflammation (223, 376). Ketone metabolism is critically important for infant survival, and interestingly, one feature of perinatal ID is an inability to produce ketones (377, 378). Finally, ketones do cross the placenta through passive diffusion to be utilized by the fetus (311, 323). There is also evidence that the placenta uses ketones as fuel preferentially to glucose (379), which may be important given maternal iron deficiency is associated with changes in placentation potentially leading to an increased incident of fetal injury during pregnancy (380).

On the basis of these independent lines of evidence, we hypothesize that βOHB supplementation would improve the cardiac function of ID offspring. Herein we show that βOHB administration throughout gestation partially mitigates the cardiac dysfunction associated with perinatal ID.

3.3 Methods

3.3.1 Animals and Treatments

The protocols described herein were approved by the University of Alberta Animal Care and Use Committee in accordance with guidelines established by the Canadian Council for Animal Care. Thirty-two female Sprague-Dawley rats aged 6 weeks were purchased from Charles River (Saint-Constant, QC, Canada) and housed at the University of Alberta Animal Care Facility, which maintains a 12-hour light/dark cycle and an ambient temperature of 23°C. Rats had *ad libitum* access to food and water throughout the study.

Two weeks before mating, female rats were randomly assigned to either a control (Ctl) or iron deficiency (ID) group. Ctl and ID rats were fed a purified diet containing 37 or 3mg/kg elemental iron, respectively; these purified diets were based on the AIN-93G formula and differed only by the amount of ferric citrate added. After two weeks on their respective diets, rats were housed overnight with male rats (fed a standard rodent chow) until pregnancy was confirmed by presence of sperm in a vaginal smear (defined as gestational day [GD]0). Thereafter, dams were individually housed, and those in the ID group were fed a purified diet containing 10 mg/kg elemental iron, whereas Ctl dams remained on their prescribed purified control diet. Maternal food intake, and Hb levels were assessed weekly throughout pregnancy; Hb values were assessed using a HemoCue Hb201+ hemoglobinometer from 10uL of blood collected from saphenous venipuncture.

From GD0-GD21, a subgroup of ID dams were administered ketones (KID group) daily in the form of a β-Hydroxybutyrate (βOHB) solution (Sigma H6501; 0.3g/kg in saline) by subcutaneous injection. Ctl dams and the remaining ID dams received an equivalent volume of saline (1.2mL/kg) by subcutaneous injection daily. All dams also received two unshelled sunflower seeds daily for enrichment.

Beginning on the day of birth (defined as postnatal day [PD]0), dams were fed the standard rodent chow. At this time, litters were reduced to ten offspring (five males and five females) to standardize postnatal conditions. At postnatal day 21, remaining offspring were weaned; same-sex littermates were group housed in separate cages and fed the standard diet.

3.3.2 Echocardiography

Cardiac structure and function were assessed by thoracic echocardiography (Vevo 3100, Visualsonics, Toronto, ON, Canada) in a subgroup of offspring at PD3 (MX400 transducer) and PD13 (MX550s transducer). Animals were anesthetized (isoflurane in oxygen; 2.5% for induction and 1.5-1.8% for maintenance), and limbs were fixes to electrodes with tape and conductive electrogel (SignaGel, WA, USA); electrogram and respiratory rate were continuously recorded. Body temperature was maintained with heated ultrasound transmission gel, a heated platform, and a heat lamp. For rats at PD13, the chest and upper abdomen were depilated (Nair® extra gentle). A single operator who was blinded to experimental groups performed all assessments.

Parasternal M mode tracings were used to quantify: left atrium diameter, LV end-diastolic and end-systolic diameters (LVID), septal (IVS) and posterior wall (LVPW) thicknesses, ejection fraction (EF), fractional shortening (FS), stroke volume (SV), cardiac output (CO), and oxygen delivery (DO_2). The trans mitral flow velocity was obtained from the apical four chambers view to measure: early filling (E) and atrial (A) pulse wave and tissue velocity, as well as isovolumetric relaxation time (IVRT), isovolumetric contraction time (IVCT), and aortic ejection time (AET). The trans mitral flow velocity was obtained from the apical four chambers view to measure: early filling (E) and atrial (A) pulse wave and tissue velocity. The trans tricuspid flow velocity was obtained from a modified apical four chambers view to measure: early filling (E) and atrial (A) pulse wave and tissue velocity. Pulmonary artery Doppler imaging was used to measure pulmonary acceleration time (PAT), pulmonary ejection time (PET), and pulmonary valve peak velocity (PV peak velocity). Pulmonary vein Doppler imaging was used to measure S (systolic) wave, D (diastolic) wave, A (atrial systolic reversal) wave, as well as the atrial systolic

reversal duration. Aortic spectral Doppler imaging was used to measure descending aorta velocity. All values were measured under steady state conditions and averaged from at least three cardiac cycles taking care to exclude cycles that took place during inhalation.

3.3.3 Quantitative Reverse-Transcriptase PCR

At PD0, PD4, and PD14, pups were weighed and euthanized by decapitation; at PD14, offspring were anesthetized with 5% isoflurane in pure oxygen prior to euthanasia. Free flowing blood was collected for hemoglobin assessments (Hemocue Hb201+). Offspring organs were quickly excised, weighed, and flash-frozen in liquid nitrogen. All tissues were stored at -80°C prior to analyses.

Total RNA was isolated from frozen hearts using TRIzol reagent (Invitrogen®) according to the manufacturer's instructions. First strand cDNA synthesis was performed using 5× All-In-One RT MasterMix, according to the manufacturer's instructions (Applied Biological Materials – abm; G486). Quantitative real-time PCR was performed in white 384-well reaction plates with PowerUp SYBR Green Master Mix (Applied Biosystems, A25742) in the LightCycler 480 (Roche Life Science), as previously described (137). Primer sequences were purchased from Integrated DNA technologies (IDT, Coralville, IA). Quantitative PCR data was analyzed using the relative gene expression (ΔΔCt) method with *Actb* as the housekeeping gene.

3.3.4 Statistical Analysis

N values throughout represent the number of treated dams or litters; any replicates obtained from littermates of the same sex were pooled and treated as n=1. Results are expressed as mean ± standard error of the mean (SEM). For maternal outcomes in pregnancy, data were analyzed by fitting a mixed-effects model for gestational treatment (Ctl vs. ID vs. KID) and time as

implemented in GraphPad Prism 8.3.0; Tukey's post-hoc test was used for multiple comparisons between groups at gestational days. Offspring data were analyzed by one-way ANOVA followed by a Tukey or Sidak post hoc test for multiple comparisons. Mann-Whitney U test was used for non-continuous data sets with two groups (i.e. litter size).

3.4 Results

Feeding dams an iron-restricted diet prior to and throughout pregnancy caused a progressive decline in maternal Hb levels throughout gestation, cumulating in a -35% and -37% decrease in ID and KID groups respectively by GD21 (**Figure 3.1a**). Despite the severity of anemia, there were no differences in maternal weight gain throughout pregnancy (**Figure 3.1b**), and litter sizes were unaffected (P=0.41), nor were any offspring found dead in any groups in the postnatal period. Maternal glucose levels decreased over the course of pregnancy, though they remained slightly elevated in both ID and KID groups, particularly in the latter stages of gestation (**Figure 3.1c**). Finally, maternal blood βOHB levels, assessed weekly immediately prior to the daily injection of ketones (or vehicle), tended to decrease by mid-gestation, but rose by GD21; interestingly, βOHB levels were decreased in both ID and KID groups (**Figure 3.1d**).

As expected, Hb levels in ID and KID offspring were markedly reduced in the neonatal period compared to the CTL offspring (**Table 3.1**). Offspring βOHB levels in the ID group tended to differ from control and KID groups, although this did not reach significance (P=0.08); however, recognizing that the last injection of ketones in the KID was made 24h prior to tissue collection at PD0, a sub-analysis whereby only Ctl and ID offspring βOHB levels were compared revealed a reduction in the latter group (unadjusted P=0.018). Male and female ID and KID offspring were growth restricted at birth, and remained so throughout the 2wk postnatal period (**Table 3.1,**

3.2). ID and KID offspring had exhibited reduced organs weights (expressed as absolute weights), with the exception of brains and hearts (**Table 3.1, 3.2**). After normalizing to bodyweight, liver and spleen weight were increased in ID and KID offspring, albeit only on or after PD4. Relative brain and heart weights remained elevated across all postnatal days in ID and KID offspring –a hallmark of asymmetric growth restriction (**Table 3.1, 3.2**). To further characterize the nature of the cardiomegaly observed in ID and KID offspring, echocardiography was performed. In male offspring (**Table 3.3**), LVPW thickness at PD13 was increased in ID, but not in KID offspring; a similar trend was seen at PD3, though this difference did not reach statistical significance. In female offspring (**Table 3.4**), LVPW thickness was also increased in ID, albeit this change was most pronounced at PD3 in the KID group. Left ventricular chamber volume size was not affected by ID or ketone treatment.

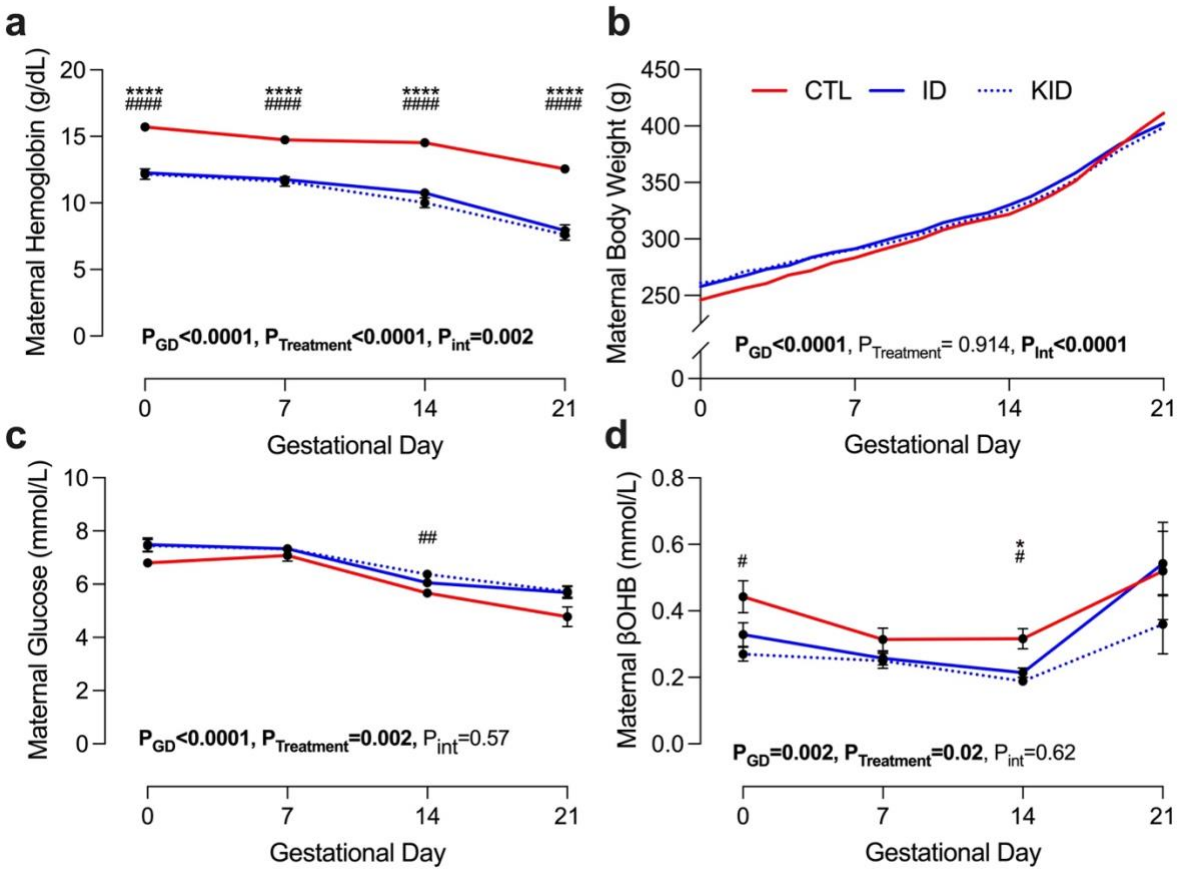

Figure 3.1. Maternal parameters. In control (CTL), iron-deficient (ID), and ketone treated iron-deficient (KID) dams on gestational days 0, 7, 14, 21. Data are mean ±SEM; each bar represents data from n=9-12 dams. Data are analyzed by two-way ANOVA with Tukey's post hoc test; stated p values reflect overall outcomes, and stars represent post-hoc outcomes (*P<0.05, **P<0.01, ***P<0.001, ****P<0.0001 ID versus Ctl; #P<0.05, ##P<0.01, ###P<0.001, ####P<0.0001 KID versus Ctl).

Table 3.1. Neonatal hemoglobin, blood glucose and ketone levels, and organ weights in males.

Male Offspring		**PD0**		**P Value**		**PD4**		**P Value**		**PD14**		**P Values**
	Ctl (n=6–7)	**ID** (n=5–7)	**KID** (n=6)		**Ctl** (n=7)	**ID** (n=8)	**KID** (n=8–9)		**Ctl** (n=7)	**ID** (n=7)	**KID** (n=9)	
Hb (g/dL)	12.6±0.4	5.4±0.5****	4.7±0.4****	**<0.0001**	9.2±0.5	4.9±0.3****	5.1±0.3****	**<0.0001**	7.7±0.3	6.1±0.3**	5.8±0.4***	**0.0008**
Ket (mmol/L)	0.76±0.06	0.53±0.05	0.69±0.10	0.08	1.21±0.07	1.38±0.11	1.44±0.18	0.49	1.36±0.04	1.58±0.23	1.25±0.11	0.29
Glucose (mmol/L)	6.1±0.5	6.1±0.8	4.9±0.4	0.30	7.2± 0.2	6.78 ± 0.3	6.3±0.1*	**0.02**	9.8±0.4	9.9±0.4	10.0±0.4	0.93
Bodyweight (g)	6.9±0.3	5.85±0.15**	5.70 ±0.2**	**0.002**	11.5±0.4	7.9 ±0.6***	7.9±0.5***	**0.0002**	36.0±1.0	30.5±1.4	29.8±2.2	**0.04**
Heart (mg)	28.0±1.5	37.0±0.9***	37.3±1.5***	**0.0002**	56.5±2.1	59.0±3.8	59.3±3.3	0.81	152.1±2.7	174.0±8.5	173.2±6.6	0.05
Kidney (mg)	64.1±4.3	55.1±1.4	54.8±3.2	0.08	133.4±8.5	102.1±5.8**	99.9±5.9**	**0.004**	407.0 ±12.7	356.1±19.5	347.2±26.3	0.14
Liver (mg)	315.5± 18.3	261.1±14.6	256.7±16.9	**0.04**	383.6±13.8	307.7±17.9**	291.6±15.6**	**0.002**	1049.0±37.8	958.0±56.9	927.2±68.0	0.34
Spleen (mg)	14.8±2.0	10.9±1.1	8.7±1.1*	**0.03**	50.9±3.9	32.6±4.0**	34.4±3.3*	**0.005**	146.1±5.1	157.9±13.8	147.4±10.7	0.71
Brain (mg)	169.3±6.2	166.1±4.4	171.0±5.3	0.81	350.4±11.8	288.6±13.0**	289.8±13.1**	**0.005**	1010.0±14.4	916.2± 21.1*	923.4±26.6*	**0.02**
Heart (mg/g)	4.1±0.1	6.3±0.2****	6.6±0.2****	**<0.0001**	4.9±0.1	7.6±0.4****	7.5±0.2****	**<0.0001**	4.2±0.05	5.73±0.2**	6.0±0.3***	**0.0002**
Kidney (mg/g)	9.3±0.4	9.4±0.2	9.6± 0.3	0.81	11.5±0.4	13.2±0.6	12.5± 0.3	0.07	11.3±0.2	11.7±0.2	11.7±0.2	0.37
Liver (mg/g)	45.7±1.6	44.4±1.7	45.0± 2.6	0.88	33.4±0.5	39.8±1.6**	37.1±0.8*	**0.002**	29.2±0.3	31.5±1.1	31.1±0.3	**0.04**
Spleen (mg/g)	2.1±0.3	1.9±0.2	1.5±0.2	0.13	4.4 ±0.3	4.0 ±0.2	4.3 ±0.2	0.52	4.0±0.1	5.2±0.4*	5.0±0.2*	**0.02**
Brain (mg/g)	24.5±0.4	28.4±0.7***	30.1±0.7****	<**0.0001**	30.5±0.5	37.6±1.6**	37.3±1.2**	**0.001**	28.2±0.6	30.4±1.2	32.0±1.6	0.15

Data are mean±SEM. Comparisons between group was performed using a one-way ANOVA followed by Sidak posthoc test.

*P<0.05, **P<0.01, ***P<0.001, ****P<0.0001 versus Ctl; #P<0.05, ##P<0.01, ###P<0.001, ####P<0.0001 versus ID.

Table 3.2. Neonatal hemoglobin, blood glucose and ketone levels, and organ weights in females.

Female Offspring		**PD0**		**P Value**		**PD4**		**P Value**		**PD14**		**P Values**
	Ctl (n=5–6)	**ID** (n=6–7)	**KID** (n=8–9)		**Ctl** (n=7)	**ID** (n=7–8)	**KID** (n=9)		**Ctl** (n=7)	**ID** (n=6–7)	**KID** (n=9)	
Hb (g/dL)	12.0±0.6	5.3±0.3****	6.0±0.6****	**<0.0001**	8.8±0.3	5.1±0.3****	5.2±0.3****	<**0.0001**	7.7±0.4	5.9±0.3**	5.9±0.1**	**0.0005**
Ket (mmol/L)	0.77±0.06	0.72±0.12	0.61±0.07	0.39	1.12±0.09	1.20±0.13	1.33±0.15	0.51	1.48±0.09	1.65±0.14	1.16±0.09**	**0.009**
Gluc (mmol/L)	5.7±0.4	4.8±0.9	5.3±0.6	0.64	7.2±0.1	6.6±0.2*	6.5±0.1**	**0.006**	10.2±0.3	9.9±0.4	10.1±0.3	0.88
Bodyweight (g)	6.3±0.3	5.1±0.3*	5.6±0.2	**0.02**	11.0±0.4	7.7±0.4****	8.0±0.3****	<**0.0001**	34.8±0.7	28.6±1.3*	28.9±1.9*	**0.01**
Heart (mg)	28.1±1.7	34.8±1.5*	35.2±1.4**	**0.006**	59.0±2.9	60.7±2.2	61.9±2.3	0.72	152.1±4.8	174.6±10.0	167.3±7.3	0.16
Kidney (mg)	60.8±5.1	50.1±1.8	51.6±2.7	0.09	134.0±9.0	102.9±3.9**	104.1±4.4**	**0.002**	410.9±13.3	348.2±19.7	336.2±22.2*	**0.03**
Liver (mg)	319.2±33.6	218.5±16.4*	250.1±13.4	**0.01**	394.8±17.1	292.7±13.3***	311.7±11.1***	**<0.0001**	1071.0±2.8	926.0±5.5	926.0±6.0	0.11
Spleen (mg)	14.4±1.9	9.7±1.0*	9.0±0.8*	**0.01**	48.8±5.3	34.7±2.0*	34.3±2.5*	**0.01**	148.2±4.5	141.3± 13.5	144.4±8.8	0.89
Brain (mg)	168.6±7.9	167.2±7.8	168.9±4.4	0.98	324.4±16.8	282.8±7.9	300.9±11.1	0.08	962.5±14.0	899.6±18.3	906.0±20.9	0.06
Heart (mg/g)	4.4± 0.1	6.6±0.2***	6.4±0.4***	**0.0002**	5.3±0.1	7.9±0.3****	7.8±0.1****	<**0.0001**	4.4±0.1	6.1±0.3***	5.9±0.3***	**0.0002**
Kidney (mg/g)	9.5±0.4	10.0±0.7	9.1±0.2	0.36	12.0±0.5	13.5±0.1	13.1±0.4	0.14	11.8±0.3	12.2±0.2	11.7±0.4	0.59
Liver (mg/g)	50.7±4.0	43.3±2.4	44.2±0.9	0.09	35.8±0.8	38.1±1.3	39.2±0.9	0.08	30.8±0.3	32.3±0.9	32.1±0.4	0.20
Spleen (mg/g)	2.2±0.3	1.9±0.1	1.6±0.1*	**0.04**	4.4±0.4	4.4±0.1	4.3±0.2	0.94	4.3±0.1	4.9±0.4	5.1±0.2	0.09
Brain (mg/g)	26.6±0.8	31.5±2.3	30.2±0.8	0.07	29.3±0.9	37.0±1.3***	37.9±1.0****	<**0.0001**	27.7±0.4	31.8±1.2	32.3±1.7	0.05

Data are mean±SEM. Comparisons between group was performed using a one-way ANOVA followed by Sidak posthoc test. *P<0.05, **P<0.01, ***P<0.001, ****P<0.0001 versus Ctl; #P<0.05, ##P<0.01, ###P<0.001, ####P<0.0001 versus ID.

Table 3.3. Neonatal left ventricular wall thickness and chamber diameters in males.

Male Offspring	**PD3**			**P Value**	**PD13**			**P Value**
	Ctl (n=6-7)	**ID** (n=7-8)	**KID** (n=8-9)		**Ctl** (n=7)	**ID** (n=6-7)	**KID** (n=6–9)	
LVPW,d	0.73±0.05	0.88±0.04	0.83±0.03	0.07	1.03±0.06	1.23±0.03	1.09±0.04	**0.02**
LVPW,s	1.01±0.03	1.03±0.06	1.04±0.04	0.91	1.55±0.06	1.55±0.05	1.55±0.09	0.99
IVS,d	0.74±0.03	0.70±0.04	0.73±0.04	0.80	0.87±0.07	0.91±0.03	0.90±0.06	0.87
IVS,s	1.04±0.03	0.93±0.05	1.07±0.07	0.21	1.43±0.09	1.35±0.08	1.31±0.10	0.64
Vol,d	39.9±2.3	31.9±2.4	35.5±2.2	0.08	85.2±8.2	84.8±4.9	81.4±5.1	0.88
Vol,s	8.6±0.9	10.3±1.1	8.1±0.6	0.19	20.3±4.5	33.5±4.5	24.1±3.6	0.11

Data are mean±SEM. Comparisons between group was performed using a one-way ANOVA followed by Sidak posthoc test. *P<0.05, **P<0.01, ***P<0.001, ****P<0.0001 versus Ctl; #P<0.05, ##P<0.01, ###P<0.001, ####P<0.0001 versus ID. Interventricular septum in diastole, IVS,d; interventricular septum in systole, IVS,s; left ventricle posterior wall in diastole, LVPW,d; left ventricle posterior wall in systole, LVPW,s; left ventricle volume in diastole, Vol,d; left ventricle volume in systole, Vol,s.

Table 3.4. Neonatal left ventricular wall thickness and chamber diameters in females.

Female Offspring	PD3			P Value	PD13			P Value
	Ctl (n=7)	**ID** (n=8)	**KID** (n=9)		**Ctl** (n=7)	**ID** (n=7)	**KID** (n=8)	
LVPW,d	0.72±0.04	0.83±0.04	0.86±0.02*	**0.01**	1.01±0.06	1.07±0.03	1.15±0.04	0.12
LVPW,s	1.01±0.04	1.09±0.09	1.11±0.04	0.19	1.53±0.06	1.45±0.05	1.56±0.05	0.37
IVS,d	0.72±0.03	0.73±0.04	0.72±0.03	0.99	0.88±0.04	0.90±0.04	0.95±0.03	0.35
IVS,s	1.06±0.02	1.01±0.06	1.05±0.04	0.76	1.44±0.06	1.30±0.05	1.41±0.04	0.15
Vol,d	40.0±2.6	32.1±3.5	36.2±1.9	0.16	81.8±5.6	83.7±6.4	77.7±6.3	0.77
Vol,s	10.1±1.0	9.9±1.6	8.9±0.8	0.74	17.0±2.3	30.5±5.0	21.4±3.7	0.07

Data are mean±SEM. Comparisons between group was performed using a one-way ANOVA followed by Sidak posthoc test. *P<0.05, **P<0.01, ***P<0.001, ****P<0.0001 versus Ctl; #P<0.05, ##P<0.01, ###P<0.001, ####P<0.0001 versus ID. Interventricular septum in diastole, IVS,d; interventricular septum in systole, IVS,s; left ventricle posterior wall in diastole, LVPW,d; left ventricle posterior wall in systole, LVPW,s; left ventricle volume in diastole, Vol,d; left ventricle volume in systole, Vol,s.

Cardiac function was assessed in neonates by echocardiography; indices of systolic function from male offspring are shown in **Table 3.5** and from female offspring in **Table 3.6**. Compared to Ctl, male ID offspring exhibited signs of systolic dysfunction, characterized by a reduced cardiac contractility (i.e. reduced ejection fraction and fractional shortening) at PD3 and PD13, as well as reduced ascending aortic velocity at PD13. Similar outcomes were observed in female ID offspring, which exhibited evidence of systolic dysfunction, again defined by a reduction in ejection fraction and fractional shortening, as well as a reduced mitral valve systolic wave velocity at PD13. Therefore, despite male ID offspring having proportionally larger hearts, cardiac output was comparable to that of Ctl offspring, culminating in a reduced oxygen delivery due to the anemia in the pups. βOHB treatment in ID offspring improved ejection fraction and fractional shortening, which was associated with an increased cardiac output at PD3 in both males (**Table 3.5**) and females (**Table 3.6**). The increased cardiac output was attributed to increased stroke volume in both males and females since no changes in heart rate were evident between groups. The cardiac changes in KID offspring were associated with increased oxygen delivery in both male and females at PD3, though these effects diminished with time, and were no longer significant at PD13.

Table 3.5. Neonatal systolic function in males.

Male Offspring		**PD3**		**P Values**		**PD13**		**P Values**
	Ctl (n=7)	**ID** (n=7–8)	**KID** (n=8–9)		**Ctl** (n=7)	**ID** (n=7)	**KID** (n=9)	
HR (bpm)	272±13	259±13	278±10	0.49	348±14	293±11	323±7	**0.008**
EF (%)	78±1	65±3***	74±3###	**0.0003**	78±4	61±4*	70±4	**0.04**
FS (%)	46±1	37±1***	44±1###	**0.0002**	47±3	33±3*	41±3.5	**0.03**
SV / BW (mL/g)	2.7±0.08	2.8±0.2	3.4±0.2*#	**0.006**	1.8±0.1	1.7±0.1	1.9±0.1	0.48
CO / BW (mL/min*g)	0.74±0.04	0.70±0.02	0.95±0.04***###	**<0.0001**	0.64±0.06	0.50±0.05	0.61±0.03	0.13
DO2 / BW (mL/min*g)	0.091±0.008	0.046±0.003****	0.064±0.003*#	<**0.0001**	0.071±0.008	0.040±0.003**	0.051±0.004*	**0.002**
MV S' (mm/s)	18±2	16±1	18±2	0.80	23±1	20±1	20±1	0.05
Asc Aorta Vel (mm/s)	378±25	501±73	580±46	0.09	919±57	589±49**	475±41***	**0.0003**
Desc Aorta Vel (mm/s)	521±30	488±47	507±33	0.85	753±29	712±38	786±47	0.44

Data are mean±SEM. Comparisons between group was performed using a one-way ANOVA followed by Sidak posthoc test.

*P<0.05, **P<0.01, ***P<0.001, ****P<0.0001 versus Ctl; #P<0.05, ##P<0.01, ###P<0.001, ####P<0.0001 versus ID. Ascending aorta velocity, Asc Aorta Vel; bodyweight, BW; cardiac output, CO; descending aorta velocity, Desc Aorta Vel; ejection fraction, EF; fractional shortening, FS; heart rate, HR; mitral valve systolic wave, MV S'; oxygen delivery, DO2; stroke volume, SV.

Table 3.6. Neonatal systolic function in females.

Female Offspring		**PD3**		**P Values**		**PD13**		**P Values**
	Ctl (n=6-7)	**ID** (n=6-8)	**KID** (n=8-9)		**Ctl** (n=5-7)	**ID** (n=7)	**KID** (n=9)	
HR (bpm)	282±13	271±11	281±7	0.72	339±10	306±5.41	326±12	0.11
EF (%)	75±2	70±2	76±1	0.09	80±2	65±4*	73±3	**0.03**
FS (%)	43±2	38±2	43±1	0.09	48±2	36±3*	43±3	**0.02**
SV / BW (mL/g)	2.7±0.1	2.9±0.3	3.4±0.1	**0.04**	1.9±0.1	1.8±0.1	2.0±0.2	0.71
CO / BW (mL/min*g)	0.77±0.05	0.76±0.048	0.96±0.041*#	**0.007**	0.63±0.03	0.57±0.04	0.64±0.05	0.43
DO2 / BW (mL/min*g)	0.090±0.006	0.051±0.003****	0.070±0.005*#	**<0.0001**	0.064±0.006	0.044±0.004*	0.052±0.005	**0.03**
MV S' (mm/s)	15±1	15±0.7	14 ±0.7	0.39	24 ± 0.9	20±0.8**	20±0.8**	**0.004**
Asc Aorta Vel (mm/s)	444±28	489±34	588±62	0.18	883±58	896±127	633±80	0.07
Desc Aorta Vel (mm/s)	495±22	492±24	546±29	0.25	780± 29	763±51	692±55	0.27

Data are mean±SEM. Comparisons between group was performed using a one-way ANOVA followed by Sidak posthoc test. *P<0.05, **P<0.01, ***P<0.001, ****P<0.0001 versus Ctl; #P<0.05, ##P<0.01, ###P<0.001, ####P<0.0001 versus ID. Ascending aorta velocity, Asc Aorta Vel; bodyweight, BW; cardiac output, CO; descending aorta velocity, Desc Aorta Vel; ejection fraction, EF; fractional shortening, FS; heart rate, HR; mitral valve systolic wave, MV S'; oxygen delivery, DO2; stroke volume, SV.

Indices of diastolic function from male offspring are shown in **Table 3.7,** and from female offspring in **Table 3.8**. Primary measures of diastolic dysfunction, including E/A, E/e' and TEI index were not different among groups in either male or female offspring. However, some subtle differences were apparent in male offspring, particularly at PD13, where ID was associated with reduced MV A, MV E, and MV e' velocities in males, with the former two being at least partially reversed by ketone supplementation. Differences were even more subtle in female offspring, which included reduced IVCT at PD3, albeit only in the KID group, and reduced MV a' velocities in ID and KID offspring at PD13. Notably, AET values were increased in ID male and female offspring at PD13 which was reversed by ketones in only the males, this may reflect reduced blood viscosity due to anemia.

Indices of pulmonary artery and venous flow, as well as flow into the right ventricle are shown in males in **Table 3.9** and in females in **Table 3.10**. PAT/PET, one of the primary measures of pulmonary artery flow was elevated in KID male offspring compared to control at PD3, which may indicate improved right ventricular function. Other differences were noted, including increased PET at PD13 in ID, which was partially reversed by ketone supplementation in both male and female offspring. Finally, pulmonary vein systolic wave (S wave) was also increased when compared to Ctl in both male and female PD3 KID offspring, as well as at PD13 in female offspring. Increased pulmonary vein systolic wave velocities could be indicative of improved diastolic function in these groups, which is consistent with a trend towards an increased S/D ratio in both males and females.

Table 3.7. Neonatal diastolic function in males.

Male Offspring		**PD3**		**P Values**		**PD13**		**P Values**
	Ctl (n=6-7)	**ID (**n=8)	**KID** (n=7–9)		**Ctl** (n=7)	**ID** (n=6–7)	**KID** (n=9)	
LA diameter (mm)	1.9±0.1	1.7±0.1	1.7±0.1	0.49	2.4±0.1	2.6±0.2	2.6±0.2	0.88
E/A	1.4± 0.3	1.1±0.1	1.1±0.1	0.28	1.3±0.1	1.5±0.2	1.1±0.1	0.19
AET (ms)	103±5	110±5	106±5	0.61	70±3	84±4*	82±2*	**0.01**
IVCT (ms)	17±1	16±2	12±1	0.11	24±2	26±3	21±1	0.21
IVRT (ms)	26±3	25±4	19±1	0.19	23±2	28±2	27±1	0.10
MV A (mm/s)	392±83	428±39	511±26	0.24	585±30	439±56*	568±20#	**0.02**
MV E (mm/s)	443±42	438±22	518±15	0.07	724±53	578±18*	632±24	**0.03**
MV a’ (mm/s)	15±1	17±2	16±1	0.58	25±3	18±1	20±2	0.15
MV e’ (mm/s)	13±1	12±1	12±1	0.33	32±3	21±1**	23±2**	**0.003**
TEI index	0.42±0.03	0.37±0.04	0.31±0.02	0.07	0.64±0.05	0.66±0.07	0.59±0.03	0.06
e’/a’	0.88±0.04	0.70±0.05*	0.75±0.05	**0.04**	1.27±0.13	1.22±0.10	1.19±0.11	0.86
E/e’	34±3	40±4	45±2	0.14	23±1	27±1	29±2	0.06

Data are mean±SEM. Comparisons between group was performed using a one-way ANOVA followed by Sidak posthoc test. *P<0.05, **P<0.01, ***P<0.001, ****P<0.0001 versus Ctl; #P<0.05, ##P<0.01, ###P<0.001, ####P<0.0001 versus ID. Aortic ejection time, AET; early left ventricular filling velocity, E or MV E; late left ventricular filling velocity, A or MV A; early mitral valve filling velocity, e' or MV e'; isovolumetric contraction time, IVCT; isovolumetric relaxation time, IVRT; late left ventricular filling velocity, A or MV A; late mitral valve filling velocity, a' or MV a'; left atrium diameter, LA diameter; myocardial performance index, TEI index

Table 3.8. Neonatal diastolic function in females.

Female Offspring		**PD3**		**P Values**		**PD13**		**P Values**
	Ctl (n=6-7)	**ID** (n=7-8)	**KID** (n=9)		**Ctl** (n=7)	**ID** (n=7)	**KID** (n=7-9)	
LA diameter (mm)	1.9±0.1	1.8±0.1	1.8±0.04	0.48	2.5± 0.1	2.4±0.1	2.7±0.2	0.24
E/A	1.2±0.2	1.2±0.06	1.1±0.05	0.85	1.4± 0.1	1.3±0.07	1.2±0.08	0.50
AET (ms)	100±4	103±6	102±2	0.89	70±3	85±3**	76±3	**0.009**
IVCT (ms)	20±1	18±2	12±1**#	**0.004**	23±2	20±2	23±2	0.43
IVRT (ms)	24±2	24±1	21±1	0.39	23±1	27±1	25±2	0.14
MV A (mm/s)	435±48	444±24	455±25	0.90	555±31	521±21	602±45	0.30
MV E (mm/s)	491±30	496±20	506±16	0.88	706±28	656±25	719±22	0.21
MV a’ (mm/s)	14±2	16±1	13±1	0.35	29±20	21±1*	22±2*	**0.008**
MV e’ (mm/s)	14±1	12±1	12±1	0.34	29±2	22±1	24±2	0.09
TEI index	0.44±0.04	0.80±0.38	0.35±0.02	0.33	0.69±0.06	0.56±0.03	0.63±0.03	0.16
e’/a’	1.16±0.14	0.82±0.04	0.94±0.12	0.12	1.04±0.04	1.09±0.10	1.06±0.06	0.89
E/E’	37±4	43±4	45±4	0.41	26±3	30±3	32±3	0.42

Data are mean±SEM. Comparisons between group was performed using a one-way ANOVA followed by Sidak posthoc test. *P<0.05, **P<0.01, ***P<0.001, ****P<0.0001 versus Ctl; #P<0.05, ##P<0.01, ###P<0.001, ####P<0.0001 versus ID. Aortic ejection time, AET; early left ventricular filling velocity, E or MV E; late left ventricular filling velocity, A or MV A; early mitral valve filling velocity, e' or MV e'; isovolumetric contraction time, IVCT; isovolumetric relaxation time, IVRT; late left ventricular filling velocity, A or MV A; late mitral valve filling velocity, a' or MV a'; left atrium diameter, LA diameter; myocardial performance index, TEI index

Table 3.9. Neonatal pulmonary and right heart function in males.

Male Offspring		**PD3**		**P Value**		**PD13**		**P Value**
	Ctl (n=5–7)	**ID** (n=7–8)	**KID** (n=8–9)		**Ctl** (n=3–7)	**ID** (n=6–7)	**KID** (n=8–9)	
S wave (mm/s)	146±20	209±20	226±13*	**0.02**	190±29	213±18	215±16	0.67
D wave (mm/s)	231±16	267±12	262±6	0.09	269±35	309±25	290±16	0.57
A wave (mm/s)	49±4	108±25	96±12	0.10	96±17	121±13	120±18	0.61
A duration (ms)	27±10	25±4	20±3	0.56	24±8	29±6	22±3	0.58
S/D	0.64±0.08	0.78±0.06	0.86±0.04	0.06	0.99±0.44	0.69±0.04	0.74±0.04	0.65
PAT (ms)	20±1	22±2	24±2	0.17	24±2	25±1	26±1	0.39
PET (ms)	101±5	99±5	94±2	0.53	85±2	98±2***	91±1*#	**0.0004**
PV (mm/s)	562±65	659±61	719±63	0.24	633±43	689±40	776±42	0.07
PAT/PET	0.19±0.01	0.23±0.01	0.25±0.02*	**0.02**	0.29±0.02	0.26±0.01	0.29±0.01	0.17
TV A (mm/s)	351±31	356±21	344±11	0.89	366±28	346±20	376±74	0.81
TV E (mm/s)	594±51	617±49	669±30	0.47	585±44	540±21	585±28	0.50
TV E/A	0.60±0.04	0.60±0.05	0.52±0.03	0.29	0.63±0.04	0.63±0.03	0.63±0.00	1.00

Data are mean±SEM. Comparisons between group was performed using a one-way ANOVA followed by Sidak posthoc test. *P<0.05, **P<0.01, ***P<0.001, ****P<0.0001 versus Ctl; #P<0.05, ##P<0.01, ###P<0.001, ####P<0.0001 versus ID. Early right ventricular filling velocity, E or TV E; late right ventricular filling velocity, A or TV A; pulmonary artery acceleration time, PAT; pulmonary artery ejection time, PET; pulmonary artery peak velocity, PV; pulmonary vein atrial reversal, A wave; pulmonary vein atrial reversal duration, A duration; pulmonary vein diastolic wave, D wave; pulmonary vein systolic wave, S wave.

Table 3.10. Neonatal pulmonary and right heart function in females.

Female Offspring		**PD3**		**P Value**		**PD13**		**P Value**
	Ctl (n=3-7)	**ID** (n=8)	**KID** (n=9)		**Ctl** (n=5–7)	**ID** (n=6–7)	**KID** (n=9)	
S wave (mm/s)	174±17	218±13	229±13*	**0.04**	167±19	241±23	238±19	**0.03**
D wave (mm/s)	254±12	267±21	269±14	0.77	331±22	287±34	300±12	0.43
A wave (mm/s)	47±7	106±8*	83±12	**0.03**	96±20	106±6	113±12	0.65
A duration (ms)	14±2	19±3	22±2	0.14	18±3	23±4	22± 23	0.65
S/D	0.69±0.05	0.85±0.07	0.86±0.06	0.11	0.51±0.05	0.96±0.23	0.79±0.06	0.07
PAT (ms)	20±0.95	25±2	23±1	0.08	23±1	24±1	22±1	0.28
PET (ms)	94±3	96±3	94±2	0.90	83±2	93±1*	88±2	**0.02**
PV (mm/s)	608±50	650±36	613±48	0.73	652±20	766±35	766±48	0.09
PAT/PET	0.21±0.01	0.26±0.02	0.25±0.017	0.11	0.28 ± 0.01	0.26 ± 0.01	0.25 ± 0.01	0.15
TV A (mm/s)	360±10	381±23	443±42	0.16	358±25	369±18	430±55	0.40
TV E (mm/s)	570±27	636±42	664±33	0.19	544±21	608±39	605±41	0.38
TV E/A	0.64±0.02	0.60±0.02	0.62±0.06	0.82	0.66±0.05	0.61±0.01	0.70±0.05	0.44

Data are mean±SEM. Comparisons between group was performed using a one-way ANOVA followed by Sidak posthoc test. *P<0.05, **P<0.01, ***P<0.001, ****P<0.0001 versus Ctl; #P<0.05, ##P<0.01, ###P<0.001, ####P<0.0001 versus ID. Early right ventricular filling velocity, E or TV E; late right ventricular filling velocity, A or TV A; pulmonary artery acceleration time, PAT; pulmonary artery ejection time, PET; pulmonary artery peak velocity, PV; pulmonary vein atrial reversal, A wave; pulmonary vein atrial reversal duration, A duration; pulmonary vein diastolic wave, D wave; pulmonary vein systolic wave, S wave.

Markers of ketone metabolism were assessed in male (**Table 3.11**) and female (**Table 3.12**) offspring at PD0, PD4 and PD14. In all offspring, cardiac Oxct1 was not different among groups. BDH2 was reduced in ID and KID groups compared to controls at PD0 and 4, as well as a marked increase in BDH1 at PD4 and 14. In the liver—the primary site of ketogenesis—Hmgcs2 was not different among groups (in either sex). BDH1 was reduced at PD4 in ID and KID groups, as were BDH2 and CD36 at PD0. In contrast to males, cardiac BDH1 was increased in ID and KID offspring at PD0, whereas BDH2 was reduced at PD4 and 14. Liver BDH2 at PD0 was reduced in ID and KID female offspring, whereas at PD4, BDH1 decreased in ID and KID offspring, and BDH2 and Mct were elevated in these groups.

Maternal ID and ketone treatment also affected expression of genes that encode oxidative stress resistance factors in male (**Figure 3.2**) and female offspring (**Figure 3.3**). In male offspring, metallothionine (Mt2) was increased by ketone treatment at PD0, and antioxidants Sod2 and *Cat* were reduced at PD4. Furthermore *Il-1β,* a marker of cardiac inflammation, was increased in male ID offspring at PD0 and PD4, this effect was reversed by βOHB treatment. Finally, *BNip3* was increased in male KID offspring at PD0 and in ID offspring at PD4. In the females, Mt2 was similarly increased in ID and KID offspring at PD0 (but not at other time points assessed), but no definitive trend in antioxidant gene expression was evident, except at PD14, where ID females had reduced Sod2, and this was reversed with maternal ketone supplementation. Notably, at PD0, KID female hearts exhibited increased IL-1*β* as well as increased *Bnip3* in both ID and KID offspring.

Table 3.11. Ketone metabolism genes in males.

Male Offspring		**PD0**		**P Value**		**PD4**		**P Value**		**PD14**		**P Values**
	Ctl (n=5–7)	**ID** (n=6–7)	**KID** (n=4–7)		**Ctl** (n=6–7)	**ID** (n=6–7)	**KID** (n=5–10)		**Ctl** (n=5–7)	**ID** (n=5–7)	**KID** (n=7–10)	
Heart												
Bdh1	1.00±0.06	1.17±0.07	1.09±0.06	0.21	1.00± 0.07	1.86±0.18**	1.72±0.14**	**0.0008**	1.00±0.22	2.75±0.70	3.10±0.59	**0.05**
Bdh2	1.00±0.09	0.70±0.02	0.82±0.09	**0.03**	1.00± 0.05	0.86±0.03	0.74±0.04**#	**0.002**	1.00±0.08	0.92±0.02	0.87±0.05	0.26
Oxct1	1.00±0.04	0.91±0.05	0.96±0.04	0.39	1.00± 0.06	1.07±0.08	0.86±0.05	0.07	1.00±0.09	0.98±0.14	1.24±0.15	0.33
Liver												
Bdh1	1.00±0.07	0.91±0.12	0.84±0.08	0.52	1.00± 0.07	0.63±0.07**	0.60±0.03***	**<0.0001**	1.00±0.13	0.96±0.07	0.76±0.04	0.08
Bdh2	1.00±0.11	0.55±0.04*	0.90±0.13	**0.01**	1.00± 0.18	0.76±0.10	1.02±0.24	0.59	1.00±0.20	1.48±0.49	0.85±0.10	0.28
Mct1	1.00±0.10	0.92±0.04	0.79±0.04	0.11	1.00± 0.09	1.22±0.07	1.11±0.07	0.17	1.00±0.08	0.74±0.07	0.87±0.05	**0.03**
Cd36	1.00±0.18	0.63±0.08*	0.46±0.03	**0.01**	1.00± 0.21	0.59±0.07*	0.69±0.18	0.25	1.00±0.10	1.38±0.35	0.93±0.06	0.22
Hmgcs2	1.00±0.13	0.85±0.10	1.02±0.20	0.66	1.00± 0.13	0.85±0.07	0.83±0.07	0.71	1.00±0.14	1.20±0.29	0.78±0.04	0.19

Data are mean±SEM. Comparisons between group was performed using a one-way ANOVA followed by Sidak posthoc test. *P<0.05, **P<0.01, ***P<0.001, ****P<0.0001 versus Ctl; #P<0.05, ##P<0.01, ###P<0.001, ####P<0.0001 versus ID.

Table 3.12. Ketone metabolism genes females.

Female Offspring	PD0			P Value	PD4			P Value	PD14			P Values
	Ctl (n=5–7)	**ID** (n=6–7)	**KID** (n=4–7)		**Ctl** (n=6–7)	**ID** (n=6–7)	**KID** (n=5–10)		**Ctl** (n=5–7)	**ID** (n=5–7)	**KID** (n=7–10)	
Heart												
Bdh1	1.00±0.13	1.68±0.10**	1.66±0.10***	**0.0006**	1.00±0.14	1.16±0.07	1.13±0.06	0.46	1.00±0.19	1.50±0.32	1.68±0.24	0.17
Bdh2	1.00±0.06	0.78±0.07	1.03±0.08	0.08	1.00±0.06	0.81±0.04*	0.82±0.05*	**0.03**	1.00±0.12	0.81±0.06	0.69±0.04*	**0.02**
Oxct1	1.00±0.13	1.18±0.07	1.14±0.06	0.38	1.00±0.07	0.96±0.05	0.99±0.07	0.91	1.00±0.16	0.89±0.07	1.01±0.10	0.77
Liver												
Bdh1	1.00±0.11	0.66±0.11	0.80±0.08	0.08	1.00±0.07	0.72±0.08	0.70±0.06*	**0.01**	1.00±0.04	0.89±0.06	0.94±0.08	0.54
Bdh2	1.00±0.14	0.53±0.06*	0.78±0.06	**0.005**	1.00±0.12	1.90±0.25*	1.95±0.22*	**0.009**	1.00±0.10	1.16±0.15	1.53±0.24	0.16
Mct1	1.00±0.15	0.94±0.09	0.88±0.05	0.67	1.00±0.08	1.26±0.04*	1.22±0.08	**0.04**	1.00±0.08	0.97±0.07	0.92±0.07	0.70
Cd36	1.00±0.10	1.58±0.81	0.60±0.06*	0.27	1.00±0.22	0.86±0.07	0.65±0.11	0.22	1.00±0.07	1.09±0.15	1.38±0.12	**0.07**
Hmgcs2	1.00±0.10	0.82±0.09	0.88±0.10	0.49	1.00±0.08	1.24±0.13	1.25±0.10	0.22	1.00±0.08	0.81±0.07	1.03±0.10	0.21

Data are mean±SEM. Comparisons between group was performed using a one-way ANOVA followed by Sidak posthoc test. *P<0.05, **P<0.01, ***P<0.001, ****P<0.0001 versus Ctl; #P<0.05, ##P<0.01, ###P<0.001, ####P<0.0001 versus ID.

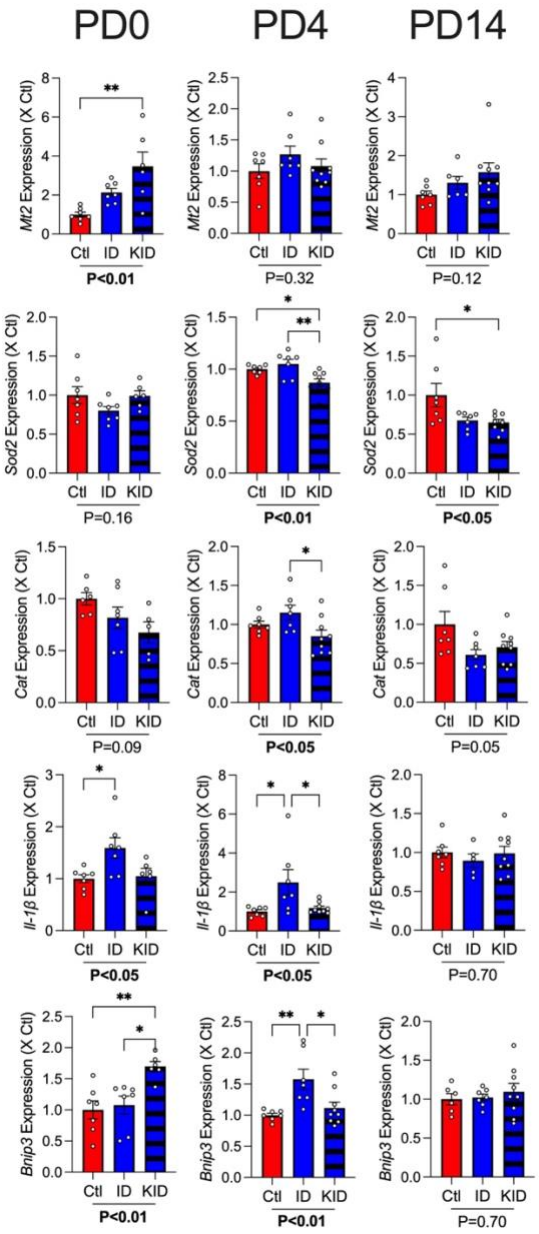

Figure 3.2. RT-qPCR of cardiac injury and oxidative stress in males. In control (CTL), iron-deficient (ID), and ketone treated iron-deficient (KID) offspring on postnatal day (PD) 0, 4, and 14. Data are mean ±SEM. Data are analyzed by one way ANOVA with Tukey's post hoc test; stated p values reflect overall outcomes, and stars represent post-hoc outcomes (*P<0.05, **P<0.01, ***P<0.001, ****P<0.0001).

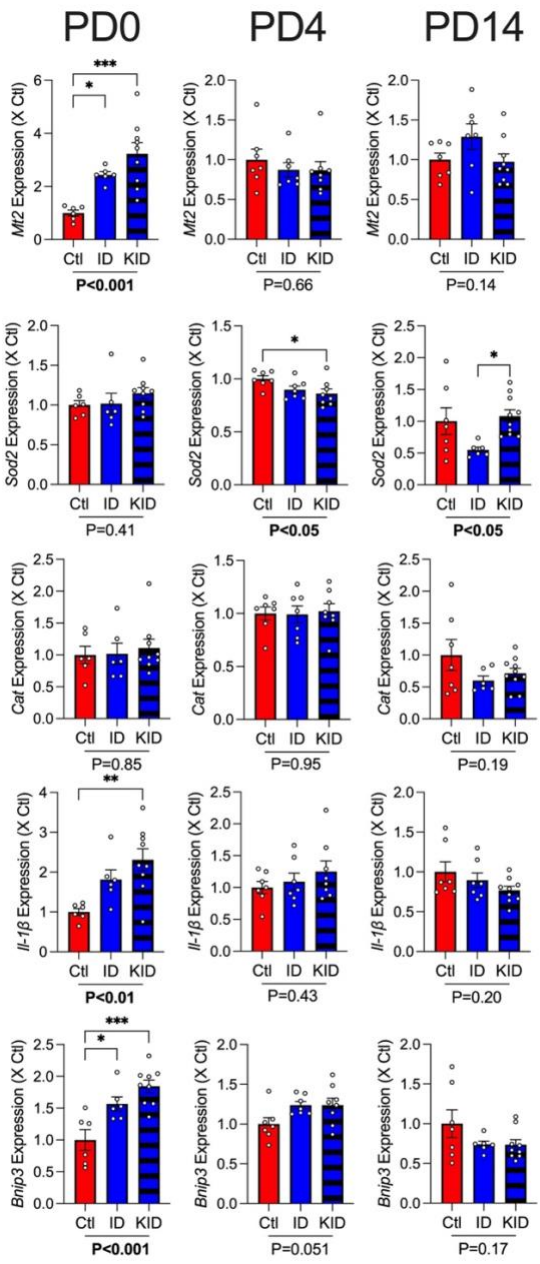

Figure 3.3. RT-qPCR of cardiac injury and oxidative stress in females. Control (CTL), iron-deficient (ID), and ketone treated iron-deficient (KID) in offspring on postnatal day (PD) 0, 4, and 14. Data are mean ±SEM. Data are analyzed by one way ANOVA with Tukey's post hoc test; stated p values reflect overall outcomes, and stars represent post-hoc outcomes (*P<0.05, **P<0.01, ***P<0.001, ****P<0.0001).

3.5 Discussion

Iron deficiency remains the most common nutritional deficiency worldwide, and pregnant women and infants are among the most susceptible subgroups. While iron supplements are widely available and commonly prescribed during pregnancy and in early infancy, the intractability of ID belies the effectiveness of this strategy. As noted above, some of the challenges with iron supplementation include poor compliance (because iron supplements can cause gastrointestinal discomfort), and many cases of ID are attributed to poor intestinal uptake, where supplements are of little benefit. Consequently, there is value in investigating alternative treatments to prevent or mitigate the deleterious short- and long-term effects associated with perinatal ID. We and others have previously shown that ketones exhibit cardioprotective effects in several preclinical disease models (375, 381-384). Here, we investigated the use of daily maternal βOHB-supplementation throughout pregnancy as a means to improve offspring cardiac effects caused by ID. To summarize the results, perinatal ID caused: (1) asymmetrical growth restriction, characterized by increased brain and heart weights; (2) systolic dysfunction and diminished systemic O2 delivery, as well as alterations in diastolic and pulmonary function in male and female offspring; (3) alterations in expression of genes related to metabolic function as well as inflammation and oxidative stress within the heart. Moreover, ketone supplementation in ID dams (4) prevented systolic dysfunction in offspring and altered gene expression related to inflammation and oxidative stress in the neonatal period.

We previously reported that maternal iron restriction (and resultant offspring ID) is associated with altered growth and development in the neonatal period, which included marked cardiomegaly. Interestingly, despite having larger hearts, ID results in systolic dysfunction in neonates, which thereby mitigates increases in CO and impairs the heart's ability to overcome the hypoxemia caused by anemia (**Chapter 2**). Here, we show that ketone supplementation during pregnancy reversed this systolic dysfunction in ID neonates, which enables the larger hearts to

increase cardiac contractility, CO, and total oxygen delivery. Notably, βOHB supplementation improved CO in the absence of an increase in wall thickness; this is important because cardiac hypertrophy during periods of rapid growth and development could lead to persistent structural changes that predispose the offspring to cardiac complications with age (385). Finally subtitle changes in cardiac function (e.g. MV A wave velocity and PET in males, and AET in females) were improved at PD13 indicating there may be some lasting effects of ketone supplementation.

Despite improving heart function at PD3, maternal ketone supplementation had no effect on body weight or organ weights at PD0 or PD4. Although we do not have a definitive explanation for this, it is possible that the timing of ketone supplementation was not optimal for this model. Dam ketone supplementation was restricted to pregnancy for both practical as well as conceptual reasons. Pragmatically, this treatment regimen was chosen to avoid repeated handling and injecting neonatal pups, which can increase in incidence of maternal cannibalism in this and other models of developmental stress (unpublished observations). Conceptually, since ID fetuses deviate most from their normal growth trajectories in the last week of gestation (Hanna et al.)— where fetal body weights increase 3-fold from GD18-21— we reasoned that offspring would be most amenable to treatments that improve cardiac function during this developmental period. However, a recent study showed that the provision of high FiO2 did not result in increased oxygen consumption in the ID fetus, despite exhibiting marked growth restriction and enlarged placentas (**Chapter 4**). One interpretation of these findings is that ID imposes constraints on fetal growth and metabolism throughout pregnancy (possibly by impairing placental development and function) such that fetal circulatory adaptations do not result in improved oxygen and nutrient delivery to tissues. In this scenario, ketone supplementation as a therapeutic strategy to improve

fetal cardiac function would be effective only if the metabolic constraint imposed by ID (i.e. placental dysfunction) is prevented or removed. Postnatal ketone supplementation could be an alternative strategy to improve neonatal offspring cardiac function in this model, although the short and long-term benefits of a comparatively late intervention as opposed to a gestational treatment should also be considered. Notwithstanding the inability to reverse growth restriction in ID offspring, the utility of ketone supplementation could make neonates more resilient to stressors associated with impaired oxygen delivery. Indeed, neonatal anemia is associated with increased incidence of ischemic bowel injury (386), and the beneficial effects of ketone supplementation on neonatal heart function could improve blood flow and reduce a potentially life-threatening scenario.

To gain some insights into the mechanisms by which maternal βOHB supplementation improves offspring cardiac function, we assessed gene expression patterns of a number of important signaling cascades. Maternal iron restriction was associated with reduced expression of a number of genes involved in ketone metabolism, including reduced BDH1 and BDH2 in the liver, which is responsible for conversion of AcAc to BHB, and could explain the reduced ketone levels in ID neonates and elsewhere (377). Exogenous ketone administration reversed liver BDH2 in males and females, which is consistent with reports showing their levels are influenced by elevated ketone levels, either by ketogenic diet feeding or diabetic ketoacidosis (387, 388). Since elevated ketone levels affect the endogenous ketone metabolism, the beneficial effects of maternal βOHB supplementation could reside in either direct actions of ketones on the heart, or via indirect mechanism affecting ketone signaling. Interestingly, while cardiac BDH1 was elevated in ID males and females, only ID females exhibited a increase in BDH2 expression. This could reflect

a compensation that ensures efficient ketone utilization in the heart in female offspring, and the lack of compensation could, at least in part, contribute to the cardiac dysfunction that is more pronounced in the male ID offspring.

Consistent with other studies showing βOHB has antioxidant and anti-inflammatory effects in the myocardium (375, 383), ketone supplementation resulted in *Mt2* expression at PD0 (a gene which encodes oxidative stress resistance factors) as well as expression of *Sod2* and *Cat,* albeit in a sex-dependent manner. Moreover, while *Il-1β*— a marker of cardiac inflammation was increased in male ID offspring, the effects were blunted in KID offspring. Altogether, these results could suggest maternal ketone supplementation may be protective through pathways related to inflammation and oxidative stress. However, KID was also associated with elevated I*l-1β* expression, as well as *Bnip3* a marker of heart injury (389), at PD0 and PD4 in males and females. The elevation of these inflammatory (*Il-1β*) and apoptotic (*Bnip3*) markers warrants caution, as this may suggest increased inflammation due to ketone supplementation, and could drive deleterious long-term changes such as a reduced endowment of cardiomyocytes or an increase in fibrosis; both of which may lead to long term cardiovascular consequences (1). Indeed, there is some evidence that diets which elevate circulating ketones can result in harm to the fetus (316, 390). Thus, while maternal ketone supplementation did not cause obvious dysfunction or exacerbate growth restriction in the offspring in the present study, the potential short and long-term risks of treatment should be considered in tandem with the observed benefits. Indeed, in the context of the DOHaD hypothesis, adverse consequences of perinatal intervention treatments could result in long-term health outcomes that do not manifest until later life.

In conclusion, we showed that perinatal ID results in systolic dysfunction in the hearts of ID offspring, and exogenous βOHB supplementation improved cardiac output and total oxygen delivery in the hearts of these offspring. Moreover, ketone supplementation affected gene expression related to inflammation and oxidative stress, but not ketone metabolism, which may suggest involvement of these pathways. While further work is required to investigate the safety profile of βOHB, this suggests βOHB supplementation may be a useful therapy for pregnant women and young children affected by ID and/or anemia.

Data Availability:

All supporting data are included within the main article and the supplementary file.

Funding:

This research was funded by the Canadian Institutes of Health Research (MOP142396 and PS183846 SLB), the Heart and Stroke Foundation of Canada (G-20-0029380 to SLB), the Stollery Children's Hospital Foundation and the Alberta Women's Health Foundation through the Women and Children's Health Research Institute. SLB is a Canada Research Chair (Tier 2) in developmental and integrative pharmacology.

Chapter 4

Use of Photoacoustic Imaging to Study the Effects of Anemia on Placental Oxygen Saturation in Normoxic and Hypoxic Conditions

Ronan M. N. Noble[1,2,3], Raven Kirschenman[1,4], Alyssa Wiedemeyer[1,2,3], Vaishvi Patel[1], Jad-Julian Rachid[1,2,3], Roger J. Zemp[2,5], Sandra T. Davidge[1,2,4,6], Stephane L. Bourque[1,2,3,7]

Affiliations:

1. Women and Children's Health Research Institute, University of Alberta, Edmonton, Alberta, Canada

2. Cardiovascular Research Centre, University of Alberta, Edmonton, Alberta, Canada

3. Department of Pediatrics, University of Alberta, Edmonton, Alberta, Canada

4. Department of Obstetrics and Gynecology, University of Alberta, Edmonton, Alberta, Canada

5. Department of Electrical and Computer Engineering, University of Alberta, Edmonton, Alberta, Canada

6. Department of Physiology, University of Alberta, Edmonton, Alberta, Canada

7. Department of Anesthesiology and Pain Medicine, University of Alberta, Edmonton, Alberta, Canada

PUBLISHED:

Accepted in Reproductive Sciences

4.1 Abstract

We aimed to evaluate fetal and placental oxygen saturation (sO2) in anemic and non-anemic pregnant rats throughout gestation using photoacoustic imaging (PAI). Female Sprague Dawley rats were fed an iron-restricted or iron-replete diet before and during pregnancy. On gestational days 13, 18, and 21, PAI was coupled with high resolution ultrasound to measure oxygenation of the fetus, whole placenta, mesometrial triangle, as well as the maternal and fetal faces of the placenta. PAI was performed in 3D, which allowed sO2 to be measured within an entire region, as well as in 2D, which enabled SO2 measurements in response to a hypoxic event in real time. Both 3D and 2D PAI were performed at varying levels of FiO2 (fraction of inspired oxygen). Iron restriction caused anemia in dams and fetuses, a reduction in fetal body weight, and an increase in placental weight, but overall had minimal effects on sO2. Reductions in FiO2 caused corresponding reductions in sO2 which correlated to the severity of the hypoxic challenge. Regional differences in sO2 were evident within the placenta, and between the placenta and fetus. In conclusion, PAI enables non-invasive measurement of sO2 both rapidly and with a high degree of sensitivity. The lack of overt changes in SO2 levels between control and anemic fetuses may suggest reduced oxygen extraction and utilization in the latter group, which could be attributed to compensatory changes in growth and developmental trajectories.

4.2 Introduction

The placenta is a specialized organ that controls oxygen, nutrient and waste exchange between the mother and fetus throughout pregnancy. It also serves as an important signaling hub via the production of hormones and cytokines. During early pregnancy, placentation occurs in a relatively hypoxic environment, where low oxygen levels prevent early trophoblast differentiation (391). In the following weeks, vascular remodeling results in increased perfusion, resulting in improved oxygen and nutrient delivery to the placenta and fetus. Impaired oxygen delivery to the placenta or fetus, such as in cases of maternal hypoxemia or placental insufficiency, can result in severe pregnancy complications, including intrauterine growth restriction (IUGR), developmental anomalies, or fetal demise (392, 393). Measurements of fetal or placental oxygen delivery would be useful to evaluate fetal exposure to a hypoxic environment this would also allow for distinguishing between cases of constitutional smallness versus IUGR due to placental insufficiency and other complications of pregnancy. Cord blood gas analysis can be performed at the time of delivery; however, this is a poor predictor of hypoxic injury (394); and at this point any damage from hypoxia would have already occurred. Instead, there is a need to assess placental function and oxygenation directly throughout gestation, though this comes with challenges.

In clinical practice, placental health is routinely assessed via ultrasound (also called sonography or ultrasonography). Sonography allows for the assessment of size and shape of the placenta and fetus, as well as flow velocity profiles through the umbilical cord. However umbilical artery velocities have been shown to have limited abilities to detect placental abnormalities in both early and low risk pregnancies (395-398). For these reasons, its use as a screening tool for placental insufficiency (and associated IUGR) is contentious (395, 396). Cordocentesis allows for direct measurements of fetal blood oxygenation, but it is invasive, and cannot provide information on the regional heterogeneity of placental dysfunction. Thus, there is a need for clinical tools that assess perfusion and oxygenation of the conceptus, which could allow earlier detection of placental dysfunction and enable timely intervention.

Photoacoustic imaging (PAI) is a novel approach that has been used primarily to study tumor vascularization (399). Recent improvements in resolution and penetration depth have made imaging tissues like the placenta possible (400-404). PAI employs a laser directed at small regions of tissue which, when absorbed, produces a sound wave that is detected by ultrasound. PAI, like a pulse oximeter, can differentiate molecules such as oxygenated and deoxygenated hemoglobin (Hb) based on absorption spectra (850 nm and 750 nm respectively) (405, 406). This enables spatial imaging within a two- or three-dimensional field, that can be overlaid with B-mode ultrasound images. Additionally, unlike cordocentesis, PAI is non-invasive and therefore allows for serial measurements of the fetus. However, due to the novelty of the technique, how various physiologic variables influence PAI assessments during pregnancy is not clear.

Globally, the incidence of anemia (defined as a reduction of Hb based on trimester) during pregnancy is 36.5%, with the majority of cases attributed to iron deficiency (ID) (211). Anemia in pregnancy is associated with complications, including increased risk of postpartum hemorrhage, placental abruption, preterm birth, and fetal malformation (407). Moreover, because anemia is a risk factor for a number of complications in pregnancy (e.g. IUGR, preeclampsia) (408), developing technologies to screen as well as study these complications within the context of anemia is critical. However, since blood oxygen saturation (sO2) reflects the ratio of oxygenated to deoxygenated hemoglobin, rather than Hb concentrations per se, it is unclear how anemia affects PAI measurements.

The objective of this study was to evaluate placental oxygen saturation in pregnant dams with and without iron deficient anemia (IDA) using PAI. To further explore the impact of anemia on placental and fetal oxygenation, PAI assessments were performed in conditions where control and anemic dams were exposed to an acute hypoxic episode.

4.3 Methods

4.3.1 Animals and Treatments

The protocols described herein were approved by the University of Alberta Animal Care and Use Committee in accordance with guidelines established by the Canadian Council for Animal Care. Female Sprague-Dawley rats (6 wk of age) were purchased from Charles River and housed at the University of Alberta Animal Care Facility, which maintains a 12-hour light/dark cycle and an ambient temperature of 23°C. Rats had *ad libitum* access to food and water throughout. Purified diets used in this study were based on the AIN-93G formula and differed only by the amount of ferric citrate added. Two weeks before mating, female rats were assigned to either a control (Ctl) or IDA groups: rats in the Ctl group were fed a purified control diet containing 37 mg/kg diet of elemental iron, and those in the IDA group were fed a purified diet containing 3 mg/kg diet of elemental iron. After two weeks on their respective diets, female rats were repeatedly housed overnight with male rats (fed a standard rodent chow) until pregnancy was confirmed by presence of sperm in a vaginal smear the next morning (defined as gestational day [GD]0).

4.3.2 Photoacoustic Imaging (PAI)

All dams underwent PAI on GD13, 18, and 21 (term = 22 days). Prior to imaging, dams were induced with 5% isoflurane and maintained at 1.5-2.0% isoflurane carried in 1.5 mL/min of medical-grade gas (composition described below). Depth of anesthesia was monitored continuously and isoflurane was adjusted as needed to maintain a heart rate of at least 70% of the baseline throughout (with exception during the hypoxia challenge). Each animal was anesthetized for a maximum of 2 hours per day. After induction, the abdomen was shaved and the remaining hair was removed by applying depilatory cream (Nair® extra gentle) for a maximum of 30 seconds (to prevent skin irritation). Dams were then placed supine on a heated physiological monitoring stage.

Photoacoustic images were acquired with either the MX250 (15-30 MHz; for GD13 and GD18 assessments) or MX201 (10-22 MHz; for GD21 assessments) connected to the Vevo 3100 LAZR-X photoacoustic imaging system (Fujifilm Visualsonics Inc., Toronto, Canada). The MX250 and MX201 transducers have an axial resolution of 75 and 100μm, respectively, and a medium optical fibre with a width of 24mm; in rats, the MX250 transducer provides sufficient resolution at the earlier gestational stages, whereas the MX201 transducer provides a depth of field to capture larger fetuses at the end of gestation. For each scan the amniotic sac was positioned within the optical focus between 12 and 17 mm with care taken that the both the placenta and the fetus were not obstructed by artifacts (e.g. bubbles, and skin reverberations). Time Gain Compensation was adjusted to add gain to deeper structures and was saved as a pre-set to ensure consistency between animals. The images used to quantify oxygen saturation were collected using 750 nm and 850 nm wavelengths in the built-in Oxyhemo mode.

Two sequential imaging protocols were used in the same cohort of pregnant rats at each gestational age. In the first protocol, photoacoustic scans were performed in a 3-dimensional (3D) mode, allowing for recordings of oxygen saturation across the entire placenta and fetus; this approach was used to evaluate the effects of ID on blood oxygenation in various regions of the fetoplacental unit. The first protocol was performed when dams were administered FiO2 (fraction of inspired oxygen) of 21% and 100%. Collectively this protocol took no longer than 30 minutes.

The second imaging protocol was performed immediately after the first using a 2-dimensional (2D) mode, which allowed for a response to hypoxia to be measured in real time. The placenta was positioned longitudinally so that the following 5 distinct regions of the fetoplacental unit could be imaged simultaneously in one plane: the whole fetus, the whole placenta, the mesometrial triangle (which connects the uterine horn and the placenta), as well as the fetal face of the placenta (i.e. the labyrinth at GD18 and GD21) and the maternal face (i.e. the basal zone at GD18 and GD21). Care was made to ensure planar sections fell within the central region of the placenta and fetus, which proved relatively easy

given the space constraints of the amniotic sac. Baseline images were taken at 21% FiO2, after which the FiO2 was reduced to 4% for 40 seconds and subsequently increased to 100% for up to 80 seconds (after which tachypnea caused the placenta to shift out of the imaging plane). This was done to assess the impact of ID on temporal changes in blood oxygenation following an acute episode of hypoxia (e.g. as might occur during a maternal hypotensive episode).

Tissue oxygenation measurements were quantified from acquired images using VevoLAZR software (Fujifilm Visualsonics Inc., Toronto, Canada). Regions of interest were manually defined: whole placenta, fetal face, maternal face, fetus in both 3D and 2D; as well as skin in 2D.

4.3.3 Tissue Collection

Upon completion of imaging on GD21, dams were anesthetized to a surgical plane (3% isoflurane, maintenance at 100% FiO2) and euthanized by excision of the heart. Fetuses and placentas were removed, cleaned and weighed. Fetuses were then decapitated and blood was collected for blood Hb assessments (HemoCue 201 + system).

4.3.4 Statistical Analysis

In all cases the n values reflect the dam or litter; when multiple placentas or fetuses from the same litter were measured, mean values were calculated and considered n = 1. Data were analyzed by two-way ANOVA or by fitting a mixed-effects model for the effects of iron-restriction and time as implemented in GraphPad Prism 8.3.0. Sidak's post-hoc test was used for multiple comparisons. The Mann-Whitney U test was used for non-continuous data (i.e. litter size and number of resorptions).

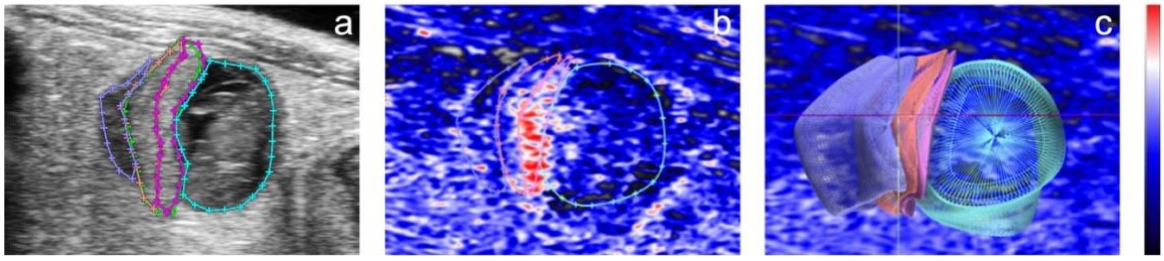

Figure 4.1. 3D photoacoustic imaging (PAI) of placental oxygenation at gestational day 13. Regions highlighted are the mesometrial triangle (dark blue), maternal face of the placenta (orange), fetal face of the placenta (pink), and fetus (teal). In panels B and C bright red represents 100% sO2 dark blue represents 0% sO2 or an absence of hemoglobin.

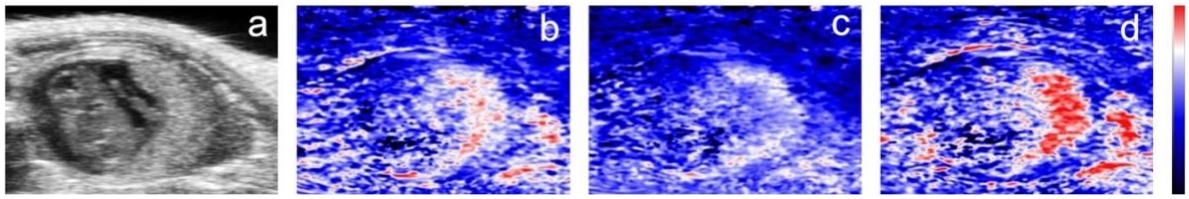

Figure 4.2. 2D photoacoustic imaging (PAI) of placental oxygenation at gestational day 13. From left to right: (a) B-mode ultrasound image of the fetus, umbilical cord, placenta, and mesometrial triangle. PAI images of oxygen challenge through normoxia (b), hypoxia (c), and recovery (d). In panels b through d bright red represents 100% sO2 dark blue represents 0% sO2 or an absence of hemoglobin.

4.4 Results

Dietary iron restriction prior to and throughout pregnancy caused a progressive decline in maternal Hb levels, culminating in a 50% decrease by GD21 (**Figure 4.3a**). ID fetuses were also anemic (-48% in males and -43% in females) and growth restricted (-20% in males, and -16% in females) (**Figure 4.3b, c**) compared to their control counterparts. Placental efficiency (the ratio of fetal weight to placental weight) was decreased by 35% in both males and females (**Figure 4.3e**). Finally, anemia was associated with increased reabsorptions (mean of 2 vs 0, P=0.04) and correspondingly reduced litter sizes (-49%; P=0.007).

In the first protocol, oxygen saturations were measured at various regions of the feto-placental unit in 3-D at an FiO2 of 21% and 100%. This allowed for the whole of the placenta and fetus to be assessed rather than a single plane. IDA was associated with increased sO2 in the mesometrial triangle at GD13, as well as the whole placenta and fetal face at GD21; the effect of IDA was most pronounced when dams were exposed to FiO2 of 100% (**Table 4.1**). In all regions assessed, higher FiO2 were associated with higher sO2, except within the mesometrial triangle at GD21 (**Table 4.1**).

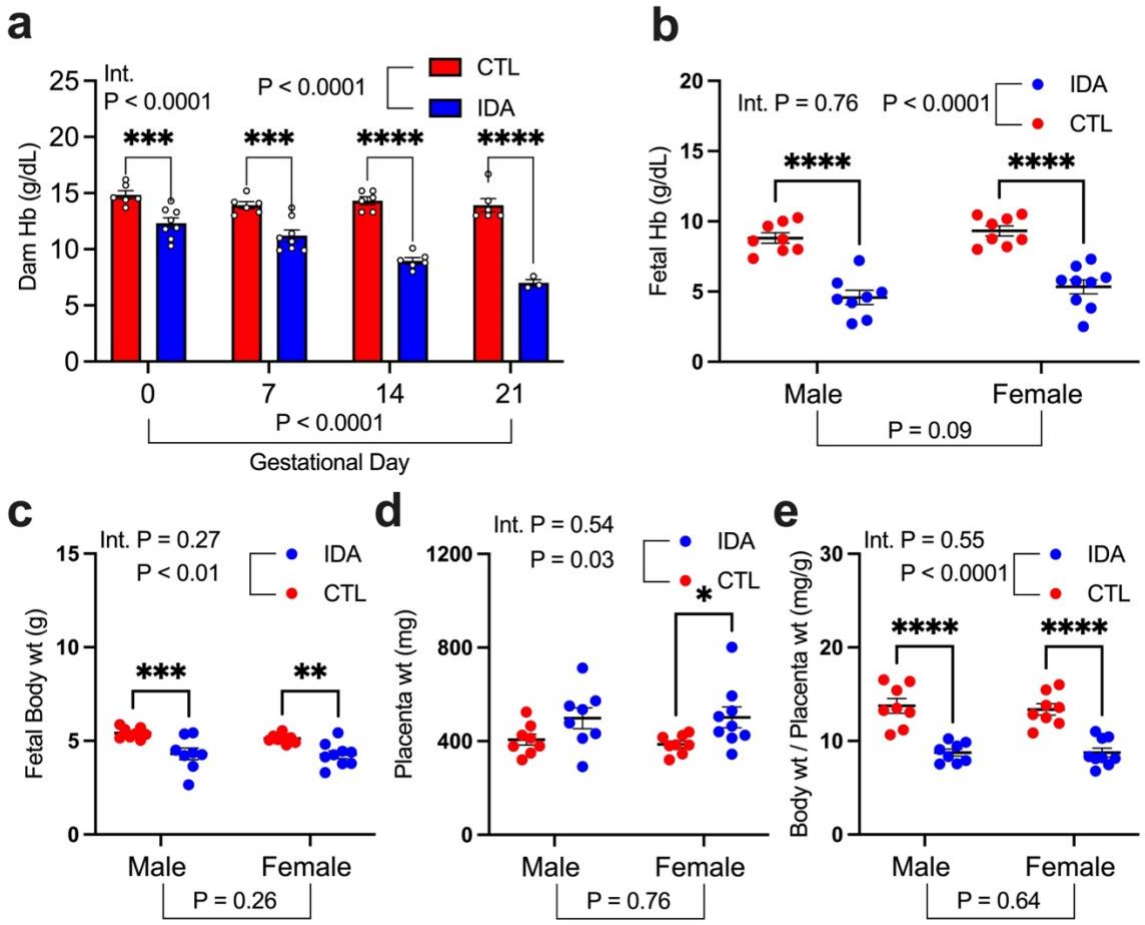

Figure 4.3. Maternal and fetal parameters. Maternal Hb (a), fetal Hb (b), fetal bodyweight (c), placenta weight (d), placental efficiency (e) in CTL and IDA groups. Results are expressed as mean ± SEM. Comparisons between groups were performed using two-way ANOVA followed by Tukey multiple comparisons test. *$p < 0.05$, **$p < 0.01$, ***$p < 0.001$, ****$p < 0.0001$. The Mann-Whitney U test was used for non-continuous data (i.e., litter size and reabsorptions).

Table 4.1. 3D oxygenation of regions of the placenta, the fetus, and the mesometrial triangle.

Region	21% FiO2		100% FiO2		P Values		
	Ctl	IDA	Ctl	IDA	FiO2	IDA	Int.
GD13							
Whole Placenta	61.96 ± 2.10 (8)	62.46 ± 1.84 (12)	71.98 ± 2.18 (8)	75.21 ± 1.15 (12)	**<0.0001**	0.41	0.30
Maternal Face	58.98 ± 3.07 (6)	58.08 ± 2.21 (12)	70.78 ± 3.10 (6)	72.18 ± 1.39 (12)	**<0.0001**	0.93	0.55
Fetal Face	67.55 ± 2.91 (6)	68.95 ± 2.20 (12)	74.52 ± 4.25 (6)	79.96 ± 1.31 (12)	**0.0004**	0.27	0.33
Mesometrial Triangle	55.12 ± 2.61 (6)	60.09 ± 1.20 (11)	62.90 ± 1.88 (6)	68.40 ± 1.70* (11)	**<0.0001**	**0.03**	0.85
Fetus	51.64 ± 2.83 (6)	52.90 ± 1.84 (13)	58.60 ± 2.82 (6)	55.79 ± 1.43 (13)	**0.02**	0.77	0.33
GD18							
Whole Placenta	56.12 ± 1.86 (5)	56.43 ± 1.58 (5)	62.49 ± 1.90 (5)	59.03 ± 2.64 (5)	**0.003**	0.57	0.11
Maternal Face	54.76 ± 2.36 (4)	51.61 ± 3.55 (5)	59.84 ± 1.62 (4)	55.42 ± 3.97 (5)	**0.03**	0.41	0.71
Fetal Face	58.35 ± 2.91 (4)	59.56 ± 2.05 (5)	63.89 ± 2.97 (4)	61.66 ± 1.87 (5)	**0.02**	0.21	0.88
Mesometrial Triangle	54.98 ± 3.96 (3)	54.40 ± 2.53 (5)	63.38 ± 0.51 (3)	64.47 ± 1.77 (5)	**0.005**	0.93	0.70
Fetus	48.93 ± 0.96 (5)	52.06 ± 1.89 (11)	59.06 ± 1.20 (5)	60.41 ± 2.36 (11)	**<0.0001**	0.50	0.26
GD21							
Whole Placenta	61.85 ± 2.45 (5)	62.77 ± 1.40 (6)	64.14 ± 1.08 (4)	72.83 ± 2.69* (5)	**0.009**	**0.01**	0.09
Maternal Face	57.46 ± 3.00 (4)	58.58 ± 1.87 (6)	61.30 ± 0.98 (4)	66.49 ± 3.09 (5)	**0.03**	0.34	0.42
Fetal Face	63.35 ± 2.45 (4)	66.19 ± 1.26 (6)	66.77 ± 1.28 (4)	77.29 ± 2.68* (5)	**0.003**	**0.02**	0.05
Mesometrial Triangle	60.28 ± 2.82 (4)	57.70 ± 3.80 (3)	62.73 ± 3.18 (4)	66.84 ± 2.09 (3)	0.13	0.81	0.34
Fetus	53.01 ± 3.03 (4)	50.38 ± 1.97 (5)	58.33 ± 2.05 (4)	58.51 ± 2.03 (5)	**0.01**	0.65	0.48

Results are expressed as mean ± SEM. Ctl, control; IDA, iron deficient anemic. *P<0.05 vs Ctl (Tukey post hoc test, 2-way ANOVA outcomes).

To determine if the LAZR-X could measure differences in sO2 between proximal regions at different scales (e.g. whole placenta versus whole fetus, maternal face to fetal face), an ad hoc analysis was performed in which control and IDA treatment groups were pooled. As expected, sO2 values were reduced in the fetus compared to the placenta at 21% FiO2 (GD13: -15%, P=0.0008; GD21: -17%, P=0.001) and 100% FiO2 (GD13: -22%, P<0.0001; GD21: -14%, P=0.02). Interestingly, sO2 values increased from the maternal face to fetal face at 21% FiO2 (GD13: +16%, P=0.0005; GD21: +12%, P=0.0004) and 100% FiO2 (GD13: +13%, P=0.002; GD21: +8%, P=0.001).

When comparing 3D images with 2D baseline images at FiO2 of 21% (i.e. prior to induction of hypoxia) there were no differences in sO2 values at either GD18 or GD21, although at GD13, sO2 values obtained from 2D mode were increased compared to those obtained in 3D mode (Ctl: +9.7%, P=0.01; ID: +8.2%, P=0.001;), which may reflect increased sO2 levels within the central placenta compared to the peripheral sections.

In the second protocol, a central plane of the fetoplacental unit was imaged continuously in real time. Baseline images were taken at 21% FiO2 (normoxia), after which FiO2 was reduced to 4% for 40 seconds, and subsequently increased to 100%. After brief delay, changes in FiO2 were reflected in sO2 levels in the fetus and placenta (**Figure 4.4**). Despite the severity of the challenge, only minimal differences between Ctl and IDA groups were evident. At GD13, sO2 in the whole placenta and fetal face of IDA fetuses, though not statistically elevated, reached higher peak values during exposure to FiO2 of 100% (**Figure 4.4a, b**); a similar pattern was observed in the maternal face of the placenta at GD13 (**Figure 4.4c**), but multiple comparisons did not reach significance. No other effects of IDA were evident in any regions at any timepoints assessed.

Qualitatively, skin sO2 was lowest irrespective of FiO2, but tended to be the most responsive in terms of timing and magnitude. At GD13, regional differences were evident; the whole placenta and fetal face

tended to have higher sO2 levels than the maternal face of the placenta, the fetus, or the mesometrial triangle, albeit responses to the acute hypoxic episode were similar. At GD18 and GD21, no regional differences were evident. Finally, at GD13, during the acute hypoxic challenge, the maternal face of the placenta exhibited a pronounced lag in the time it took to reach minimum sO2 levels (86±4s; n=14) compared to all other regions analyzed (whole placenta: 74±6s; fetal face: 69±7s; mesometrial triangle: 70±2s; fetus: 70±1s; skin: 68±4s; n=13-14 for all measurements; $P<0.001$ for all pairwise comparisons by Holm-Sidak test).

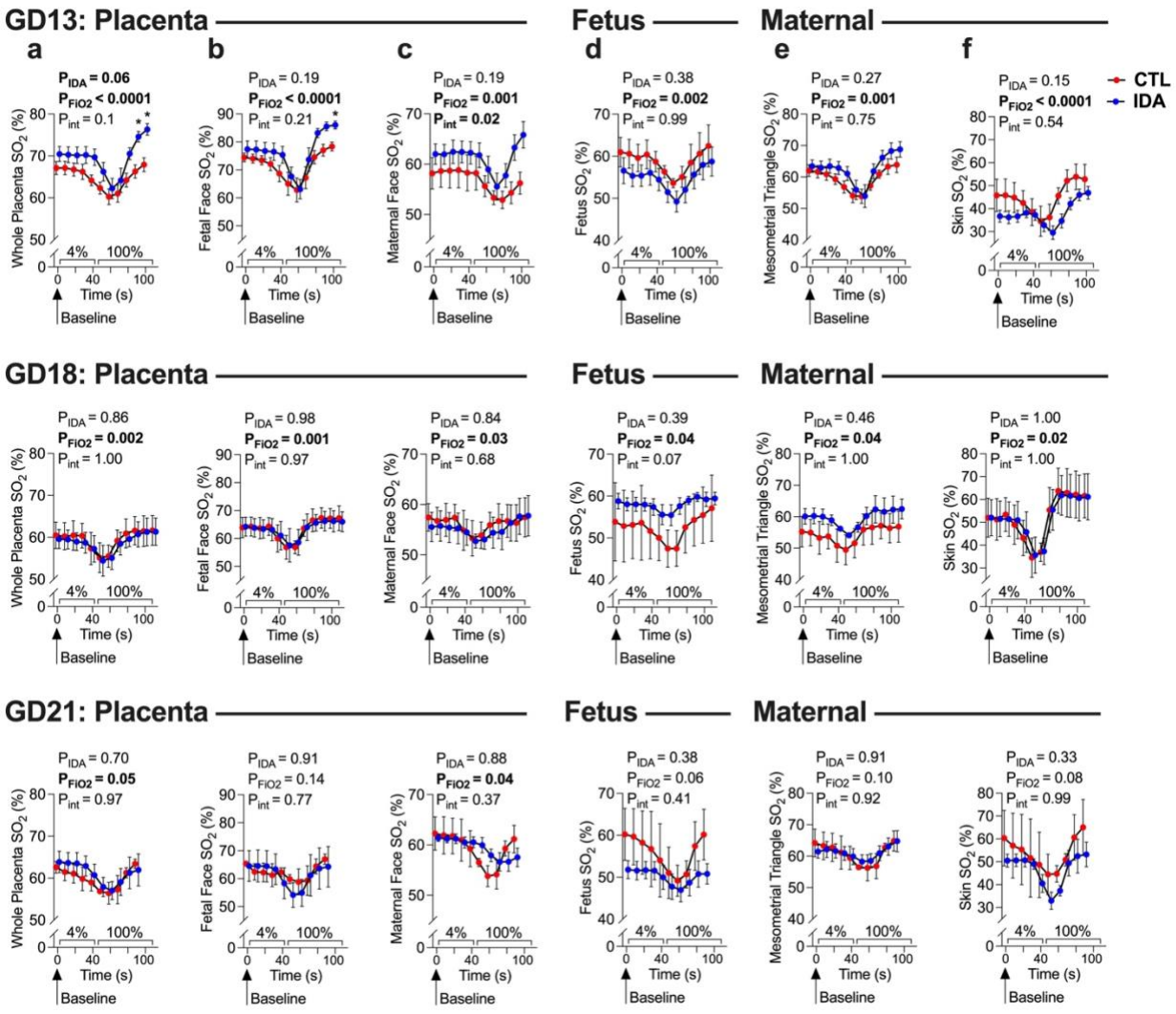

Figure 4.4. 2D time intensity curves obtained over a baseline (21% oxygen), hypoxia (4% oxygen), and hyperoxygenation (100% oxygen). Whole placenta (a), fetal face (b), maternal face (c), fetus (d), mesometrial triangle (e), and maternal skin (f), in CTL and IDA groups. Top, middle, and bottom panels depict gestational days 13, 18, 21 respectively. Results are expressed as mean ± SEM. Comparisons between groups were performed using two-way ANOVA.

4.5 Discussion

The goal of this study was to determine whether maternal anemia affects placental and fetal oxygenation throughout gestation, as assessed by PAI. To summarize, maternal iron restriction caused: (1.) progressively severe maternal anemia throughout pregnancy and severe anemia and growth restriction in fetus by GD21; (2.) no effects on maternal, placental and fetal oxygenation throughout pregnancy when dams were exposed to FiO2 21%; (3.) increased placental oxygenation (particularly on the fetal face) when dams were exposed to FiO2 100% on GD21; (4.) minimal differences in tissue oxygenation when dams underwent an acute hypoxic episode. These findings may suggest reduced oxygen extraction and utilization by IDA fetuses in late gestation.

Outside of pregnancy, oxygen delivery to most tissues exceeds metabolic demands (344), and therefore the reduced oxygen carrying capacity associated with mild anemia can be buffered by increased tissue oxygen extraction (409, 410). However, there is a limit to this reserve; in cases of severe anemia, oxygen extraction exceeds supply and results in impaired tissue oxygenation (411-413). During gestation, physiological reserve is diminished, in part due to increased metabolic demands imposed by growth and development of the fetus and placenta, as well as a reliance on the maternal circulation for oxygen and nutrient supply. We therefore expected sO2 levels to decrease in IDA groups as maternal tissue, placentas, and fetuses may already extract a large portion of delivered oxygen. Contrary to our hypothesis, we found that tissue sO2 were largely unaffected by anemia at all gestational days. In fact, sO2 were increased in the fetal face of the placenta in IDA at GD21 with exposure to FiO2 of 100%, suggesting overall reduced oxygen extraction. This was surprising, because GD21 not only reflects the period during which maternal and fetal anemia are most severe (i.e. low resources), but the last 3 days of gestation also represents a period during which fetal weight increases 3-4-fold (i.e. high metabolic demand) (380).

This seemingly paradoxical finding could be explained in the context of fetal resource allocation in the wake of a suboptimal uterine environment. We and others have shown that IDA results in maladaptive changes in the placenta; despite being larger, IDA placentas have proportionally smaller labyrinth zones (380) with reduced vascularization (414). The placentas are therefore less efficient, and unable to sustain optimal growth and development, particularly as anemia worsens and metabolic demands of the fetus increase throughout pregnancy (380). When faced with this suboptimal in utero environment, the fetus may alter its developmental trajectories in an effort to reduce energy expenditure, and allocate the limited resources available to essential processes that ensure survival (223, 380). In this way, the lower growth rate of the IDA fetus is sustainable despite a less-efficient placenta and the relative hypoxemia induced by maternal anemia, and the transient provision of excess oxygen (i.e., exposure to FiO2 100%) is not used by the fetus. This could explain why sO2 levels in the fetal face of the placenta remain elevated in the IDA group, but fetal values are unchanged. Similarly, the acute exposure to hypoxia had comparable effects on sO2 levels in the IDA group as controls despite overall reduced fetal oxygen delivery (due by anemia) (223) because of the proportionally smaller IDA fetus.

In addition to measuring differences between compartments (i.e. fetus, placenta), we also show that the newest generation of PAI could clearly measure differences in sO2 between the maternal and fetal faces of the placenta at GD13 in rats. Notably, these differences could not be detected using 2D imaging, but only using the sensitive 3D imaging, which measures oxygenation over the whole region rather than a single plane. This is perhaps not surprising because placental vascularization is not homogenous, and this central planar image is unlikely to reflect oxygenation of the entire placenta. This finding is consistent with a report by Arthuis et al. that showed 2D PAI could not detect placental regional differences in sO2 at GD14 in rats (404), whereas Yamaleyeva et al. could using 3D PAI at GD14 in mice (403); an important caveat here is that GD14 represents a comparatively later developmental timepoint compared to rats, since gestational length is 4 days shorter in mice (term=GD18). Despite the increased sensitivity of the 3D imaging approach, we also show that a single plane (as assessed using 2D imaging) is sensitive to

changes in inspired oxygen, and can be measured in real time. Therefore, PAI could be used to measure oxygenation noninvasively in the context of acute fetal or maternal distress.

Although PAI has been used in the clinical setting, it has mostly been adopted as a research tool to measure blood flow, oxygenation, or metabolite clearance in peripheral tissues (e.g., tumour, muscle) and the vasculature (415-417). Feto-placental imaging by PAI could be useful for monitoring fetal well-being. However, currently depth of penetration remains a limitation for its use in obstetrics, since imaging tissues with a depth beyond 3.5 cm is not feasible. However, PAI may be a practical choice in many cases, particularly in the third trimester of pregnancy, when the placenta is pressed closer to the surface (418, 419). It is important to remember that PAI is a relatively new technology, with commercially available lasers only recently entering the market. The development of powerful lasers which can quickly switch between wavelengths, in this case to excite oxygenated and deoxygenated Hb; as well as ultrasound transducers sensitive enough to measure these signals is currently underway, with these advancements PAI's applications in obstetrics could be more widespread. there are other imaging modalities that could be used to measure oxygen saturation and delivery (e.g., MRI (420)), PAI offers advantages, including real-time imaging, portability, and cost-effectiveness. Most importantly, due to the ubiquity of sonography use at the bedside, PAI could be easily integrated as a standard of care, particularly with the ongoing developments of 3D photoacoustic tomography which will further improve resolution.

In conclusion, photoacoustic imaging offers a method to measure fetal, placental, and maternal oxygenation noninvasively. To our surprise these results show that IDA results in little or no differences in tissue oxygenation as measured with the current system, which may reflect fetal and placental adaptations to ensure fetal survival in a suboptimal gestational environment. This technology has the potential to determine the role of placental and fetal hypoxia in several different disease models, regardless of fetal or maternal hemoglobin.

Funding information

This research was funded by the Canadian Institutes of Health Research (MOP142396 and PS183846 SLB), the Heart and Stroke Foundation of Canada (G-20-0029380 to SLB), the Stollery Children's Hospital Foundation and the Alberta Women's Health Foundation through the Women and Children's Health Research Institute. SLB is a Canada Research Chair (Tier 2) in developmental and integrative pharmacology.

Data Availability

All data supporting the findings of this study are available within the paper.

Statements and Declarations

Competing Interests: RJZ is founder and shareholder of CliniSonix Inc. and IllumiSonix Inc., which, however, did not support this work. RJZ is also a Scientific Advisory Board member of FUJIFILM Visualsonics, which, however, did not support this work.

Ethics approval: The protocols described herein were approved by the University of Alberta Animal Care and Use Committee in accordance with guidelines established by the Canadian Council for Animal Care.

Consent to participate: Not applicable

Consent for publication: Not applicable

Availability of data and material: All data supporting the findings of this study are available within the paper.

Code availability: Not applicable

Chapter 5

Broccoli Sprouts Promote Sex-Dependent Cardiometabolic Health and Longevity in Long Evans Rats

Ronan M. N. Noble [1,2*], Forough Jahandideh [2,3*], Edward A. Armstrong [1], Stephane L. Bourque[1,2,3,4,], and Jerome Y. Yager [1,2]

1. Department of Pediatrics, University of Alberta, Edmonton, AB T6G 2G3, Canada

2. Women and Children's Health Research Institute, University of Alberta, Edmonton, AB

3. Department of Anesthesiology & Pain Medicine, University of Alberta, Edmonton, AB

4. Department of Pharmacology, University of Alberta, Edmonton, AB T6G 2G3, Canada

* denotes equal contribution

PUBLISHED:

Noble *et al.* Int J Environ Res Public Health 2022. Oct 18;19(20):13468

5.1 Abstract

Antioxidants and anti-inflammatory compounds are potential candidates to prevent age-related chronic diseases. Broccoli sprouts (BrSp) are a rich source of sulforaphane—a bioactive metabolite known for its antioxidant and anti-inflammatory properties. We tested the effect of chronic BrSp feeding on age-related decline in cardiometabolic health and lifespan in rats. Male and female Long-Evans rats were fed a control diet with or without dried BrSp (300 mg/kg body weight, 3 times per week) from 4 months of age until death. Body weight, body composition, blood pressure, heart function, and glucose and insulin tolerance were measured at 10, 16, 20, and 22 months of age. Behavioral traits were also examined at 18 months of age. BrSp feeding prolonged life span in females, whereas in males the positive effects on longevity were more pronounced in a subgroup of males (last 25% of survivors). Despite having modest effects on behavior, BrSp profoundly affected cardiometabolic parameters in a sex-dependent manner. BrSp-fed females had a lower body weight and visceral adiposity while BrSp-fed males exhibited improved glucose tolerance and reduced blood pressure when compared to their control counterparts. These findings highlight the sex-dependent benefits of BrSp on improving longevity and delaying cardiometabolic decline associated with aging in rats.

5.2 Introduction

Aging is a complex biologic process associated with structural and biochemical changes that result in progressive functional decline (171). Free radical and related oxidants are believed to be involved in this process. Oxidative stress is thought to activate the immune system generating inflammatory responses that further exacerbate oxidative stress; the resulting cyclic pattern leads to progressive physiological decline, culminating into increased morbidity, and eventual mortality (421). Uncontrolled oxidative stress has been suggested as one of the primary causes of cardiovascular disease and other major health problems (422). Reduction of oxidative stress on the other hand, has the potential to reverse the age-related functional deficits in rodents (423, 424). Antioxidant molecules, acting directly or indirectly to protect cells against oxidative stress, have the potential to prevent age-related diseases. Direct antioxidants, such as ascorbate and tocopherols (exogenous antioxidants) as well as glutathione, α-lipoic acid, and ubiquinols (endogenous antioxidants), are redox active compounds able to scavenge reactive oxygen species. Direct antioxidants are typically short-lived, requiring replenishment or regeneration as they are consumed in mediating their antioxidant effects. In contrast, indirect antioxidants mediate their effects by supporting endogenous antioxidant function and are more efficient in reducing oxidative stress and its associated dysfunctions. Indirect antioxidants are able to activate the Kelch-like ECH-Associating protein 1 nuclear factor erythroid 2 related factor 2-antioxidant response element (Keap1-Nrf2-ARE) pathway, an important cellular defense mechanism. Keap1-Nrf2-ARE regulatory pathway activation results in transcriptional induction of various cytoprotective proteins that play a role in the regeneration of the direct antioxidant glutathione (425). Age-associated decline in Nrf2 signaling activity has been suggested as an important factor in the development of age-related onset of neurodegenerative disorders (171). Restoration of endogenous cytoprotective mechanisms through increased Nrf2 activity is believed to be an effective strategy to protect against age-related physiological decline (171).

Many functional foods containing bioactive compounds with antioxidant and anti-inflammatory properties are promising agents for the prevention of age-related chronic diseases (426). Sulforaphane is

an aliphatic isothiocyanate and an Nrf2 activator with antioxidant properties (427). Broccoli sprouts (BrSp) contain the highest concentration of glucoraphanin, a glucosinolate hydrolyzed by myrosinase to sulforaphane. Crushing of the plant cells by chewing or food preparation releases myrosinase from intracellular vesicles, after which glucoraphanin hydrolyze to yield sulforaphane. Young BrSp contain higher amounts of glucosinolates (20–50 times more) than mature market-stage broccoli (264) and may therefore be a better choice for its health-promoting properties. Indeed, we have shown that maternal BrSp feeding during pregnancy confers protection and mitigates brain injury and neurodevelopmental delays in a rat model of induced intra-uterine growth restriction and prenatal inflammation (428, 429). In adult rodents, long-term consumption of BrSp promotes cardiovascular and metabolic health and mitigates organ damage in diabetes and hypertension (430-432). Despite these well documented effects, the long-term effects of BrSp feeding on age-related physiological decline has yet to be reported. Therefore, the aim of this study was to determine the effects of long-term BrSp feeding on cardiometabolic health, behavioral traits, and longevity in rats. Since age-related complications have shown a sex-specific pattern (433), we studied both male and female rats.

5.3 Materials and Methods

5.3.1 Animals and Treatments

The experimental protocols described herein were approved by the University of Alberta Animal Care and Use Committee in accordance with the guidelines established by the Canadian Council of Animal Care. Twelve-week-old Long-Evans rats (bred in-house) and housed at the University of Alberta animal care facility under a light/dark cycle of 12 h and an ambient temperature of 22 °C with 40–60% relative humidity. Fifty-six rats were bred in total. An estimated standard deviation of 20% of the mean, an overall effect of 25% for cardiometabolic parameters with 80% power and an α of 0.05 meant a sample size of at least 10 per group was required. All rats had *ad libitum* access to a standard rodent chow (5L0D; PicoLab, St Louis, MO, USA) and water throughout the study. At 12 weeks of age, males and females were

randomized to the control or BrSp groups. Body weight was monitored monthly for all animals starting at 4 months of age.

Broccoli seeds were purchased from Mumm's Sprouting Seeds (Parkside, SK). Seeds were sprouted for 4 days and greened for 4 h before harvesting. The sprouts were then air dried for 7 days before use. Rats were fed 300 mg/kg body weight BrSp 3 days per week (Monday, Wednesday, Friday, to limit rat agitation) beginning at 4 months of age until death/euthanasia. A quantity of 300 mg/kg BrSp was the maximum amount Long-Evans rats ate entirely in our pilot experiments and is consistent with amounts used in other studies (432, 434).

5.3.2 Body Composition and Metabolic Parameters

Body composition as well as oral glucose tolerance tests (oGTT) and insulin tolerance tests (ITT) were assessed in all rats after 0, 6, 12, 16, and 18 months of treatment (corresponding to 4, 10, 16, 20, and 22 months of age, respectively). Body composition was assessed in conscious rats using a whole-body composition analyzer (EchoMRI 4-in-1/1000, Echo Medical Systems LLC, Houston, TX, USA) throughout the study. For oGTT, rats were fasted overnight (16 h). Baseline blood glucose levels were assessed using a glucometer (AccuChek Aviva Nano, Roche Diagnostics) from a saphenous venipuncture. Rats were then administered a glucose solution (0.5 g D-glucose per mL water) by oral gavage at a dose of 2 g/kg body weight. Blood glucose concentrations were assessed at 15, 30, 60, 90, and 120 min post-glucose administration by saphenous venipuncture.

For the ITT, rats underwent a fast of 4 h prior to blood sampling. Baseline glucose levels were assessed from a saphenous venipuncture using an AccuChek Aviva Nano blood glucometer (Roche Diagnostics). Rats then received an intraperitoneal injection of insulin (1.0IU/kg body weight for males or 0.75 IU/kg body weight for females). Blood glucose concentrations were then assessed at 15, 30, 60, 90, and 120 min post-insulin injection by saphenous venipuncture.

5.3.3 Tail-Cuff Plethysmography

Systolic blood pressure was measured non-invasively by tail-cuff plethysmography (CODA, Kent Scientific, Torington, CT). Animals were lightly sedated (1% isoflurane, 1 L/min oxygen via nose-cone) and maintained on a temperature-controlled platform (kept at 37 °C). After equilibrating to isoflurane for 10 min, a total of 20 separate BP recordings (cycles) were taken in a single session. Integrity of BP measurements were evaluated based on whether meaningful diastolic BP and heart rate recordings could be collected in tandem, though these parameters were not analyzed. Systolic BP data from any cycle where heart rate or diastolic BP recordings could not be calculated were excluded from analysis.

5.3.4 Echocardiography

Rats were lightly anaesthetized (2.0% Isoflurane, 1 L/min oxygen via nose-cone), kept on a temperature-controlled warming pad (kept at 37 °C), and imaged in the supine position using a high-resolution imaging system and a 16–23 Mhz transducer (Vevo2100, VisualSonics Inc., Toronto, ON, Canada). A single operator who was blinded to experimental groups performed all assessments. Parasternal short axis M mode tracings of the left ventricle (LV) were recorded at the widest point of the heart, with the M mode cursor placed perpendicular to the anterior and posterior wall of the left ventricle. LV end-diastolic and end-systolic diameters (LVID), and septal (IVS) and posterior wall (LVPW) thicknesses were measured. LV mass was calculated according to the troy formula (LV mass = $1.053 \times 0.8 \times ([\text{LVIDd} + \text{LVPWd} + \text{IVSd}]^3 - [\text{LVIDd}]^3)$), where 1.053 is the specific gravity of the myocardium. Stroke volume (SV) and cardiac output (CO) were calculated with ventricular end-systolic and end-diastolic volumes obtained from M mode images. The trans mitral flow velocity was obtained from the apical four chambers view. The ratio of peak early filling (E) and atrial velocity (A) was measured with pulse wave Doppler imaging. E and A wave images were used to quantify isovolumic relaxation and contraction time, as well as aortic ejection time, which were then combined to calculate a TEI index. All values were measured under steady state conditions and averaged from three cardiac cycles taking care to exclude cycles that took place during inhalation.

5.3.5 Behavioral Tests

All behavioral tests were performed after 14 months of treatment (i.e., at 18 months of age). For the tapered beam, hind limb function was determined using the raised tapered beam test (435). Tapered beam test provides a sensitive measure of bilateral motor function based on foot faults (slips) made by a rodent traversing a gradually narrowing beam (436). Briefly, animals walked the beam in two consecutive recorded trials, albeit only the second trial was scored. Half faults (score = 1) were defined as an instance in which a portion of the hind paw used the side or lower ledge for weight bearing. Full foot faults (score = 2) were recorded when the full hind paw used the bottom ledge for support. Performance in the tapered beam task was assessed by analyzing the sum of the foot faults during the second trial.

The elevated plus maze was used to assess anxiety-related behavior in rats, as well as measures of locomotion (437). Rats were placed in an elevated structure with two opposing enclosed arms (15 cm high walls) and two opposing open arms. Each arm was 10 cm wide and 50 cm long. Rats were placed in the center of the apparatus, facing an open arm and behavior was recorded for 5 min. Recordings were analyzed for entries and time spent in each arm type (open versus closed).

Finally, the open field test was used to assess exploratory activity in an unfamiliar environment; this test also provides measures of anxiety-related behaviors (438), as well as locomotor activity. Rats were placed in the center of an opaque box (60cm × 60cm × 60cm) and video recorded for 5 min to track exploratory and thigmotactic behaviors (439). Time spent in the center region of the box (defined as an average body length from the edge of the box) and total distance travelled were recorded and analyzed using tracking software.

5.3.6 Lifespan Estimation

Animals were inspected twice weekly for general health status. Established criteria for humane endpoints were used to estimate lifespan, and evaluations were performed by a clinical veterinarian. Criteria for

humane endpoints included excessive loss of body weight (>20% of body weight from their top weight), breathing abnormalities (respiratory distress, labored breathing, increased or decreased respiratory rate, cyanosis), uncontrolled bleeding, presence of big (>3 cm) or ulcerated and necrotic tumors, limb paralysis, dermatitis, malocclusion, or behavioral indicators of pain or severe distress (e.g., hunched posture, extensive porphyrin staining, piloerection). Post-mortems were performed on euthanized rats, as well as those found dead in their cages.

5.3.7 Statistical Analyses

Data are presented as mean ± SEM. Outcomes were analyzed by two-way ANOVA for the effects of intervention (BrSp-feeding) and time, followed with Holm–Sidak post hoc test where main effects were found. Area under the curve (AUC) and behavioral data were analyzed either by Student's t-test or Mann–Whitney test as appropriate. Data were assessed for normality by the Shapiro–Wilk test prior to analyses. All statistical analyses were conducted using Prism 9.0 (GraphPad Software Inc., San Diego, U.S.A.).

5.4 Results

5.4.1 Survival and Mean Age at Death

Offspring lifespan, estimated based on established criteria for humane endpoints, are shown in **Figure 5.1**. Average age at the time of death in male rats was 648 ± 25 days (Ctl), and 661 ± 39 (BrSp), and in female rats was 726 ± 41 (Ctl) and 826 ± 29 (BrSp). Log-rank analysis revealed no overall effect of BrSP-feeding on lifespan in males (P=0.26, **Figure 5.1a**, left). However, survival curves of control and BrSp-fed male rats tended to separate at older ages (beyond the point of 2 years), and while there were no differences in lifespan in the oldest 50% of surviving rats (**Figure 5.1a**, middle), mean age at death for the oldest 25% of rats was higher in BrSp-fed rats (838 ± 18 days) than controls (754 ± 17 days; P=0.01, **Figure 5.1a**, right). In females, BrSp feeding improved survival, and the benefits were evident when considering all rats (P=0.04, **Figure 5.1b**, left), as well as the oldest 50% of survivors (**Figure 5.1b**,

middle), although differences in the oldest 25% of female survivors did not reach statistical significance ($p = 0.06$; **Figure 5.1b**, right).

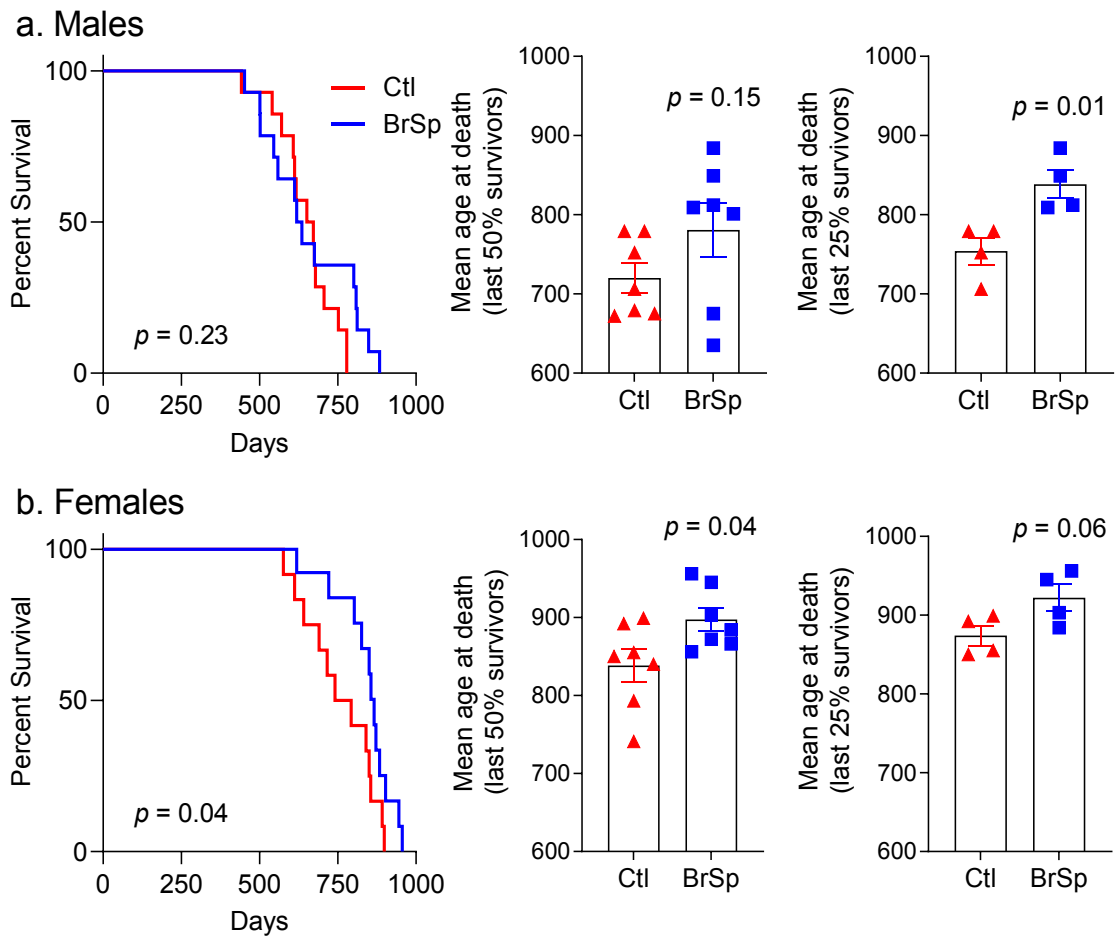

Figure 5.1. Survival in male and female rats supplemented with or without broccoli sprouts (BrSp). Kaplan–Meier curves showing survival in (a) males and (b) females. Middle panels depict mean age at death of the oldest 50% survivors of male and female rats. Similarly, right panels depict mean age at death of the oldest 25% survivors of male and female rats.

5.4.2 Cause of Death

With the exception of 4 males (1 Ctl and 3 BrSp-fed) and 1 female (1 Ctl) found deceased, all rats were euthanized based on criteria for humane endpoints. The criteria used to determine humane endpoints are appended. Weight loss and presence of tumors were the predominant criteria for euthanasia. Cases of malocclusion and severe dermatitis were also considered causes for euthanasia; however, since these conditions would otherwise not be considered terminal, these subjects were censured, and therefore not included in survival calculations show in **Figure 5.1**. Co-morbidities evident at postmortem are also shown in **Table 5.1**. Evidence of cardiopulmonary disease and complications of the kidney, liver, and brain function were present in all animals at the time of death, though it is unclear whether any or all of these complications contributed to morbidity and mortality. **Table 5.1** summarizes the data on the number of rats with more than one morbidity (cardiopulmonary, kidney, liver, brain, or tumor) at the time of death.

Table 5.1. Number and % of rats with more than one health complication at the time of death.

Groups	N	Total	%
Male-Ctl	11	13	84.6%
Male-BrSp	8	12	66.7%
Female-Ctl	8	11	72.7%
Female-BrSp	7	12	58.3%

* Rats found dead (n = 5) or euthanized prematurely solely due to malocclusion (n = 3) are excluded.

5.4.3 Body Weight and Composition

Body weight in male offspring was not affected by BrSp feeding (**Figure 5.2a**). In contrast, BrSp-fed females gained less weight compared to their control counterparts (**Figure 5.2b**). As expected, aging was associated with changes in body composition (**Figure 5.3**). All rats, irrespective of sex or treatment, tended to gain fat (**Figure 5.3a,d**) at the expense of lean mass (**Figure 5.3b,e**) as they aged. BrSp had no effect on age-related changes in body composition in either sex. Interestingly, whereas abdominal circumferences, a surrogate of abdominal adiposity, was unaffected by BrSp-feeding in males (P_{BrSp}=0.35, **Figure 5.3c**), BrSp-feeding tended to mitigate this increase in females compared to their control counterparts (P_{BrSp}=0.06, **Figure 5.3f**).

5.4.4 Glucose Homeostasis

BrSp modestly affected glucose handling parameters, albeit in a sex-dependent manner (**Figure 5**). BrSp-feeding was associated with reduced fasting blood glucose levels in males (P_{BrSp}=0.02, **Figure 5.4a**), although no differences were apparent in glucose (**Figure 5b**) or insulin sensitivity (**Figure 5.4c**). In contrast, BrSp-feeding did not improve fasting glucose levels (**Figure 5d**), nor glucose or insulin sensitivity (**Figure 5.4d**) in females.

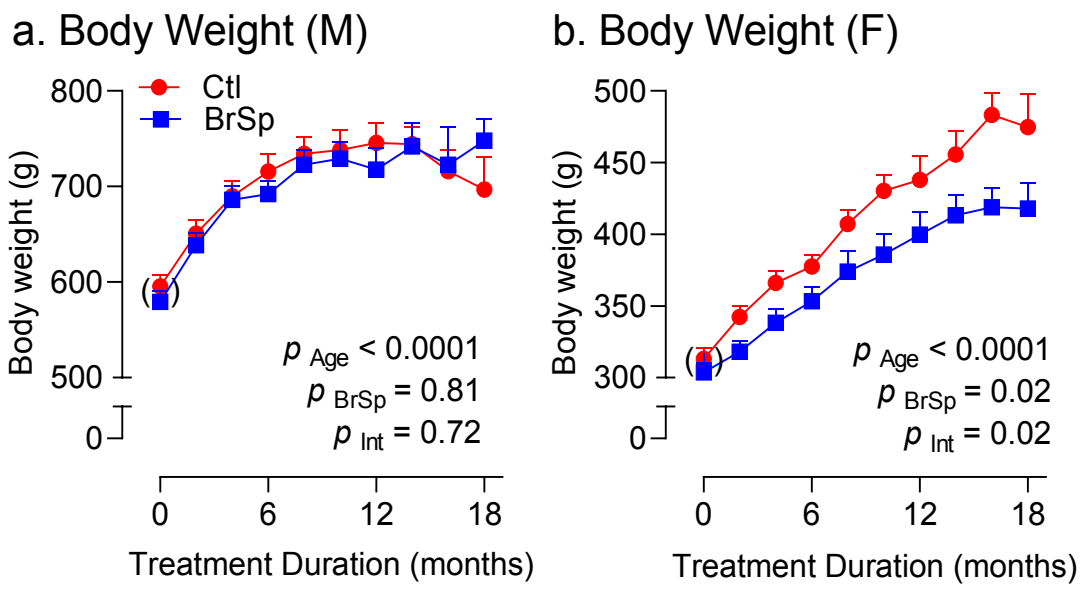

Figure 5.2. Body weight over time in male (a) and female (b) rats. Data is presented as Mean ± SEM for n = 6–14 offspring from separate litters in each group and analyzed by two-way ANOVA.

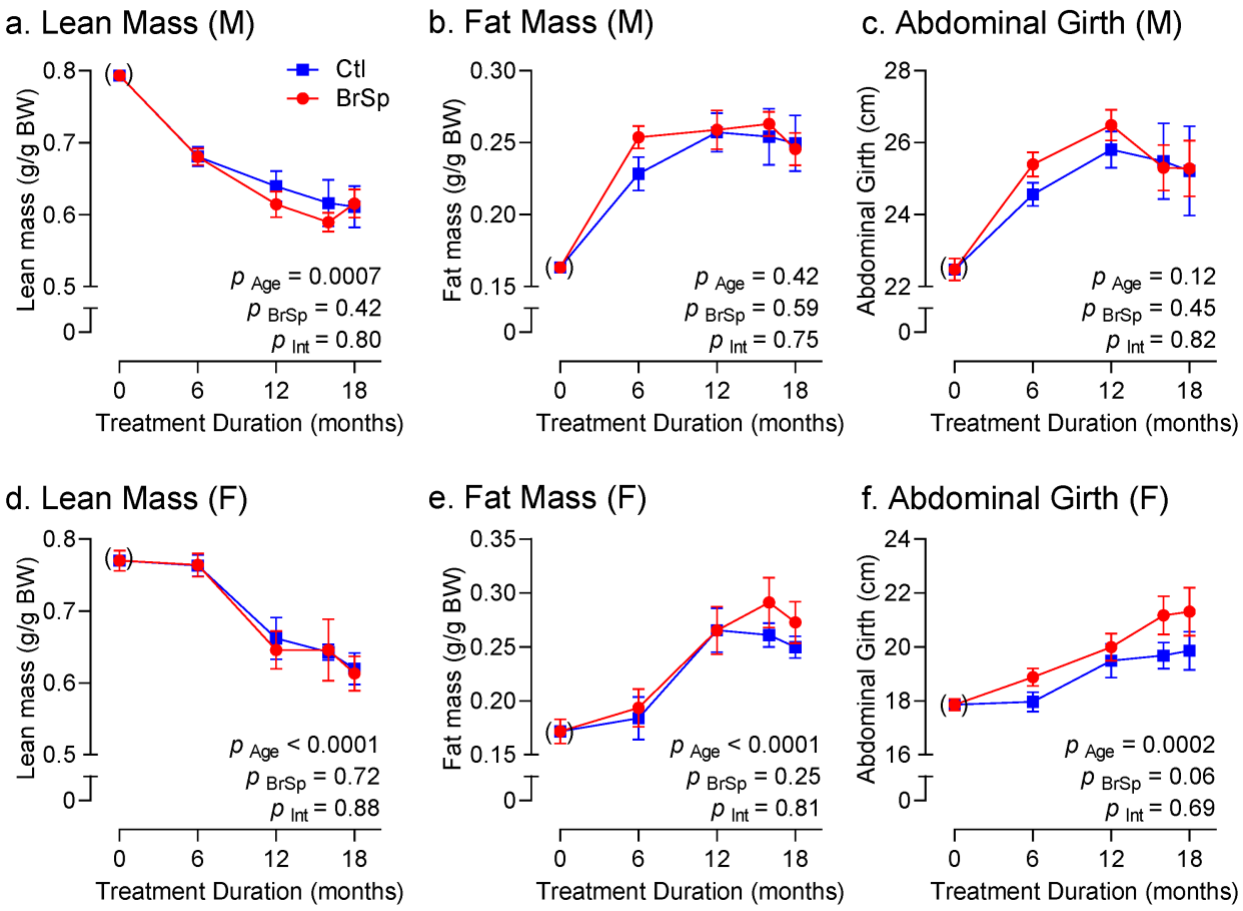

Figure 5.3. Body composition and waist circumference. In (a–c) males and (d–f) females, including (a,d) lean mass, (b,e) fat mass, and (c,f) abdominal girth. Data is presented as Mean ± SEM for n = 6–14 rats in each group and analyzed by two-way ANOVA.

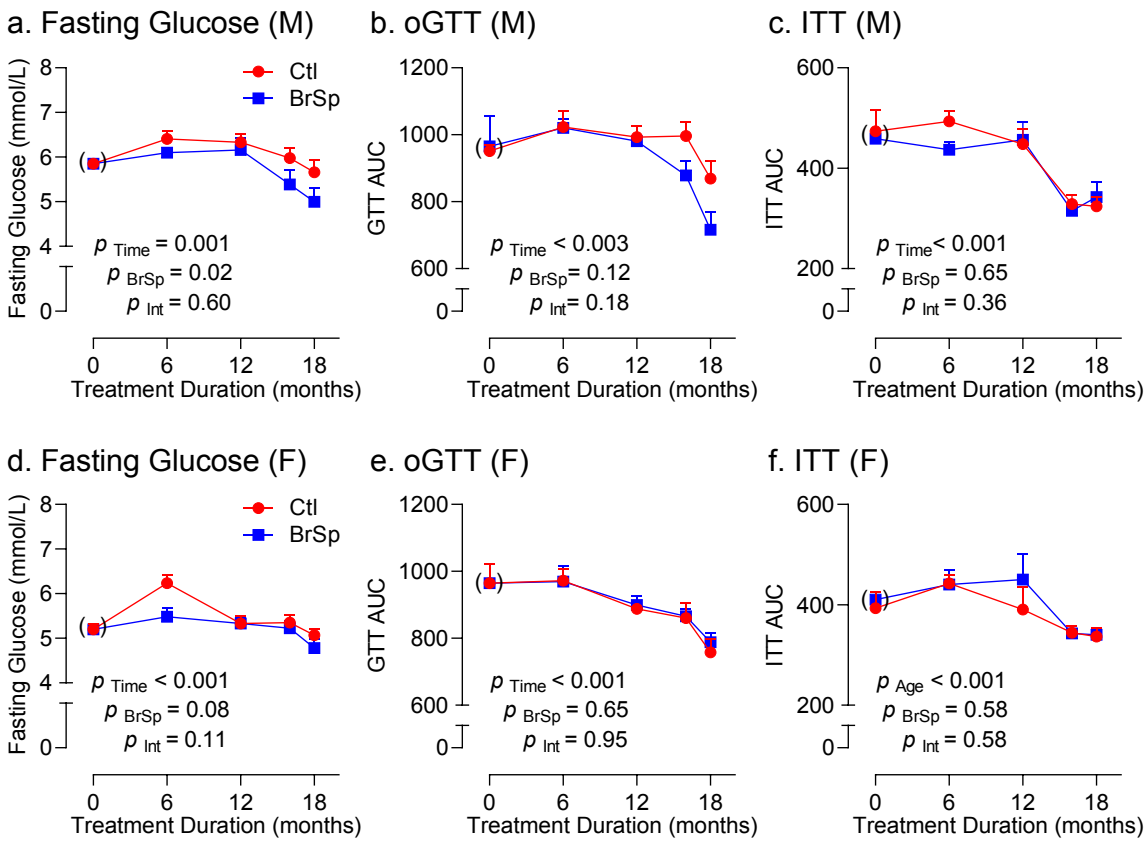

Figure 5.4. Changes in fasting blood glucose and area under the curve for GTT, and ITT in male (a) and female (b) rats over time. Data is presented as Mean ± SEM for *n* = 6–14 offspring from separate litters in each group and analyzed by two-way ANOVA.

5.4.5 Blood Pressure and Cardiac Function

BrSp-feeding had a pronounced blood pressure lowering effect in males that was evident in all ages (**Figure 5.5a**). Consistent with these data, echocardiographic measurements revealed reduced cardiac size in BrSp-fed males compared to controls, reflected in left-ventricular internal diameter at end-diastole (LVIDd), as well as in corrected left ventricular mass (**Table 5.2**). Cardiac output was also reduced in BrSp-fed males compared to controls as indicated by a significant interaction between time and treatment (P_{Int}=0.004, **Table 5.3**), whereas E/A ratio tended to increase upon BrSp feeding in males (P_{Int}=0.06, **Table 5.3**).

BrSp-feeding was also associated with a blood pressure lowering effect in females, albeit this was largely attributed to differences recorded after 18 months of treatment (**Figure 5b**). This effect could not be attributed to attrition, since paired analysis of those female rats surviving at 16 and 18 months of age yielded similar systolic blood pressure differences (Ctl-F (16 mo.): 132 ± 3mmHg [n = 9]; BrSp-F (16 mo.): 128 ± 4 mmHg [n = 11]; p = 0.57; Ctl-F (18 mo.): 142 ± 4mmHg [n = 9]; BrSp-F (18 mo.): 124 ± 5mmHg [n = 11]; p = 0.01). BrSp-feeding had modest effects on cardiac morphology and function in the females, albeit an interaction was observed in corrected LV mass, attributed to an un-sustained increase in controls at the penultimate time point (16 months; **Table 5.2**). Finally, like males, cardiac output also tended to be lower in BrSp-fed females (**Table 5.3**).

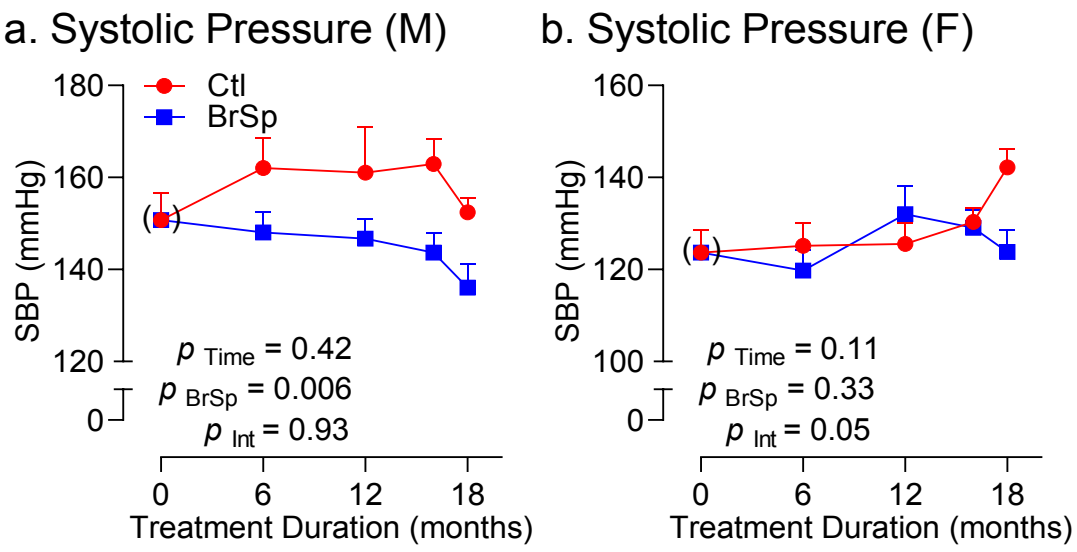

Figure 5.5. Systolic blood pressure in (a) male and (b) female offspring over time. Data is presented as Mean ± SEM for n = 6–14 offspring from separate litters in each group and analyzed by two-way ANOVA.

Table 5.2. Echocardiographic measurements (cardiac morphometry) in rats fed a control or BrSp diet.

		Ctl					BrSp					p-value		
		0 Months	**6 Months**	**12 Months**	**16 Months**	**18 Months**	**0 Months**	**6 Months**	**12 Months**	**16 Months**	**18 Months**	**Time**	**BrSp**	**Int**
Male Offspring	IVSd, mm	1.7 ± 0.0	2.2 ± 0.1	2.4 ± 0.1	2.2 ± 0.1	2.4 ± 0.1	1.7 ± 0.0	2.2 ± 0.1	2.4 ± 0.1	2.1 ± 0.0	2.2 ± 0.1	**0.008**	0.37	0.51
	IVSs, mm	2.3 ± 0.3	3.6 ± 0.2	3.8 ± 0.2	3.6 ± 0.1	4.0 ± 0.2	2.3 ± 0.3	3.6 ± 0.1	4.0 ± 0.1	3.5 ± 0.1	3.8 ± 0.2	**0.02**	0.85	0.40
	LVIDd, mm	7.9 ± 0.6	8.4 ± 0.2	8.8 ± 0.2	9.2 ± 0.3	8.8 ± 0.2	8.0 ± 0.3	8.3 ± 0.2	8.1 ± 0.2	8.2 ± 0.5	8.4 ± 0.4	0.61	**0.04**	0.31
	LVIDs, mm	3.7 ± 0.6	4.2 ± 0.3	4.4 ± 0.3	4.5 ± 0.3	4.0 ± 0.4	3.7 ± 0.6	3.8 ± 0.3	3.5 ± 0.1	3.9 ± 0.4	3.7 ± 0.3	0.75	0.18	0.60
	LVPWd, mm	2.2 ± 0.2	2.2 ± 0.1	2.3 ± 0.1	2.0 ± 0.2	2.3 ± 0.2	2.2 ± 0.2	2.3 ± 0.1	2.1 ± 0.1	2.1 ± 0.2	2.2 ± 0.1	0.72	0.88	0.78
	LVPWs, mm	3.4 ± 0.1	3.6 ± 0.2	3.7 ± 0.1	3.7 ± 0.2	3.8 ± 0.2	3.5 ± 0.0	3.8 ± 0.1	3.6 ± 0.1	3.6 ± 0.1	3.8 ± 0.1	0.81	0.88	0.79
	Corrected LV mass, g	1.0 ± 0.1	1.3 ± 0.05	1.5 ± 0.06	1.4 ± 0.09	1.4 ± 0.07	1.0 ± 0.1	1.2 ± 0.04	1.3 ± 0.06	1.2 ± 0.06	1.3 ± 0.07	**0.03**	**0.04**	0.17
Female Offspring	IVSd, mm	1.9 ± 0.1	1.9 ± 0.1	1.8 ± 0.0	1.9 ± 0.1	1.9 ± 0.1	1.9 ± 0.1	1.9 ± 0.1	1.8 ± 0.0	1.9 ± 0.1	1.9 ± 0.0	0.32	0.60	0.95
	IVSs, mm	3.2 ± 0.2	3.2 ± 0.1	3.4 ± 0.1	3.4 ± 0.1	3.3 ± 0.1	3.2 ± 0.2	3.2 ± 0.1	3.3 ± 0.1	3.2 ± 0.1	3.3 ± 0.1	0.69	0.49	0.99
	LVIDd, mm	6.1 ± 0.2	6.7 ± 0.2	6.8 ± 0.2	7.3 ± 0.2	7.4 ± 0.2	6.1 ± 0.2	6.2 ± 0.3	7.1 ± 0.1	7.1 ± 0.3	7.0 ± 0.2	**0.003**	0.46	0.25
	LVIDs, mm	2.8 ± 0.1	3.0 ± 0.2	2.8 ± 0.2	3.4 ± 0.2	3.3 ± 0.3	2.8 ± 0.1	2.8 ± 0.3	3.1 ± 0.1	3.6 ± 0.3	3.3 ± 0.3	**0.04**	0.76	0.47
	LVPWd, mm	2.3 ± 0.2	1.7 ± 0.1	2.1 ± 0.1	2.1 ± 0.2	1.9 ± 0.1	2.3 ± 0.2	2.0 ± 0.1	2.0 ± 0.1	1.9 ± 0.1	2.1 ± 0.1	0.37	0.57	0.11
	LVPWs, mm	3.8 ± 0.1	3.1 ± 0.1	3.5 ± 0.1	3.6 ± 0.2	3.6 ± 0.2	3.8 ± 0.1	3.2 ± 0.1	3.5 ± 0.1	3.2 ± 0.1	3.5 ± 0.2	0.08	0.50	0.33
	Corrected LV mass, g	0.72 ± 0.03	0.69 ± 0.03	0.77 ± 0.04	0.92 ± 0.06	0.82 ± 0.04	0.72 ± 0.03	0.72 ± 0.04	0.79 ± 0.04	0.77 ± 0.03	0.82 ± 0.05	**0.006**	0.74	**0.05**

Times (in months) reflect duration of BrSp feeding. Values are expressed as means ± SEM; n = 6–14 animals/group. Male or female offspring in control and BrSp supplemented groups were compared over time with a 2-way ANOVA. LV, left ventricular; IVSd and IVSs, interventricular septum at diastole and systole, respectively; LVIDd and LVIDs, LV internal diameter at diastole and systole, respectively; LVPWd and LVPWs, LV posterior wall at diastole and systole, respectively.

Table 5.3. Systolic and diastolic function in rats fed a control or BrSp diet.

		Ctl					BrSp					p-Value		
		0 Months	**6 Months**	**12 Months**	**16 Months**	**18 Months**	**0 Months**	**6 Months**	**12 Months**	**16 Months**	**18 Months**	**Time**	**BrSp**	**Int**
Male Offspring	LV end-diastolic volume, µl	340.6 ± 25.9	389.6 ± 24.5	427.5 ± 19.4	471.8 ± 29.5	404.1 ± 32.1	340.6 ± 25.9	380.1 ± 20.2	355.5 ± 14.6	369.9 ± 44.5	412.2 ± 41.8	0.51	0.14	0.11
	LV end-systolic volume, µl	63.2 ± 19.0	84.4 ± 15.1	96.6 ± 15.7	96.6 ± 13.6	76.4 ± 13.2	63.2 ± 19.0	66.2 ± 10.9	54.3 ± 4.9	69.8 ± 14.8	59.9 ± 10.6	0.79	0.12	0.50
	Hear rate (bpm)	394.3 ± 7.8	332.1 ± 14.6	333.6 ± 12.6	328.9 ± 5.4	325.8 ± 17.7	426.2 ± 0.7	351.1 ± 9.8	315.8 ± 12.1	288.2 ± 15.8	309.5 ± 17.7	0.06	0.30	0.14
	Stroke volume, mL	277.4 ± 10.2	305.2 ± 13.1	330.9 ± 14.8	375.2 ± 28.0	327.6 ± 21.6	277.4 ± 10.2	313.9 ± 13.0	301.2 ± 10.8	300.1 ± 33.7	328.4 ± 24.3	0.55	0.19	0.13
	Cardiac output, mL/min	113.6 ± 2.9	100.5 ± 4.5	110.4 ± 6.7	123.0 ± 8.5	106.0 ± 8.4	113.6 ± 2.9	109.7 ± 4.6	94.5 ± 3.9	84.1 ± 6.9**	102.9 ± 8.4	0.92	0.08	**0.003**
	Cardiac output, mL/min.g	0.18 ± 0.00	0.13 ± 0.01	0.14 ± 0.01	0.15 ± 0.01	0.14 ± 0.01	0.19 ± 0.00	0.14 ± 0.01	0.12 ± 0.01	0.10 ± 0.00	0.15 ± 0.02	0.17	0.34	**0.004**
	Mitral Flow Doppler													
	E, mm/s	918.4 ± 57.1	936.4 ± 49.7	886.2 ± 28.4	892.4 ± 76.4	917.1 ± 79.4	918.4 ± 57.1	838.1 ± 34.7	861.5 ± 40.5	807.1 ± 67.9	912.1 ± 90.2	0.72	0.24	0.77
	A, mm/s	998.1 ± 50.1	747.4 ± 72.2	754.4 ± 69.7	758.2 ± 86.6	827.0 ± 81.7	964.4 ± 0.0	718.9 ± 39.6	665.3 ± 51.7	485.4 ± 34.5	714.5 ± 72.8	0.18	0.10	0.48
	E/A	0.93 ± 0.08	1.31 ± 0.08	1.25 ± 0.11	1.08 ± 0.06	1.06 ± 0.06	0.93 ± 0.08	1.18 ± 0.05	1.32 ± 0.08	1.57 ± 0.13	1.28 ± 0.11	0.46	0.12	**0.03**
	TEI index	0.52 ± 0.05	0.44 ± 0.03	0.57 ± 0.04	0.46 ± 0.02	0.52 ± 0.04	0.52 ± 0.05	0.46 ± 0.04	0.55 ± 0.02	0.51 ± 0.06	0.57 ± 0.06	**0.02**	0.41	0.83
Female Offspring	LV end-diastolic volume, µl	190.4 ± 9.2	240.9 ± 16.6	250.4 ± 12.8	289.8 ± 21.4	294.8 ± 14.7	194.0 ± 29.9	220.0 ± 17.5	258.8 ± 10.8	279.2 ± 20.8	274.4 ± 14.6	**<0.001**	0.61	0.55
	LV end-systolic volume, µl	20.0 ± 4.0	33.9 ± 4.9	29.2 ± 5.6	47.1 ± 6.6	40.2 ± 9.4	17.3 ± 4.8	28.4 ± 5.4	32.9 ± 3.8	55.8 ± 12.8	44.9 ± 9.3	**0.007**	0.62	0.62
	Hear rate (bpm)	505.7 ± 11.6	398.5 ± 12.9	403.3 ± 15.0	370.4 ± 21.1	370.3 ± 11.5	484.3 ± 10.8	383.6 ± 19.8	403.3 ± 15.9	357.2 ± 16.3	332.5 ± 26.7	**0.004**	0.29	0.76
	Stroke volume, mL	170.4 ± 5.2	207.0 ± 12.7	221.2 ± 8.7	242.6 ± 17.4	258.2 ± 13.8	176.7 ± 25.0	191.6 ± 15.1	225.9 ± 8.6	213.3 ± 12.3	229.5 ± 9.3	**0.002**	0.17	0.42
	Cardiac output, mL/min	86.2 ± 4.6	82.7 ± 6.0	88.5 ± 3.4	89.3 ± 7.0	95.9 ± 6.4	85.3 ± 10.2	72.4 ± 5.9	90.6 ± 4.4	76.2 ± 5.4	76.8 ± 7.2	0.09	**0.04**	0.24
	Cardiac output, mL/min.g	0.20 ± 0.02	0.17 ± 0.1	0.16 ± 0.01	0.16 ± 0.01	0.18 ± 0.02	0.21 ± 0.03	0.15 ± 0.01	0.17 ± 0.01	0.14 ± 0.01	0.14 ± 0.2	0.48	0.06	0.22
	Mitral Flow Doppler													
	E, mm/s	824.2 ± 0.0	837.1 ± 47.2	885.5 ± 56.3	827.1 ± 72.4	786.4 ± 43.9	832.6 ± 0.0	780.1 ± 44.6	889.0 ± 42.9	902.5 ± 53.7	797.9 ± 61.1	0.13	0.99	0.77
	A, mm/s	906.5 ± 0.0	854.4 ± 46.5	760.4 ± 60.2	661.4 ± 54.2	789.3 ± 41.2	926.7 ± 0.0	778.5 ± 51.9	764.0 ± 60.7	660.0 ± 42.8	766.9 ± 83.4	0.12	0.58	0.91
	E/A	0.91 ± 0.00	0.96 ± 0.03	1.24 ± 0.20	1.27 ± 0.13	1.05 ± 0.08	0.90 ± 0.00	1.10 ± 0.06	1.20 ± 0.10	1.46 ± 0.11	1.30 ± 0.20	0.10	0.28	0.75
	TEI index	0.54 ± 0.05	0.48 ± 0.05	0.58 ± 0.04	0.55 ± 0.07	0.54 ± 0.05	0.54 ± 0.05	0.44 ± 0.03	0.50 ± 0.03	0.50 ± 0.07	0.50 ± 0.03	0.11	0.22	0.96

Times (in months) reflect duration of BrSp feeding. Values are expressed as means ± SEM; n = 6–14 animals/group. Male or female offspring in control and BrSp supplemented groups were compared over time with a 2-way ANOVA.

5.4.6 Behavioral Analyses

Table 4.4 summarizes the parameters measured for activity and anxiety behavioral traits in rats. Male and female rats in both treatment groups performed similarly in the open field maze when total time in center and total distance was measured. In contrast, total mobile time was higher in BrSp-fed males (P=0.03) but not females (P=0.13). No differences were observed in performance in the elevated plus maze parameters between the control and BrSp groups in either sex. On the tapered beam test, BrSp-fed females tended to have fewer left foot faults compared to their control counterparts (P=0.06), whereas no such differences were evident between treatment groups in males.

Table 5.4. Behavioral analysis of rats subjected to open field, elevated plus maze, and tapered beam tests.

Behavioral Test	Parameters	Male			Female		
		Ctl	BrSp	p-Value	Ctl	BrSp	p-Value
Open Field Test	Total distance traveled (m)	13.6 ± 1.9	16.2 ± 2.9	0.44	20.1 ± 1.2	21.8 ± 1.4	0.35
	Time mobile (sec)	53 ± 5	77 ± 10	**0.03**	79.11 ± 4.46	88 ± 4	0.13
	Time in inner zone (sec)	37 ± 10	48 ± 12	0.49	27.69 ± 3.16	32 ± 5	0.48
Elevated Plus Maze	Time in open arm (sec)	118 ± 29	92 ± 26	0.41	125 ± 20	150 ± 21	0.41
	Time in closed arm (sec)	125 ± 20	150 ± 21	0.53	99 ± 19	100 ± 19	0.98
	Entries into open arm	6.4 ± 0.8	7.0 ± 1.1	0.66	9.4 ± 0.8	11.3 ± 1.6	0.35
	Entries into closed arm	5.8 ± 0.7	5.9 ± 1.5	0.97	8.4 ± 1.1	7.0 ± 0.8	0.30
	Open arm avoidance Index	53.9 ± 5.8	43.8 ± 8.2	0.31	52.1 ± 5.4	43.6 ± 5.7	0.30
Tapered beam	Total foot faults	3.4 ± 0.6	3.5 ± 0.5	0.86	1.3 ± 0.4	0. 9 ± 0.2	0.43
	Right foot faults	1.9 ± 0.4	2.1 ± 0.6	0.80	0.5 ± 0.2	0.3 ± 0.1	0.39
	Left foot faults	1. 5 ± 0.3	1.4 ± 0.4	0.97	1.0 ± 0.3	0.4 ± 0.1	0.06

5.5 Discussion

Aging is characterized by a decline of cellular, tissue, and organ function, and is typically associated with a loss of homeostasis and decreased adaptability to stress. This loss of functionality and diminished adaptability yields a greater vulnerability to disease and mortality (440). Indeed, aging is the main risk factor for cardiovascular and metabolic diseases, which have become particularly pressing issues as the global aging population continues to grow. Functional foods contain bioactive compounds that, in many cases, promote health due to their pleiotropic effects, and thus may mitigate age-related functional decline and improve longevity. The objective of this study was to assess the effects of long-term BrSp feeding on longevity in rats, as well as on cardiometabolic health parameters. To summarize the outcomes, BrSp feeding of rodents, starting at 4 months of age caused (1) extended life span in rats, albeit this was observed predominantly in females; (2) reduced body weight gain in females; (3) modest improvements in glucose handling in males; (4) marked blood pressure reduction in males; and (5) modest changes in behavioral traits in both sexes.

As expected, aging was associated with an increase in body weight in all rats, which was accompanied by a decrease in lean mass and concomitant increase in fat mass. The increase in abdominal girth, which has been reported to be a reliable surrogate of abdominal fat (441), paralleled the increase fat mass, suggesting the age-related increase in fat is largely attributed to accumulation of visceral fat. However, in BrSp-fed females, rise in abdominal girth tended to be lower, which may indicate a propensity for more subcutaneous, and hence healthier, fat accumulation compared to control females. Yet despite the tendency to reduced abdominal fat accumulation, there were no apparent changes in glucose handling (i.e., fasting glucose or

glucose tolerance) in females. In contrast, only male BrSp-fed rats exhibited improved fasting glucose levels despite no differences in body composition, which is consistent with other reports in male rats using sulforaphane (171), and underscores that body composition is by no means the sole determinant of glucose homeostasis. This is perhaps best exemplified by the observation that among all groups over time, fasting glucose levels as well as GTT and ITT AUCs remained largely unchanged (or even decreased), despite increases in body weight and fat deposition, which has been reported by others (442-444).

The pronounced sexually dimorphic effect of BrSp-feeding, aside from body weight gain observed only in females, was on BP regulation in males. At all times assessed, BrSp feeding caused a 10–15mmHg reduction in systolic BP, which coincided with lower LV mass (assessed by echocardiography), reflecting a diminished cardiac afterload (445). The benefits of blood pressure reduction on longevity are well documented (446), and studies indicate that even modest reductions of 1–2mmHg can impart survival benefits (447). Although overall survival in males was not affected by BrSp-feeding, the oldest surviving males were invariably BrSp-fed. In contrast, BP profiles of control and BrSp-fed females were largely superimposable throughout the experiments, and yet the latter group exhibited a clear survival advantage. The survival benefit could be attributed, in part, to BrSp-feeding mitigating the marked rise in BP in control rats at 24 months of age (after 18 months of treatment)—a consistent finding among all control rats assessed at that time ($n = 9$), suggesting this was not a spurious observation. Although the cause of this BP rise is unclear, it may be attributed, in part, to hormonal changes. The increasing incidence of hypertension occurring at older ages in women than in men (448), is attributed to hormonal changes following menopause; hormonal changes accompanying reproductive

senescence in rats may occur at even more advanced ages (449, 450). Therefore, it is not altogether unexpected that marked BP rises occur beyond 18 months of age. Other potential mechanistic effects may be attributed to the vascular inflammation seen in spontaneously hypertensive rats. Wu *et al.* (451), found that feeding BrSp to spontaneously hypertensive rats reduced the presence of intra-luminal inflammatory cells seen on pathologic examination, and this coincided with a reduction in the onset of hypertension. However, the latter does not explain the sex differences seen in our study, as the former did not compare the sexes.

Notwithstanding, how BrSp mitigates this late-stage BP rise remains unclear. Despite the overall modest effects of BrSp on the measured cardiometabolic parameters in females, survival benefit was quite compelling in all the females; BrSp-fed females lived longer than their control counterparts. The small albeit significant reduction in cardiac output could indicate an overall decrease in metabolic demands in females, which has been linked to longevity (452, 453). However, cardiac output was sporadically reduced in BrSp-fed males as well, which may explain the less robust survival advantage in this group.

Aging is associated with structural and biochemical changes that culminate in profound functional changes over time; increased tendencies to anxiety and depression-like behaviors (454-456) and impaired performance in tasks requiring coordinated control of motor and reflex responses (457) have been described in aged rodents. To this end, control and BrSp-fed rats underwent a series of behavioral tests, including the tapered beam test, which evaluates motor coordination and balance, as well as elevated plus maze and open field tests, which evaluate locomotor activities as well as anxiety-like behaviors, respectively (438). BrSp-fed females

tended to have fewer foot faults than their control counterparts, which could reflect improved neurological function with treatment in these animals. In contrast, no apparent improvements in locomotor function were evident in males. However, BrSp-fed males exhibited increased time active within the open field, which may reflect better exploratory activity compared to control counterparts. Despite this benefit, though other well-documented outcomes reflecting anxiety (e.g., time spent in the center of the open field and ventures into the open-arms of the elevated plus maze) were not affected by BrSp in males or females. Notably, the outcomes of these tests probe state-like anxiety, in which situations create anxiety (458), rather than trait anxiety, which reflect fears that are not apparent to others (459). Therefore, it is possible that the beneficial effects of BrSp on trait-anxiety may be more pronounced, and thus future studies investigating whether this treatment may be useful in mitigating anxiety-like behaviors in other contexts requires further investigation.

There are other limitations to this study that warrant discussion. First, because the primary objective of this study was to assess longevity, post-mortem tissue collection invariably occurred from previously moribund animals, thus precluding biochemical analyses. As such, measures of oxidative stress and inflammation (such as reactive oxygen species and malondialdehyde) were not measured in this study. Therefore, mechanisms by which long-term BrSp-consumption promotes health and longevity remain unclear. However, the present study sets the stage for such mechanistic studies, which in turn may provide insights into the sex-differences in beneficial effects of BrSp reported herein. Similarly, variability from time of death to post-mortem tissue collection introduces a large error in histological and immunohistochemical examination. It is well known that small sample sizes decrease statistical power and decrease the flexibility of effect

sizes. There is the potential that this study was underpowered and larger groups may have resulted in significance (e.g., **Figure 5.1**). Finally, despite low calorie content of BrSp, it is possible that BrSp feeding may have affected overall food consumption. Although intermittent food intake assessments did not reveal differences between control and BrSp-fed rats in either sex (data not shown), the use of non-purified rodent chow, which are less consistent in their nutritional make-up and indeed less nutritive overall than purified diets, made food intake parameter difficult to assess. Whether BrSp affects satiety is important because the effects of reduced food consumption on longevity are well documented.

Overall, this study clearly demonstrated the positive effects of chronic BrSp consumption on longevity in rats. Body weight, visceral adiposity, glucose handling, and blood pressure were positively affected by BrSp consumption in rats throughout their life span in a sex-specific manner. Rats fed with BrSp also exhibited improved activity and bilateral motor function when older. This highlights the potential of chronic BrSp consumption on improving cardiometabolic health and neurological dysfunctions associated with aging, which can eventually lead to improved longevity in the aging population.

Author Contributions: Conceptualization, R.M.N.N., F.J., E.A.A., S.L.B. and J.Y.Y.; methodology, R.M.N.N., F.J. and E.A.A.; validation, F.J. and S.L.B.; formal analysis, F.J.; investigation, R.M.N.N., F.J. and E.A.A.; resources, S.L.B. and J.Y.Y.; data Curation, F.J.; writing—original draft preparation, F.J.; writing—review and editing, R.M.N.N., F.J., S.L.B. and J.Y.Y.; visualization, F.J. and S.L.B.; supervision, S.L.B. and J.Y.Y.; project administration,

S.L.B. and J.Y.Y.; funding acquisition, S.L.B. and J.Y.Y. All authors have read and agreed to the published version of the manuscript.

Funding: This research was funded by the Canadian Institutes of Health Research, grant number MOP142396 (to S.L.B.) and the Women and Children's Health Research Institute (to J.Y.Y.).

Institutional Review Board Statement: The experimental protocols described herein were approved by the University of Alberta Animal Care and Use Committee in accordance with the guidelines established by the Canadian Council of Animal Care (protocol number AUP00000364).

Informed Consent Statement: Not applicable.

Data Availability Statement: Data and information related to this study are available upon reasonable request from corresponding authors.

Conflicts of Interest: The authors declare no conflict of interest. The funders had no role in the design of the study; in the collection, analyses, or interpretation of data; in the writing of the manuscript, or in the decision to publish the results.

Chapter 6
Summary and Conclusions

6.1 Perinatal Iron Deficiency and Cardiovascular Disease

Nutritional causes of non-communicable disease have likely been recognized for longer than some may imagine. We do know for example, that gout has been liked to a diet of excess for over 2000 years (460). However, it was not until much more recently that we began to understand how poor nutrition during development could shape an individual's lifelong health.

In the 1900's several studies began to link conditions at birth with an increased probability of cardiometabolic syndromes later in adulthood. James Neal first offered the "Thrifty Genotype" hypothesis to attempt to explain this phenomenon, suggesting some humans evolved a state of high insulin resistance to survive periods of nutrient scarcity (461). However, this claim came with controversy. Early humans did not appear to put on fat in periods between nutrient scarcity (462), furthermore present-day individuals who should have carried this evolutionary adaptation did not experience an increased incidence of diabetes or glucose intolerance (463). Neal's work did however set the stage for David Barker's "Thrifty Phenotype" hypothesis, which proposed an association between poor fetal nutrition and a following development of type 2 diabetes. Here relative scarcity was thought to alter development in utero causing a lasting change in glucose-insulin metabolism. This initial work eventually led to the Developmental Origins of Heath and Disease (DOHaD) hypothesis, which provides a framework to study how the environmental factors during early life can permanently influence lifelong health.

In this thesis, I first had the opportunity to investigate iron deficiency, which during pregnancy, predispose offspring to chronic disease in later life. However, recognizing many who develop under ideal circumstances will still experience chronic disease, I then investigated a broccoli sprouts as a therapy to help mitigate the diseases associated with normal ageing. Collectively, the focus of this thesis is therefore to evaluate the alterations in cardiovascular function due to nutritional restriction or nutritional supplementation.

Anemia has been declared a global health priority by the WHO and represents a leading cause of disability across all populations (234). ID is the chief cause of anemia and the most common nutritional deficiency worldwide, conservatively ID affects 2 billion people per year (199). Because of ID's tendency to affect pregnant women, women of childbearing age, and young children, this disease therefore represents a highly relevant in the field of study. Perinatal ID is associated with an increased prevalence of both maternal and neonatal mortality, as well as morbidities such as pre-term birth and intrauterine growth restriction (214, 464, 465). By virtue of ID's abilities to alter growth trajectories, it may come to no surprise that ID has implications in the field of developmental programing. We and others have shown that perinatal ID increases the risk of long term cardiovascular, metabolic, and cognitive dysfunction (225). Because ID impacts the long-term health of offspring, the overall burden of disease due to ID is likely larger than previously appreciated. Cardiovascular disease alone is the leading cause of death worldwide and is responsible for roughly 30% of all deaths (466). If we can understand the mechanisms by which ID programs cardiovascular disease, and find more effective treatments for perinatal ID, we could substantially reduce the overall burden of disease across all peoples.

6.2 Summary of Work

The mechanisms by which perinatal ID affects cardiovascular dysfunction are not presently clear. Our laboratory has shown maternal ID causes sex- and organ-specific patterns of fetal hypoxia, mitochondrial dysfunction, and increased ROS generation, collectively these result in reduced nephron endowment in fetal kidneys (137, 223, 224). In **Chapter 2** of this thesis, we extended our investigation of perinatal ID to the offspring's heart. We first showed that perinatal ID results in offspring which are born small and exhibit organ specific growth restriction. Organs deemed "vital" (i.e., the heart and brain) remained the same weight, at the expense of other organs (i.e., liver and kidney). This was likely driven at least partially, by impaired systemic oxygen delivery in the neonatal hearts. The physiological response to anemia in an adult heart is an increased cardiac output to compensate for the corresponding reduction in oxygen carrying capacity (467); in fact, the lower hematocrit in cases of anemia results in reduced blood viscosity, which makes increases in cardiac contractility less energetically demanding. However, even after adjusting to the reduced bodyweight, the enlarged hearts of ID offspring did not increase cardiac output, in part because of diminished cardiac contractility. This is, to my best knowledge, the first study to show perinatal ID causes a decrease in neonatal ejection fraction. These finding presents an important co-morbidity that leaves the perinatal ID infant at a greater risk for injury in its first months of life. Interestingly these changes also occurred in a sex specific manner the extent of systolic dysfunction for example appeared more severe in males than in females. This is not to say females were protected however, as this phenomena appeared reversed in measures of diastolic dysfunction where here the females were more effected.

Because other forms of neonatal anemia (e.g., hemoglobin Barts disease) are associated with an initial period of increased cardiac output, we speculated these changes were due to the biochemical effect of ID. Further analysis showed a diminished expression of proteins associated with cardiac contractility and structure. Finally, when the hearts were assessed by histology, the approximation of cardiomyocyte number appeared reduced. This occurred at a time-point after cardiomyocyte proliferation ended, indicating that offspring exposed to perinatal ID will enter adulthood with less cardiomyocytes than control offspring. As previously discussed in **Chapter 1,** a reduced cardiomyocyte endowment could decrease the hearts resistance to injury as well as accelerate age related cardiovascular decline. Collectively, these findings have important implications for both the short- and long-term cardiac health of perinatal ID offspring.

The need for treatments of ID in pregnancy is perhaps not obvious given that iron supplementation appears straightforward and easily accessible. Though iron supplementation is currently recommended in anemic mothers, oral iron supplements, which are commonly used to treat ID anemia in pregnancy, are associated with gastrointestinal discomfort which can affect compliance. Furthermore, there are also circumstances in which iron supplementation is simply not effective. For example, ID during pregnancy is sometimes caused by poor intestinal absorption of iron, and in these cases, oral supplementation is of little benefit. To make matters worse, iron supplementation can be deleterious, resulting in oxidative stress in the fetuses and placenta, local inflammation in the placenta, and hepatic damage in the dams (255). In other cases, iron supplementation improves anemia and iron status in the mothers, but has little effect on the fetus (217, 242). Consequently, new interventions that can be used alone or in combination with existing treatments to prevent the adverse effects of perinatal ID are needed.

In **Chapter 3**, we explored a potential intervention to improve cardiac function in perinatal ID offspring. Our findings suggest ketone supplementation could be an effective intervention (if applied in the proper context and found to be safe during pregnancy). Our results first confirmed the cardiac dysfunction in **Chapter 2**, and that ketone supplementation resulted in improved cardiac contractility and total oxygen delivery. Furthermore, ketone supplementation reduced markers of cardiac inflammation and heart injury in ID offspring. This is also one of the first papers to test ketone supplementation during pregnancy. While further mechanistic work is required, we saw no obvious signs of fetal or maternal injury due to ketone supplementation. Elevated circulating ketones (e.g., ketogenic diet, DKA) are largely considered to be harmful to both the mother and fetus. Because ketones have been shown to be protective in a number of other diseases, our hope is this study will encourage more people to investigate ketones as a supplement in other models of pathological pregnancies.

This also highlights one of the challenges regarding treatments during pregnancy. Due to a higher degree of developmental plasticity earlier in life, these early interventions may have the largest potential to alter developmental trajectories. However, this increased plasticity could also raise the offspring's susceptibility to side effects, either within the target organ or in other organ systems which fall beyond the scope of the study. Furthermore, while these changes may drive a beneficial adaptation in the short term, the long-term effects (which may be either positive or negative) must also be studied. This can be exemplified by the use of corticosteroids prior to delivery, which are given prior to a preterm delivery to mature the fetal lung. This is common practice to improve morbidity and mortality rates in preterm babies (468). Unfortunately, animal

as well epidemiological studies indicate that this practice also is associated with alterations in endocrine, renal, and brain development, which may eventually lead to increases in blood pressure as well as mental and behavior disorders later in development (469, 470). When investigating therapies during development the relative increase in sensitivity to perturbations must be considered, and care must be taken to investigate the influences of varying organ systems both in the short and long term. It is only then that the benefits and harms of these treatments can be balanced to optimize the health of the mother and child.

In **Chapter 4** we tested ultrasound guided photoacoustic imaging as a modality to measure placental oxygenation both noninvasively and in real time. This technology could effectively measure differences in oxygenation between distinct regions within the placenta with a resolution on the scale of millimeters. Moreover, despite a severe anemia due to ID, there appears to be minimal differences between ID and control placental percent oxygenation, indicating a fetal adaption to the anemia; this may explain why the elevated cardiac output due to ketone supplementation in **Chapter 3** did not appear to improve organ specific growth restriction. Further, photoacoustic imaging could prove a useful technique to look at hemodynamics as well as placental oxygen delivery in several models of developmental programing. This study will hopefully identify photoacoustic imaging as a potential technology to study placenta pathology both in humans and in preclinical models.

However even if treatments during pregnancy or in early life have the potential to improve growth trajectories and ultimately leave individuals healthier in adulthood, many will still develop cardiovascular disease. In fact, as the global life expectancy increases so has the

percentage of deaths from non-communicable diseases, including cardiometabolic syndrome and cardiovascular disease (471, 472). In **Chapter 5** we tested another nutritional compound, broccoli sprouts, to see if chronic consumption would improve the cardiometabolic decline associated with ageing. As previously discussed, broccoli sprouts act on the NRF2 pathway which causes an inhibition of inflammation, as well as activate the antioxidant response element pathway which causes an overall increase in endogenous antioxidant function. Previous epidemiological studies have linked cruciferous vegetable consumption with reductions in all-cause mortality (257), however the observational nature of this work increases the risk of residual confounders caused by unmeasured covariates. Testing broccoli sprout's role on longevity, in a prospective animal model, was critical to validate the health effects of sulforaphane. In fact, our work represents the first study to show broccoli sprouts have a direct improvement in lifespan. Additionally, the treatment herein appeared to reduce visceral obesity in females as well as improve glucose handling and blood pressure in males; again, highlighting the importance of studying both sexes. Broccoli sprout consumption therefore has the potential to reduce incidence of cardiometabolic diseases commonly associated with ageing, which could ultimately improve lifespan and the quality of life of our population.

Because the programing of perinatal ID is also driven by both oxidative stress and inflammation, it stands to reason that broccoli sprouts may demonstrate protective effects in our model. In fact, our collaborators have shown broccoli sprouts are neuroprotective in rat models of both placental insufficiency and fetal inflammation (428, 429). I originally hoped to build on the work of **Chapter 5** and test the protective effects of broccoli sprouts in maternal ID, however in the interest of time I will instead leave this work in the capable hands of my peers.

6.3 Limitations and Remaining Questions

While these four studies addressed the hypotheses we set out to test, there are several limitations or future directions that should be discussed. The work from **Chapter 2** brings several new hypotheses to question. First, while we demonstrate alterations in protein expression as well as reduction in cardiomyocyte endowment that persisted throughout the final timepoint of the study, we can only assume that these changes could affect long term function in adulthood. I believe these findings warrant a future study, where the long-term programing effects of perinatal ID on adult cardiac function could be investigated. Currently, this is something on which we can only speculate through observations of left ventricular hypertrophy, as well as several other cardiovascular changes outside of the heart (140). Studies using prenatal hypoxia as a model of developmental stress are associated with lasting cardiac dysfunction (473-476). However, while we see evidence of hypoxia in our model of ID, current studies are underway to determine whether the heart itself is hypoxic or not. Finally, it is interesting that male systolic function was reduced to a larger extent than females, one potential cause of this could be the reduction in calmodulin found in male but not female offspring. Within the heart calmodulin is responsible for the regulation of action potential and is typically thought to control heartrate. While we observed no differences in heartrate calmodulin may represent an interesting protein of future study which could explain some of the sex specific differences in cardiac function observed.

The work in **Chapter 2** is however not without limitations, there are a number of other techniques and investigations which could further improve this study. First while the offspring were born growth restricted, their size could have been better characterized. In future works care will be taken to measure parameters such as abdominal circumference, body surface area, crown

rump length and tibia length. This would also provide several different parameters which scale differently to growth (linearly, quadratically) than bodyweight which could then be used to normalize parameters of cardiac function. Furthermore, the limitations of the assessment of cardiac function should also be addressed. It is worth noting that unlike human echocardiography, rats are sedated in our case with isoflurane prior to imaging. Isoflurane is a volatile anesthetic which lowers heart rate, ejection fraction (independent of preload and afterload), and tidal volume while increasing stroke volume and respiratory rate; all of these parameters have the potential to confound particular findings. While on the topic of echocardiography many of our measures of systolic function were also measured based on geometric assumptions and therefore changes in cardiac structure (namely aspect ratio) could alter estimated volumes. To name one example a more spherical ventricle (which occurs in preterm infants) would cause ejection fraction and fractional shortening to be underestimated. Other parameters such as an integral method of cardiac output, or even a load independent measure such as a pressure volume loop (which is admittedly far more invasive) would provide further clarity.

Much like **Chapter 5,** this may also pose an ideal opportunity to test whether perinatal ID shortens lifespan, allowing a link to be established between the cardiovascular dysfunction previously found, and an increase in mortality. Furthermore, perinatal ID did cause both systolic and diastolic dysfunction in the offspring hearts (shown in **Chapter 2** and again validated in **Chapter 3**). It is my perspective that this is an important finding with major clinical implications. A logical next step would be to validate that these changes exist in human neonates, as this could have the potential to inform clinical management.

While **Chapter 3** suggested exogenous ketones are a promising supplement to alter the deleterious effects of maternal iron deficiency, this project failed to illuminate the underlying mechanisms which drove these changes. There are a number of different pathways which ketones exhibit protective effects (outlined in **Chapter 1**), and it is likely several of these factors act on the ID hearts studied in **Chapter 3**. Now that the ketone treatment has been shown to elicit positive functional changes, I believe a future study is warranted to uncover the underlying mechanisms as well as confirm ketones safety as a supplement during pregnancy. Indeed, a major limitation of **Chapter 3** is that (1.) ketones were not studied in control mothers to see how they affected the physiology of normal animals, and (2.) that other organs were not studied both in the short and long term to test the effects of maternal ketone supplementation other organ systems. As discussed in **Chapter 3** in some parameters the ketone treated offspring appeared sicker than their controls, therefore ketones may represent a U-shaped curve by which high doses have the potential to harm the offspring (something which was confirmed by early pilot studies). There are a number of mechanisms by which ketones have could elicit cardioprotective effects (anti-oxidant, anti-inflammatory, ATP production, mitochondrial quality control, epigenetic changes, ect.) and therefore further work to understand the mechanisms by which ketones improved cardiac function may help predict potential harmful effects of this therapy allowing this treatment to be further studied in the context of maternal health.

On the same note, the nature of the longevity study which makes up **Chapter 5** required animals to be euthanized at the end of their life when they were already close to succumbing from diseases associated with ageing. This precluded biochemical analyses, again leaving the mechanism by which broccoli sprout supplementation improves the cardiometabolic health of

these animals unclear. Again, further work would be required to uncover these changes. However within **Chapter 5** an obvious limitation is that other nutrients within the broccoli sprout supplementation were not controlled for, therefore while sulforaphane may have been the primary compound responsible for these findings there may be other molecules within broccoli sprouts that also played a role. One example would be fibre which has been shown to reduce lipid uptake and may have been partially responsible for the decrease in fat mass. In my opinion this just further highlights the benefits of studying nutrient supplements instead of just individual molecules, potential synergistic effects are always of interest and should be explored further.

Chapter 4 assessed photoacoustic imaging in healthy and anemic pregnancies. Because no differences were seen between the two groups, this technology's ability to distinguish placental pathology remains unclear. An interesting area for future study would be to investigate photoacoustic imagining in placentas with clear anatomical injuries such as placental infarcts. One limitation was that fetal heart rate was not measured during photoacoustic imaging, this was because the fetoplacental unit had to be carefully aligned with the imaging probe and then enclosed in a box to prevent retinal injury of the operator. However, in the future investigators could consider using a second probe to measure fetal heartrate immediately prior to an imaging sequence and therefore more tightly control for fetal circulatory parameters during analysis as opposed to only maintaining a consistent maternal heartrate.

6.4 Final Remarks

Perinatal ID undoubtably has a large impact on both the short and long term health of offspring. Unlike many other developmental stressors, perinatal ID represents a deficiency which could be almost entirely preventable; however, there are still several challenges which must be overcome.

A common challenge in the field of DOHaD is that the mother will often preferentially take up nutrients at the expense of the fetus, ID does not appear to be an exception. While iron supplementation during pregnancy (particularly intravenous iron) does appear to improve some measures of neonatal health (e.g., birthweight), hemoglobin (a direct measure of iron status) improves in the mother but not the neonate indicating iron supplementation primarily benefits the mother (246). This is supported by work from our group which shows there are minimal correlations between neonatal and maternal hematologic indices and iron statuses (477); and highlights the challenges associated with identifying which fetuses have become ID. One may postulate that instead of treating ID during pregnancy, a superior option may be prevention. This is supported by evidence that suggests optimization of iron status prior to pregnancy is the most effective way to reduce the deleterious effects of ID (215, 216). Hopefully, further work to identify the overall burden of disease caused by ID in pregnancy will draw attention to the importance of this deficiency, particularly in women of reproductive age.

However, due to the sheer commonness of ID, as well as challenges with oral supplementation, many women will still become ID during pregnancy. Fortunately, animal studies have shown promising results by which therapies prevent dysfunction driven by developmental stressors (370). A second challenge associated with treating ID lies in the sex specific programing effects. Because the dysfunction found in our study was sex specific (highlighted in **Chapters 2** and **3**), one may postulate that treatments may also affect these offspring differently. How each sex responds to therapies should therefore be considered when devising future treatments. Further, it is understandable that transitioning from animal models to humans is even more challenging when the intended therapy is to be used in pregnancy. Naturally occurring compounds or

nutritional supplements which have either already undergone FDA approval (such as broccoli sprouts or ketones) may warrant particular attention, as less steps may be required to ultimately bring these treatments to patients. Finally, it is important to remember that DOHaD is just one driver of disease in adulthood; there are many genetic, environmental, and physiological causes for disease. Prevention does not end after development, and therefore care should also be taken to improve lifelong health in the decades following birth.

References

1. Bourque SL, Davidge ST. Developmental programming of cardiovascular function: a translational perspective. Clin Sci (Lond). 2020;134(22):3023-46.

2. Schneider MB, Umpierrez GE, Ramsey RD, Mabie WC, Bennett KA. Pregnancy complicated by diabetic ketoacidosis: maternal and fetal outcomes. Diabetes Care. 2003;26(3):958-9.

3. Writing Group M, Lloyd-Jones D, Adams RJ, Brown TM, Carnethon M, Dai S, et al. Heart disease and stroke statistics--2010 update: a report from the American Heart Association. Circulation. 2010;121(7):e46-e215.

4. Mishra S. Does modern medicine increase life-expectancy: Quest for the Moon Rabbit? Indian Heart J. 2016;68(1):19-27.

5. Warraich HJ, Hernandez AF, Allen LA. How Medicine Has Changed the End of Life for Patients With Cardiovascular Disease. J Am Coll Cardiol. 2017;70(10):1276-89.

6. Canadian Institutes of Health Research. Health Research - Investing in Canada's Future 2004- 2005 [Available from: http://www.cihr-irsc.gc.ca/e/28901.html.

7. Kermack WO, McKendrick AG, McKinlay PL. Death-rates in Great Britain and Sweden. Some general regularities and their significance. Int J Epidemiol. 2001;30(4):678-83.

8. Forsdahl A. [Points which enlighten the high mortality rate in the county of Finnmark. Can the high mortality rate today be a consequence of bad conditions of life in childhood and adolescence?]. Tidsskr Nor Laegeforen. 1973;93(10):661-7.

9. Forsdahl A. Are poor living conditions in childhood and adolescence an important risk factor for arteriosclerotic heart disease? Br J Prev Soc Med. 1977;31(2):91-5.

10. Barker DJ, Osmond C. Infant mortality, childhood nutrition, and ischaemic heart disease in England and Wales. Lancet. 1986;1(8489):1077-81.

11. Balarajan R. Ethnic differences in mortality from ischaemic heart disease and cerebrovascular disease in England and Wales. BMJ. 1991;302(6776):560-4.

12. Barker DJ, Winter PD, Osmond C, Margetts B, Simmonds SJ. Weight in infancy and death from ischaemic heart disease. Lancet. 1989;2(8663):577-80.

13. Barker DJ. In utero programming of chronic disease. Clin Sci (Lond). 1998;95(2):115-28.

14. Hwang JK, Kang HN, Ahn JH, Lee HJ, Park HK, Kim CR. Effects of Ponderal Index on Neonatal Mortality and Morbidities in Extremely Premature Infants. J Korean Med Sci. 2022;37(24):e198.

15. Tran NN, Tran M, Panigrahy A, Brady KM, Votava-Smith JK. Association of Cerebrovascular Stability Index and Head Circumference Between Infants With and Without Congenital Heart Disease. Pediatr Cardiol. 2022;43(7):1624-30.

16. Barker DJ, Osmond C, Simmonds SJ, Wield GA. The relation of small head circumference and thinness at birth to death from cardiovascular disease in adult life. BMJ. 1993;306(6875):422-6.

17. Barker DJ, Meade TW, Fall CH, Lee A, Osmond C, Phipps K, Stirling Y. Relation of fetal and infant growth to plasma fibrinogen and factor VII concentrations in adult life. BMJ. 1992;304(6820):148-52.

18. Hales CN, Barker DJ, Clark PM, Cox LJ, Fall C, Osmond C, Winter PD. Fetal and infant growth and impaired glucose tolerance at age 64. BMJ. 1991;303(6809):1019-22.

19. Barker DJ, Bull AR, Osmond C, Simmonds SJ. Fetal and placental size and risk of hypertension in adult life. BMJ. 1990;301(6746):259-62.

20. Berry G. The analysis of mortality by the subject-years method. Biometrics. 1983;39(1):173-84.

21. Hockaday TD, Yajnik CS. --to: Hales CN, Barker DJP (1992) Type 2 (non-insulin-dependent) diabetes mellitus: the thrifty phenotype hypothesis. Diabetologia 35:595-601. Diabetologia. 2003;46(2):303-4.

22. Hales CN, Barker DJ. The thrifty phenotype hypothesis. Br Med Bull. 2001;60:5-20.

23. De Rooij SR, Bleker LS, Painter RC, Ravelli AC, Roseboom TJ. Lessons learned from 25 Years of Research into Long term Consequences of Prenatal Exposure to the Dutch famine 1944-45: The Dutch famine Birth Cohort. Int J Environ Health Res. 2022;32(7):1432-46.

24. Roseboom TJ, van der Meulen JH, Osmond C, Barker DJ, Ravelli AC, Bleker OP. Plasma lipid profiles in adults after prenatal exposure to the Dutch famine. Am J Clin Nutr. 2000;72(5):1101-6.

25. Roseboom TJ, van der Meulen JH, Osmond C, Barker DJ, Ravelli AC, Schroeder-Tanka JM, et al. Coronary heart disease after prenatal exposure to the Dutch famine, 1944-45. Heart. 2000;84(6):595-8.

26. Kyle UG, Pichard C. The Dutch Famine of 1944-1945: a pathophysiological model of long-term consequences of wasting disease. Curr Opin Clin Nutr Metab Care. 2006;9(4):388-94.

27. Ravelli AC, van der Meulen JH, Michels RP, Osmond C, Barker DJ, Hales CN, Bleker OP. Glucose tolerance in adults after prenatal exposure to famine. Lancet. 1998;351(9097):173-7.

28. Stanner SA, Bulmer K, Andres C, Lantseva OE, Borodina V, Poteen VV, Yudkin JS. Does malnutrition in utero determine diabetes and coronary heart disease in adulthood? Results from the Leningrad siege study, a cross sectional study. BMJ. 1997;315(7119):1342-8.

29. Stanner SA, Yudkin JS. Fetal programming and the Leningrad Siege study. Twin Res. 2001;4(5):287-92.

30. Dickinson H, Moss TJ, Gatford KL, Moritz KM, Akison L, Fullston T, et al. A review of fundamental principles for animal models of DOHaD research: an Australian perspective. J Dev Orig Health Dis. 2016;7(5):449-72.

31. Romanus S, Neven P, Soubry A. Extending the Developmental Origins of Health and Disease theory: does paternal diet contribute to breast cancer risk in daughters? Breast Cancer Res. 2016;18(1):103.

32. Barker DJ. The developmental origins of adult disease. J Am Coll Nutr. 2004;23(6 Suppl):588S-95S.

33. Stearns SC, Medzhitov R. Evolutionary medicine. Sunderland, Massachussetts: Sinauer Associates, Inc., Publishers; 2016. xix, 306 pages : color illustrations p.

34. Lee PA, Chernausek SD, Hokken-Koelega AC, Czernichow P, International Small for Gestational Age Advisory B. International Small for Gestational Age Advisory Board consensus development conference statement: management of short children born small for gestational age, April 24-October 1, 2001. Pediatrics. 2003;111(6 Pt 1):1253-61.

35. Physical status: the use and interpretation of anthropometry. Report of a WHO Expert Committee. World Health Organ Tech Rep Ser. 1995;854:1-452.

36. Sheridan C. Intrauterine growth restriction--diagnosis and management. Aust Fam Physician. 2005;34(9):717-23.

37. Sharma D, Shastri S, Sharma P. Intrauterine Growth Restriction: Antenatal and Postnatal Aspects. Clin Med Insights Pediatr. 2016;10:67-83.

38. Thornburg KL. The programming of cardiovascular disease. J Dev Orig Health Dis. 2015;6(5):366-76.

39. Morton JS, Cooke CL, Davidge ST. In Utero Origins of Hypertension: Mechanisms and Targets for Therapy. Physiol Rev. 2016;96(2):549-603.

40. Sutton EF, Gilmore LA, Dunger DB, Heijmans BT, Hivert MF, Ling C, et al. Developmental programming: State-of-the-science and future directions-Summary from a Pennington Biomedical symposium. Obesity (Silver Spring). 2016;24(5):1018-26.

41. Blencowe H, Krasevec J, de Onis M, Black RE, An X, Stevens GA, et al. National, regional, and worldwide estimates of low birthweight in 2015, with trends from 2000: a systematic analysis. Lancet Glob Health. 2019;7(7):e849-e60.

42. Giussani DA. The fetal brain sparing response to hypoxia: physiological mechanisms. J Physiol. 2016;594(5):1215-30.

43. Giussani DA, Davidge ST. Developmental programming of cardiovascular disease by prenatal hypoxia. J Dev Orig Health Dis. 2013;4(5):328-37.

44. Nardozza LM, Caetano AC, Zamarian AC, Mazzola JB, Silva CP, Marcal VM, et al. Fetal growth restriction: current knowledge. Arch Gynecol Obstet. 2017;295(5):1061-77.

45. Rosenberg A. The IUGR newborn. Semin Perinatol. 2008;32(3):219-24.

46. Gilbert JS, Cox LA, Mitchell G, Nijland MJ. Nutrient-restricted fetus and the cardio-renal connection in hypertensive offspring. Expert Rev Cardiovasc Ther. 2006;4(2):227-37.

47. Symonds ME, Gardner DS. Experimental evidence for early nutritional programming of later health in animals. Curr Opin Clin Nutr Metab Care. 2006;9(3):278-83.

48. Embleton ND, Skeath T. Catch-Up Growth and Metabolic and Cognitive Outcomes in Adolescents Born Preterm. Nestle Nutr Inst Workshop Ser. 2015;81:61-71.

49. Embleton ND, Korada M, Wood CL, Pearce MS, Swamy R, Cheetham TD. Catch-up growth and metabolic outcomes in adolescents born preterm. Arch Dis Child. 2016;101(11):1026-31.

50. Nguyen MT, Ouzounian JG. Evaluation and Management of Fetal Macrosomia. Obstet Gynecol Clin North Am. 2021;48(2):387-99.

51. Bowers K, Laughon SK, Kiely M, Brite J, Chen Z, Zhang C. Gestational diabetes, pre-pregnancy obesity and pregnancy weight gain in relation to excess fetal growth: variations by race/ethnicity. Diabetologia. 2013;56(6):1263-71.

52. Marshall NE, Biel FM, Boone-Heinonen J, Dukhovny D, Caughey AB, Snowden JM. The Association between Maternal Height, Body Mass Index, and Perinatal Outcomes. Am J Perinatol. 2019;36(6):632-40.

53. Su R, Zhu W, Wei Y, Wang C, Feng H, Lin L, et al. Relationship of maternal birth weight on maternal and neonatal outcomes: a multicenter study in Beijing. J Perinatol. 2016;36(12):1061-6.

54. Jolly MC, Sebire NJ, Harris JP, Regan L, Robinson S. Risk factors for macrosomia and its clinical consequences: a study of 350,311 pregnancies. Eur J Obstet Gynecol Reprod Biol. 2003;111(1):9-14.

55. Jin WY, Lin SL, Hou RL, Chen XY, Han T, Jin Y, et al. Associations between maternal lipid profile and pregnancy complications and perinatal outcomes: a population-based study from China. BMC Pregnancy Childbirth. 2016;16:60.

56. Usta A, Usta CS, Yildiz A, Ozcaglayan R, Dalkiran ES, Savkli A, Taskiran M. Frequency of fetal macrosomia and the associated risk factors in pregnancies without gestational diabetes mellitus. Pan Afr Med J. 2017;26:62.

57. Koo S, Kim JY, Park JH, Roh GS, Lim NK, Park HY, Kim WH. Binge alcohol drinking before pregnancy is closely associated with the development of macrosomia: Korean pregnancy registry cohort. PLoS One. 2022;17(7):e0271291.

58. Little SE, Edlow AG, Thomas AM, Smith NA. Estimated fetal weight by ultrasound: a modifiable risk factor for cesarean delivery? Am J Obstet Gynecol. 2012;207(4):309 e1-6.

59. Gu S, An X, Fang L, Zhang X, Zhang C, Wang J, et al. Risk factors and long-term health consequences of macrosomia: a prospective study in Jiangsu Province, China. J Biomed Res. 2012;26(4):235-40.

60. McGrath RT, Glastras SJ, Hocking SL, Fulcher GR. Large-for-Gestational-Age Neonates in Type 1 Diabetes and Pregnancy: Contribution of Factors Beyond Hyperglycemia. Diabetes Care. 2018;41(8):1821-8.

61. Thorn SR, Rozance PJ, Brown LD, Hay WW, Jr. The intrauterine growth restriction phenotype: fetal adaptations and potential implications for later life insulin resistance and diabetes. Semin Reprod Med. 2011;29(3):225-36.

62. Ross MG, Beall MH. Adult sequelae of intrauterine growth restriction. Semin Perinatol. 2008;32(3):213-8.

63. Gluckman PD, Hanson MA, Buklijas T, Low FM, Beedle AS. Epigenetic mechanisms that underpin metabolic and cardiovascular diseases. Nat Rev Endocrinol. 2009;5(7):401-8.

64. Wit JM, Boersma B. Catch-up growth: definition, mechanisms, and models. J Pediatr Endocrinol Metab. 2002;15 Suppl 5:1229-41.

65. Lizarraga-Mollinedo E, Carreras-Badosa G, Xargay-Torrent S, Remesar X, Mas-Pares B, Prats-Puig A, et al. Catch-up growth in juvenile rats, fat expansion, and dysregulation of visceral adipose tissue. Pediatr Res. 2022;91(1):107-15.

66. de Zegher F, Garcia Beltran C, Lopez-Bermejo A, Ibanez L. Metformin for Rapidly Maturing Girls with Central Adiposity: Less Liver Fat and Slower Bone Maturation. Horm Res Paediatr. 2018;89(2):136-40.

67. Stettler N, Zemel BS, Kumanyika S, Stallings VA. Infant weight gain and childhood overweight status in a multicenter, cohort study. Pediatrics. 2002;109(2):194-9.

68. Ibanez L, Ong K, Dunger DB, de Zegher F. Early development of adiposity and insulin resistance after catch-up weight gain in small-for-gestational-age children. J Clin Endocrinol Metab. 2006;91(6):2153-8.

69. Malpique R, Bassols J, Lopez-Bermejo A, Diaz M, Villarroya F, Pavia J, et al. Liver volume and hepatic adiposity in childhood: relations to body growth and visceral fat. Int J Obes (Lond). 2018;42(1):65-71.

70. Leunissen RW, Kerkhof GF, Stijnen T, Hokken-Koelega AC. Effect of birth size and catch-up growth on adult blood pressure and carotid intima-media thickness. Horm Res Paediatr. 2012;77(6):394-401.

71. Goedegebuure WJ, Van der Steen M, Smeets CCJ, Kerkhof GF, Hokken-Koelega ACS. SGA-born adults with postnatal catch-up have a persistently unfavourable metabolic health profile and increased adiposity at age 32 years. Eur J Endocrinol. 2022;187(1):15-26.

72. Kesavan K, Devaskar SU. Intrauterine Growth Restriction: Postnatal Monitoring and Outcomes. Pediatr Clin North Am. 2019;66(2):403-23.

73. Dulloo AG, Jacquet J, Montani JP. Pathways from weight fluctuations to metabolic diseases: focus on maladaptive thermogenesis during catch-up fat. Int J Obes Relat Metab Disord. 2002;26 Suppl 2:S46-57.

74. Dulloo AG. Regulation of fat storage via suppressed thermogenesis: a thrifty phenotype that predisposes individuals with catch-up growth to insulin resistance and obesity. Horm Res. 2006;65 Suppl 3:90-7.

75. Summermatter S, Marcelino H, Arsenijevic D, Buchala A, Aprikian O, Assimacopoulos-Jeannet F, et al. Adipose tissue plasticity during catch-up fat driven by thrifty metabolism: relevance for muscle-adipose glucose redistribution during catch-up growth. Diabetes. 2009;58(10):2228-37.

76. Embleton ND. Early nutrition and later outcomes in preterm infants. World Rev Nutr Diet. 2013;106:26-32.

77. Ong KK, Kennedy K, Castaneda-Gutierrez E, Forsyth S, Godfrey KM, Koletzko B, et al. Postnatal growth in preterm infants and later health outcomes: a systematic review. Acta Paediatr. 2015;104(10):974-86.

78. Lampl M, Jeanty P. Timing is everything: a reconsideration of fetal growth velocity patterns identifies the importance of individual and sex differences. Am J Hum Biol. 2003;15(5):667-80.

79. Intapad S, Ojeda NB, Dasinger JH, Alexander BT. Sex differences in the developmental origins of cardiovascular disease. Physiology (Bethesda). 2014;29(2):122-32.

80. Dasinger JH, Alexander BT. Gender differences in developmental programming of cardiovascular diseases. Clin Sci (Lond). 2016;130(5):337-48.

81. Talbot CPJ, Dolinsky VW. Sex differences in the developmental origins of cardiometabolic disease following exposure to maternal obesity and gestational diabetes (1). Appl Physiol Nutr Metab. 2019;44(7):687-95.

82. Ward AM, Moore VM, Steptoe A, Cockington RA, Robinson JS, Phillips DI. Size at birth and cardiovascular responses to psychological stressors: evidence for prenatal programming in women. J Hypertens. 2004;22(12):2295-301.

83. Jones A, Beda A, Ward AM, Osmond C, Phillips DI, Moore VM, Simpson DM. Size at birth and autonomic function during psychological stress. Hypertension. 2007;49(3):548-55.

84. Hatano N, Mori Y, Oh-hora M, Kosugi A, Fujikawa T, Nakai N, et al. Essential role for ERK2 mitogen-activated protein kinase in placental development. Genes Cells. 2003;8(11):847-56.

85. Dzubur A, Gacic E, Mekic M. Comparison of Patients with Acute Myocardial Infarction According to Age. Med Arch. 2019;73(1):23-7.

86. Yang D, Li J, Yuan Z, Liu X. Effect of hormone replacement therapy on cardiovascular outcomes: a meta-analysis of randomized controlled trials. PLoS One. 2013;8(5):e62329.

87. Menazza S, Murphy E. The Expanding Complexity of Estrogen Receptor Signaling in the Cardiovascular System. Circ Res. 2016;118(6):994-1007.

88. Mercuro G, Deidda M, Piras A, Dessalvi CC, Maffei S, Rosano GM. Gender determinants of cardiovascular risk factors and diseases. J Cardiovasc Med (Hagerstown). 2010;11(3):207-20.

89. Iorga A, Cunningham CM, Moazeni S, Ruffenach G, Umar S, Eghbali M. The protective role of estrogen and estrogen receptors in cardiovascular disease and the controversial use of estrogen therapy. Biol Sex Differ. 2017;8(1):33.

90. Kander MC, Cui Y, Liu Z. Gender difference in oxidative stress: a new look at the mechanisms for cardiovascular diseases. J Cell Mol Med. 2017;21(5):1024-32.

91. Colombo J, Gustafson KM, Carlson SE. Critical and Sensitive Periods in Development and Nutrition. Ann Nutr Metab. 2019;75 Suppl 1(Suppl 1):34-42.

92. Neithercott T. 6 ways to take a bite out of heart disease. Diabetes Forecast. 2012;65(2):31-4.

93. McGill HC, Jr., McMahan CA, Gidding SS. Preventing heart disease in the 21st century: implications of the Pathobiological Determinants of Atherosclerosis in Youth (PDAY) study. Circulation. 2008;117(9):1216-27.

94. Rehman B, Muzio MR. Embryology, Week 2-3. StatPearls. Treasure Island (FL)2023.

95. Lilly LS. Pathophysiology of Heart Disease : a Collaborative Project of Medical Students and Faculty. Philadelphia :Lippincott Williams & Wilkins; 2003.

96. Finnemore A, Groves A. Physiology of the fetal and transitional circulation. Semin Fetal Neonatal Med. 2015;20(4):210-6.

97. Morton SU, Brodsky D. Fetal Physiology and the Transition to Extrauterine Life. Clin Perinatol. 2016;43(3):395-407.

98. Sharma A FS, Calvert J. Adaptation for life: a review of neonatal physiology. Anaesth Intensive Care Med 2014;15((3)):89–95.

99. Kotaska K, Urinovska R, Klapkova E, Prusa R, Rob L, Binder T. Re-evaluation of cord blood arterial and venous reference ranges for pH, pO(2), pCO(2), according to spontaneous or cesarean delivery. J Clin Lab Anal. 2010;24(5):300-4.

100. Tan CMJ, Lewandowski AJ. The Transitional Heart: From Early Embryonic and Fetal Development to Neonatal Life. Fetal Diagn Ther. 2020;47(5):373-86.

101. Piquereau J, Ventura-Clapier R. Maturation of Cardiac Energy Metabolism During Perinatal Development. Front Physiol. 2018;9:959.

102. Xiong F, Lin T, Song M, Ma Q, Martinez SR, Lv J, et al. Antenatal hypoxia induces epigenetic repression of glucocorticoid receptor and promotes ischemic-sensitive phenotype in the developing heart. J Mol Cell Cardiol. 2016;91:160-71.

103. Lv J, Ma Q, Dasgupta C, Xu Z, Zhang L. Antenatal Hypoxia and Programming of Glucocorticoid Receptor Expression in the Adult Rat Heart. Front Physiol. 2019;10:323.

104. Xue Q, Dasgupta C, Chen M, Zhang L. Foetal hypoxia increases cardiac AT(2)R expression and subsequent vulnerability to adult ischaemic injury. Cardiovasc Res. 2011;89(2):300-8.

105. Lamadema N, Burr S, Brewer AC. Dynamic regulation of epigenetic demethylation by oxygen availability and cellular redox. Free Radic Biol Med. 2019;131:282-98.

106. Camuzi D, de Amorim ISS, Ribeiro Pinto LF, Oliveira Trivilin L, Mencalha AL, Soares Lima SC. Regulation Is in the Air: The Relationship between Hypoxia and Epigenetics in Cancer. Cells. 2019;8(4).

107. Kietzmann T, Petry A, Shvetsova A, Gerhold JM, Gorlach A. The epigenetic landscape related to reactive oxygen species formation in the cardiovascular system. Br J Pharmacol. 2017;174(12):1533-54.

108. Radford EJ, Ito M, Shi H, Corish JA, Yamazawa K, Isganaitis E, et al. In utero effects. In utero undernourishment perturbs the adult sperm methylome and intergenerational metabolism. Science. 2014;345(6198):1255903.

109. Gilsbach R, Preissl S, Gruning BA, Schnick T, Burger L, Benes V, et al. Dynamic DNA methylation orchestrates cardiomyocyte development, maturation and disease. Nat Commun. 2014;5:5288.

110. Gilsbach R, Schwaderer M, Preissl S, Gruning BA, Kranzhofer D, Schneider P, et al. Distinct epigenetic programs regulate cardiac myocyte development and disease in the human heart in vivo. Nat Commun. 2018;9(1):391.

111. Li R, Jia Z, Trush MA. Defining ROS in Biology and Medicine. React Oxyg Species (Apex). 2016;1(1):9-21.

112. Duhig K, Chappell LC, Shennan AH. Oxidative stress in pregnancy and reproduction. Obstet Med. 2016;9(3):113-6.

113. Marseglia L, D'Angelo G, Manti S, Arrigo T, Barberi I, Reiter RJ, Gitto E. Oxidative stress-mediated aging during the fetal and perinatal periods. Oxid Med Cell Longev. 2014;2014:358375.

114. Martini S, Aceti A, Della Gatta AN, Beghetti I, Marsico C, Pilu G, Corvaglia L. Antenatal and Postnatal Sequelae of Oxidative Stress in Preterm Infants: A Narrative Review Targeting Pathophysiological Mechanisms. Antioxidants (Basel). 2023;12(2).

115. Tain YL, Hsu CN. Oxidative Stress-Induced Hypertension of Developmental Origins: Preventive Aspects of Antioxidant Therapy. Antioxidants (Basel). 2022;11(3).

116. Brennan LJ, Goulopoulou S, Bourque SL. Prenatal therapeutics and programming of cardiovascular function. Pharmacol Res. 2019;139:261-72.

117. Mistry HD, Williams PJ. The importance of antioxidant micronutrients in pregnancy. Oxid Med Cell Longev. 2011;2011:841749.

118. Berkelhamer SK, Farrow KN. Developmental regulation of antioxidant enzymes and their impact on neonatal lung disease. Antioxid Redox Signal. 2014;21(13):1837-48.

119. Huang ST, Vo KC, Lyell DJ, Faessen GH, Tulac S, Tibshirani R, et al. Developmental response to hypoxia. FASEB J. 2004;18(12):1348-65.

120. Huppertz B, Weiss G, Moser G. Trophoblast invasion and oxygenation of the placenta: measurements versus presumptions. J Reprod Immunol. 2014;101-102:74-9.

121. Luo ZC, Fraser WD, Julien P, Deal CL, Audibert F, Smith GN, et al. Tracing the origins of "fetal origins" of adult diseases: programming by oxidative stress? Med Hypotheses. 2006;66(1):38-44.

122. Tong W, Xue Q, Li Y, Zhang L. Maternal hypoxia alters matrix metalloproteinase expression patterns and causes cardiac remodeling in fetal and neonatal rats. Am J Physiol Heart Circ Physiol. 2011;301(5):H2113-21.

123. Walton SL, Bielefeldt-Ohmann H, Singh RR, Li J, Paravicini TM, Little MH, Moritz KM. Prenatal hypoxia leads to hypertension, renal renin-angiotensin system activation and exacerbates salt-induced pathology in a sex-specific manner. Sci Rep. 2017;7(1):8241.

124. Walton SL, Singh RR, Little MH, Bowles J, Li J, Moritz KM. Prolonged prenatal hypoxia selectively disrupts collecting duct patterning and postnatal function in male mouse offspring. J Physiol. 2018;596(23):5873-89.

125. Aljunaidy MM, Morton JS, Cooke CM, Davidge ST. Prenatal hypoxia and placental oxidative stress: linkages to developmental origins of cardiovascular disease. Am J Physiol Regul Integr Comp Physiol. 2017;313(4):R395-R9.

126. Aplin J. Maternal influences on placental development. Semin Cell Dev Biol. 2000;11(2):115-25.

127. Belkacemi L, Nelson DM, Desai M, Ross MG. Maternal undernutrition influences placental-fetal development. Biol Reprod. 2010;83(3):325-31.

128. Anderson RN. Deaths: leading causes for 2000. Natl Vital Stat Rep. 2002;50(16):1-85.

129. Murphy VE, Smith R, Giles WB, Clifton VL. Endocrine regulation of human fetal growth: the role of the mother, placenta, and fetus. Endocr Rev. 2006;27(2):141-69.

130. Gurusinghe S, Tambay A, Sethna CB. Developmental Origins and Nephron Endowment in Hypertension. Front Pediatr. 2017;5:151.

131. Hughson M, Farris AB, 3rd, Douglas-Denton R, Hoy WE, Bertram JF. Glomerular number and size in autopsy kidneys: the relationship to birth weight. Kidney Int. 2003;63(6):2113-22.

132. Lumbers ER, Kandasamy Y, Delforce SJ, Boyce AC, Gibson KJ, Pringle KG. Programming of Renal Development and Chronic Disease in Adult Life. Front Physiol. 2020;11:757.

133. Bertram JF, Douglas-Denton RN, Diouf B, Hughson MD, Hoy WE. Human nephron number: implications for health and disease. Pediatr Nephrol. 2011;26(9):1529-33.

134. Low Birth W, Nephron Number Working G. The Impact of Kidney Development on the Life Course: A Consensus Document for Action. Nephron. 2017;136(1):3-49.

135. Luyckx VA, Brenner BM. Clinical consequences of developmental programming of low nephron number. Anat Rec (Hoboken). 2020;303(10):2613-31.

136. Baum M. Role of the kidney in the prenatal and early postnatal programming of hypertension. Am J Physiol Renal Physiol. 2010;298(2):F235-47.

137. Woodman AG, Mah RL, Kinney S, Holody CD, Wiedemeyer AR, Noble RMN, et al. Perinatal iron deficiency causes sex-dependent alterations in renal retinoic acid signaling and nephrogenesis. J Nutr Biochem. 2023;112:109227.

138. Woodman AG, Mah R, Keddie DL, Noble RMN, Holody CD, Panahi S, et al. Perinatal iron deficiency and a high salt diet cause long-term kidney mitochondrial dysfunction and oxidative stress. Cardiovasc Res. 2020;116(1):183-92.

139. Bourque SL, Komolova M, Nakatsu K, Adams MA. Long-term circulatory consequences of perinatal iron deficiency in male Wistar rats. Hypertension. 2008;51(1):154-9.

140. Woodman AG, Noble RMN, Panahi S, Gragasin FS, Bourque SL. Perinatal iron deficiency combined with a high salt diet in adulthood causes sex-dependent vascular dysfunction in rats. J Physiol. 2019;597(18):4715-28.

141. Ream M, Ray AM, Chandra R, Chikaraishi DM. Early fetal hypoxia leads to growth restriction and myocardial thinning. Am J Physiol Regul Integr Comp Physiol. 2008;295(2):R583-95.

142. Xu Y, Williams SJ, O'Brien D, Davidge ST. Hypoxia or nutrient restriction during pregnancy in rats leads to progressive cardiac remodeling and impairs postischemic recovery in adult male offspring. FASEB J. 2006;20(8):1251-3.

143. Rueda-Clausen CF, Morton JS, Lopaschuk GD, Davidge ST. Long-term effects of intrauterine growth restriction on cardiac metabolism and susceptibility to ischaemia/reperfusion. Cardiovasc Res. 2011;90(2):285-94.

144. Reyes LM, Kirschenman R, Quon A, Morton JS, Shah A, Davidge ST. Aerobic exercise training reduces cardiac function in adult male offspring exposed to prenatal hypoxia. Am J Physiol Regul Integr Comp Physiol. 2015;309(5):R489-98.

145. Paradis AN, Gay MS, Wilson CG, Zhang L. Newborn hypoxia/anoxia inhibits cardiomyocyte proliferation and decreases cardiomyocyte endowment in the developing heart: role of endothelin-1. PLoS One. 2015;10(2):e0116600.

146. Bae S, Xiao Y, Li G, Casiano CA, Zhang L. Effect of maternal chronic hypoxic exposure during gestation on apoptosis in fetal rat heart. Am J Physiol Heart Circ Physiol. 2003;285(3):H983-90.

147. van Amerongen MJ, Engel FB. Features of cardiomyocyte proliferation and its potential for cardiac regeneration. J Cell Mol Med. 2008;12(6A):2233-44.

148. Tong W, Zhang L. Fetal hypoxia and programming of matrix metalloproteinases. Drug Discov Today. 2012;17(3-4):124-34.

149. Rueda-Clausen CF, Morton JS, Davidge ST. Effects of hypoxia-induced intrauterine growth restriction on cardiopulmonary structure and function during adulthood. Cardiovasc Res. 2009;81(4):713-22.

150. Sarvari SI, Rodriguez-Lopez M, Nunez-Garcia M, Sitges M, Sepulveda-Martinez A, Camara O, et al. Persistence of Cardiac Remodeling in Preadolescents With Fetal Growth Restriction. Circ Cardiovasc Imaging. 2017;10(1).

151. Fouzas S, Karatza AA, Davlouros PA, Chrysis D, Alexopoulos D, Mantagos S, Dimitriou G. Neonatal cardiac dysfunction in intrauterine growth restriction. Pediatr Res. 2014;75(5):651-7.

152. Sehgal A, Doctor T, Menahem S. Cardiac function and arterial biophysical properties in small for gestational age infants: postnatal manifestations of fetal programming. J Pediatr. 2013;163(5):1296-300.

153. Iruretagoyena JI, Gonzalez-Tendero A, Garcia-Canadilla P, Amat-Roldan I, Torre I, Nadal A, et al. Cardiac dysfunction is associated with altered sarcomere ultrastructure in intrauterine growth restriction. Am J Obstet Gynecol. 2014;210(6):550 e1-7.

154. Rodgers JL, Jones J, Bolleddu SI, Vanthenapalli S, Rodgers LE, Shah K, et al. Cardiovascular Risks Associated with Gender and Aging. J Cardiovasc Dev Dis. 2019;6(2).

155. Dhingra R, Vasan RS. Age as a risk factor. Med Clin North Am. 2012;96(1):87-91.

156. Lakatta EG, Levy D. Arterial and cardiac aging: major shareholders in cardiovascular disease enterprises: Part I: aging arteries: a "set up" for vascular disease. Circulation. 2003;107(1):139-46.

157. Lakatta EG, Levy D. Arterial and cardiac aging: major shareholders in cardiovascular disease enterprises: Part II: the aging heart in health: links to heart disease. Circulation. 2003;107(2):346-54.

158. Group SR, Lewis CE, Fine LJ, Beddhu S, Cheung AK, Cushman WC, et al. Final Report of a Trial of Intensive versus Standard Blood-Pressure Control. N Engl J Med. 2021;384(20):1921-30.

159. Lakatta EG. Age-associated cardiovascular changes in health: impact on cardiovascular disease in older persons. Heart Fail Rev. 2002;7(1):29-49.

160. Correia LC, Lakatta EG, O'Connor FC, Becker LC, Clulow J, Townsend S, et al. Attenuated cardiovascular reserve during prolonged submaximal cycle exercise in healthy older subjects. J Am Coll Cardiol. 2002;40(7):1290-7.

161. Savage DD, Levy D, Dannenberg AL, Garrison RJ, Castelli WP. Association of echocardiographic left ventricular mass with body size, blood pressure and physical activity (the Framingham Study). Am J Cardiol. 1990;65(5):371-6.

162. Takemura G, Kanoh M, Minatoguchi S, Fujiwara H. Cardiomyocyte apoptosis in the failing heart--a critical review from definition and classification of cell death. Int J Cardiol. 2013;167(6):2373-86.

163. Goldspink DF, Burniston JG, Tan LB. Cardiomyocyte death and the ageing and failing heart. Exp Physiol. 2003;88(3):447-58.

164. Rizvi F, Preston CC, Emelyanova L, Yousufuddin M, Viqar M, Dakwar O, et al. Effects of Aging on Cardiac Oxidative Stress and Transcriptional Changes in Pathways of Reactive Oxygen Species Generation and Clearance. J Am Heart Assoc. 2021;10(16):e019948.

165. Bernhard D, Laufer G. The aging cardiomyocyte: a mini-review. Gerontology. 2008;54(1):24-31.

166. Pagan LU, Gomes MJ, Gatto M, Mota GAF, Okoshi K, Okoshi MP. The Role of Oxidative Stress in the Aging Heart. Antioxidants (Basel). 2022;11(2).

167. Martin-Fernandez B, Gredilla R. Mitochondria and oxidative stress in heart aging. Age (Dordr). 2016;38(4):225-38.

168. North BJ, Sinclair DA. The intersection between aging and cardiovascular disease. Circ Res. 2012;110(8):1097-108.

169. Prabhu SD, Frangogiannis NG. The Biological Basis for Cardiac Repair After Myocardial Infarction: From Inflammation to Fibrosis. Circ Res. 2016;119(1):91-112.

170. Marvasti TB, Alibhai FJ, Yang GJ, Li SH, Wu J, Yau T, Li RK. Heart Failure Impairs Bone Marrow Hematopoietic Stem Cell Function and Responses to Injury. J Am Heart Assoc. 2023;12(11):e027727.

171. Bose C, Alves I, Singh P, Palade PT, Carvalho E, Borsheim E, et al. Sulforaphane prevents age-associated cardiac and muscular dysfunction through Nrf2 signaling. Aging Cell. 2020;19(11):e13261.

172. Gazoti Debessa CR, Mesiano Maifrino LB, Rodrigues de Souza R. Age related changes of the collagen network of the human heart. Mech Ageing Dev. 2001;122(10):1049-58.

173. Biernacka A, Frangogiannis NG. Aging and Cardiac Fibrosis. Aging Dis. 2011;2(2):158-73.

174. Shiraishi I, Takamatsu T, Minamikawa T, Onouchi Z, Fujita S. Quantitative histological analysis of the human sinoatrial node during growth and aging. Circulation. 1992;85(6):2176-84.

175. Inoue S, Shinohara F, Niitani H, Gotoh K. A new method for the histological study of aging changes in the sinoatrial node. Jpn Heart J. 1986;27(5):653-60.

176. Moghtadaei M, Jansen HJ, Mackasey M, Rafferty SA, Bogachev O, Sapp JL, et al. The impacts of age and frailty on heart rate and sinoatrial node function. J Physiol. 2016;594(23):7105-26.

177. Kistler PM, Sanders P, Fynn SP, Stevenson IH, Spence SJ, Vohra JK, et al. Electrophysiologic and electroanatomic changes in the human atrium associated with age. J Am Coll Cardiol. 2004;44(1):109-16.

178. Sanders P, Morton JB, Kistler PM, Spence SJ, Davidson NC, Hussin A, et al. Electrophysiological and electroanatomic characterization of the atria in sinus node disease: evidence of diffuse atrial remodeling. Circulation. 2004;109(12):1514-22.

179. Thery C, Gosselin B, Lekieffre J, Warembourg H. Pathology of sinoatrial node. Correlations with electrocardiographic findings in 111 patients. Am Heart J. 1977;93(6):735-40.

180. Ho SY, Sanchez-Quintana D. Anatomy and pathology of the sinus node. J Interv Card Electrophysiol. 2016;46(1):3-8.

181. Choi S, Baudot M, Vivas O, Moreno CM. Slowing down as we age: aging of the cardiac pacemaker's neural control. Geroscience. 2022;44(1):1-17.

182. Yildiz O. Vascular smooth muscle and endothelial functions in aging. Ann N Y Acad Sci. 2007;1100:353-60.

183. Seals DR, Jablonski KL, Donato AJ. Aging and vascular endothelial function in humans. Clin Sci (Lond). 2011;120(9):357-75.

184. Heffernan KS, Fahs CA, Ranadive SM, Patvardhan EA. L-arginine as a nutritional prophylaxis against vascular endothelial dysfunction with aging. J Cardiovasc Pharmacol Ther. 2010;15(1):17-23.

185. Shannon OM, Clifford T, Seals DR, Craighead DH, Rossman MJ. Nitric oxide, aging and aerobic exercise: Sedentary individuals to Master's athletes. Nitric Oxide. 2022;125-126:31-9.

186. Pantopoulos K. Iron metabolism and the IRE/IRP regulatory system: an update. Ann N Y Acad Sci. 2004;1012:1-13.

187. Chua AC, Graham RM, Trinder D, Olynyk JK. The regulation of cellular iron metabolism. Crit Rev Clin Lab Sci. 2007;44(5-6):413-59.

188. Benson CS, Shah A, Stanworth SJ, Frise CJ, Spiby H, Lax SJ, et al. The effect of iron deficiency and anaemia on women's health. Anaesthesia. 2021;76 Suppl 4:84-95.

189. Lynch S, Pfeiffer CM, Georgieff MK, Brittenham G, Fairweather-Tait S, Hurrell RF, et al. Biomarkers of Nutrition for Development (BOND)-Iron Review. J Nutr. 2018;148(suppl_1):1001S-67S.

190. Ems T, St Lucia K, Huecker MR. Biochemistry, Iron Absorption. StatPearls. Treasure Island (FL)2023.

191. Yiannikourides A, Latunde-Dada GO. A Short Review of Iron Metabolism and Pathophysiology of Iron Disorders. Medicines (Basel). 2019;6(3).

192. Andrews NC. Disorders of iron metabolism. N Engl J Med. 1999;341(26):1986-95.

193. Saboor M, Zehra A, Hamali HA, Mobarki AA. Revisiting Iron Metabolism, Iron Homeostasis and Iron Deficiency Anemia. Clin Lab. 2021;67(3).

194. Nemeth E, Ganz T. Hepcidin-Ferroportin Interaction Controls Systemic Iron Homeostasis. Int J Mol Sci. 2021;22(12).

195. Afsar RE, Kanbay M, Ibis A, Afsar B. In-depth review: is hepcidin a marker for the heart and the kidney? Mol Cell Biochem. 2021;476(9):3365-81.

196. Saneela S, Iqbal R, Raza A, Qamar MF. Hepcidin: A key regulator of iron. J Pak Med Assoc. 2019;69(8):1170-5.

197. Wang CY, Babitt JL. Hepcidin regulation in the anemia of inflammation. Curr Opin Hematol. 2016;23(3):189-97.

198. Pak M, Lopez MA, Gabayan V, Ganz T, Rivera S. Suppression of hepcidin during anemia requires erythropoietic activity. Blood. 2006;108(12):3730-5.

199. Petry N, Olofin I, Hurrell RF, Boy E, Wirth JP, Moursi M, et al. The Proportion of Anemia Associated with Iron Deficiency in Low, Medium, and High Human Development Index Countries: A Systematic Analysis of National Surveys. Nutrients. 2016;8(11).

200. Taylor CL, Brannon PM. Introduction to workshop on iron screening and supplementation in iron-replete pregnant women and young children. Am J Clin Nutr. 2017;106(Suppl 6):1547S-54S.

201. Allen LH. Anemia and iron deficiency: effects on pregnancy outcome. Am J Clin Nutr. 2000;71(5 Suppl):1280S-4S.

202. DeLoughery TG. Iron Deficiency Anemia. Med Clin North Am. 2017;101(2):319-32.

203. Camaschella C. Iron-deficiency anemia. N Engl J Med. 2015;372(19):1832-43.

204. Balendran S, Forsyth C. Non-anaemic iron deficiency. Aust Prescr. 2021;44(6):193-6.

205. Zhu XY, Wu TT, Wang HM, Li X, Ni LY, Chen TJ, et al. Correlates of Nonanemic Iron Deficiency in Restless Legs Syndrome. Front Neurol. 2020;11:298.

206. Beard JL. Iron biology in immune function, muscle metabolism and neuronal functioning. J Nutr. 2001;131(2S-2):568S-79S; discussion 80S.

207. Garcia-Casal MN, Pena-Rosas JP, Pasricha SR. Rethinking ferritin cutoffs for iron deficiency and overload. Lancet Haematol. 2014;1(3):e92-4.

208. Suchdev PS, Williams AM, Mei Z, Flores-Ayala R, Pasricha SR, Rogers LM, Namaste SM. Assessment of iron status in settings of inflammation: challenges and potential approaches. Am J Clin Nutr. 2017;106(Suppl 6):1626S-33S.

209. McLean E, Cogswell M, Egli I, Wojdyla D, de Benoist B. Worldwide prevalence of anaemia, WHO Vitamin and Mineral Nutrition Information System, 1993-2005. Public Health Nutr. 2009;12(4):444-54.

210. Lopez A, Cacoub P, Macdougall IC, Peyrin-Biroulet L. Iron deficiency anaemia. Lancet. 2016;387(10021):907-16.

211. Stevens GA, Finucane MM, De-Regil LM, Paciorek CJ, Flaxman SR, Branca F, et al. Global, regional, and national trends in haemoglobin concentration and prevalence of total and severe anaemia in children and pregnant and non-pregnant women for 1995-2011: a systematic analysis of population-representative data. Lancet Glob Health. 2013;1(1):e16-25.

212. Bastian TW, von Hohenberg WC, Mickelson DJ, Lanier LM, Georgieff MK. Iron Deficiency Impairs Developing Hippocampal Neuron Gene Expression, Energy Metabolism, and Dendrite Complexity. Dev Neurosci. 2016;38(4):264-76.

213. Acharya G, Sitras V. Oxygen uptake of the human fetus at term. Acta Obstet Gynecol Scand. 2009;88(1):104-9.

214. Breymann C. Iron Deficiency Anemia in Pregnancy. Semin Hematol. 2015;52(4):339-47.

215. Breymann C, Auerbach M. Iron deficiency in gynecology and obstetrics: clinical implications and management. Hematology Am Soc Hematol Educ Program. 2017;2017(1):152-9.

216. Georgieff MK. Iron deficiency in pregnancy. Am J Obstet Gynecol. 2020;223(4):516-24.

217. Pena-Rosas JP, De-Regil LM, Gomez Malave H, Flores-Urrutia MC, Dowswell T. Intermittent oral iron supplementation during pregnancy. Cochrane Database Syst Rev. 2015;2015(10):CD009997.

218. Kassebaum NJ, Collaborators GBDA. The Global Burden of Anemia. Hematol Oncol Clin North Am. 2016;30(2):247-308.

219. Rahman MM, Abe SK, Rahman MS, Kanda M, Narita S, Bilano V, et al. Maternal anemia and risk of adverse birth and health outcomes in low- and middle-income countries: systematic review and meta-analysis. Am J Clin Nutr. 2016;103(2):495-504.

220. Dewey KG, Oaks BM. U-shaped curve for risk associated with maternal hemoglobin, iron status, or iron supplementation. Am J Clin Nutr. 2017;106(Suppl 6):1694S-702S.

221. Domellof M. Meeting the Iron Needs of Low and Very Low Birth Weight Infants. Ann Nutr Metab. 2017;71 Suppl 3:16-23.

222. Roberts H, Bourque SL, Renaud SJ. Maternal iron homeostasis: effect on placental development and function. Reproduction. 2020;160(4):R65-R78.

223. Woodman AG, Care AS, Mansour Y, Cherak SJ, Panahi S, Gragasin FS, Bourque SL. Modest and Severe Maternal Iron Deficiency in Pregnancy are Associated with Fetal Anaemia and Organ-Specific Hypoxia in Rats. Sci Rep. 2017;7:46573.

224. Woodman AG, Mah R, Keddie D, Noble RMN, Panahi S, Gragasin FS, et al. Prenatal iron deficiency causes sex-dependent mitochondrial dysfunction and oxidative stress in fetal rat kidneys and liver. FASEB J. 2018;32(6):3254-63.

225. Alwan NA, Hamamy H. Maternal Iron Status in Pregnancy and Long-Term Health Outcomes in the Offspring. J Pediatr Genet. 2015;4(2):111-23.

226. Erick M. Breast milk is conditionally perfect. Med Hypotheses. 2018;111:82-9.

227. Zimmermann MB. Global look at nutritional and functional iron deficiency in infancy. Hematology Am Soc Hematol Educ Program. 2020;2020(1):471-7.

228. Zhao G, Xu G, Zhou M, Jiang Y, Richards B, Clark KM, et al. Prenatal Iron Supplementation Reduces Maternal Anemia, Iron Deficiency, and Iron Deficiency Anemia in a Randomized Clinical Trial in Rural China, but Iron Deficiency Remains Widespread in Mothers and Neonates. J Nutr. 2015;145(8):1916-23.

229. Lupton JR, Blumberg JB, L'Abbe M, LeDoux M, Rice HB, von Schacky C, et al. Nutrient reference value: non-communicable disease endpoints--a conference report. Eur J Nutr. 2016;55 Suppl 1:S1-10.

230. American College of O, Gynecologists' Committee on Practice B-O. Anemia in Pregnancy: ACOG Practice Bulletin, Number 233. Obstet Gynecol. 2021;138(2):e55-e64.

231. Fisher AL, Nemeth E. Iron homeostasis during pregnancy. Am J Clin Nutr. 2017;106(Suppl 6):1567S-74S.

232. Ziegler EE, O'Donnell AM, Nelson SE, Fomon SJ. Body composition of the reference fetus. Growth. 1976;40(4):329-41.

233. Miller EM. The reproductive ecology of iron in women. Am J Phys Anthropol. 2016;159(Suppl 61):S172-95.

234. Pasricha SR, Tye-Din J, Muckenthaler MU, Swinkels DW. Iron deficiency. Lancet. 2021;397(10270):233-48.

235. Aztlan-James EA, McLemore M, Taylor D. Multiple Unintended Pregnancies in U.S. Women: A Systematic Review. Womens Health Issues. 2017;27(4):407-13.

236. Suominen P, Punnonen K, Rajamaki A, Irjala K. Serum transferrin receptor and transferrin receptor-ferritin index identify healthy subjects with subclinical iron deficits. Blood. 1998;92(8):2934-9.

237. Georgieff MK, Krebs NF, Cusick SE. The Benefits and Risks of Iron Supplementation in Pregnancy and Childhood. Annu Rev Nutr. 2019;39:121-46.

238. Cockell KA, Miller DC, Lowell H. Application of the Dietary Reference Intakes in developing a recommendation for pregnancy iron supplements in Canada. Am J Clin Nutr. 2009;90(4):1023-8.

239. van der Merwe LF, Eussen SR. Iron status of young children in Europe. Am J Clin Nutr. 2017;106(Suppl 6):1663S-71S.

240. Soppi ET. Iron deficiency without anemia - a clinical challenge. Clin Case Rep. 2018;6(6):1082-6.

241. Screening for Iron Deficiency Anemia and Iron Supplementation in Pregnant Women to Improve Maternal Health and Birth Outcomes: Recommendation Statement. Am Fam Physician. 2016;93(2):133-6.

242. Pena-Rosas JP, De-Regil LM, Garcia-Casal MN, Dowswell T. Daily oral iron supplementation during pregnancy. Cochrane Database Syst Rev. 2015;2015(7):CD004736.

243. Paganini D, Zimmermann MB. The effects of iron fortification and supplementation on the gut microbiome and diarrhea in infants and children: a review. Am J Clin Nutr. 2017;106(Suppl 6):1688S-93S.

244. Krebs NF, Domellof M, Ziegler E. Balancing Benefits and Risks of Iron Fortification in Resource-Rich Countries. J Pediatr. 2015;167(4 Suppl):S20-5.

245. Pavord S, Daru J, Prasannan N, Robinson S, Stanworth S, Girling J, Committee BSH. UK guidelines on the management of iron deficiency in pregnancy. Br J Haematol. 2020;188(6):819-30.

246. Lewkowitz AK, Gupta A, Simon L, Sabol BA, Stoll C, Cooke E, et al. Intravenous compared with oral iron for the treatment of iron-deficiency anemia in pregnancy: a systematic review and meta-analysis. J Perinatol. 2019;39(4):519-32.

247. Miller HJ, Hu J, Valentine JK, Gable PS. Efficacy and tolerability of intravenous ferric gluconate in the treatment of iron deficiency anemia in patients without kidney disease. Arch Intern Med. 2007;167(12):1327-8.

248. Casanueva E, Viteri FE. Iron and oxidative stress in pregnancy. J Nutr. 2003;133(5 Suppl 2):1700S-8S.

249. Scholl TO. Iron status during pregnancy: setting the stage for mother and infant. Am J Clin Nutr. 2005;81(5):1218S-22S.

250. Ziaei S, Norrozi M, Faghihzadeh S, Jafarbegloo E. A randomised placebo-controlled trial to determine the effect of iron supplementation on pregnancy outcome in pregnant women with haemoglobin > or = 13.2 g/dl. BJOG. 2007;114(6):684-8.

251. Bateman DN, Eagling V, Sandilands EA, Jackson G, Crawford C, Hawkins L, et al. Iron overdose epidemiology, clinical features and iron concentration-effect relationships: the UK experience 2008-2017. Clin Toxicol (Phila). 2018;56(11):1098-106.

252. Sun CF, Liu H, Hao YH, Hu HT, Zhou ZY, Zou KX, et al. Association between gestational anemia in different trimesters and neonatal outcomes: a retrospective longitudinal cohort study. World J Pediatr. 2021;17(2):197-204.

253. Gragasin FS, Ospina MB, Serrano-Lomelin J, Kim SH, Kokotilo M, Woodman AG, et al. Maternal and Cord Blood Hemoglobin as Determinants of Placental Weight: A Cross-Sectional Study. J Clin Med. 2021;10(5).

254. Pena-Rosas JP, De-Regil LM, Dowswell T, Viteri FE. Intermittent oral iron supplementation during pregnancy. Cochrane Database Syst Rev. 2012;7(7):CD009997.

255. Toblli JE, Cao G, Oliveri L, Angerosa M. Effects of iron polymaltose complex, ferrous fumarate and ferrous sulfate treatments in anemic pregnant rats, their fetuses and placentas. Inflamm Allergy Drug Targets. 2013;12(3):190-8.

256. Kwok CS, Gulati M, Michos ED, Potts J, Wu P, Watson L, et al. Dietary components and risk of cardiovascular disease and all-cause mortality: a review of evidence from meta-analyses. Eur J Prev Cardiol. 2019;26(13):1415-29.

257. Zhang X, Shu XO, Xiang YB, Yang G, Li H, Gao J, et al. Cruciferous vegetable consumption is associated with a reduced risk of total and cardiovascular disease mortality. Am J Clin Nutr. 2011;94(1):240-6.

258. Aune D, Giovannucci E, Boffetta P, Fadnes LT, Keum N, Norat T, et al. Fruit and vegetable intake and the risk of cardiovascular disease, total cancer and all-cause mortality-a systematic review and dose-response meta-analysis of prospective studies. Int J Epidemiol. 2017;46(3):1029-56.

259. Wang Q, King L, Wang P, Jiang G, Huang Y, Dun C, et al. Higher Levels of Urinary Thiocyanate, a Biomarker of Cruciferous Vegetable Intake, Were Associated With Lower Risks of Cardiovascular Disease and All-Cause Mortality Among Non-smoking Subjects. Front Nutr. 2022;9:919484.

260. Pan JH, Abernathy B, Kim YJ, Lee JH, Kim JH, Shin EC, Kim JK. Cruciferous vegetables and colorectal cancer prevention through microRNA regulation: A review. Crit Rev Food Sci Nutr. 2018;58(12):2026-38.

261. Nho CW, Jeffery E. The synergistic upregulation of phase II detoxification enzymes by glucosinolate breakdown products in cruciferous vegetables. Toxicol Appl Pharmacol. 2001;174(2):146-52.

262. Wei YF, Hao YY, Gao S, Li XQ, Liu FH, Wen ZY, et al. Pre-diagnosis Cruciferous Vegetables and Isothiocyanates Intake and Ovarian Cancer Survival: A Prospective Cohort Study. Front Nutr. 2021;8:778031.

263. Pollock RL. The effect of green leafy and cruciferous vegetable intake on the incidence of cardiovascular disease: A meta-analysis. JRSM Cardiovasc Dis. 2016;5:2048004016661435.

264. Egner PA, Chen JG, Wang JB, Wu Y, Sun Y, Lu JH, et al. Bioavailability of Sulforaphane from two broccoli sprout beverages: results of a short-term, cross-over clinical trial in Qidong, China. Cancer Prev Res (Phila). 2011;4(3):384-95.

265. Li B, Kim DS, Yadav RK, Kim HR, Chae HJ. Sulforaphane prevents doxorubicin-induced oxidative stress and cell death in rat H9c2 cells. Int J Mol Med. 2015;36(1):53-64.

266. Danilov CA, Chandrasekaran K, Racz J, Soane L, Zielke C, Fiskum G. Sulforaphane protects astrocytes against oxidative stress and delayed death caused by oxygen and glucose deprivation. Glia. 2009;57(6):645-56.

267. Brandenburg LO, Kipp M, Lucius R, Pufe T, Wruck CJ. Sulforaphane suppresses LPS-induced inflammation in primary rat microglia. Inflamm Res. 2010;59(6):443-50.

268. Greco T, Fiskum G. Brain mitochondria from rats treated with sulforaphane are resistant to redox-regulated permeability transition. J Bioenerg Biomembr. 2010;42(6):491-7.

269. Kensler TW, Egner PA, Agyeman AS, Visvanathan K, Groopman JD, Chen JG, et al. Keap1-nrf2 signaling: a target for cancer prevention by sulforaphane. Top Curr Chem. 2013;329:163-77.

270. Santilli F, Guagnano MT, Vazzana N, La Barba S, Davi G. Oxidative stress drivers and modulators in obesity and cardiovascular disease: from biomarkers to therapeutic approach. Curr Med Chem. 2015;22(5):582-95.

271. Padayatty SJ, Katz A, Wang Y, Eck P, Kwon O, Lee JH, et al. Vitamin C as an antioxidant: evaluation of its role in disease prevention. J Am Coll Nutr. 2003;22(1):18-35.

272. Xue M, Momiji H, Rabbani N, Barker G, Bretschneider T, Shmygol A, et al. Frequency Modulated Translocational Oscillations of Nrf2 Mediate the Antioxidant Response Element Cytoprotective Transcriptional Response. Antioxid Redox Signal. 2015;23(7):613-29.

273. Houghton CA, Fassett RG, Coombes JS. Sulforaphane and Other Nutrigenomic Nrf2 Activators: Can the Clinician's Expectation Be Matched by the Reality? Oxid Med Cell Longev. 2016;2016:7857186.

274. Ladak Z. Sulforaphane Protects Brain Cells from Oxygen & Glucose Deprivation: University of Alberta; 2021.

275. Ladak Z, Garcia E, Yoon J, Landry T, Armstrong EA, Yager JY, Persad S. Sulforaphane (SFA) protects neuronal cells from oxygen & glucose deprivation (OGD). PLoS One. 2021;16(3):e0248777.

276. Fahey JW, Talalay P. Antioxidant functions of sulforaphane: a potent inducer of Phase II detoxication enzymes. Food Chem Toxicol. 1999;37(9-10):973-9.

277. Wu JH, Batist G. Glutathione and glutathione analogues; therapeutic potentials. Biochim Biophys Acta. 2013;1830(5):3350-3.

278. Forman HJ, Zhang H, Rinna A. Glutathione: overview of its protective roles, measurement, and biosynthesis. Mol Aspects Med. 2009;30(1-2):1-12.

279. Arai Y, Martin-Ruiz CM, Takayama M, Abe Y, Takebayashi T, Koyasu S, et al. Inflammation, But Not Telomere Length, Predicts Successful Ageing at Extreme Old Age: A Longitudinal Study of Semi-supercentenarians. EBioMedicine. 2015;2(10):1549-58.

280. Jurk D, Wilson C, Passos JF, Oakley F, Correia-Melo C, Greaves L, et al. Chronic inflammation induces telomere dysfunction and accelerates ageing in mice. Nat Commun. 2014;2:4172.

281. Negi G, Kumar A, Sharma SS. Nrf2 and NF-kappaB modulation by sulforaphane counteracts multiple manifestations of diabetic neuropathy in rats and high glucose-induced changes. Curr Neurovasc Res. 2011;8(4):294-304.

282. Moustafa PE, Abdelkader NF, El Awdan SA, El-Shabrawy OA, Zaki HF. Extracellular Matrix Remodeling and Modulation of Inflammation and Oxidative Stress by Sulforaphane in Experimental Diabetic Peripheral Neuropathy. Inflammation. 2018;41(4):1460-76.

283. Navarro SL, Schwarz Y, Song X, Wang CY, Chen C, Trudo SP, et al. Cruciferous vegetables have variable effects on biomarkers of systemic inflammation in a randomized controlled trial in healthy young adults. J Nutr. 2014;144(11):1850-7.

284. Zurbau A, Au-Yeung F, Blanco Mejia S, Khan TA, Vuksan V, Jovanovski E, et al. Relation of Different Fruit and Vegetable Sources With Incident Cardiovascular Outcomes: A Systematic Review and Meta-Analysis of Prospective Cohort Studies. J Am Heart Assoc. 2020;9(19):e017728.

285. Pan J, Wang R, Pei Y, Wang D, Wu N, Ji Y, et al. Sulforaphane alleviated vascular remodeling in hypoxic pulmonary hypertension via inhibiting inflammation and oxidative stress. J Nutr Biochem. 2023;111:109182.

286. Wang H, Tian Y, Zhang Q, Liu W, Meng L, Jiang X, Xin Y. Essential role of Nrf2 in sulforaphane-induced protection against angiotensin II-induced aortic injury. Life Sci. 2022;306:120780.

287. Hung CN, Huang HP, Wang CJ, Liu KL, Lii CK. Sulforaphane inhibits TNF-alpha-induced adhesion molecule expression through the Rho A/ROCK/NF-kappaB signaling pathway. J Med Food. 2014;17(10):1095-102.

288. Yang X, Liu P, Zhao X, Yang C, Li B, Liu Y, Liu Y. Sulforaphane inhibits cytokine-stimulated chemokine and adhesion molecule expressions in human corneal fibroblasts: Involvement of the MAPK, STAT, and NF-kappaB signaling pathways. Exp Eye Res. 2022;216:108946.

289. Murashima M, Watanabe S, Zhuo XG, Uehara M, Kurashige A. Phase 1 study of multiple biomarkers for metabolism and oxidative stress after one-week intake of broccoli sprouts. Biofactors. 2004;22(1-4):271-5.

290. Bahadoran Z, Mirmiran P, Hosseinpanah F, Rajab A, Asghari G, Azizi F. Broccoli sprouts powder could improve serum triglyceride and oxidized LDL/LDL-cholesterol ratio in type 2 diabetic patients: a randomized double-blind placebo-controlled clinical trial. Diabetes Res Clin Pract. 2012;96(3):348-54.

291. Elkashty OA, Tran SD. Sulforaphane as a Promising Natural Molecule for Cancer Prevention and Treatment. Curr Med Sci. 2021;41(2):250-69.

292. Klomparens EA, Ding Y. The neuroprotective mechanisms and effects of sulforaphane. Brain Circ. 2019;5(2):74-83.

293. Grunwald S, Stellzig J, Adam IV, Weber K, Binger S, Boll M, et al. Longevity in the red flour beetle Tribolium castaneum is enhanced by broccoli and depends on nrf-2, jnk-1 and foxo-1 homologous genes. Genes Nutr. 2013;8(5):439-48.

294. Qi Z, Ji H, Le M, Li H, Wieland A, Bauer S, et al. Sulforaphane promotes C. elegans longevity and healthspan via DAF-16/DAF-2 insulin/IGF-1 signaling. Aging (Albany NY). 2021;13(2):1649-70.

295. Cahill GF, Jr. Fuel metabolism in starvation. Annu Rev Nutr. 2006;26:1-22.

296. Selvaraj S, Kelly DP, Margulies KB. Implications of Altered Ketone Metabolism and Therapeutic Ketosis in Heart Failure. Circulation. 2020;141(22):1800-12.

297. Lopaschuk GD, Karwi QG, Ho KL, Pherwani S, Ketema EB. Ketone metabolism in the failing heart. Biochim Biophys Acta Mol Cell Biol Lipids. 2020;1865(12):158813.

298. Halestrap AP. Monocarboxylic acid transport. Compr Physiol. 2013;3(4):1611-43.

299. van Hasselt PM, Ferdinandusse S, Monroe GR, Ruiter JP, Turkenburg M, Geerlings MJ, et al. Monocarboxylate transporter 1 deficiency and ketone utilization. N Engl J Med. 2014;371(20):1900-7.

300. Moller N. Ketone Body, 3-Hydroxybutyrate: Minor Metabolite - Major Medical Manifestations. J Clin Endocrinol Metab. 2020;105(9).

301. Shimazu T, Hirschey MD, Newman J, He W, Shirakawa K, Le Moan N, et al. Suppression of oxidative stress by beta-hydroxybutyrate, an endogenous histone deacetylase inhibitor. Science. 2013;339(6116):211-4.

302. Youm YH, Nguyen KY, Grant RW, Goldberg EL, Bodogai M, Kim D, et al. The ketone metabolite beta-hydroxybutyrate blocks NLRP3 inflammasome-mediated inflammatory disease. Nat Med. 2015;21(3):263-9.

303. Rahman M, Muhammad S, Khan MA, Chen H, Ridder DA, Muller-Fielitz H, et al. The beta-hydroxybutyrate receptor HCA2 activates a neuroprotective subset of macrophages. Nat Commun. 2014;5:3944.

304. Kolb H, Kempf K, Rohling M, Lenzen-Schulte M, Schloot NC, Martin S. Ketone bodies: from enemy to friend and guardian angel. BMC Med. 2021;19(1):313.

305. Newman JC, Verdin E. beta-Hydroxybutyrate: A Signaling Metabolite. Annu Rev Nutr. 2017;37:51-76.

306. Aubert G, Martin OJ, Horton JL, Lai L, Vega RB, Leone TC, et al. The Failing Heart Relies on Ketone Bodies as a Fuel. Circulation. 2016;133(8):698-705.

307. Newbern D, Freemark M. Placental hormones and the control of maternal metabolism and fetal growth. Curr Opin Endocrinol Diabetes Obes. 2011;18(6):409-16.

308. Riskin-Mashiah S, Damti A, Younes G, Auslander R. Normal fasting plasma glucose levels during pregnancy: a hospital-based study. J Perinat Med. 2011;39(2):209-11.

309. Phelps RL, Metzger BE, Freinkel N. Carbohydrate metabolism in pregnancy. XVII. Diurnal profiles of plasma glucose, insulin, free fatty acids, triglycerides, cholesterol, and individual amino acids in late normal pregnancy. Am J Obstet Gynecol. 1981;140(7):730-6.

310. Metzger BE, Ravnikar V, Vileisis RA, Freinkel N. "Accelerated starvation" and the skipped breakfast in late normal pregnancy. Lancet. 1982;1(8272):588-92.

311. Rudolf MC, Sherwin RS. Maternal ketosis and its effects on the fetus. Clin Endocrinol Metab. 1983;12(2):413-28.

312. Patel MS, Johnson CA, Rajan R, Owen OE. The metabolism of ketone bodies in developing human brain: development of ketone-body-utilizing enzymes and ketone bodies as precursors for lipid synthesis. J Neurochem. 1975;25(6):905-8.

313. King JC. Physiology of pregnancy and nutrient metabolism. Am J Clin Nutr. 2000;71(5 Suppl):1218S-25S.

314. van der Louw EJ, Williams TJ, Henry-Barron BJ, Olieman JF, Duvekot JJ, Vermeulen MJ, et al. Ketogenic diet therapy for epilepsy during pregnancy: A case series. Seizure. 2017;45:198-201.

315. Husari KS, Cervenka MC. The ketogenic diet all grown up-Ketogenic diet therapies for adults. Epilepsy Res. 2020;162:106319.

316. Sussman D, van Eede M, Wong MD, Adamson SL, Henkelman M. Effects of a ketogenic diet during pregnancy on embryonic growth in the mouse. BMC Pregnancy Childbirth. 2013;13:109.

317. Sussman D, Germann J, Henkelman M. Gestational ketogenic diet programs brain structure and susceptibility to depression & anxiety in the adult mouse offspring. Brain Behav. 2015;5(2):e00300.

318. Marshall NE, Abrams B, Barbour LA, Catalano P, Christian P, Friedman JE, et al. The importance of nutrition in pregnancy and lactation: lifelong consequences. Am J Obstet Gynecol. 2022;226(5):607-32.

319. Hamdi K, Bastani P, Gafarieh R, Mozafari H, Hashemi SH, Ghotbi MH. The influence of maternal ketonuria on fetal well-being tests in postterm pregnancy. Arch Iran Med. 2006;9(2):144-7.

320. Onyeije CI, Divon MY. The impact of maternal ketonuria on fetal test results in the setting of postterm pregnancy. Am J Obstet Gynecol. 2001;184(4):713-8.

321. Jovanovic L, Metzger BE, Knopp RH, conley MR, Park E, Lee YJ, et al. The Diabetes in Early Pregnancy Study: beta-hydroxybutyrate levels in type 1 diabetic pregnancy compared with normal pregnancy. NICHD-Diabetes in Early Pregnancy Study Group (DIEP). National Institute of Child Health and Development. Diabetes Care. 1998;21(11):1978-84.

322. Hirata Y, Shimazaki S, Suzuki S, Henmi Y, Komiyama H, Kuwayama T, et al. beta-hydroxybutyrate suppresses NLRP3 inflammasome-mediated placental inflammation and lipopolysaccharide-induced fetal absorption. J Reprod Immunol. 2021;148:103433.

323. Soni S, Martens MD, Takahara S, Silver HL, Maayah ZH, Ussher JR, et al. Exogenous ketone ester administration attenuates systemic inflammation and reduces organ damage in a lipopolysaccharide model of sepsis. Biochim Biophys Acta Mol Basis Dis. 2022;1868(11):166507.

324. Taegtmeyer H, Young ME, Lopaschuk GD, Abel ED, Brunengraber H, Darley-Usmar V, et al. Assessing Cardiac Metabolism: A Scientific Statement From the American Heart Association. Circ Res. 2016;118(10):1659-701.

325. De Jong KA, Lopaschuk GD. Complex Energy Metabolic Changes in Heart Failure With Preserved Ejection Fraction and Heart Failure With Reduced Ejection Fraction. Can J Cardiol. 2017;33(7):860-71.

326. Abdul Kadir A, Clarke K, Evans RD. Cardiac ketone body metabolism. Biochim Biophys Acta Mol Basis Dis. 2020;1866(6):165739.

327. Matsumura N, Zordoky BN, Robertson IM, Hamza SM, Parajuli N, Soltys CM, et al. Co-administration of resveratrol with doxorubicin in young mice attenuates detrimental late-occurring cardiovascular changes. Cardiovasc Res. 2018;114(10):1350-9.

328. Halabi A, Sen J, Huynh Q, Marwick TH. Metformin treatment in heart failure with preserved ejection fraction: a systematic review and meta-regression analysis. Cardiovasc Diabetol. 2020;19(1):124.

329. Kamel AM, Sabry N, Farid S. Effect of metformin on left ventricular mass and functional parameters in non-diabetic patients: a meta-analysis of randomized clinical trials. BMC Cardiovasc Disord. 2022;22(1):405.

330. van der Pol A, van Gilst WH, Voors AA, van der Meer P. Treating oxidative stress in heart failure: past, present and future. Eur J Heart Fail. 2019;21(4):425-35.

331. Svensson EC, Madar A, Campbell CD, He Y, Sultan M, Healey ML, et al. TET2-Driven Clonal Hematopoiesis and Response to Canakinumab: An Exploratory Analysis of the CANTOS Randomized Clinical Trial. JAMA Cardiol. 2022;7(5):521-8.

332. Ho KL, Zhang L, Wagg C, Al Batran R, Gopal K, Levasseur J, et al. Increased ketone body oxidation provides additional energy for the failing heart without improving cardiac efficiency. Cardiovasc Res. 2019;115(11):1606-16.

333. Ko A, Kwon HE, Kim HD. Updates on the ketogenic diet therapy for pediatric epilepsy. Biomed J. 2022;45(1):19-26.

334. Nielsen R, Moller N, Gormsen LC, Tolbod LP, Hansson NH, Sorensen J, et al. Cardiovascular Effects of Treatment With the Ketone Body 3-Hydroxybutyrate in Chronic Heart Failure Patients. Circulation. 2019;139(18):2129-41.

335. Fischer T, Och U, Klawon I, Och T, Gruneberg M, Fobker M, et al. Effect of a Sodium and Calcium DL-beta-Hydroxybutyrate Salt in Healthy Adults. J Nutr Metab. 2018;2018:9812806.

336. Neudorf H, Durrer C, Myette-Cote E, Makins C, O'Malley T, Little JP. Oral Ketone Supplementation Acutely Increases Markers of NLRP3 Inflammasome Activation in Human Monocytes. Mol Nutr Food Res. 2019;63(11):e1801171.

337. Cuenoud B, Hartweg M, Godin JP, Croteau E, Maltais M, Castellano CA, et al. Metabolism of Exogenous D-Beta-Hydroxybutyrate, an Energy Substrate Avidly Consumed by the Heart and Kidney. Front Nutr. 2020;7:13.

338. Chu Y, Zhang C, Xie M. Beta-Hydroxybutyrate, Friend or Foe for Stressed Hearts. Front Aging. 2021;2.

339. Denic S, Agarwal MM. Nutritional iron deficiency: an evolutionary perspective. Nutrition. 2007;23(7-8):603-14.

340. Garzon S, Cacciato PM, Certelli C, Salvaggio C, Magliarditi M, Rizzo G. Iron Deficiency Anemia in Pregnancy: Novel Approaches for an Old Problem. Oman Med J. 2020;35(5):e166.

341. Gambling L, Dunford S, Wallace DI, Zuur G, Solanky N, Srai SK, McArdle HJ. Iron deficiency during pregnancy affects postnatal blood pressure in the rat. J Physiol. 2003;552(Pt 2):603-10.

342. Lisle SJ, Lewis RM, Petry CJ, Ozanne SE, Hales CN, Forhead AJ. Effect of maternal iron restriction during pregnancy on renal morphology in the adult rat offspring. Br J Nutr. 2003;90(1):33-9.

343. Bourque SL, Komolova M, McCabe K, Adams MA, Nakatsu K. Perinatal iron deficiency combined with a high-fat diet causes obesity and cardiovascular dysregulation. Endocrinology. 2012;153(3):1174-82.

344. Beck KC, Randolph LN, Bailey KR, Wood CM, Snyder EM, Johnson BD. Relationship between cardiac output and oxygen consumption during upright cycle exercise in healthy humans. J Appl Physiol (1985). 2006;101(5):1474-80.

345. Duncker DJ, Bache RJ. Regulation of coronary blood flow during exercise. Physiol Rev. 2008;88(3):1009-86.

346. van Veldhuisen DJ, Anker SD, Ponikowski P, Macdougall IC. Anemia and iron deficiency in heart failure: mechanisms and therapeutic approaches. Nat Rev Cardiol. 2011;8(9):485-93.

347. Naito Y, Tsujino T, Matsumoto M, Sakoda T, Ohyanagi M, Masuyama T. Adaptive response of the heart to long-term anemia induced by iron deficiency. Am J Physiol Heart Circ Physiol. 2009;296(3):H585-93.

348. Maeder MT, Khammy O, dos Remedios C, Kaye DM. Myocardial and systemic iron depletion in heart failure implications for anemia accompanying heart failure. J Am Coll Cardiol. 2011;58(5):474-80.

349. Anand IS, Gupta P. Anemia and Iron Deficiency in Heart Failure: Current Concepts and Emerging Therapies. Circulation. 2018;138(1):80-98.

350. Toblli JE, Cao G, Rivas C, Giani JF, Dominici FP. Intravenous iron sucrose reverses anemia-induced cardiac remodeling, prevents myocardial fibrosis, and improves cardiac function by attenuating oxidative/nitrosative stress and inflammation. Int J Cardiol. 2016;212:84-91.

351. Thammavong K, Luewan S, Jatavan P, Tongsong T. Foetal haemodynamic response to anaemia. ESC Heart Fail. 2020.

352. Das N, Menon NG, de Almeida LGN, Woods PS, Heynen ML, Jay GD, et al. Proteomics Analysis of Tears and Saliva From Sjogren's Syndrome Patients. Front Pharmacol. 2021;12:787193.

353. Cox J, Neuhauser N, Michalski A, Scheltema RA, Olsen JV, Mann M. Andromeda: a peptide search engine integrated into the MaxQuant environment. J Proteome Res. 2011;10(4):1794-805.

354. Cox J, Mann M. MaxQuant enables high peptide identification rates, individualized p.p.b.-range mass accuracies and proteome-wide protein quantification. Nat Biotechnol. 2008;26(12):1367-72.

355. Spitzer M, Wildenhain J, Rappsilber J, Tyers M. BoxPlotR: a web tool for generation of box plots. Nat Methods. 2014;11(2):121-2.

356. Guo Y, Pu WT. Cardiomyocyte Maturation: New Phase in Development. Circ Res. 2020;126(8):1086-106.

357. Parajuli P, Ahmed AA. Left Atrial Enlargement. StatPearls. Treasure Island (FL)2022.

358. Kalisch-Smith JI, Ved N, Szumska D, Munro J, Troup M, Harris SE, et al. Maternal iron deficiency perturbs embryonic cardiovascular development in mice. Nat Commun. 2021;12(1):3447.

359. Alnuwaysir RIS, Hoes MF, van Veldhuisen DJ, van der Meer P, Grote Beverborg N. Iron Deficiency in Heart Failure: Mechanisms and Pathophysiology. J Clin Med. 2021;11(1).

360. Nikolaou M, Chrysohoou C, Georgilas TA, Giamouzis G, Giannakoulas G, Karavidas A, et al. Management of iron deficiency in chronic heart failure: Practical considerations for clinical use and future directions. Eur J Intern Med. 2019;65:17-25.

361. Garcia M, Mulvagh SL, Merz CN, Buring JE, Manson JE. Cardiovascular Disease in Women: Clinical Perspectives. Circ Res. 2016;118(8):1273-93.

362. Bishop SP, Zhang J, Ye L. Cardiomyocyte Proliferation from Fetal- to Adult- and from Normal- to Hypertrophy and Failing Hearts. Biology (Basel). 2022;11(6).

363. Krenz M, Robbins J. Impact of beta-myosin heavy chain expression on cardiac function during stress. J Am Coll Cardiol. 2004;44(12):2390-7.

364. Georgieff MK. Iron assessment to protect the developing brain. Am J Clin Nutr. 2017;106(Suppl 6):1588S-93S.

365. Rineau E, Gaillard T, Gueguen N, Procaccio V, Henrion D, Prunier F, Lasocki S. Iron deficiency without anemia is responsible for decreased left ventricular function and reduced mitochondrial complex I activity in a mouse model. Int J Cardiol. 2018;266:206-12.

366. Rineau E, Gueguen N, Procaccio V, Genevieve F, Reynier P, Henrion D, Lasocki S. Iron Deficiency without Anemia Decreases Physical Endurance and Mitochondrial Complex I Activity of Oxidative Skeletal Muscle in the Mouse. Nutrients. 2021;13(4).

367. Perez-Riverol Y, Bai J, Bandla C, Garcia-Seisdedos D, Hewapathirana S, Kamatchinathan S, et al. The PRIDE database resources in 2022: a hub for mass spectrometry-based proteomics evidences. Nucleic Acids Res. 2022;50(D1):D543-D52.

368. Deutsch EW, Bandeira N, Perez-Riverol Y, Sharma V, Carver JJ, Mendoza L, et al. The ProteomeXchange consortium at 10 years: 2023 update. Nucleic Acids Res. 2023;51(D1):D1539-D48.

369. Perez-Riverol Y, Xu QW, Wang R, Uszkoreit J, Griss J, Sanchez A, et al. PRIDE Inspector Toolsuite: Moving Toward a Universal Visualization Tool for Proteomics Data Standard Formats and Quality Assessment of ProteomeXchange Datasets. Mol Cell Proteomics. 2016;15(1):305-17.

370. Tain YL, Hsu CN. Developmental Origins of Chronic Kidney Disease: Should We Focus on Early Life? Int J Mol Sci. 2017;18(2).

371. Milman N. Iron and pregnancy--a delicate balance. Ann Hematol. 2006;85(9):559-65.

372. Lopaschuk GD, Ussher JR. Evolving Concepts of Myocardial Energy Metabolism: More Than Just Fats and Carbohydrates. Circ Res. 2016;119(11):1173-6.

373. Puchalska P, Crawford PA. Multi-dimensional Roles of Ketone Bodies in Fuel Metabolism, Signaling, and Therapeutics. Cell Metab. 2017;25(2):262-84.

374. Anders HJ, Suarez-Alvarez B, Grigorescu M, Foresto-Neto O, Steiger S, Desai J, et al. The macrophage phenotype and inflammasome component NLRP3 contributes to nephrocalcinosis-related chronic kidney disease independent from IL-1-mediated tissue injury. Kidney Int. 2018;93(3):656-69.

375. Byrne NJ, Soni S, Takahara S, Ferdaoussi M, Al Batran R, Darwesh AM, et al. Chronically Elevating Circulating Ketones Can Reduce Cardiac Inflammation and Blunt the Development of Heart Failure. Circ Heart Fail. 2020;13(6):e006573.

376. Symington EA, Baumgartner J, Malan L, Wise AJ, Ricci C, Zandberg L, Smuts CM. Maternal iron-deficiency is associated with premature birth and higher birth weight despite routine antenatal iron supplementation in an urban South African setting: The NuPED prospective study. PLoS One. 2019;14(9):e0221299.

377. Bartholmey SJ, Sherman AR. Impaired ketogenesis in iron-deficient rat pups. J Nutr. 1986;116(11):2180-9.

378. Cotter DG, d'Avignon DA, Wentz AE, Weber ML, Crawford PA. Obligate role for ketone body oxidation in neonatal metabolic homeostasis. J Biol Chem. 2011;286(9):6902-10.

379. Shambaugh GE, 3rd, Koehler RA, Freinkel N. Fetal fuels II: contributions of selected carbon fuels to oxidative metabolism in rat conceptus. Am J Physiol. 1977;233(6):E457-61.

380. Roberts H, Woodman AG, Baines KJ, Jeyarajah MJ, Bourque SL, Renaud SJ. Maternal Iron Deficiency Alters Trophoblast Differentiation and Placental Development in Rat Pregnancy. Endocrinology. 2021;162(12).

381. Yurista SR, Matsuura TR, Sillje HHW, Nijholt KT, McDaid KS, Shewale SV, et al. Ketone Ester Treatment Improves Cardiac Function and Reduces Pathologic Remodeling in Preclinical Models of Heart Failure. Circ Heart Fail. 2021;14(1):e007684.

382. Santos-Gallego CG, Requena-Ibanez JA, Picatoste B, Fardman B, Ishikawa K, Mazurek R, et al. Cardioprotective Effect of Empagliflozin and Circulating Ketone Bodies During Acute Myocardial Infarction. Circ Cardiovasc Imaging. 2023;16(4):e015298.

383. Takahara S, Soni S, Maayah ZH, Ferdaoussi M, Dyck JRB. Ketone therapy for heart failure: current evidence for clinical use. Cardiovasc Res. 2022;118(4):977-87.

384. Takahara S, Soni S, Phaterpekar K, Kim TT, Maayah ZH, Levasseur JL, et al. Chronic exogenous ketone supplementation blunts the decline of cardiac function in the failing heart. ESC Heart Fail. 2021;8(6):5606-12.

385. Stegeman R, Paauw ND, de Graaf R, van Loon RLE, Termote JUM, Breur J. The etiology of cardiac hypertrophy in infants. Sci Rep. 2021;11(1):10626.

386. Kalteren WS, Bos AF, van Oeveren W, Hulscher JBF, Kooi EMW. Neonatal anemia relates to intestinal injury in preterm infants. Pediatr Res. 2022;91(6):1452-8.

387. Asif S, Kim RY, Fatica T, Sim J, Zhao X, Oh Y, et al. Hmgcs2-mediated ketogenesis modulates high-fat diet-induced hepatosteatosis. Mol Metab. 2022;61:101494.

388. Liskiewicz D, Liskiewicz A, Nowacka-Chmielewska MM, Grabowski M, Pondel N, Grabowska K, et al. Differential Response of Hippocampal and Cerebrocortical Autophagy and Ketone Body Metabolism to the Ketogenic Diet. Front Cell Neurosci. 2021;15:733607.

389. Chaanine AH, Gordon RE, Kohlbrenner E, Benard L, Jeong D, Hajjar RJ. Potential role of BNIP3 in cardiac remodeling, myocardial stiffness, and endoplasmic reticulum: mitochondrial calcium homeostasis in diastolic and systolic heart failure. Circ Heart Fail. 2013;6(3):572-83.

390. Tanner HL, Dekker Nitert M, Callaway LK, Barrett HL. Ketones in Pregnancy: Why Is It Considered Necessary to Avoid Them and What Is the Evidence Behind Their Perceived Risk? Diabetes Care. 2021;44(1):280-9.

391. Caniggia I, Winter J, Lye SJ, Post M. Oxygen and placental development during the first trimester: implications for the pathophysiology of pre-eclampsia. Placenta. 2000;21 Suppl A:S25-30.

392. Abaci Turk E, Stout JN, Ha C, Luo J, Gagoski B, Yetisir F, et al. Placental MRI: Developing Accurate Quantitative Measures of Oxygenation. Top Magn Reson Imaging. 2019;28(5):285-97.

393. Gumina DL, Su EJ. Mechanistic insights into the development of severe fetal growth restriction. Clin Sci (Lond). 2023;137(8):679-95.

394. Hafstrom M, Ehnberg S, Blad S, Noren H, Renman C, Rosen KG, Kjellmer I. Developmental outcome at 6.5 years after acidosis in term newborns: a population-based study. Pediatrics. 2012;129(6):e1501-7.

395. Schild RL, Maringa M, Siemer J, Meurer B, Hart N, Goecke TW, et al. Weight estimation by three-dimensional ultrasound imaging in the small fetus. Ultrasound Obstet Gynecol. 2008;32(2):168-75.

396. Fraser KH, Poelma C, Zhou B, Bazigou E, Tang MX, Weinberg PD. Ultrasound imaging velocimetry with interleaved images for improved pulsatile arterial flow measurements: a new correction method, experimental and in vivo validation. J R Soc Interface. 2017;14(127).

397. Bamfo JE, Odibo AO. Diagnosis and management of fetal growth restriction. J Pregnancy. 2011;2011:640715.

398. Khong SL, Kane SC, Brennecke SP, da Silva Costa F. First-trimester uterine artery Doppler analysis in the prediction of later pregnancy complications. Dis Markers. 2015;2015:679730.

399. Li J, Chen Y, Ye W, Zhang M, Zhu J, Zhi W, Cheng Q. Molecular breast cancer subtype identification using photoacoustic spectral analysis and machine learning at the biomacromolecular level. Photoacoustics. 2023;30:100483.

400. Yamaleyeva LM, Brosnihan KB, Smith LM, Sun Y. Preclinical Ultrasound-Guided Photoacoustic Imaging of the Placenta in Normal and Pathologic Pregnancy. Mol Imaging. 2018;17:1536012118802721.

401. Bayer CL, Wlodarczyk BJ, Finnell RH, Emelianov SY. Ultrasound-guided spectral photoacoustic imaging of hemoglobin oxygenation during development. Biomed Opt Express. 2017;8(2):757-63.

402. Vincely VD, Bayer CL. Functional photoacoustic imaging for placental monitoring: A mini review. IEEE Trans Ultrason Ferroelectr Freq Control. 2023;PP.

403. Yamaleyeva LM, Sun Y, Bledsoe T, Hoke A, Gurley SB, Brosnihan KB. Photoacoustic imaging for in vivo quantification of placental oxygenation in mice. FASEB J. 2017;31(12):5520-9.

404. Arthuis CJ, Novell A, Raes F, Escoffre JM, Lerondel S, Le Pape A, et al. Real-Time Monitoring of Placental Oxygenation during Maternal Hypoxia and Hyperoxygenation Using Photoacoustic Imaging. PLoS One. 2017;12(1):e0169850.

405. Neprokin A, Broadway C, Myllyla T, Bykov A, Meglinski I. Photoacoustic Imaging in Biomedicine and Life Sciences. Life (Basel). 2022;12(4).

406. Yao J, Wang LV. Photoacoustic tomography: fundamentals, advances and prospects. Contrast Media Mol Imaging. 2011;6(5):332-45.

407. Shi H, Chen L, Wang Y, Sun M, Guo Y, Ma S, et al. Severity of Anemia During Pregnancy and Adverse Maternal and Fetal Outcomes. JAMA Netw Open. 2022;5(2):e2147046.

408. Ali AA, Rayis DA, Abdallah TM, Elbashir MI, Adam I. Severe anaemia is associated with a higher risk for preeclampsia and poor perinatal outcomes in Kassala hospital, eastern Sudan. BMC Res Notes. 2011;4:311.

409. Haisjackl M, Luz G, Sparr H, Germann R, Salak N, Friesenecker B, et al. The effects of progressive anemia on jejunal mucosal and serosal tissue oxygenation in pigs. Anesth Analg. 1997;84(3):538-44.

410. Wardle SP, Garr R, Yoxall CW, Weindling AM. A pilot randomised controlled trial of peripheral fractional oxygen extraction to guide blood transfusions in preterm infants. Arch Dis Child Fetal Neonatal Ed. 2002;86(1):F22-7.

411. Charlot K, Antoine-Jonville S, Moeckesch B, Jumet S, Romana M, Waltz X, et al. Cerebral and muscle microvascular oxygenation in children with sickle cell disease: Influence of hematology, hemorheology and vasomotion. Blood Cells Mol Dis. 2017;65:23-8.

412. Raj A, Bertolone SJ, Mangold S, Edmonds HL, Jr. Assessment of cerebral tissue oxygenation in patients with sickle cell disease: effect of transfusion therapy. J Pediatr Hematol Oncol. 2004;26(5):279-83.

413. Nahavandi M, Tavakkoli F, Hasan SP, Wyche MQ, Castro O. Cerebral oximetry in patients with sickle cell disease. Eur J Clin Invest. 2004;34(2):143-8.

414. Lewis RM, Doherty CB, James LA, Burton GJ, Hales CN. Effects of maternal iron restriction on placental vascularization in the rat. Placenta. 2001;22(6):534-9.

415. Riksen JJM, Nikolaev AV, van Soest G. Photoacoustic imaging on its way toward clinical utility: a tutorial review focusing on practical application in medicine. J Biomed Opt. 2023;28(12):121205.

416. Tsuge I, Munisso MC, Kosaka T, Takaya A, Sowa Y, Liu C, et al. Preoperative visualization of midline-crossing subcutaneous arteries in transverse abdominal flaps using photoacoustic tomography. J Plast Reconstr Aesthet Surg. 2023;84:165-75.

417. Qiu T, Peng C, Huang L, Yang J, Ling W, Li J, et al. ICG clearance test based on photoacoustic imaging for assessment of human liver function reserve: An initial clinical study. Photoacoustics. 2023;31:100511.

418. Fadl S, Moshiri M, Fligner CL, Katz DS, Dighe M. Placental Imaging: Normal Appearance with Review of Pathologic Findings. Radiographics. 2017;37(3):979-98.

419. Elsayes KM, Trout AT, Friedkin AM, Liu PS, Bude RO, Platt JF, Menias CO. Imaging of the placenta: a multimodality pictorial review. Radiographics. 2009;29(5):1371-91.

420. Aughwane R, Ingram E, Johnstone ED, Salomon LJ, David AL, Melbourne A. Placental MRI and its application to fetal intervention. Prenat Diagn. 2020;40(1):38-48.

421. De la Fuente M, Miquel J. An update of the oxidation-inflammation theory of aging: the involvement of the immune system in oxi-inflamm-aging. Curr Pharm Des. 2009;15(26):3003-26.

422. Cervantes Gracia K, Llanas-Cornejo D, Husi H. CVD and Oxidative Stress. J Clin Med. 2017;6(2).

423. Liu R, Liu IY, Bi X, Thompson RF, Doctrow SR, Malfroy B, Baudry M. Reversal of age-related learning deficits and brain oxidative stress in mice with superoxide dismutase/catalase mimetics. Proc Natl Acad Sci U S A. 2003;100(14):8526-31.

424. Masood A, Nadeem A, Mustafa SJ, O'Donnell JM. Reversal of oxidative stress-induced anxiety by inhibition of phosphodiesterase-2 in mice. J Pharmacol Exp Ther. 2008;326(2):369-79.

425. Sharifi-Rad M, Anil Kumar NV, Zucca P, Varoni EM, Dini L, Panzarini E, et al. Lifestyle, Oxidative Stress, and Antioxidants: Back and Forth in the Pathophysiology of Chronic Diseases. Front Physiol. 2020;11:694.

426. Chakrabarti S, Jahandideh F, Wu J. Food-derived bioactive peptides on inflammation and oxidative stress. Biomed Res Int. 2014;2014:608979.

427. Bai Y, Cui W, Xin Y, Miao X, Barati MT, Zhang C, et al. Prevention by sulforaphane of diabetic cardiomyopathy is associated with up-regulation of Nrf2 expression and transcription activation. J Mol Cell Cardiol. 2013;57:82-95.

428. Black AM, Armstrong EA, Scott O, Juurlink BJH, Yager JY. Broccoli sprout supplementation during pregnancy prevents brain injury in the newborn rat following placental insufficiency. Behav Brain Res. 2015;291:289-98.

429. Nguyen AT, Bahry AM, Shen KQ, Armstrong EA, Yager JY. Consumption of broccoli sprouts during late gestation and lactation confers protection against developmental delay induced by maternal inflammation. Behav Brain Res. 2016;307:239-49.

430. Rubattu S, Di Castro S, Cotugno M, Bianchi F, Mattioli R, Baima S, et al. Protective effects of Brassica oleracea sprouts extract toward renal damage in high-salt-fed SHRSP: role of AMPK/PPARalpha/UCP2 axis. J Hypertens. 2015;33(7):1465-79.

431. Xu Z, Wang S, Ji H, Zhang Z, Chen J, Tan Y, et al. Broccoli sprout extract prevents diabetic cardiomyopathy via Nrf2 activation in db/db T2DM mice. Sci Rep. 2016;6:30252.

432. Puspitasari A, Handayani N. Broccoli sprouts juice prevents lens protein aggregation in streptozotocin-induced diabetic rat. Int J Ophthalmol. 2019;12(9):1380-5.

433. Hagg S, Jylhava J. Sex differences in biological aging with a focus on human studies. Elife. 2021;10.

434. Yagishita Y, Fahey JW, Dinkova-Kostova AT, Kensler TW. Broccoli or Sulforaphane: Is It the Source or Dose That Matters? Molecules. 2019;24(19).

435. Carter RJ, Morton J, Dunnett SB. Motor coordination and balance in rodents. Curr Protoc Neurosci. 2001;Chapter 8:Unit 8 12.

436. Ardesch DJ, Balbi M, Murphy TH. Automated touch sensing in the mouse tapered beam test using Raspberry Pi. J Neurosci Methods. 2017;291:221-6.

437. Turner KM, Burne TH. Comprehensive behavioural analysis of Long Evans and Sprague-Dawley rats reveals differential effects of housing conditions on tests relevant to neuropsychiatric disorders. PLoS One. 2014;9(3):e93411.

438. Prut L, Belzung C. The open field as a paradigm to measure the effects of drugs on anxiety-like behaviors: a review. Eur J Pharmacol. 2003;463(1-3):3-33.

439. Schmitt U, Hiemke C. Combination of open field and elevated plus-maze: a suitable test battery to assess strain as well as treatment differences in rat behavior. Prog Neuropsychopharmacol Biol Psychiatry. 1998;22(7):1197-215.

440. Fedarko NS. The biology of aging and frailty. Clin Geriatr Med. 2011;27(1):27-37.

441. Maio MT, Hannan JL, Komolova M, Adams MA. Caloric restriction prevents visceral adipose tissue accumulation and maintains erectile function in aging rats. J Sex Med. 2012;9(9):2273-83.

442. Ghezzi AC, Cambri LT, Botezelli JD, Ribeiro C, Dalia RA, de Mello MA. Metabolic syndrome markers in wistar rats of different ages. Diabetol Metab Syndr. 2012;4(1):16.

443. Carrascosa JM, Ruiz P, Martinez C, Pulido JA, Satrustegui J, Andres A. Insulin receptor kinase activity in rat adipocytes is decreased during aging. Biochem Biophys Res Commun. 1989;160(1):303-9.

444. Escriva F, Agote M, Rubio E, Molero JC, Pascual-Leone AM, Andres A, et al. In vivo insulin-dependent glucose uptake of specific tissues is decreased during aging of mature Wistar rats. Endocrinology. 1997;138(1):49-54.

445. Bornstein AB, Rao SS, Marwaha K. Left Ventricular Hypertrophy. StatPearls. Treasure Island (FL)2023.

446. Franco OH, Peeters A, Bonneux L, de Laet C. Blood pressure in adulthood and life expectancy with cardiovascular disease in men and women: life course analysis. Hypertension. 2005;46(2):280-6.

447. Hardy ST, Loehr LR, Butler KR, Chakladar S, Chang PP, Folsom AR, et al. Reducing the Blood Pressure-Related Burden of Cardiovascular Disease: Impact of Achievable Improvements in Blood Pressure Prevention and Control. J Am Heart Assoc. 2015;4(10):e002276.

448. Fryar CD, Ostchega Y, Hales CM, Zhang G, Kruszon-Moran D. Hypertension Prevalence and Control Among Adults: United States, 2015-2016. NCHS Data Brief. 2017(289):1-8.

449. Sengupta P. The Laboratory Rat: Relating Its Age With Human's. Int J Prev Med. 2013;4(6):624-30.

450. Lu KH, Hopper BR, Vargo TM, Yen SS. Chronological changes in sex steroid, gonadotropin and prolactin secretions in aging female rats displaying different reproductive states. Biol Reprod. 1979;21(1):193-203.

451. Wu L, Noyan Ashraf MH, Facci M, Wang R, Paterson PG, Ferrie A, Juurlink BH. Dietary approach to attenuate oxidative stress, hypertension, and inflammation in the cardiovascular system. Proc Natl Acad Sci U S A. 2004;101(18):7094-9.

452. Piper MD, Skorupa D, Partridge L. Diet, metabolism and lifespan in Drosophila. Exp Gerontol. 2005;40(11):857-62.

453. Golbidi S, Daiber A, Korac B, Li H, Essop MF, Laher I. Health Benefits of Fasting and Caloric Restriction. Curr Diab Rep. 2017;17(12):123.

454. Watkins RE, Coates R, Ferroni P. Measurement of aging anxiety in an elderly Australian population. Int J Aging Hum Dev. 1998;46(4):319-32.

455. Moreno-Torres A, Pujol J, Soriano-Mas C, Deus J, Iranzo A, Santamaria J. Age-related metabolic changes in the upper brainstem tegmentum by MR spectroscopy. Neurobiol Aging. 2005;26(7):1051-9.

456. Melancon MO, Lorrain D, Dionne IJ. Exercise and sleep in aging: emphasis on serotonin. Pathol Biol (Paris). 2014;62(5):276-83.

457. Wallace JE, Krauter EE, Campbell BA. Motor and reflexive behavior in the aging rat. J Gerontol. 1980;35(3):364-70.

458. Avgustinovich DF, Lipina TV, Bondar NP, Alekseyenko OV, Kudryavtseva NN. Features of the genetically defined anxiety in mice. Behav Genet. 2000;30(2):101-9.

459. Gokdemir O, Cetinkaya C, Gumus H, Aksu I, Kiray M, Ates M, et al. The effect of exercise on anxiety- and depression-like behavior of aged rats. Biotech Histochem. 2020;95(1):8-17.

460. Nuki G, Simkin PA. A concise history of gout and hyperuricemia and their treatment. Arthritis Res Ther. 2006;8 Suppl 1(Suppl 1):S1.

461. Neel JV. Diabetes mellitus: a "thrifty" genotype rendered detrimental by "progress"? Am J Hum Genet. 1962;14(4):353-62.

462. Speakman JR. A nonadaptive scenario explaining the genetic predisposition to obesity: the "predation release" hypothesis. Cell Metab. 2007;6(1):5-12.

463. Spielman RS, Fajans SS, Neel JV, Pek S, Floyd JC, Oliver WJ. Glucose tolerance in two unacculturated Indian tribes of Brazil. Diabetologia. 1982;23(2):90-3.

464. Scholl TO. Maternal iron status: relation to fetal growth, length of gestation, and iron endowment of the neonate. Nutr Rev. 2011;69 Suppl 1(Suppl 1):S23-9.

465. Brichta CE, Godwin J, Norlin S, Kling PJ. Impact and interactions between risk factors on the iron status of at-risk neonates. J Perinatol. 2022;42(8):1103-9.

466. Mortality GBD, Causes of Death C. Global, regional, and national age-sex specific all-cause and cause-specific mortality for 240 causes of death, 1990-2013: a systematic analysis for the Global Burden of Disease Study 2013. Lancet. 2015;385(9963):117-71.

467. Metivier F, Marchais SJ, Guerin AP, Pannier B, London GM. Pathophysiology of anaemia: focus on the heart and blood vessels. Nephrol Dial Transplant. 2000;15 Suppl 3:14-8.

468. Surbek D, Drack G, Irion O, Nelle M, Huang D, Hoesli I. Antenatal corticosteroids for fetal lung maturation in threatened preterm delivery: indications and administration. Arch Gynecol Obstet. 2012;286(2):277-81.

469. Alhamoud I, Legan SK, Gattineni J, Baum M. Sex differences in prenatal programming of hypertension by dexamethasone. Exp Biol Med (Maywood). 2021;246(13):1554-62.

470. Raikkonen K, Gissler M, Kajantie E. Associations Between Maternal Antenatal Corticosteroid Treatment and Mental and Behavioral Disorders in Children. JAMA. 2020;323(19):1924-33.

471. Mendoza W, Miranda JJ. Global Shifts in Cardiovascular Disease, the Epidemiologic Transition, and Other Contributing Factors: Toward a New Practice of Global Health Cardiology. Cardiol Clin. 2017;35(1):1-12.

472. Vaduganathan M, Mensah GA, Turco JV, Fuster V, Roth GA. The Global Burden of Cardiovascular Diseases and Risk: A Compass for Future Health. J Am Coll Cardiol. 2022;80(25):2361-71.

473. Hula N, Vu J, Quon A, Kirschenman R, Spaans F, Liu R, et al. Sex-specific effects of prenatal hypoxia on the cardiac endothelin system in adult offspring. Am J Physiol Heart Circ Physiol. 2022;322(3):H442-H50.

474. Hula N, Spaans F, Vu J, Quon A, Kirschenman R, Cooke CM, et al. Placental treatment improves cardiac tolerance to ischemia/reperfusion insult in adult male and female offspring exposed to prenatal hypoxia. Pharmacol Res. 2021;165:105461.

475. Shah A, Matsumura N, Quon A, Morton JS, Dyck JRB, Davidge ST. Cardiovascular susceptibility to in vivo ischemic myocardial injury in male and female rat offspring exposed to prenatal hypoxia. Clin Sci (Lond). 2017;131(17):2303-17.

476. Rueda-Clausen CF, Morton JS, Oudit GY, Kassiri Z, Jiang Y, Davidge ST. Effects of hypoxia-induced intrauterine growth restriction on cardiac siderosis and oxidative stress. J Dev Orig Health Dis. 2012;3(5):350-7.

477. Sanni OB, Chambers T, Li JH, Rowe S, Woodman AG, Ospina MB, Bourque SL. A systematic review and meta-analysis of the correlation between maternal and neonatal iron status and haematologic indices. EClinicalMedicine. 2020;27:100555.

Appendix

Table S1. Criteria used for humane endpoint and euthanasia in rats

Parameter	Condition
Weight loss	Body weight loss of more than 20% from their top weight
Breathing abnormalities	Respiratory distress, labored breathing, increased or decreased respiratory rate, cyanosis
Bleeding/open sores	When there is a prolapse of rectum/vagina/penis or rat cannot urinate
Tumor volume or burden	Tumor(s) ulcerated, necrotic, exceeding 3 cm or impairing function (interfere with quality of life)
Limb paralysis	
Dermatitis	
Malocclusion	

Table S2. Observed morbidities at the time of euthanasia in control and broccoli sprout- fed rats

Groups	Rat ID	Age (days)	Humane endpoint criteria	Cardiopulmonary	Kidney	Liver	Brain	Tumor	Other conditions
	1	608	Weight Loss	1	1				
	2	570	Weight Loss	1	1				
	3	779	Breathing Problems/pain	1		1		1	Hemangiosarcoma
	4	779	Unknown (eaten)						
	5	752	Weight Loss		1				
	6	612	Weight Loss	1	1				
Male-	7	617	Movement issues				1		
Chow	8	672	Rear leg paralysis	1	1				
	9	706	Weight Loss	1	1		1	1	
	10	679	Tumor	1	1			1	
	11	540	Weight Loss	1	1		1		
	12	442	Weight loss	1	1				
	13	651	Weight Loss	1	1	1	1		Fast Clotting blood
	14	675	Weight Loss	1	1	1			
Sum				**11**	**11**	**3**	**4**	**3**	
	1	501	Unknown (eaten)						
	2	559	Weight Loss/problems Breathing	1					
	3	452	Unknown (FD)					1	
	4	809	Weight Loss	1				1	
	5	849	Weight Loss	1	1	1			Hyperperfusion
Male-	6	884	Weight Loss	1	1		1		
Broccoli	7	502	Unknown (eaten)						
	8	612	Weight Loss Problems	1					
	9	812	Breathing/not eating	1		1			
	10	801	Malocclusion	1	1	1		1	
	11	635	Weight Loss		1				
	12	545	Weight Loss	1	1				

	13	619	Weight Loss	1	1				
	14	675	Weight Loss	1	1	1			
Sum				**10**	**7**	**4**	**1**	**3**	
Female-Chow	1	641	Malocclusion						
	2	557	Malocclusion						
	3	793	Tumor					1	
	4	840	Weight Loss	1	1		1		Porphyrin from nose
	5	855	Tumor	1		1		1	
	6	612	Tumor	1				1	
	7	690	Weight Loss					1	
	8	576	Tumor	1				1	
	9	899	Malocclusion	1			1		
	10	476	Difficulty breathing	1					
	11	741	Weight Loss/pain	1	1	1	1	1	
	12	716	Unknown (FD)						
	13	892	Weight Loss	1	1				
	14	850	Weight Loss	1	1	1		1	
Sum				**9**	**4**	**3**	**3**	**7**	
Female-Broccoli	1	826	Tumors	1				1	
	2	608	Malocclusion						
	3	638	Dermatitis	1					Dermatitis
	4	872	Weight Loss		1	1	1		
	5	856	Tumor					1	
	6	884	Impaired hindlimb movement		1		1		Loss of hindlimb function
	7	945	Impaired hindlimb movement						
	8	956	Unknown						
	9	619	Tumor					1	
	10	866	Tumor	1	1			1	
	11	803	Weight Loss	1	1		1		Abnormal stomach
	12	721	Tumors		1			1	
	13	903	Malocclusion		1				
	14	850	Tumor	1	1			1	
Sum				**5**	**7**	**1**	**3**	**6**	